

---

# Feasibility of alternative manufacturing processes for winding and stator components of electric machines

**Author:** Nathan Dodd

---

December 2021

*A Thesis submitted to the University of Sheffield for the degree of Doctor of Engineering in the Faculty of Engineering*

*Supervision: Prof Russell Goodall, Dr. Graeme Heron, Dr. Erica Ballantyne, Ben Kitcher, Dr. David Curtis*

# Abstract

---

One of the features of the 21<sup>st</sup> Century is the development of new electric vehicles. This has been accelerated at this time through a combination of political will and consumer adoption. The technologies that can be used in the manufacture of electric vehicles range from the tried and tested to the state of the art. One of the major aspects of an electric vehicle is, naturally, the electric motor (electric machine) which provides the drive to the vehicle. The science and understanding of how to design electric machines is fairly well known. However, it is in the application and mass manufacturability of electric machines of the required capability and at the required scale that there is much less knowledge. The research conducted in this thesis aims to bridge the gap between manufacturing technology and business operations impact, providing a holistic view on the performance of processes and identifying areas for opportunity and concern. The research conducted in this thesis has been centred on the components of the stator and windings.

The manufacturing implications of a shift from windings to hairpins has been considered, with an analysis of the manufacturing route employed in wire winding and hairpin winding produced and examined. A comprehensive study of potential alternative materials for windings and hairpins for conducted, revealing that aluminium has the potential to be a cheaper and lighter winding material to copper. Following these results, a review of the manufacturing efficacy of alternative joining methodologies for Al-Cu hairpin assembly was performed, with the highest potential being seen in friction stir, laser beam and cold press joining. This research was backed up with a structural analysis of the potential benefits of incorporating a hollow section in a hairpin design to reduce the thermal expansion of the hairpin component.

A review of stamping as a method of stator laminate production was considered alongside the creation of a stamping model for stator production and an evaluation of innovative stator manufacturing processes. Following an analysis of the stamping manufacturing route employed in stator production, areas for operational improvements were identified. This knowledge was incorporated into the development of a stamping process manufacturing model. A further study was produced to develop a tool wear dynamic system within the stamping model, with the resulting sub-model used within the system. The stamping model was used to generate a greater understanding of the effect of various stamping parameters on the overall performance of a stamping operation. An analysis of alternative stator materials was produced, identifying METLGAS and cobalt iron as potential alternatives to electrical steel, where electrical steel remains the best material from an overall cost and mass perspective. A feasibility study of slinky style stator as an alternative manufacturing process was conducted, with the

results demonstrating the need to create bespoke stator designs to reduce the stresses as a result of bending.

Laser cutting was identified as a potential alternative to stamping in the mass manufacture of stators. A laser cutting model was developed and an evaluation of laser cutting as an alternative approach was performed. The development of a laser cutting manufacturing model required incorporating a laser optimisation procedure. The optimisation procedure was able to achieve either cost or time efficient results based on any given set of manufacturing parameters. The optimisation model showed that different manufacturing setups are required based on the type of optimisation being considered. A full analysis of laser cutting process parameters was performed, with considerations to cost and time factors, allowing identification of areas of opportunity such as improving the changeover function with an automated transit system.

Experiments were performed using a laser cutting machine. Samples were manufactured and a series of tests were performed to ascertain the feasibility of performing cuts as stacks. The act of cutting multiple laminates in a single operation is henceforth referred to as *polystromata*. The polystromata cut samples were also tested for their electro-magnetic performance qualities post cutting. A materials study of laser cut samples using microscopy was conducted to understand the effect of polystromata cutting.

An economic and operational comparison of stamping and laser cutting was performed, using the knowledge gained throughout the studies conducted within this research. The comparison study was able to identify performance trade-offs of stamping and laser cutting for various stator design parameters. Laser cutting was found to be more suitable than stamping for smaller sized machines. A follow-up study of the economic order quantity of raw materials for stator production was performed.

# Acknowledgements

---

Perhaps it is a fault of mine that I would prefer to use these words to share my appreciation towards those not simply based on their technical support during this project, else I would be giving much thanks to Mr. Google and his often-overlooked brother Bing. I would like to use my acknowledgments to commit in writing a brief journal of thanks, but I would also like use these words to plant a flag in the sand, and though it is often self-defeating to try and live the future all at once, during these years I have realised the way I wish to travel forward... if not quite to where.

In 2016 I started an engineering doctorate in earnest. I look back and realise that at this time I was still a boy in man's clothes. I have seen countless accounts of people who have struggled and suffered during the course of doctoral research, and despite my flippancy towards the idea at first, I too found my own particular set of challenges and circumstances which found me at despair. In that despair, that crucible of doubt and rage, I did too suffer. In these difficult times I developed a character that speaks almost unrecognisably to that boy from 2016. I found a confidence and resilience in the darkness which has become a staple part of my being. At the time of writing, I approach both my 30<sup>th</sup> Birthday and the completion of this EngD with hope and vigour, and most importantly, a steadfast belief in oneself.

I have received varying degrees of help, support, and input over these past years. I give much thanks in particular to Prof. Russell Goodall who has given me both the freedom and the confidence to develop much of what are the best ideas presented in this research. I have also been the beneficiary of help and support from Dr. Erica Ballantyne and Dr. Graeme Heron whom despite no obligation to do so, have provided great insight and calming words during some difficult months.

I would like to thank my parents, Steven & Lindsay Dodd, though their technical input has been very limited, the provision of cake has been much appreciated. I also give thanks to my grandparents, grandad Bill, nana Brenda and grandad John. I would like to give special acknowledgement to my grandmother, Nana Mo, who's generosity, kindness and stoic attitude are just some of the merits of her flawless character. I hope that I can carry her great sense of humour on with me throughout my life, whilst also adding my own little dash of comic personality. I have the deepest respect and love for her, and I hope that in this success and any future successes, I can continue to make her proud.

# Nomenclature

<b>Symbol</b>	<b>Units</b>	<b>Definition</b>
$A_I$	$m^2$	Inner area of stator design
$A_O$	$m^2$	Outer area of stator design
$A_{slot}$	$m^2$	Area of single slot of stator
$A_{sq}$	$m^2$	Area of sheet size material used in stator production
$B$		Magnetic field
$c$		Correcting factor for energy used in cutting
$C_C$	£	Consumables & other
$C_{co}$	/100 hours	Other consumables
$C_D$	£	Die cost
$C_E$	£	Energy costs
$C_{eJ}$	£ / kJ	Energy cost rate per kJ
$C_{eW}$	£ / kWh	Energy cost rate per kWh
$C_G$	/operation	Gas
$C_I$	£	Maintenance costs
$C_{kg}$	£ / kg	Material cost per kg
$C_L$	£	Laser cutter
$C_m$	£	Cost of performing maintenance
$C_O$	£	Overhead costs
$C_{sps}$	£	Material value scrapped
$C_t$	£/hr	Overhead rate
$C_{ups}$	£	Material value in n stacks
$C_V$	£ / $m^3$	Material cost per $m^3$
$C_{\bar{x}}$	£	Av. Stack Cost

$C_{am}$	£	Maintenance
$C_{ao}$	£	Machine & Machining
$C_{\Sigma^*}$	£	Total costs (including raw Mats)
$C_{\Sigma\alpha}$	£	Total costs (Machining)
$D$	m	Rotor diameter
$E_{DM}$	kg	Die Mass
$E_{IC}$	kJ	Inner circumference
$E_L$	kW	Laser power rating
$E_m$	kJ	Die position return
$E_{OC}$	kJ	Outer circumference
$E_P$	kW	Laser Power usage
$E_{slots}$	kJ	Slots
$F$	%	Force factor of safety in stamping model
$F$	N	Magnetic force
$F$	N	Normal load (tool wear)
$H$	HRC	Tool hardness
$I$	Amps	Current
$k$		Torque constant
$K_{cr}$		Cutting resistance
$K_w$		Tool wear constant
$L$	m	Rotor length
$L_c$	m	Length of cut
$L_d$	m	Sheet thickness
$L_{DT}$	m	Die Travel
$L_{IC}$	m	Inner circumference
$L_{ID}$	m	Inner diameter

$L_L$	m	Actual cutting stack depth
$L_{OC}$	m	Outer circumference
$L_{OD}$	m	Outer diameter
$L_{slot}$	m	Length of single slot outline
$L_{stack}$	m	Stack length
$L_{wire}$	m	Length of wire
$n_D$		Tools required to produce stacks
$n_J$		Operations until maintenance
$n_L$		Number of machines purchased
$n_{lams}$		Total required Laminates
$n_{LC}$		Laminates cut (best case)
$n_{lps}$		Laminates per stack
$n_m$		Number of tool maintenance occurrences
$n_O$		Total operations required
$n_S$		Number of strokes until tool maintenance
$n_{slots}$		Number of slots per lamination
$n_{Stacks}$		Total number of stacks
$n_\alpha$		Number of strokes until tool failure
$P$		Power
$P_{IC}$	kN	Force to cut inner circumference
$P_{OC}$	kN	Force to cut outer circumference
$P_{slots}$	kN	Force to cut Slots
$P_\Sigma$	kN	Total force to cut material
$Q$	mm	Tool wear
$T$	N	Torque
$t_D$	mins	Die change over

$t_l$	mins	Laser maintenance
$t_L$	mins	Change over time
$t_{lam}$	secs	Av. laminate production rate
$t_m$	mins	Maintenance time
$t_{stack}$	secs	Av. stack production rate
$t_\alpha$	hours	Time to produce quantity
$U_L$	m/sec	Laser cutting speed
$V_{sps}$	$m^3$	Material scrapped
$V_{ups}$	$m^3$	Material used in n stacks
$x$	m	Energy used in cutting parameter for cutting distance
$\alpha_o$		Operations per minute
$\beta$		Laminates cut per operation
$\rho$	$kg / m^3$	Density
$\sigma_{CR}$	Pa or $N/m^1$	Cutting resistance
$\sigma_{UTS}$	Pa or $N/m^2$	Ultimate tensile strength of material
$\omega$		Angular velocity / rotor speed



# Contents

---

1	Introduction.....	14
1.1	Opening statement.....	14
1.2	Thesis aims and objectives .....	15
1.3	Thesis original contributions .....	16
1.4	General assumptions.....	17
2	Literature review .....	18
2.1	The automotive industry .....	18
2.1.1	Economic order quantity (EOQ) .....	22
2.1.2	Design for manufacture principles and application .....	22
2.2	Synchronous reluctance motor .....	24
2.2.1	Introduction to electric machines .....	24
2.2.2	Electrical steel laminations.....	26
2.2.3	Copper wire winding .....	27
2.2.4	Electric machine mechanics .....	28
2.2.5	Synchronous reluctance manufacture and assembly processes.....	29
2.2.6	Hairpin winding of stators .....	31
2.2.7	Joining methods for use in hairpin winding assembly .....	32
2.3	Stamping process mechanics .....	36
2.3.1	Stamping tool wear .....	38
2.3.2	The slinky Method .....	40
2.4	Laser cutting .....	41
2.5	Laminate performance .....	42
2.5.1	Laminate performance and cut quality as a result of stamping.....	43
2.5.2	Laminate performance and cut quality using laser cutting.....	52
2.6	Gap analysis.....	54

3	Manufacturing implications of a shift from wire winding to hairpin winding .....	55
3.1	Methodology .....	55
3.1.1	Knowledge gap .....	55
3.1.2	Approach .....	55
3.2	Introduction.....	56
3.2.1	Process route.....	56
3.3	Material selection.....	58
3.3.1	Aluminium .....	61
3.4	Temperature effect on resistivity.....	63
3.5	Joining methodology for hairpin to busbar assembly .....	65
3.5.1	Suitability parameter justification .....	65
3.5.2	Assessment of joining methods.....	69
3.6	Experimental exploration .....	70
3.6.1	Thermal expansion issue .....	71
3.7	Conclusions.....	73
4	Cost model for stator production.....	74
4.1	Methodology .....	74
4.1.1	Knowledge gap .....	74
4.1.2	Approach .....	74
4.2	Introduction.....	75
4.2.1	Understanding the operation.....	75
4.2.2	Stamping process route.....	76
4.2.3	Slinky style process route .....	77
4.2.4	SWOT analysis .....	77
4.3	Development of manufacturing cost model for stator stamping activities .....	80
4.3.1	Stamping model assumptions .....	81
4.4	Tool failure predictive model .....	86

4.4.1	Methodology .....	86
4.4.2	Wear parameters.....	86
4.4.3	Application of Taylor’s tool wear to stamping .....	87
4.4.4	The n problem .....	87
4.4.5	Tool hardness issue and solution .....	90
4.4.6	Final tool wear model implementation.....	93
4.5	Analysis of materials used in stamping process .....	94
4.5.1	Assumptions in stamping cost model.....	94
4.5.2	Results .....	95
4.5.3	Stator & rotor material alternatives.....	97
4.6	Study of manufacturing model for stamping of stator laminations.....	98
4.7	Conclusions.....	107
5	Feasibility study for a slinky style stator.....	108
5.1	Methodology .....	108
5.1.1	Knowledge gap .....	108
5.1.2	Approach .....	108
5.2	Slinky coiling trial.....	110
5.3	Introduction.....	112
5.4	Slinky coiling finite element analysis results .....	113
5.5	Slinky coiling trial experimental results.....	116
5.6	Discussion of results for slinky coiling process.....	118
5.7	Conclusions.....	120
6	Laser cutting model and evaluation as an alternative approach .....	121
6.1	Methodology .....	121
6.1.1	Knowledge gap .....	121
6.1.2	Approach .....	121
6.2	Introduction.....	122

6.2.1	Process.....	122
6.2.2	Process improvements .....	123
6.3	Development of laser cutting model.....	126
6.3.1	Assumptions in laser cutting cost model.....	127
6.3.2	Parameter sets.....	127
6.3.3	Laser cutting model .....	128
6.4	Laser model optimisation .....	130
6.4.1	Parameter set 1 .....	132
6.4.2	Parameter set 2 .....	133
6.5	Laser cutter variation .....	135
6.6	Laser cutting model analysis .....	137
6.7	Conclusions.....	142
7	Polystromata laser cutting experiment.....	143
7.1	Methodology .....	143
7.1.1	Knowledge gap .....	143
7.1.2	Approach .....	143
7.2	Introduction.....	149
7.3	Cutting of single sheet laminates .....	150
7.3.1	Single sheet laminate cutting variation.....	150
7.3.2	Laser settings effect on part quality.....	150
7.4	polystromata laser cutting .....	154
7.4.1	polystromata cutting trial 1.....	154
7.4.2	Polystromata trial 2 - geometric variance .....	155
7.4.3	SEM stack results.....	157
7.4.4	Joined layers during polystromata cutting .....	164
7.5	Polystromata laser cutting issues.....	165
7.6	Electro-magnetic performance measurement using Epstein frame .....	166

7.7	Conclusions.....	168
8	An economic and operational comparison of stamping and laser cutting .....	169
8.1	Methodology .....	169
8.1.1	Knowledge gap .....	169
8.1.2	Approach .....	169
8.2	Introduction.....	170
8.3	Economic order quantity .....	170
8.4	Assessment and evaluation of alternative technologies.....	173
8.4.1	Parameter sets.....	173
8.4.2	Scale / quantity.....	174
8.4.3	comparison of cost and time performance for different motor sizes.....	175
8.4.4	Key points of interest .....	177
8.4.5	Sheet thickness effect on results.....	179
8.5	Discussion & Conclusions .....	180
9	Thesis conclusions and further work.....	181
10	References.....	184
11	Appendices .....	194
11.1	Appendix A .....	194
11.2	Appendix B.....	195
11.3	Appendix C.....	201
11.4	Appendix D .....	202
11.5	Appendix E.....	203
11.6	Appendix F .....	204
11.7	Appendix G .....	208
11.8	Appendix H .....	212
11.9	Appendix I.....	213

# 1 Introduction

---

## 1.1 Opening statement

One of the features of the 21<sup>st</sup> Century is the continued development of the electric vehicle, which first started in the early 1900's (Idaho National Laboratory, 2016). This has been accelerated at this time through a combination of political will and consumer adoption. The technologies that can be used in the manufacture of electric vehicles range from the tried and tested to the state of the art. One of the major aspects of an electric vehicle is, naturally, the electric motor (electric machine) which provides the drive to the vehicle. The science and understanding of how to design electric machines is fairly well known. However, it is in the application and mass manufacturability of electric machines of the required capability and at the required scale that there is much less knowledge. There continues to be new manufacturing processes and new technologies developed to produce electric machine components. The stator and rotor components are currently manufactured using an established manufacturing process called stamping. Manufacturers generally rely on empirical knowledge when setting up the process, rather than fine tuning the parameters based on theory to give optimal results. An alternative to stamping is laser cutting. However, this is currently usually reserved for the manufacture of prototypes. The winding component, which sits within the stator, has seen recent technology developments which involve the use of 'hairpin' structures as opposed to wire. Improving the quality and performance of these components is only one aspect of the overall impact such decisions in manufacturing can have on the business. It is important to be able to understand and quantify how these different components and processes effect the whole manufacturing system. Studies regarding the operational impacts of these various processes are limited, as the core research tends towards greater understanding of quality and technological aspects. The research conducted in this thesis aims to bridge the gap between manufacturing technology and business operations impact, providing a holistic view on the performance of processes and identifying areas for opportunity and concern.

## 1.2 Thesis aims and objectives

The overall aim of this thesis is to provide a holistic performance review of current and future manufacturing processes in the production and assembly of stators and windings. This will be achieved by combining machining knowledge with manufacturing economics analysis techniques. The objectives of this research have been divided into six distinct chapters of work.

### *Chapter 3: Manufacturing implications of a shift from windings to hairpins*

The objective of this chapter is to develop a greater understanding of the manufacturing processes used during the winding of stators. Furthermore, the chapter aims to provide knowledge through an analysis of materials and processes such that the feasibility of alternative winding technologies can be assessed.

### *Chapter 4: Stamping model for stator production and evaluation of innovative processes*

The main objective of this chapter is to create a digital model which can be used as a manufacturing tool for optimising manufacturing processes and setting manufacturing parameters in the production of stamped laminates for stators.

### *Chapter 5: Slinky style stator manufacturing feasibility*

The objective of this chapter is to assess the opportunities and issues which occur in the production of stators using the slinky style manufacturing method. This is to be achieved through a combination of modelling and experimental analysis.

### *Chapters 6: Laser cutting model and evaluation of this as an alternative approach*

The main objective of this chapter is to create a digital model which can be used as a manufacturing tool for optimising manufacturing processes and setting manufacturing parameters in the production of laser cut laminates for stators.

### *Chapters 7: Polystromata laser cutting feasibility experiments*

The objective of this chapter is to assess the opportunities and issues which occur in the production of laminates via polystromata laser cutting. This is to be achieved through experimental analysis.

### *Chapter 8: An economic and operational comparison of stamping and polystromata laser cutting*

The objective of this chapter is to identify the relative performance benefits of stamping and laser cutting and to further identify through modelling and analysis the circumstances which affect the relative performance of stamping and laser cutting such that process recommendations are possible.

### 1.3 Thesis original contributions

The work in this thesis is spread across six distinct chapters. This thesis makes the following original contributions in each chapter.

#### *Chapter 3: Manufacturing implications of a shift from windings to hairpins*

- An analysis of the manufacturing route employed in wire winding and hairpin winding.
- A comprehensive study of potential alternative materials for windings & hairpins.
- A review of the manufacturing efficacy of alternative joining methodologies for Al-Cu hairpin assembly and confirmatory trials.
- A structural analysis of the potential benefits of incorporating a hollow section in a hairpin design.

#### *Chapter 4: Stamping model for stator production and evaluation of innovative processes*

- An analysis of the stamping manufacturing route employed in stator production.
- Development of a stamping process manufacturing model incorporating tool wear dynamics.
- An analysis of alternative stator materials
- An analysis of stamping process parameters, with considerations to cost and time factors.

#### *Chapter 5: Slinky style stator manufacturing feasibility*

- Feasibility study of slinky style stator as an alternative manufacturing process

#### *Chapters 6: Laser cutting model and evaluation of this as an alternative approach*

- An analysis of laser cutting as a potential manufacturing route for stator production.
- Development of a laser cutting process manufacturing model incorporating a laser optimisation procedure to achieve either cost / time efficiency.
- An analysis of laser cutting process parameters, with considerations to cost and time factors.

#### *Chapters 7: Polystromata laser cutting feasibility experiments*

- Manufacture and test stack laser cut samples for electro-magnetic performance qualities.
- To perform a materials study of laser cut samples using microscopy to understand effect of polystromata cut samples.

#### *Chapter 8: An economic and operational comparison of stamping and polystromata laser cutting*

- Study the performance trade-offs of stamping and laser cutting for various stator design parameters.
- An analysis of the economic order quantity of raw materials for stator production.



## 1.4 General assumptions

The research conducted in this thesis is initially considered towards the assumed case of the production of a synchronous reluctance machine. However, the research findings have applications in the manufacture of electric machine components more generally. A general machine specification was provided at the commencement of this project, and as such this has been used throughout as the assumed electric machine where specific machine specifications have been required. This same specification was provided to a corresponding project at the University of Sheffield which considered the electrical design of a new machine and the resulting thesis is anticipated to be published circa 2022 entitled '*Design of a novel synchronous reluctance traction machine with a multipart composite rotor*' (Stone, 2021)<sup>1</sup>. An inner stator diameter and rotor diameter was specified as being approximately 170mm. The length of the rotor and stator are assumed to be 100mm. The stator and rotor materials have been assumed to have comparable properties to Cogent M250-35A, as this is a standard laminate material and was readily available for use in trials.

<b>Ricardo Specification circa 2016</b>			
<b>Specification</b>	<b>Step</b>	<b>Stretch</b>	<b>Leap</b>
Power (kW)	80kW	80kW	80kW
Weight (kg)	50	30	20
Cost (\$)	700	300	150
Operating temperature	180oC	300oC	600oC
Rotor diameter (mm)	170	170	170
Stator outer diameter (mm)	291	291	291
Rotor / Stator stack height	100	100	100
Life (hours)	3000hrs	10,000hrs	50,000hrs

*Table 1 Ricardo (Industrial sponsor) specification for new machine (Atkins, 2016)*

<b>Material property</b>	<b>Units</b>	<b>Value</b>
Yield strength	N/mm <sup>2</sup>	455
Tensile Strength	N/mm <sup>2</sup>	575
Young's modulus (rolled direction)	N/mm <sup>2</sup>	185000
Young's modulus (transverse direction)	N/mm <sup>2</sup>	200000
Hardness	HV5 (VPN)	215

*Table 2 Cogent M250-35A properties (Cogent, 2008)*

Whilst best efforts have been made to use specific, known quantities in the development of a manufacturing model, some data are not reported and have been assumed. In these cases, it has been noted which data are specific or referenced and which data are assumed.

<sup>1</sup> *These projects were conducted independently of one another despite their shared origins.*

## 2 Literature review

### 2.1 The automotive industry

Manufacturing in the automotive industry has always been at the forefront of evolution. This could be taken to have begun in 1908 with the introduction of Ford's mass assembly plants and continued with the 1920s and General Motors idea of flexible assembly, the 1980s and the introduction of lean manufacturing from Honda and Toyota, and, more recently, Volkswagen introducing the 'Lego principle' into manufacturing operations (Schmitt, 2013). Modularisation such as this is a recent phenomenon which has the potential to be a real industry disrupter. The premise is to strategically plan product development and process resources such that economic gains can be achieved through efficiency, but not at the expense of product differentiation (Wu, 2019). It is a school of thought recognisable in the standardisation of parts and procedures in lean manufacturing techniques. To successfully implement modularisation requires a keen understanding of platform strategy. Platform strategy is generally concerned with the creation and management of sets of components, or modules, which can be applied to a common final assembly, the platform (Muffatto, 1999). Traditionally, there have been two areas of study with regard to platform strategy; economists who try to understand what modular platforms change from a demand perspective (market approach), and engineers who focus on technological issues and are mainly interested in innovation. With consideration of the introduction of electric vehicle platforms and the likelihood of technological advancements, planning effectively is an onerous task (Brown, 2008). Platform planning and modularisation are intrinsically linked to carmakers' ability to effectively use their production capabilities. This requires a full understanding of the operations and machining processes undertaken and a clear view as to the constraints and adaptability that these machines might offer. Fyhr (2018) demonstrates the link between micro and macro-economic thinking in the production and development of the electric vehicle industry.

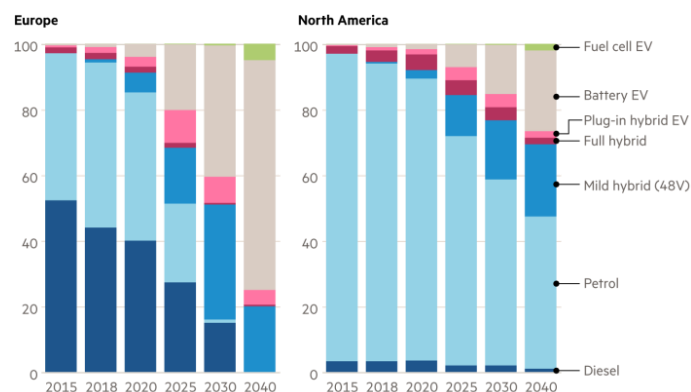


Figure 1 Future vehicle ownership by power unit projections for Europe and North America where Europe is expected to be quicker to convert to EV based vehicles (McGee, 2018)

Investment in advanced vehicle technology is substantial; Giffi et al (2018) describes the current state of play as 'high stakes poker.' It is generally agreed that electrified vehicles will in time become commonplace. However, the question of when is open to debate. Volkswagen is projected to have invested \$86 billion by 2022 in the development of electric vehicles (Cremer & Schwartz, 2017), yet customers in some markets, particularly in the United States, are reluctant to pay a premium for alternately powered vehicles (McGee, 2018). A similar feeling may be shared generally across the market, given that customers are expected to pay a premium as an 'early adopter.' This may in turn create a scenario of prolonged use of more conventional vehicles. Figure 1 shows historic and projected data on the proportion of vehicles powered by different means for both Europe and North America, where the reluctance to switch is significantly more marked in the US market.

In a global sense, the typical vehicle is likely to see significant changes, not only technologically, but also in respects of the way transport is consumed. Ride hailing (taxi) services such as Uber are ever more prevalent, and as such, automobile manufactures may feel a need to produce bespoke vehicle iterations for these purposes. Given that the automobile industry is moving towards modular vehicle development and manufacture, this could present itself as being a module type to fit that particular market. Another interesting development is that vehicle ownership itself may become far less prevalent, in favor of other ownership models, such as shared mobility fleets (Giffi, et al., 2018, p. 4). Customers are understandably hesitant to invest in electric vehicle technology in its current state, with concerns such as range and lack of charging infrastructure still prevalent. Safety, brand trust and cost are all major factors in the customer decision process. Price premiums for battery powered vehicles should reduce as production quantities increase. In fact, battery costs have already begun to shrink, reducing from \$599 per kWh in 2013 to \$273 per kWh, based on 2016 data (Randall & Watanabe, 2017). As concluded by Giffi et al (2018), companies will have to make difficult choices in terms of which technology investments to make. Another factor worth noting, perhaps not currently high on consumer priorities, but likely to be increasingly so, is the environmental impact of the product life cycle (Hernandez, et al., 2015).

A vast array of decisions is being undertaken, and will continue to be undertaken, as the automotive sector transitions into production of electric powertrain vehicles. It is the case that structural re-organisation is required to align key competences of; skills, resource, supply, development, and manufacturing (Vazquez, et al., 2018). At this same time, improvements to robotics, automation and artificial intelligence create a more complex dynamic with which to design future operational strategy. Ashwood Electric Motors (2017) is an example of a company which has invested in automated winding, welding and rotor assembly facilities. Car makers currently have to balance keeping flexibility in manufacturing capabilities with transition into bespoke electric vehicle design and processing. For

example, an electric machine supplier may invest in new technology such as a friction stir welding platform as part of manufacturing copper hairpins, but this could rapidly be rendered obsolete if advancements are made, and another material (such as aluminium) becomes standard, and a better joining technique presents itself. A process might be flexible enough to adapt (perhaps with some cost through tool change) but throughput rate, required skills, product validation and supply will all be affected. Car makers are choosing between bespoke platforms for electric vehicles and more flexible platforms. If a technological advancement occurs, or a core material becomes unavailable, what would be the best strategy to react? Answering this question correctly will have a large part in determining the companies who will best manage this disruptive transition.

Established carmakers are already able to produce a variety of vehicles on a single production line. However, McGee (2018) suggests that the main challenge to produce electric vehicles in high volumes is to develop the operations strategy. There are currently two divisive manufacturing methodologies being invested in by carmakers today; flexible platforms and bespoke platforms. Ricardo (2017, p. 3) acknowledge that as the industry transitions to electric powertrains, the product development cycle must also be adapted to meet these new demands. There are two types of electric vehicle manufacturing platform which are used by carmakers, the 'adapted electric platform' AEP and the 'new electric platform' NEP (Muniz & Belzowski, 2016); both of these have advantages and disadvantages. An AEP has to potential to reduce costs by sharing more common parts between electric and gas powertrain vehicles. However, this may also compromise the dynamics of the vehicle and also create limitations on the interior space and comfort available. An NEP may have higher costs as result of being a bespoke, dedicated platform. However, it allows the manufacturer to design a new electric vehicle without restriction. Different manufacturing platforms are currently being employed by the various carmakers and this segmented thinking is also considered by Ricardo (2017) who suggest two separate approaches to electric vehicle development; one approach is to treat all electric vehicle activity as one single, bespoke function. The alternate approach is to assimilate the electrified powertrain as a separate function within already existing functions, as if to 'tac on' the technology. Jana (2018, p. 2) points to examples of how poor platform strategy can cause major issues, describing how platform investment essentially ties manufacturing capability to the level of innovation afforded by the platform which has been developed. All products produced on these platforms will be limited by the technology which has been invested in. It is therefore essential to plan manufacturing with great care to ensure that all product lines benefit.

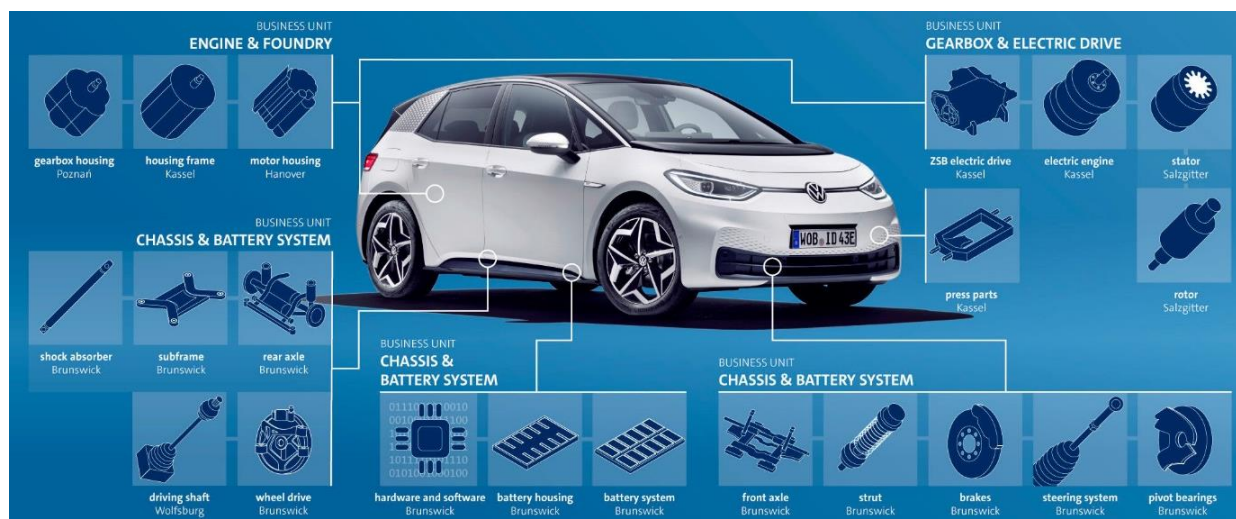


Figure 2 Schematic diagram indicating the locations where some of the parts of the VW ID.3 are produced, illustrating the Complex supply chain (Volkswagen, 2019)

Volkswagen (2019) have invested in a new manufacturing facility to produce and assemble the stator, rotor, and winding components for electric vehicles. This sits within a much wider supply chain (Figure 2). The factory, based in Salzgitter, provides a case for the operational requirements of modern stator production. The factory spans 2.8 million m<sup>2</sup> and it is proposed that it will produce 500,000 stator and rotor units per year with the eventual goal to build 2,000 units daily with 24-hour operation. The factory sits as part of a plan to launch 70 pure electric vehicle models in the next 10 years. In order to produce 70 different designs of new cars, some amount of variation in the stator design processes would be likely, and so having a manufacturing system which can adapt with greater flexibility to design variations is vitally important. Volkswagen (2019) do not comment on the cutting technology used in their stator production (which is the focus of the work of this thesis). However, given that they have issued multiple press releases regarding novel aspects of the process, such as the use of new hairpin technologies (ZEISS, 2020) and battery technologies (Volkswagen AG, 2021), it would seem likely that the stator laminations are produced by a more standard form of stamping. GROB (2019) are credited with the design and implementation of Volkswagen's new winding set up. GROB state that this consists of 12 numerically controlled bending machines, and that the ends of the copper wires (used in winding the rotor) are stripped using lasers. The hairpins (stator components, described in section 2.2.6) are press-fitted into the stator cores which are made up of steel laminations, in one working stroke.

### 2.1.1 Economic order quantity (EOQ)

Complex supply chains such as those used by Volkswagen (Figure 2) rely on a constant flow of materials into and out of the system. Here, an economic order quantity study was considered alongside manufacturing models as a way of providing further insight into stator manufacturing operations. The Economic order quantity approach is an inventory management technique which can be used to reduce the inventory costs of manufacturers (Thakker, et al., 2012, p. 648). The two sources of cost relevant to this are defined as holding costs and order costs. Holding costs take into account the costs of storage, extra work (such as handling), and risks such as obsolescence. Order costs are generally considered to comprise the cost of placing orders, including transportation of goods, and any order discounts which would be offered (Slack, 2019, p. 459). The total order quantity costs are calculated in equation ( 2.1 ) where  $C_h$  is holding cost per unit,  $\frac{Q}{2}$  is average inventory held,  $C_o$  is order costs per order and  $D$  is demand. Whilst the economic order quantity approach has limitations, in that it does not take into account any variations in base costs, transportation times and costs nor does it account for limitations of capital availability, it is generally taken that while these assumptions have to be made, the EOQ generally gives a good approximation to reality (Slack, 2019, p. 463).

$$C_t = \frac{C_h \cdot Q}{2} + \frac{C_o \cdot D}{Q} \quad ( 2.1 )$$

### 2.1.2 Design for manufacture principles and application

To properly analyse the performance of stator production processes, it is essential that underlying manufacturing principles are understood. Design for manufacture (DFM) principles are considered in this research as a method of analysing the performance characteristics of stator production processes.

Manufacturing costs can be broken down into three categories; labour, materials, and overheads. Materials are generally the largest cost (O'Driscoll, 2001). Kuo Tsai-C (2001) described engineering design as a process of developing a system, component, or process to meet desired needs. In the past, engineering design was conducted purely based on the consideration of product functionality. Design and manufacturing were typically completed in a sequential manner. The two functions of design and manufacture were therefore separate entities. In the past, designers and manufacturers worked much more independently of each other. This approach is now known as the 'over-the-wall' approach where designers effectively said, 'we design it, you build it.' There was clearly room for improvement and innovation in the design processes being employed for the time. Boothroyd (1994) suggested that Product design for manufacture and assembly can be the key to high productivity in all manufacturing

industries and noted that no improvements in operation can make a plant fully competitive if the product design is defective. The design for manufacture process leans heavily on existing knowledge, such that where suggestions for simplification are considered, it is possible to find solutions from knowledge of the process being employed. This might, for example, be understanding the implications of trying to mill a narrow radius, with the important knowledge being at what point the radius becomes so narrow as to be prohibitive. In stamping, this point where a design feature, such as the limiting radius, is not something which is calculable. Instead, the stamping industry relies on best practice approaches, which in turn mean that the suggestions for simplification are somewhat of a grey area, as it is down to the view of the designer in that moment, rather than logical, mathematical reasoning. Kuo Tsai-C (2001) says that Initially, DFM is concerned with the identification of the appropriate materials and manufacturing processes for components in a product's design, based on the combination of various capabilities and limitations of the product, so that it can be easily produced. The overall design-development cycle is shortened through the early use of manufacturing-analysis tools (Boothroyd, 1994).

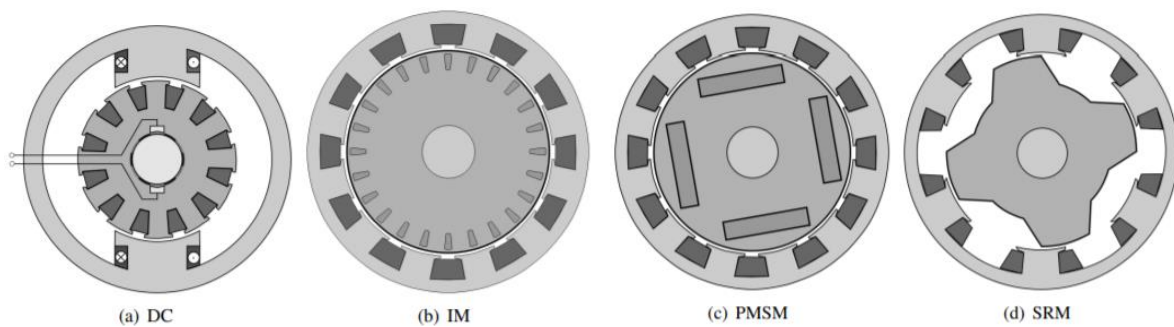
Design for assembly (Moultrie & Maier, 2014) exists alongside design for manufacture. Where in design for manufacture, the onus is on part and feature simplification, design for assembly considers how parts might later be brought together, and the issues that an operator might encounter in trying to do so. Edwards (2002) pointed out that careful consideration needs to be given to the simplicity, rate and cost of assembling components. Edwards suggested that to be effective in product design, the procedures of design for manufacture and design for assembly, are often combined as design for manufacture and assembly (DFMA). Kuo Tsai-C (2001) even went as far as to say that to remain competitive in the future, every manufacturing organisation will have to adopt the DFMA philosophy and apply cost-quantification tools at the early stages of product design. Kuo Tsai-C (2001) listed the design for assembly method developed by Boothroyd and Dewhurst (1987), noting that all parts should be assembled from one direction whenever possible.

Whilst design for manufacture is clearly a powerful tool, it is currently difficult to relate design for manufacture principles to the design of a part which is intended to be stamped. This issue stems from the knowledge gaps which currently exist within the stamping industry. Various sources, such as Tang & Gao (2007) attempt to apply DFM to stamping. However this is done in a very limited way. Tang & Gao use best practice principles for stamping and expand on these using DFM. However, it would be more useful to start with DFM and then apply it to stamping, as has been attempted in the creation of the tool used in this thesis.

## 2.2 Synchronous reluctance motor

### 2.2.1 Introduction to electric machines

Organisations such as the advanced propulsion centre (APC) in the UK provides an understanding of the key trends, themes and technologies on electric machine architectures, integration, thermal management, materials, and manufacturing. one of the challenges posed by the APC is to reduce the dependence on heavy 'rare earth' materials which are used in permanent magnets (Advanced Propulsion Centre UK, 2020). One possible solution would be to invest in electric machine technologies which do not require the use of permanent magnets, therefore eliminating the issue entire.



*Figure 3 Electric machine schematics for: (a) Direct current machine (b) induction machine (c) permanent magnet synchronous machine (d) switched reluctance machine (Finken, et al., 2008)*

Current examples of electric machines used in production vehicles include the brushless asynchronous induction machine (Figure 3.b) as used in the Tesla Model S, the brushed externally excited synchronous machine in the Renault Zoe and the brushless permanent magnet synchronous machines (Figure 3.c) in the Nissan Leaf & Tesla Model 3 (Crosse, 2019). The research conducted in this project initially considered a synchronous reluctance machine as the primary machine topology. Generally, the synchronous reluctance machine (without permanent magnet) is used for industrial purposes as opposed to powering motor vehicles (Heidari, et al., 2021).

Typically, all electric machines will include components such as rotor, stator, and windings. In Figure 3 it can be seen how similar the stator (outer component) is in the examples b, c, and d. However, there can be subtle differences in the design and implementation of components and technology depending on the type of machine being considered. As the main aim of this research is to consider the manufacturing processes involved in production of predominately stator components, it can be seen how transferable the knowledge is between different machine technologies, where the component topology is very similar.



Synchronous reluctance motors have some potential advantages for automotive in that they do not intrinsically require the use of permanent magnets, which are an important, and costly, part of some other machine designs. Permanent magnets are expensive and raise the cost of a motor (Gragger, et al., 2016). Permanent magnets require the use of 'rare earth metals' (such as neodymium, dysprosium, or samarium, depending on the type). These 'rare earth metals' are not actually so rare on the planet, but they are generally only available in limited quantities as a result of often being in geopolitically sensitive locations, whilst the addition of further supply of these metals may require environmentally harmful mining in order to meet the needs of a fully electrified automotive economy (Pitron, 2021).

Like all electric machines, synchronous machines turn electrical energy into kinetic energy using the phenomenon of electromagnetism. Synchronous machines are a subset of electrical machines which use electromagnetism to create precise, rotational output energy. There are two types of synchronous machine; non-excited and current excited. Non-excited machines rely on ferromagnetic materials in their rotors to produce magnetic flux in combination with the stator. There are three main types: hysteresis motors, synchronous reluctance motors, and permanent magnet motors. Hysteresis motors use a rotor shaft contained within a non-magnetic material which is coated with a layer of ferromagnetic material. Reluctance motors employ magnetic attraction and the phenomenon of reluctance to generate motion, and permanent magnet machines use permanent magnets in their rotors which generate a constant magnetic flux. A current excited synchronous machine uses a DC supply to power windings in a rotor, similar to the stator. These windings produce a constant magnetic field (Cavallo, 2021).

Synchronous machines were built so that the output rotational frequency equals exactly the input AC frequency, meaning that there is no 'slip'. Slip refers to an issue which is typically seen in induction machines where there is some difference between the oscillating AC frequency provided by the stator saliency (input) and the rotational frequency of the rotor (output). The synchronous reluctance machine has two major components; rotor and stator. As the names suggest, the rotor rotates, and the stator remains stationary. The stator uses electrical energy to induce a magnetic field in the form of saliency, where wound pairs of poles create the magnetic flux which then travels through the rotor. The flux cannot travel easily through airgaps in the rotor and so it is effectively forced through the rotor veins. Using the stator to control the magnetic flux, the flux is moved around the system, this is referred to as a rotating magnetic field (RMF). The rotating magnetic field can be seen in Figure 4 (A) where the rotor is aligned with the magnetic field, so no torque is produced, whereas in Figure 4 (B) there is a misalignment between the rotor and the magnetic field, leading to a torque. While there is a misalignment, the magnetic field will take a longer path through the rotor, causing what is known as reluctance, to increase. This produces a reluctance torque on the motor, as the rotor wants to get to some lower reluctance, or

back to its aligned position. Reluctance refers to the magnetic resistance in the circuit and is analogous to electrical resistance. To maintain the torque, the magnetic field must be continually rotated, thus ensuring that there is a constant misalignment between the rotor and the magnetic field. (Sahdev, 2018)

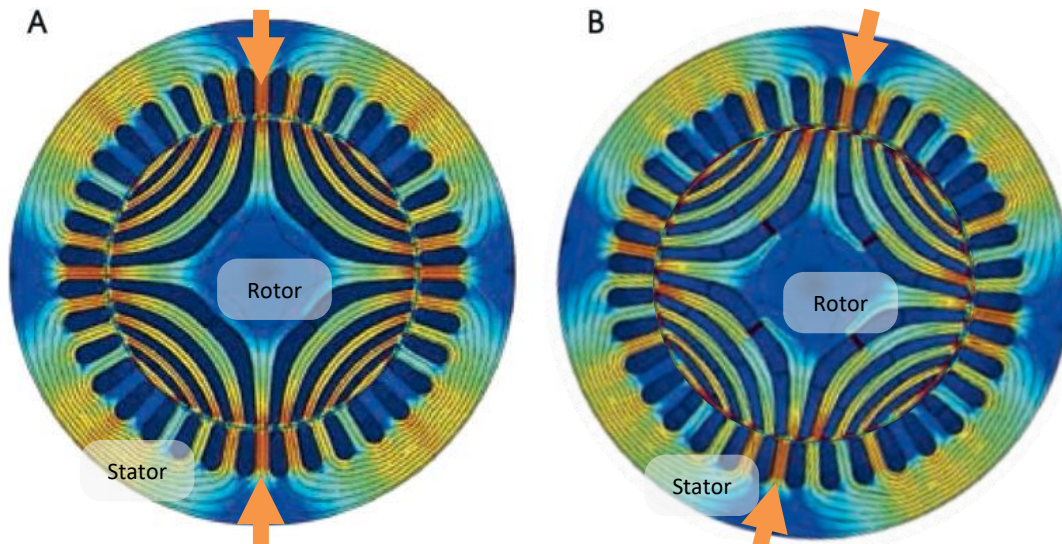


Figure 4 (A) & (B) Cross section of synchronous reluctance machine (ee.co.za, 2016)

### 2.2.2 Electrical steel laminations

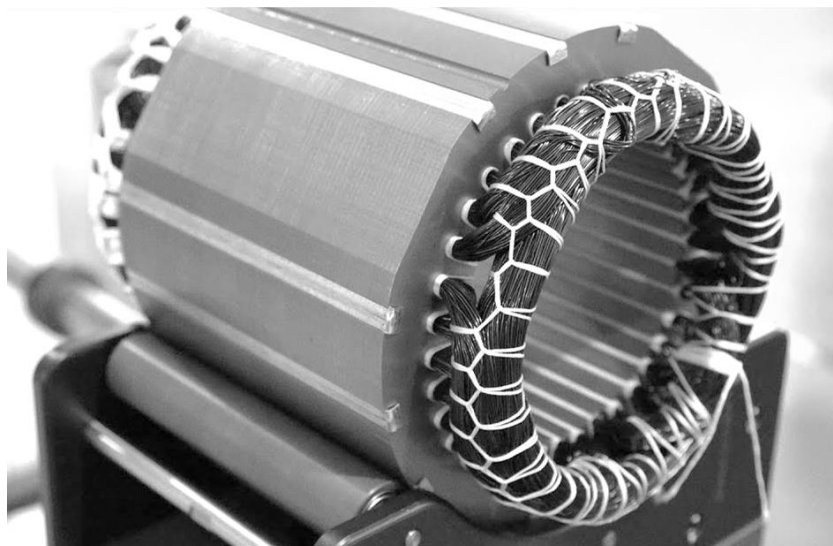
The stator and rotor are generally made from electrical steels, also known as silicon steels. Silicon steel refers to a steel which has a higher proportion of silicon in its metallurgy composition, ranging from 0%-3%. Whilst the addition of silicon restrains eddy currents and reduces losses, it is also more costly to produce (Beckley, 2011). Sheets are also coated with thin layers of material or varnish to prevent eddy currents from travelling axially. Sheet thickness also effects the performance characteristics of an electrical steel. Thinner sheets reduce losses through better eddy current restraint. However, thinner sheets cost more to produce. There is also an issue raised by Beckley (2011, p. 69), which suggests that for any given stack size, using a thinner sheet thickness results in less material actually being in the stack due to the effect of the extra surfaces / contacts as a result of using more sheets, ultimately meaning that for thinner thicknesses there is less material in the final stack. Stators and rotors for synchronous reluctance machines are normally manufactured as a series of thin laminations, such as the stator laminates in Figure 5, which are then packed tightly together to produce the final component, as in the rotor components in Figure 7. Magnetic permeability is an important function of the stator and rotor materials. Magnetic permeability refers to the change in flux density caused by a change in field strength. It is often as a relative quantity, which is multiplied by the permeability of a vacuum ( $1$  in Imperial units,  $4\pi \times 10^{-7}$  in SI) to give the physical quantity (units of Henries per metre in SI units, Gauss per Oersted in Imperial units). Silicon steels generally have a value of approximately  $18000 \text{ H m}^{-1}$  for maximum permeability (CES Edupack, 2018).



*Figure 5 Example of electrical steel stator laminations which have been stamped to create stator shape. Laminates in image are prior to being stacked and joined (Polaris Laser Laminations, 2012)*

### 2.2.3 Copper wire winding

The winding inside an electric machine is used to carry current. Normally, windings are produced using copper wire as in Figure 6. However, an alternative method is available which is discussed in section 2.2.6. The copper wire is arranged and wound around stator teeth such that magnetic flux can be induced by passing a current through the necessary part of the circuit, which ultimately provides the torque which the machine produces. An explanation of some of the fundamental mechanics of this are provided for context, as it is fundamentally these principles which the manufacturing processes are hoping to maximise.



*Figure 6 Example of wire wound stator (SMT Winding Equipment, 2017)*

### 2.2.4 Electric machine mechanics

The power the machine is capable of providing will be determined by the torque which the machine can produce. This is evidenced in equation ( 2.2 ) which shows that power,  $P$ , is a function of torque,  $T$  and angular velocity (or operating speed),  $\omega$ .

$$P = T \cdot \omega \quad ( 2.2 )$$

The torque generated by a synchronous reluctance motor is proportional to the volume of the rotor. This is most easily seen in equation ( 2.3 ) (Chapman, 2012), where  $T$  is torque,  $k$  is a constant,  $D$  is the rotor diameter and  $L$  is the rotor length. The torque produced is also affected by the electromagnetic forces which act on the rotor. In equation ( 2.3 ) the forces are considered to be a part of the constant  $k$ .

$$T = k \cdot D^2 \cdot L \quad ( 2.3 )$$

A wire carrying a current in a magnetic field will produce a force. This relationship is described in equation ( 2.4 ) where  $F$  is the force produced,  $B$  the magnetic field,  $I$  the current and  $L_{wire}$  the length of wire in the field. Increasing the number of wires, or conductors, in the field would create a pressure rather than point load, as seen in equation ( 2.5 ) (Soong, 2008). When this pressure acts upon the rotor it provides a turning force, or a torque,  $T$ . Equation ( 2.6 ) develops on equation ( 2.5 ) by considering the torque produced by current carrying wires in a magnetic field.

$$F = B \cdot I \cdot L_{wire} \quad ( 2.4 )$$

$$\sigma = \frac{F}{AREA} = B \cdot n \cdot I = B \cdot A \quad ( 2.5 )$$

$$T = F \frac{D}{2} = \sigma \times Area \times \frac{D}{2} = \sigma \pi D L \frac{D}{2} = \frac{\pi}{2} D^2 L \sigma = 2V_r \sigma \quad ( 2.6 )$$

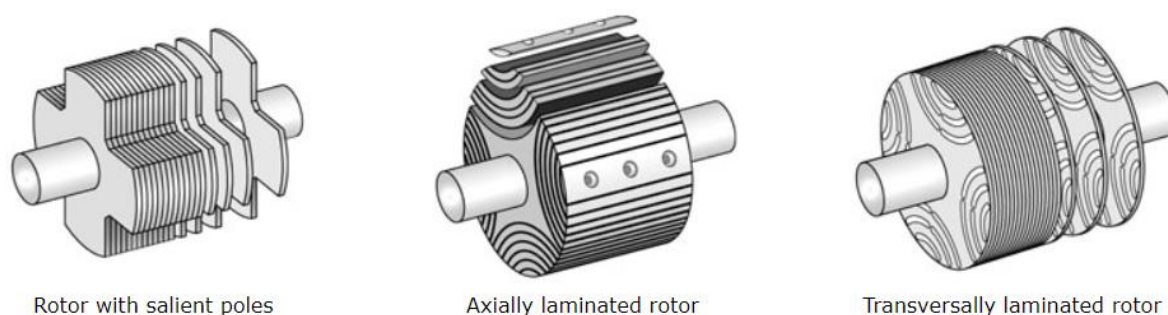
There is a clear similarity between equation ( 2.6 ) and equation ( 2.3 ). Taking  $D^2 L$  from both equations, it is possible to consider the torque of the machine.

$$k = \frac{\pi}{2} \sigma \quad \text{where } \sigma = B \cdot n \cdot I \quad ( 2.7 )$$

The potential working life of a motor is affected by the stresses induced from operating at high speeds and in a high temperature environment, as occurs from producing a high torque machine. However, ABB (2015) suggest that most electrical motors (51%) fail as a result of a bearing failure, whilst the second biggest cause of failures is related to stator windings (16%) from either over heating or over-loading. An analysis of the production and assembly of a synchronous reluctance motor is considered at this point.

### 2.2.5 Synchronous reluctance manufacture and assembly processes

A synchronous reluctance motor is made from two key parts; the stator assembly (which includes an electric winding array), and the rotor (which includes a shaft). The research conducted in this project pertains mostly to the production of the stator component. However, it is useful to identify the further assembly processes which occur within the total manufacturing system. Advanced manufacturing techniques are being developed for synchronous reluctance components, such as the use of photochemical machining (Desai, et al., 2018) and the production of stators by additive manufacturing (Pham, et al., 2021). The current manufacturing and assembly processes are described by both Youssef (2017) and Mechlar (2010). Sheet material is typically delivered as a roll, referred to as mother coil (MC) by Youssef (2017). The sheet is loaded onto a roller where it is then flattened and fed into a stamping machine. Mechlar (2010, p. 24) describes how the cut sheet sections are then annealed, which Youssef does not include in his description of the process. The annealing process has three main benefits to laminations; a reduction in stress and strain, additional grain growth and further decarbonisation. The end result of annealing is a reduction in core losses through better performance. However, this is not always the case as some steels which are produced using older methods react poorly to the annealing process (Hilinski & Johnston, 2014). Both Youssef (2017) and Mechlar (2010) identify that the stator is then assembled by collecting the punched sheets then, stacking, compression and joining, which seals the stack together. Mechlar (2010, p. 24) reports that the joining method at this stage is TIG welding. The stator slots are then electrically insulated by paper-like sleeves and the copper windings are then installed into the stator. Various winding methods and technologies exist, and Mechlar (2010) describes how copper hairpin windings are inserted into the stator slots, a method similar to that employed by Volkswagen (2019).



*Figure 7 Exploded view of alternative rotor structures (Engineering Solutions, 2021)*

The rotor component is produced by stacking punched sheets in the same way as assembling the stator, this is known as a transversally laminated rotor. Other rotor designs exist, such as the axially laminated rotor, as illustrated in Figure 7, which require alternative manufacturing and assembly processes to produce the rotor as it is not produced from standard laminations, as in the transversally laminated rotor.

Further assembly processes are undertaken, including the installation of a shaft into the rotor and the housing unit being assembled around the stator. Research by Niazi (2007) demonstrates how different rotor designs can be used to reduce cost and increase ease of manufacture for synchronous reluctance applications.

It is possible to find some limited examples of the manufacturing process route as a production stream map. However, these examples only include the general outline of processes utilised in the system (Yang, 2016, p. 67) (Tucci, 1994, p. 579). The process map in Figure 8 (Yang, 2016) includes “rotor assembly machining” and “stator assembly machining” which would ideally be avoided, as this could potentially risk creating short circuit opportunities in the assemblies. The process “coating” would also be referred to as impregnation typically. Some research has been conducted considering manual handling of parts and tools during production (Lan, 2010). More specific process or activity maps have not been found, suggesting that the current state of research is more concentrated on the overall manufacturing system and not with any particular process improvements, such as in Figure 8; it is likely that the optimisation of these steps is based on in-house knowledge and experience (and with any case-specific limitations). This hypothesis is supported by the review of stamping processes, which are noted to occur on a basis of ‘old school know how’ rather than specific requirements. Following discussion with Campbell & Brittle (2017), it was confirmed that stamping is somewhat of a *black art*. Challenged on this assertion, Campbell & Brittle suggested that in order to evaluate the manufacturability of a design, it would require an experienced eye, rather than the application of some logical rationale or mathematical model. Further to these discussions, Campbell & Brittle also mentioned another stamping method used to produce stators. This is known as the *slinky* style stator. This new process has very little material scrapped, which is an issue identified in the created tool.

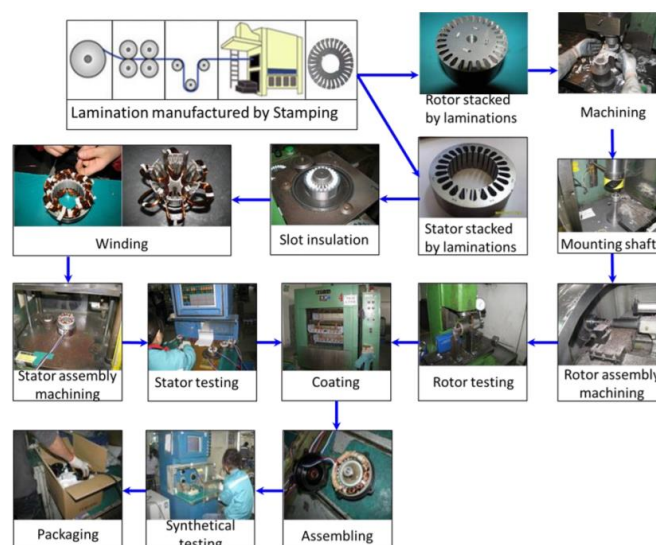


Figure 8 Example of an electric motor process route (Yang, 2016, p. 67)

### 2.2.6 Hairpin winding of stators

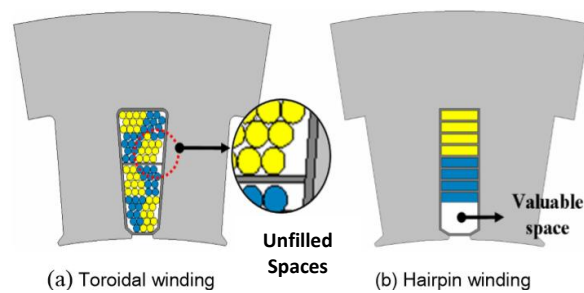


Figure 9 cross section of standard winding (a) and a hairpin winding (b) (Jung, et al., 2012)

The winding component inside an electric machine is used to carry current. Windings are arranged and wound around stator teeth such that magnetic flux can be induced by passing a current through the necessary part of the circuit. Normally, windings are produced using a copper coil, such as in Figure 9 (a). Franke, et al (2011) discusses the need to develop more efficient manufacturing processes by employing greater use of automation in the winding process. One issue with this method is the effective use of space. Jung, et al (2012, p. 2) comment that if a high slot fill factor can be achieved, the power density of the motor can be increased. This high space factor or slot fill factor is the ratio of useful material to dead space in the stator slot. The hairpin is larger in section than a standard wire, this combined with the geometrical benefits of packing square sections rather than circular sections endows the hairpin winding with a greater slot fill factor. Miljavec (2018, p. 27) discusses the benefits of using hairpin winding technology over the standard wire winding method. Miljavec suggests that better thermal conductivity of the slot is achieved as copper losses in the form of excessive heat are better transferred to the stator iron and there is a better copper fill factor. Miljavec raises the concern that tight control is required when performing joining operations between the copper hairpins. Hairpin winding assemblies can be constructed either as a continuous part, a U shape with busbar assembly, or an I shape with busbar assemblies at both ends. Concentrated windings are another possible technology. Libert & Soulard (2006) comment that this process leads to a relatively low slot fill factor and requires the production of a different type of stator, which in turns requires specialised tools. Jung, et al (2012, p. 2) point out that hairpin winding is a complicated process and cannot be applied to a motor which has a large outside diameter. Hairpin windings are joined to terminal blocks to create the electric circuit. It is here that the question of joining processes arises. There are many different methods which could be employed, and with each, a different process would be required. As an alternative to copper, to maximise weight savings, hairpins could be manufactured from aluminium (Cakal & Keysan, 2021), and in this case where hairpins join to form the circuit, there would be an aluminium-to-aluminium joint (in the more conventional design it would be copper-copper). In either case there is a requirement to connect the hairpin circuit to a copper plate at the termination point, and if aluminium is used this requires joining aluminium to copper. Some consideration of potential joining methods is appropriate at this point.

### 2.2.7 Joining methods for use in hairpin winding assembly

There are a number of challenges involved when considering methods for joining of hairpin winding components. Hairpin windings are coated with an insulation material, which protects the windings from external factors such as air or particles in the environment. The insulation also provides a barrier between the individual windings, ensuring that the circuits are not broken. It is therefore important to have a consideration for the insulation material during any further processing, such that the insulation coating can remain intact. The following joining processes are considered based on perceived manufacturing and assembly suitability across the factors of time, cost, and quality.

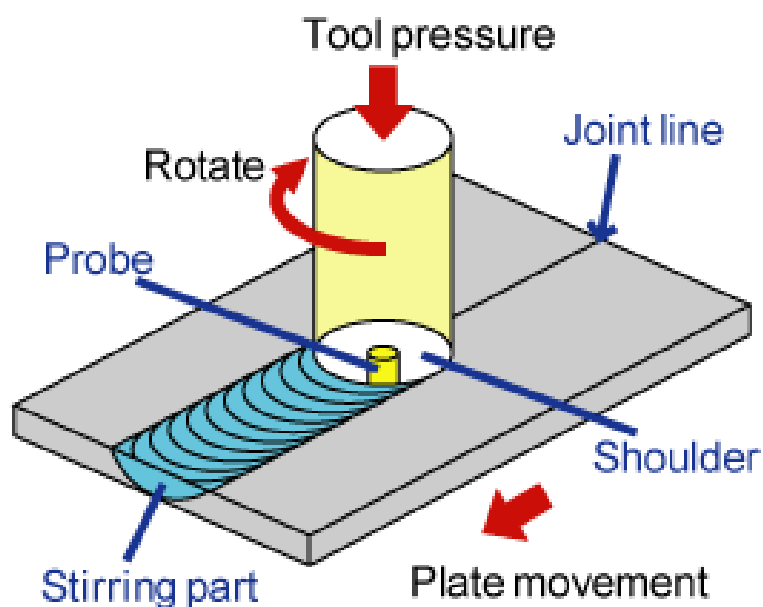
#### *Friction welding*

Weman (2012, p. 126) suggests that friction welding does not involve complete melting of the joint surfaces. The energy input is purely mechanical; friction is used to heat the surfaces of the parts. Friction welding has been used for more than 30 years. Friction can be generated either through relative motion between the workpieces or through the use of an external tool. One traditional method is to rotate one of the workpieces, a method particularly useful should at least one of the workpieces be rotationally symmetrical. It is important that at least one component is ductile when hot to allow deformation during the forge step. Friction welding can create clean, high-quality joints between a wide variety of metals (CES Edupack (2018)). Bhamji, et al. (2012) similarly concluded that linear friction welding is a viable way of joining dissimilar metals and produces welds with very good mechanical (tensile and bend) properties. Grimm (2015) has also performed trials with aluminium to copper overlap joints. Due to the nature of friction welding, no protective flux or gases are needed. However, the ability to achieve either fast speeds (for small components, rotational speeds of up to 80,000 rpm and a few kilogram loads used) or high loads requires the use of potentially expensive machinery. Nevertheless, for a mass manufacture process, high investment costs can potentially be absorbed by high quantity output. Information on the process in CES Edupack (2018) includes that the capital cost of equipment is high, but tooling costs are low, suggesting that the process is fast and can be fully automated. Weld times can range from 1 – 250 seconds, and so further work would be required to understand the process times for this application. The process is already widely used in the automobile industry, with various components joined this way. Bhamji, et al. (2012) notes that welds with very good electrical properties could be produced with little or no detectable increase in resistivity at the weld line. Bhamji, et al. (2012) also recognised that further properties of the welds, such as corrosion resistance, may also need to be characterised before being able to recommend the process in full confidence.



### *Friction stir welding*

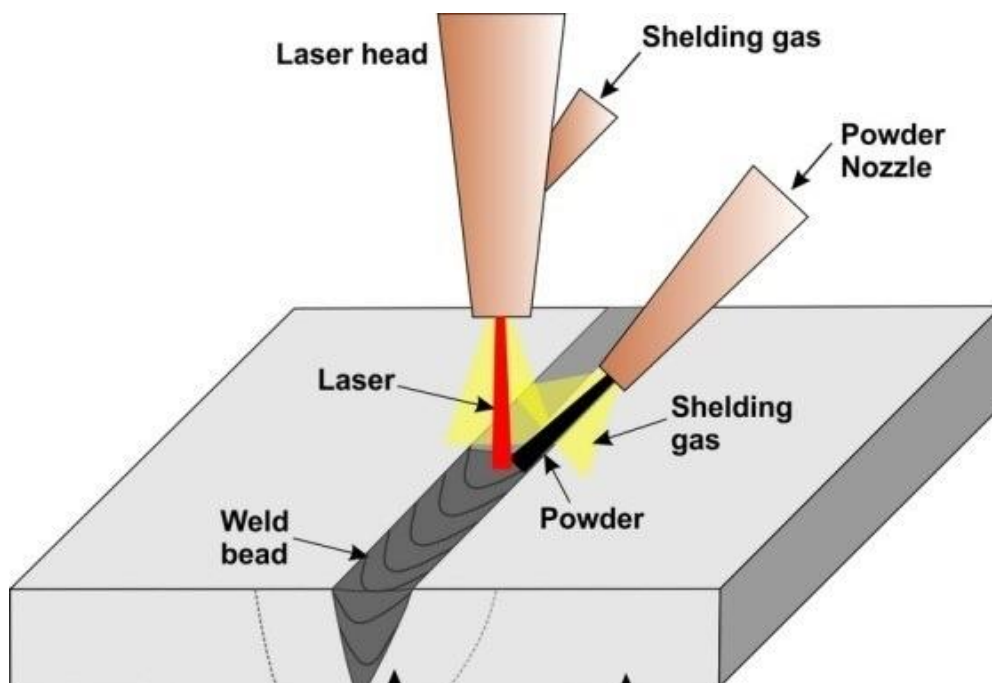
Friction stir welding was patented by the welding institute in 1991 and the process uses a specially designed non-consumable rotating tool, as illustrated in Figure 10 (Sharma, et al., 2017). The tool consists of two parts; a shoulder and a pin (or probe). The process is generally used to join long lengths of material, particularly in the aerospace, shipbuilding, and rail industries (CES Edupack, 2018). Friction stir welding is capable of creating copper to copper joins and also aluminium to aluminium joins (Weman, 2012). One benefit of friction stir welding is that there is an almost invisible weld line. However, in the application of hairpin joining this does not add any value as the hairpin component is hidden during operation. No joint preparation is necessary which simplifies the manufacturing implementation by reducing the requirement of additional processing. Friction stir welded joints have excellent fatigue strength and very little thermal stress or distortion, and no melting takes place so volume changes are avoided (CES Edupack, 2018). The formation of a hole from the tool where it stops can be a disadvantage. However unlikely to have much effect in the application of hairpin joining. The major manufacturing hurdle is the requirement to use heavy, and powerful fixtures to keep the parts of the workpiece together and pressed to the backing plate Weman (2012, p. 128). The process clearly has value in the mass manufacture of high-tech products, as demonstrated by the use of friction stir welding to join components in the 2012 apple iMac (Dilger, 2012). Friction stir spot welding is a very efficient process, with energy consumption at around 3kJ per weld to 6kJ per weld. However, the weld cycle times are typically between 2 seconds to 5 seconds (Ni & Ye, 2016).



*Figure 10 Friction stir weld schematic (CES Edupack, 2018)*

### *Laser beam welding*

In laser welding a focused beam of monochromatic light is focused on the joint, creating a plasma, and localised melting as illustrated in Figure 11. Shielding gas is often used to protect the weld. Due to the focussing capabilities of the laser, the heat input is highly concentrated in the joint region. Laser beam welding can join many different types of joint geometries and the process can also join parts of dissimilar thickness. In order to be able to weld parts together, the joints must be close fitting. CES Edupack (2018) notes that the equipment required for laser beam welding is expensive. However, it is not as costly as electron beam welding. This is partly due to the difference in atmospheric requirements, as laser welding can be conducted in air, whereas electron beam welding requires a vacuum. CES Edupack (2018) suggests that owing to the high cost of equipment, high volume or critical weld conditions would be required to justify investment, such as inaccessible joints and/or flimsy assemblies, which are recommended as being especially suitable for laser beam welding (CES Edupack (2018)). The process can be well automated providing scope for reducing cost. Materials to be laser welded should not have reflective, polished surfaces since these do not absorb energy from the beam. Copper is very reflective and as such, more power (and thus cost) would be required to create the join. It has been recommended that a blue laser might be suitable for welding copper parts (Hummel, et al., 2020). Laser welding is a mature technology in the automobile industry (Hong & Shin, 2017).



*Figure 11 (right) Laser beam welding (CES Edupack, 2018)*

### *Ultrasonic welding*

Ultrasonic welding bonds the workpieces together by vibrating them in contact at high frequency under pressure. The process can produce spot, seam, or annular welds and that most metals can be ultrasonically welded, particularly if the material is more ductile (CES Edupack, 2018). The process is ideally suited for joining thin sheets or wires (Weman, 2012). Surfaces should be thoroughly degreased before welding, as grease acts as a lubricant and degrades the quality of the weld (Weman, 2012). This would potentially create an extra process step in the workflow, that said, the process is relatively cheap, fast, and clean. The process is relatively energy efficient at around 0.6kJ to 1.5kJ per weld compared to friction stir welding at 3kJ –6kJ (Ni & Ye, 2016). This is because the major heat generation is in the weld line, not at the top surface of the specimen. Ultrasonic welding also alleges to have shorter weld cycle times, at typically less than 0.5 seconds (Ni & Ye, 2016).

### *Snap fit*

A snap fit joint works by using material elasticity in two separate parts to effectively squeeze one part into another, such as pressing two Lego pieces together. As such, it is essential that the part can tolerate relatively large elastic deflection. Snap fit joints can be produced using an automated assembly line, making it a suitable joining method for mass manufacture. However, the assembly tooling would require an initial capital investment (CES Edupack, 2018). The quality of electrical conductivity would no doubt be limited by the quality of fit, with small airgaps being a concern, similarly the potential mechanical strength of the joint is directly related to the quality of fit produced.

### 2.3 Stamping process mechanics

One of the key manufacturing processes used in stator production is stamping. Stamping refers to the process of shaping a sheet of material by punches and dies. Stamping can be used to create holes and slots in a work piece by forcing a punch through the material. Stamping can also be used to form shapes by pressing a die into a piece of material. When cutting material using a punch, there are two types of cut; an open cut and a closed cut (Klocke, 2005, p. 9). In an open cut, the punch acts more like a blade, slicing into material. The two edges of the cut do not meet. In a closed cut, the punch creates a continuous cut in the shape of the punch, in Figure 14 this is a circle. The material which is punched out of the sheet could either be scrap, or the part which is intended to be made. These two different scenarios are defined as blanking and piercing. In blanking the work piece is punched from the sheet, leaving the remaining sheet as scrap or waste. In piercing, the opposite is true, the work piece is the sheet, and the waste is the material which is removed. In creating a new part of complex shape, these operations are frequently mixed to create the final product, as demonstrated in Figure 12 (Dayton Progress Corp, 2003). The cuts produced by the tool in Figure 12 are shown in Figure 13, demonstrating the different types of features and geometries produced during the stamping operation.

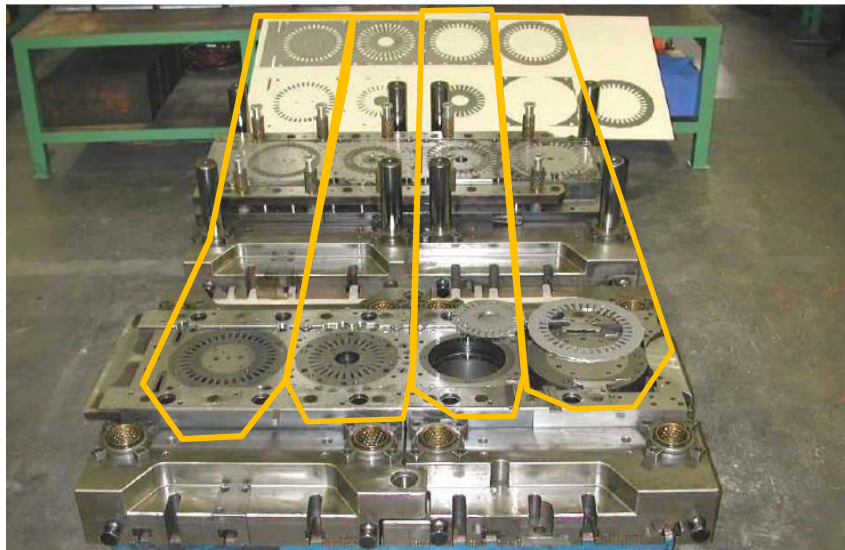


Figure 12 A four stage stamping tool for stator and rotor lamination production (Klocke, 2005, p. 23)

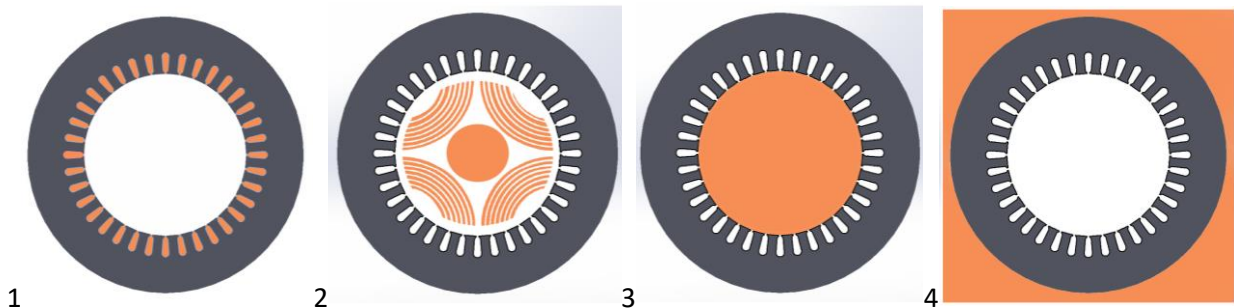


Figure 13 four stage stamping operation – cuts highlighted in orange

The design of parts which are intended to be stamped is typically conducted based on the understanding of the designer, rather than specific design principles or mathematical models. The most commonly suggested advice is to use part thickness as a guide for how small or large a feature can be (ESI, 2021) (Fonger, 2021) , and as such, alter the part thickness as required. This also means that the geometries which can viably be produced are limited by the part thickness when punching. This advice shows how the part design, rather than process, plays a more important part in the design of parts for stamping. This leaves a problem, how best to set up the process to achieve the best possible product? Further research is required to understand how the stamping process would be optimised to a given design. Whilst it is possible to design a part to be easily stampable, setting the correct parameters for the operation still requires some method of quantifying in order to achieve the best product.

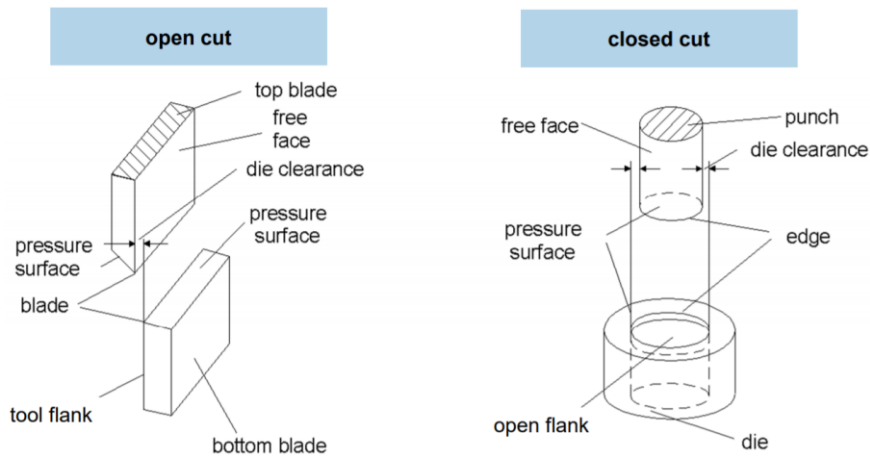


Figure 14 Open and closed cutting (Klocke, 2005, p. 9)

To be able to stamp a part, it is important to know how much force is required to create shear in the sheet material, and as such, how to properly set up the stamping press. It is possible to calculate the force,  $F$ , required to stamp a part using equation ( 2.8 ) (Klocke, 2005, p. 36), where  $L_c$  is the length of cut and  $L_d$  is equivalent to sheet thickness. The sheet material has cutting resistance,  $K_{cr}$ . The cutting resistance of a material is proportional to its ultimate tensile strength. The cutting energy used to stamp a part is a function of the force used,  $F$  and the linear distance the force is applied through,  $x$ . there is also a correcting factor  $c$ , which accounts for variables such as the material properties, the size of the die clearance and the friction. The work done (energy) is calculated by equation ( 2.10 ).

$$F = L_c \cdot L_d \cdot K_{cr} \quad ( 2.8 )$$

$$K_{cr} = 0.8 \cdot \sigma \quad ( 2.9 )$$

$$W = c \cdot x \cdot F \quad ( 2.10 )$$

### 2.3.1 Stamping tool wear

It is important to understand the wear mechanics of stamping, as reducing wear will be a method of prolonging the life of a stamping tool, thus reducing cost, and increasing productivity by reducing downtime. It is also the case that reducing tool wear will enable a better quality of cut to be consistently produced. Wear occurs on a stamped tool at either the face of the tool or the shaft, as in Figure 15. Taylor (1906) first demonstrated how tools used in machining generally wear, and these first principles are still applied today (Johansson, et al., 2017). There are three main stages to tool wear progression. The first stage is often brief and describes the period where the tool is 'broken-in.' In the second stage, the tool will wear at a steady state until it finally reaches some failure point and wear begins to run-away and progress at a higher rate.

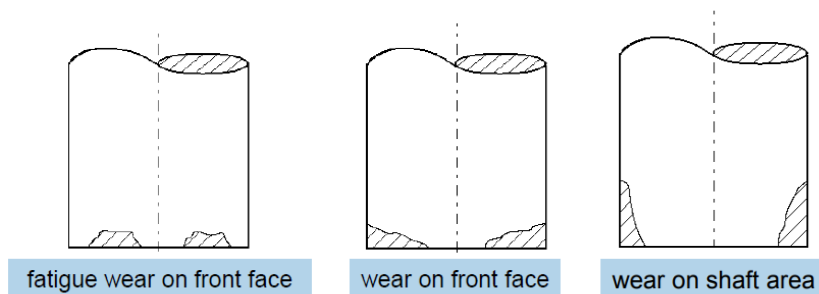


Figure 15 Schematic diagrams of tool wear, which might result from stamping parts of different thickness (Klocke, 2005, p. 21)

There is evidence of wear within the literature that closely resembles this type of wear progression (Kraemer, et al., 2015). Taylor's wear curve follows equation ( 2.11 ), where  $V$  is the cutting velocity,  $T$  tool life, and  $n$  and  $C$  are constants.

$$V T^n = C \quad ( 2.11 )$$

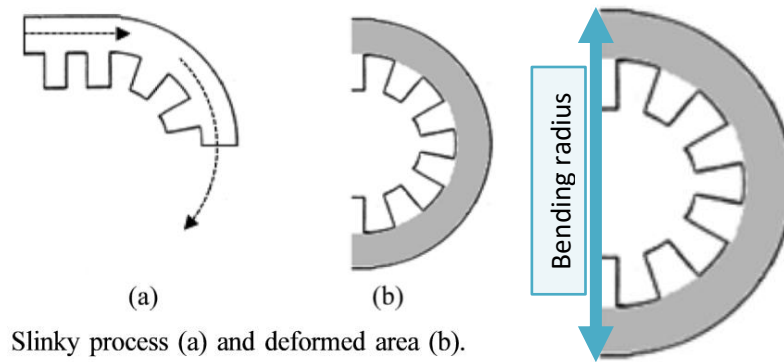
The common mechanisms of cutting tool wear are; Mechanical wear, Thermochemical wear, Chemical wear, and Galvanic wear (Kharagpur, n.d.). In the application of stamping, three main causes of tool wear stand out; friction, impact, and thermal mechanisms. Friction occurs between the tool and the sheet material during the cutting operation. Wear as a result of friction would have a greater effect on the flank of the tool, as opposed to the face. Cutting at higher speeds would create more friction, as would increasing the thickness of the sheet material. Impact occurs at the moment at which the tool first interacts with the sheet material. The face of the tool is the initial load bearing element in this action and as such, is the most susceptible part of the tool for wear as a result of impact. The force of impact is affected by the sheet thickness, sheet strength and the length of cut required. Thermal degradation is another issue for the stamping tool, with increased temperatures raising the wear rate of the tool. The

mechanisms can be linked; for example, friction naturally has a by-product of generating higher temperatures within the tool. Archard developed an equation ( 2.12 ) for predicting tool life, where  $Q$  is tool wear,  $K_w$  a constant,  $F$  normal load,  $L_d$  sheet thickness and  $H$  tool hardness. A substitution is performed where the normal load,  $F$ , is replaced by the force required to cut material as defined by ( 2.8 ).

$$Q = K_w \frac{FL_d}{H} \quad ( 2.12 )$$

$$Q = K_w \frac{L_c L_d^2 K_{cr}}{H} \quad ( 2.13 )$$

### 2.3.2 The slinky Method



*Figure 16 Slinky process schematic (Kim & Hong, 2015)*

As was identified through discussion with Campbell & Brittle (2017) an alternative stator manufacturing process is possible. The slinky method uses strips of material, rather than large sheet, to produce the stator. The strips have the tooth design stamped out and are then coiled around a mandrel to create the laminated stator. Figure 16 shows this process, with a straight strip entering the process, and then being bent around to create the correct shape. Figure 16 also shows that the back iron is the key area that deforms during this process. The process of coiling a slinky stator is very similar to mechanics of bending a beam. In a bent beam, compressive and tensile forces create stresses in the part. The neutral axis is neither under compression nor tension, and as such, there should not be any bending stress in the part along this axis. The bending phenomenon follows equation ( 2.14 ) where  $\sigma$  is bending stress,  $M$  the moment acting on the part,  $y$  is the vertical distance from the neutral axis, and  $I$  is the second moment area of neutral axis (Young & Budynas, 2002). Thicker cross sections are more difficult to bend, resulting in the need to impart greater force in the workpiece. The bending moment generated in the coiling process for the slinky stator is directly linked to the bending radius (Figure 16). For a given back iron width, there would be a minimum bending radius, and similarly for a given bending radius, a maximum back iron width. Interestingly, Youssef (2017) concludes that cutting is still the major consideration, despite the change of stator design. Youssef writes that the rolling and the punching process should be optimized for a slinky stator to reduce losses. Currently there are some techniques for the rolling process which are already patented (Lee, 2005) (Mitsuhiro, 1989) (Mitsuhiro, et al., 1990) (Yasuo & Toshihiko, 2004).

$$\sigma = \frac{My}{I} \quad ( 2.14 )$$



## 2.4 Laser cutting

There have been many recent studies which have considered and compared the various machining methods in stator production (Bayraktar & Turgut, 2018). The most commonly used methodology in mass production is stamping (or pressing). Stamping requires a high level of initial investment owing to the manufacture of dies, but once set up, is a relatively quick and consistent method. Laser cutting is an alternative manufacturing process to stamping which is typically considered for smaller batch productions or one offs (Association of Electrical and Mechanical Trades, 2018). Whilst other cutting processes exist such as Abrasive water jet and wire cut electric discharge machining, these are typically used for specific applications (Ziegler, et al., 2018). Laser cutting is of particular interest, as this appears to be the most feasible cutting alternative for mass manufacture of stator laminations. The term LASER is an acronym for Light Amplification by Stimulated Emission of Radiation. A laser works by focusing a high intensity light source into a very narrow beam, as illustrated in Figure 17. This is done by combination of mirrors and lenses. The laser beam is amplified by passing through a medium material which can be either a solid, such as a crystal, or an assist gas (Sculpteo, 2016). The high energy of the laser beam melts the workpiece at the contact point. This action of melting away material is what creates the cut in laser cutting. Separate to the assist gas there is an auxiliary gas which blows away molten material from the workpiece. The auxiliary gas can be inert or active. An inert auxiliary gas protects the surface from oxidation, whereas an active gas (usually oxygen) generates an exothermic reaction at the workpiece which increases the temperature at the cutting area, allowing thicker cuts to be produced (Genna, et al., 2020). Laser cutting is capable of dimensional tolerances in the region 0.01mm (Sołtysiak, et al., 2019). Whereas stamping is a mechanical process, laser cutting is a thermally intense process and as such, the effects of laser cutting differ somewhat from stamping. These differences are explored based on the application of cutting electric steel laminates.

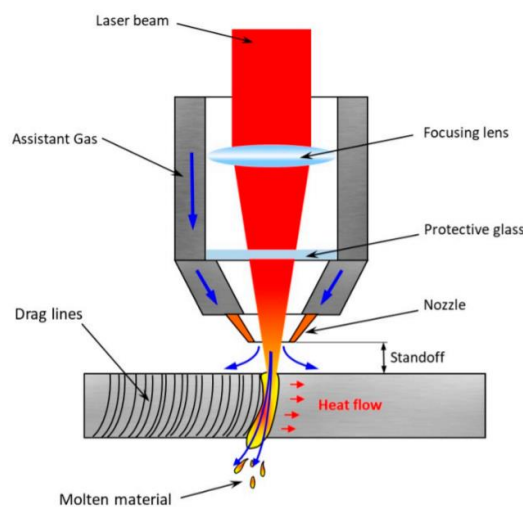


Figure 17 Schematic demonstrating laser cutting of sheet metal (Genna, et al., 2020, p. 5)

## 2.5 Laminate performance

The key performance characteristic of a stator is its ability to provide magnetic flux, and thus provide a torque to the rotor. There have been a number of studies which have considered how various manufacturing processes affect the magnetizability of a stator. Generally, each study considers a variety of magnetization scenario (frequency, strip width, orientation). There is not a single, consistent performance metric which allows simple and direct comparison of results, at least from the purview of a lay individual.

Laminate cutting appears to be the major manufacturing step which contributes to machine performance loss, with both Youssef (2017) and Bali & Muetze (2019) commenting that the cutting process is the main cause of degradation of the magnetic properties in the manufactured parts. It is understood that the electromagnetic performance of an electrical steel is affected by the state that the material is in. Residual stresses in the laminate negatively impact the performance of the stator. Boubaker, et al (2019) note that performance losses due to residual stresses have a greater effect in smaller sized stators, as there is a greater proportion of cutting edge in proportion to the whole laminate surface. The quality of cut produced in stamping is also affected by tool wear (Weiss, et al., 2018). Sharp tools are more effective at producing clean fractures. However, understanding the severity of the effect and the causes of differences are important, as this will be a key parameter in later modelling. There appear to be two main causal factors in the reduction of magnetic performance, induced stress, and edge deformation. Stresses can be thermal and/or mechanical. The laminate grain structure is susceptible to change as a result of both stress types.

Most sheet metal parts are designed based solely on the functional requirements. The stamp-ability is not considered until the design is nearly completed, or even worse, until the die design is started (Tang & Gao, 2007, p. 2680). A part design is made up from a number of features. Tang & Gao (2007) define two different types of feature; primary features and subsidiary features, and describe a primary feature as being representative of the overall shape whereas a subsidiary feature is a feature which would typically exist within the primary feature, such as holes and embossments. Tang & Gao (2007) set out a number of best practice guidelines which are based on sheet thickness, such as that;

- The diameter of a hole,  $d$  should be greater than the part thickness,  $t$  by a factor  $k$ , which is dependent upon the part thickness, namely,  $d > kt$ .
- The width of a slot should be greater than the part thickness by a factor dependent upon the part thickness
- The inside bend radius of a rib should be greater than or equal to twice the sheet thickness.

This approach is very empirical, relying on the experience of the designer to find the most suitable value of  $k$ . A risk averse designer might choose a much safer  $k$  than the next designer. Part thickness clearly plays a key role in the design of a stamped part. Campbell & Brittle (2017), Electrical machines manager & production director of MTD LTD, confirmed the importance of sheet thickness on part design. They suggested that there was no clear mathematical model to define the point a feature becomes too small relative to part thickness, rather that experience in stamping would be the ultimate way to judge the effectiveness of the part design with consideration to feature size relative to part thickness. Klocke (2005) noted that part thickness has an inherent effect on die wear. For thinner parts (<2mm), tool wear is more likely to occur on the front face of the die, including fatigue wear. As the part thickness increases, more wear occurs down the shaft of the die. Laminate thickness for electrical machines is typically chosen based on the performance of the machine, rather than manufacturability.

2.5.1 Laminate performance and cut quality as a result of stamping

The lack of knowledge regarding the implementation of manufacturing processes in stator production is further evidenced by Vandenbossche (2015) who realises the need to add greater understanding into manufacturing decisions. Vandenbossche (2015, p. 6) concludes that careful consideration of the manufacturing methods is required in order to optimise the performance of an electrical steel component. Energy losses in electric machines arise from various sources. There are losses in the electric sheet material owing to the material’s hysteresis properties and local eddy currents. There are losses as a result of laminate cutting through microstructural damage in edge area (Gmyrek & Lefik, 2017), and there are losses as a result of joining and assembly processes as a result of mechanical losses and eddy currents in the joins (Kraemer, et al., 2016).

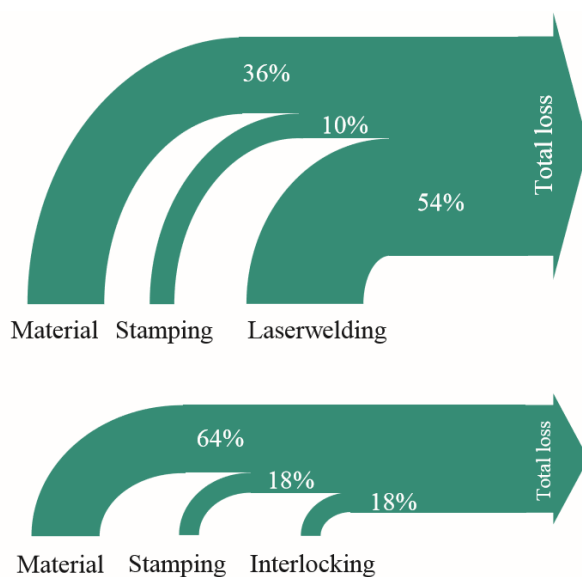


Figure 18 Sankey diagram of performance loss factors in stator production (Kraemer, et al., 2016)

The mechanics of how cutting negatively impacts on the electromagnetic performance have been discussed (Section 2.3). However, understanding the severity of the operation remains unclear. Kraemer’s (2016) research (using M330-35A sheets) indicates that stamping only has a limited impact on the overall performance of a wound stator (Figure 18) as material losses (36% & 64%) are indicated to be more than 3 times as large as any losses incurred through stamping (10% & 18%). Kramer’s conclusion is that the method used to join the laminates and create the stator core is the most detrimental. This argument does not take into account the plethora of design parameters which could also impact the efficiency of the stator and severity of each operation. It may be the case that for thicker sheets (per se), stamping becomes the pre-dominant loss factor. Another study by Bayraktar & Turgut (2018) shows that regardless of cutting technique (using M400-50A sheets), there are overall motor efficiency losses of around 15% (for 5.5kW motor). The change of cutting method had an impact between worst and best case of approximately 2.5%, as shown in Figure 19. When considering the condition of a cutting tool and how it may be monitored effectively during manufacture, it might be more pertinent to maintain a record of other factors, such as burr height, than to measure the performance of the laminate being produced.

Cutting method	WEDM	Punching	Laser	AWJ
Motor efficiency (%)	85.61	85.16	83.47	83.1
Friction and windage losses (W)	8.25	0.89	10.46	15.37
Iron losses (W)	553	562	664	712

Figure 19 Comparison of motor efficiencies & losses for cutting methods (Bayraktar & Turgut, 2018)

As touched on in other parts of this review, it is a recurring issue that stamping is not considered in a highly technical way, and by extension, the effect of stamping processes on the ultimate performance of a stator is not considered in the manufacturing set up. Al-Timimy (2018, p. 1161) writes that the effects of machining processes on the performance of stators are often overlooked. Research conducted by Al-Timimy (2018) shows that manufacturing processes reduce the performance of laminates, demonstrating an increase in the stator core losses ranging between 23.5% and 16.7% (the lower end of this range is consistent with the findings of Bayraktar & Turgut).

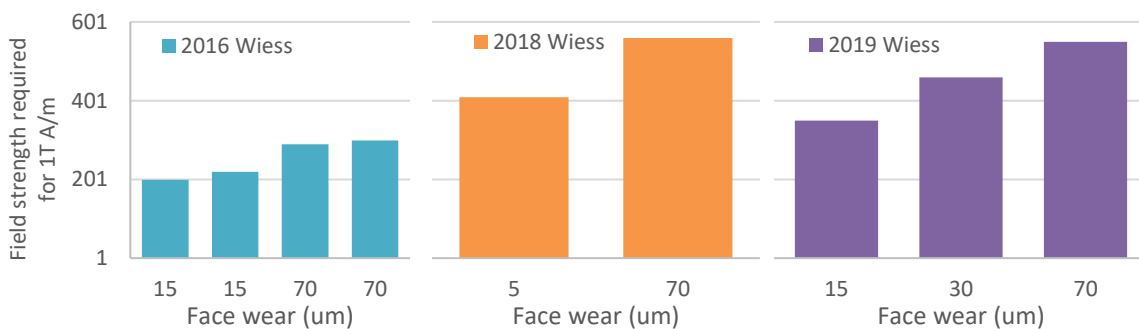


Figure 20 Effect of tool wear on performance. Data collected from (Weiss, et al., 2016),(2018),(2019)

Understanding electro-magnetic performance of laminates has many challenges. There is not a single metric which is used to compare the performance of parts, and each metric has the caveat of circumstance, such as proposed frequencies or strip widths. Weiss has produced a series of results within his work and taking the most consistent and comparable of these results, a trend appears to be present. Weiss' evidence shows that working with a tool in poorer condition reduces the laminates' ability to become magnetized. Across the range of results seen in Figure 20, there is an increase of approximately 50% in field strength required to achieve 1 Tesla A/m magnetisation. How this translates directly to machine performance losses is complex, but a decrease in the performance of the stator materials could be expected to have a negative impact (Moses, et al., 2019). Whilst tool condition has a clear impact on performance, there are also other factors which influence the performance of the produced laminate. As well as the potential for stamping parameters to affect the performance, there is also the base performance of each material and its susceptibility to influence.

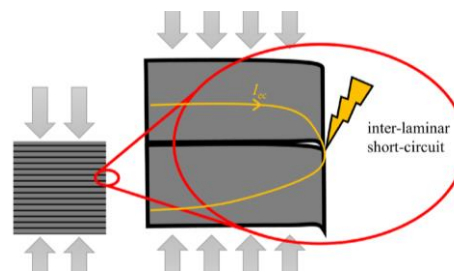


Figure 21 Inter-laminar short-circuit from axial pressure & burr (von Pfingsten & Hameyer., 2016)

Edge deformation mainly considers the effect of burr and roll over. Excessive burrs can create short circuits between the laminates (Figure 21) and as such, lower the performance of the stator. Roll-over creates an air gap at the laminate edge between layers. It has been noted from various sources that tool condition has a major impact on size of the burr created on the work piece (Kraemer, et al., 2015) (Mucha, 2010). There have also been various studies which show that the cutting clearance between tool and die also contributes heavily towards the level of burr created (Weiss, et al., 2016) (Soares, et al., 2012).

Cutting speed in stamping differs somewhat from the typical definition in a manufacturing environment. The standard units of 'speed' are strokes per minute (SPM). This cutting speed does not translate well to actual cutting tool velocity, as 1 SPM can conceivably have the same cutting velocity as 100 SPM as a result of differing rest time between strokes. Lubis & Ristiawan (2017, p. 59) show how the effect of different cutting velocities effect the quality a cut edge. Lubis & Ristiawan demonstrate in their results that a faster cutting velocity increases the shear zone of the cut edge, and by extension, reduces burr and rollover effects. Taylors's equation ( 2.11 ) (Liang, 2002) demonstrates how faster tool velocities cause the tool to wear at increasing rates. The rate of change in this case is also a function of the tool material and a wear constant.

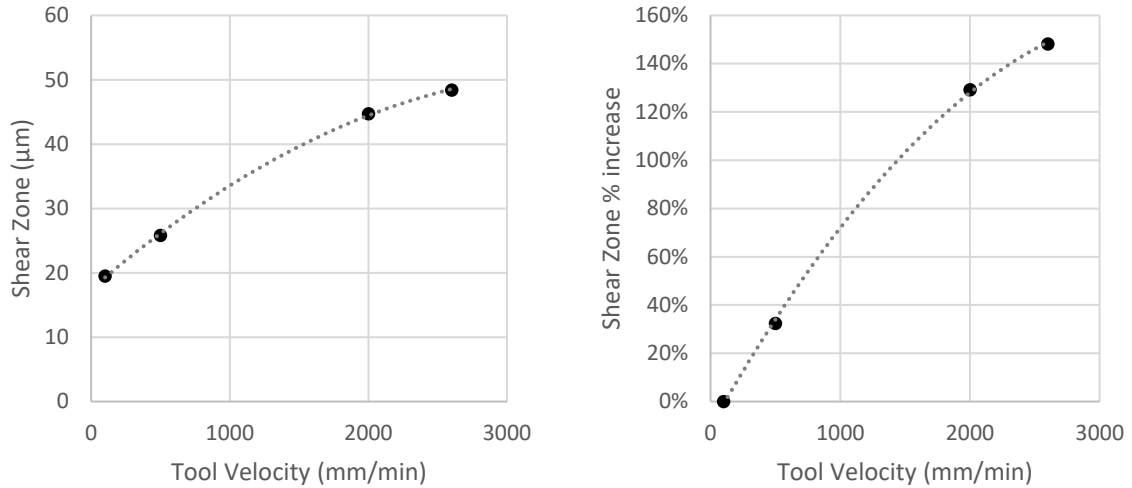


Figure 22 Lubis & Ristiawan (2017, p. 59) data for Shear zone results for a 5% clearance

Bayraktar & Turgut (2018) & Jayarama (2015) both investigate the effect of stamping on the quality of cut edge. M400-50A (Bayraktar & Turgut) and HYPERCO 50 (Jayarama) are the materials tested. Both materials are 0.5mm thick. The results for the stamped samples appear different. The M400-50A sample (Figure 23) shows a uniform shear pattern across the cross section of the sample, whereas the HYPERCO 50 (Figure 24) shows a shear zone and a large fracture zone also. Whilst it might be the case that evidence of fracture might be more visible on the M400-50A with greater magnification as used in Figure 24, the evidence suggests that stamping does not always generate a clean, full shear cut. Figure 23 also demonstrates some deformation and rounding in the upper region of the cut.

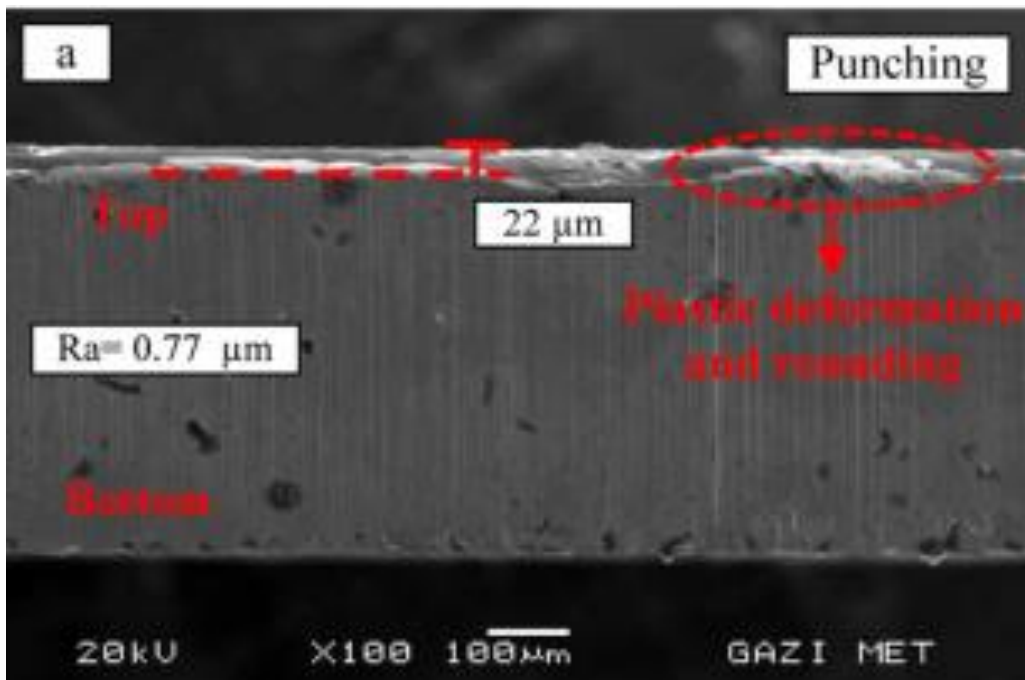
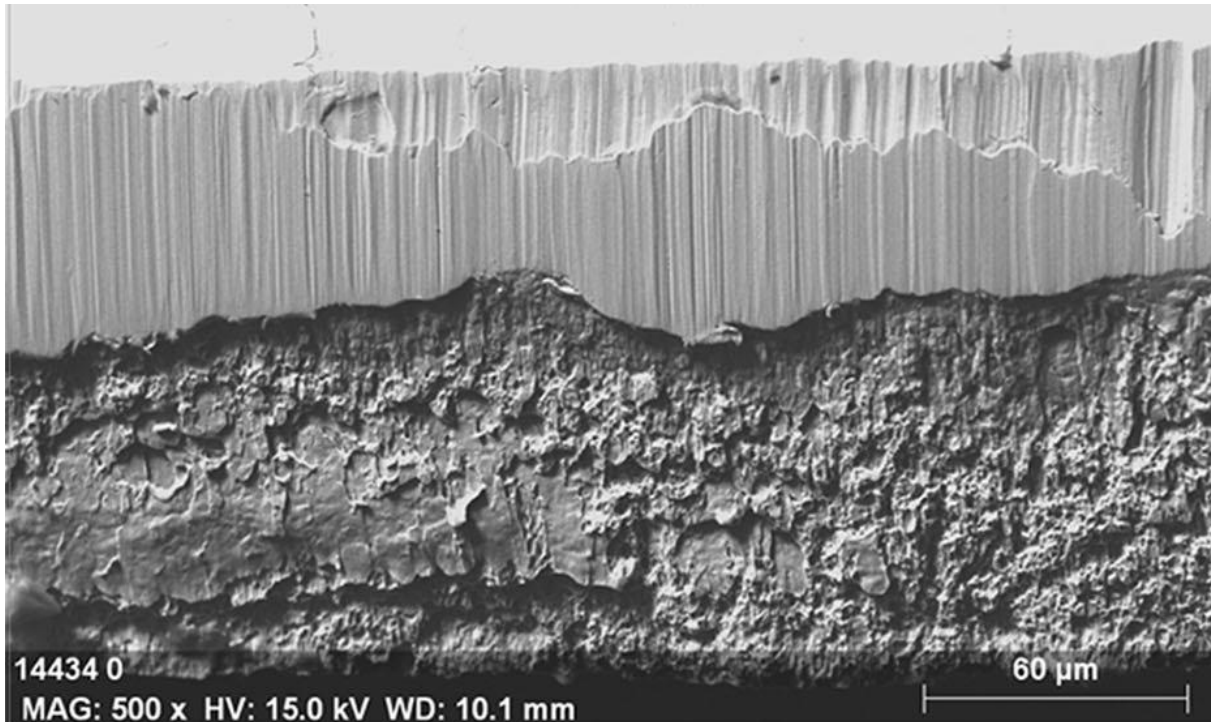


Figure 23 Examples of cut edge by Bayraktar & Turgut (2018, p. 6)



*Figure 24 Scanning Electron Microscope (SEM) of HYPERCO 50 stamped sample*

*by Jayarama (2015, p. 5)*

There appears to be very little relation between sheet thickness and burr height. Whilst there may in fact be some contribution from the sheet thickness to the burr produced, other factors have a greater effect. Sheet thickness is not commonly noted as being a contributing factor to burr height. Sheet thickness is directly related to the force required to stamp sheet material, equation ( 2.8 ), and is also a factor in the Archard equation for stamping tool wear, equation ( 2.12 ). Substitution into ( 2.12 ) creates a square root function for sheet thickness ( 2.13 ). Owing to this, small changes in sheet thickness can have much larger repercussions than initially considered. Increases in sheet thickness would also be likely to effect the flank wear through greater friction. The increased force required to punch the material would likely predominately effect the face wear of the tool. Archard's equation shows that tool hardness effects the wear rate of a tool. The strength of the material being punched directly effects the force required to punch the material. Another important material property is the ductility of the material. More ductile materials are considered to be more susceptible to greater burr heights. The force required to punch through a material is proportional to the length of cut intended. Whilst not considered within this research, the complexity of cut, such as sharp narrow angles, also affects the way the tool wears and the process requirements to create the geometry.

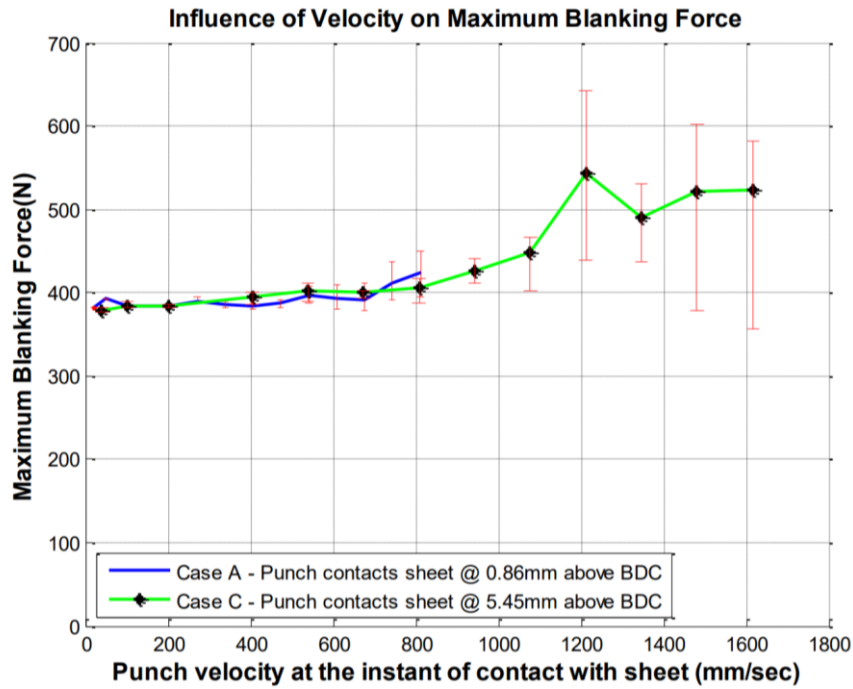


Figure 25 Influence of cutting velocity (Subramonian, 2013, p. 51)

It is interesting to note that the force created by increasing the tool velocity does not appear to follow a direct 1:1 relationship. The result of vastly increasing tool velocity as in Figure 25 is only an approximately 50% increase in force at contact with the worksheet. Hirsch (2011) provides an insight into the generation of tool wear as a result of cutting speed. Hirsch has investigated the force and vibration response of a part during stamping and notes that the excess oscillation of the punch leads to an increase of wear as a result of the extra distance travelled by the punch under friction during this oscillation phase.

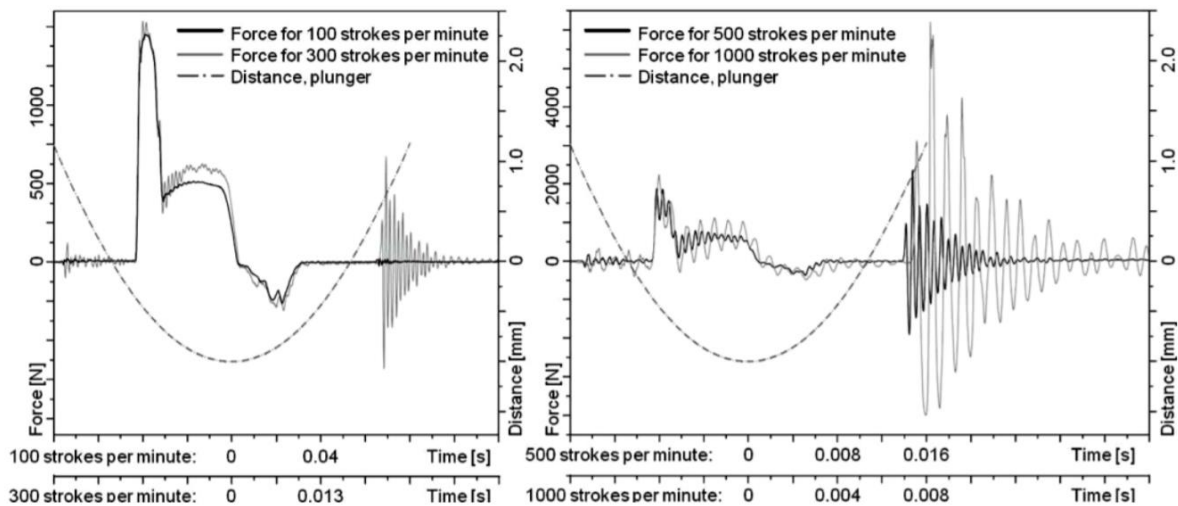


Figure 26 Forces in the blanking process (Hirsch, 2011)



Weiss, et al (2016) performed a series of experiments, measuring the quality of laminate stamping over a series of parameters. The findings show that tool wear, or cutting-edge wear, negatively impacts on the electromagnetic performance of the electrical steels. One aspect of the research was an indicative study between worn and sharp stamping tool performance. The sharp punch and die were considered to have a radius of  $15\ \mu\text{m}$ , with the worn punch and die having face wear of  $70\ \mu\text{m}$  and flank wear  $100\ \mu\text{m}$ . Cutting velocities considered were 60 and 200 strokes per minute. The results of this study indicate that a worn tool leads to an increase in sheet deformation. Low speed and sharp tools minimize the area effected by work hardening. However, the impact of cutting speed variation (over the range tested) is not as significant as the tool wear state. Weiss also notes that tool wear state has a more detrimental effect on losses in the RD (rolled direction) compared to the transverse direction. In further research by Weiss, et al (2018), the effect of material properties is also considered. Weiss concludes that materials with higher UTS have a greater sensitivity to punching parameters. Weiss (2018) also notes from his work in this field, that the energy used during the punching operation is greater for a worn tool, as opposed to a sharp tool. While Weiss does not comment on the rate at which a tool might wear, or after how many operations the tool conditions presented in his research would present, these factors are considered in research by Kraemer (2015). A general understanding of the factors affecting tool wear in stamping are described by Hedrick (2016), who notes that stamping with increased force causes the die to erode and break down at a much quicker rate. Use of excessive force also applies greater side and top loads to the tooling section, increasing the probability of cracking. A poorly maintained press decreases tool life. Hedrick (2016) also reiterates the need to keep the tool in good maintenance to prolong its life.

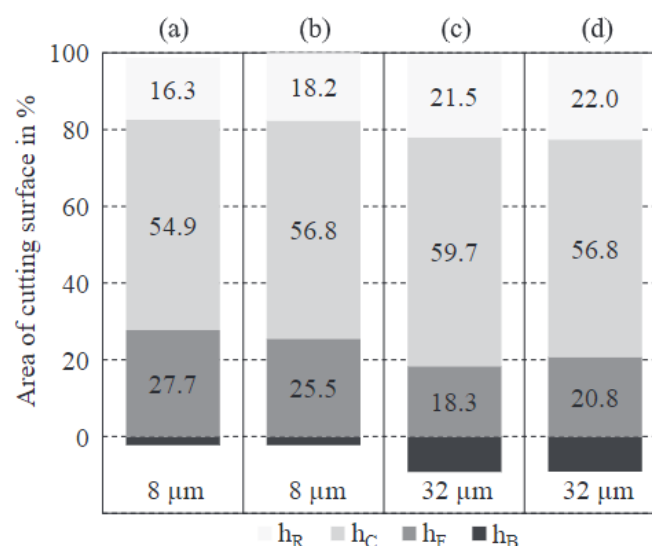


Figure 27 Weiss et al (2016, p. 253) Cutting surface parameters for electrical steel sheet, CCL 30mm;

(a) sharp, 60 SPM,  $0^\circ$ ; (b) sharp, 60 SPM,  $90^\circ$ ; (c) worn, 60 SPM,  $90^\circ$ ; (d) worn, 200 SPM,  $90^\circ$

A series of experiments were performed on behalf of Kraemer (2015) by Kienle + Spiess GmbH. A stamping press with maximum stamping force of 110 tons was used and a stroke speed 300 SPM. Both the punch and die used were manufactured from *hardened tool steel* AISI D6 with a hardness of approximately 63 HRC. The material being stamped was M330-35. Kraemer (2015) identifies from Figure 30 that flank wear is the most important factor in considering tool life, as it shows the largest amount of wear compared to tip and face wear. It is also clear that there is a link between face wear and burr height, as both graphs show very similar growth structures. It can be observed from Kraemer's results, that tool wear as a result of stamping occurrences negatively impacts the quality of laminate produced, through increased burr height. The availability of tungsten carbide as an alternative die material can offset this issue by offering longer tool life at the expense of greater tool cost. General Carbide (2019) suggest that a tungsten carbide tool can achieve four times the life of a standard tool steel, which is not unrealistic given Mucha's (2010) results (Figure 28)

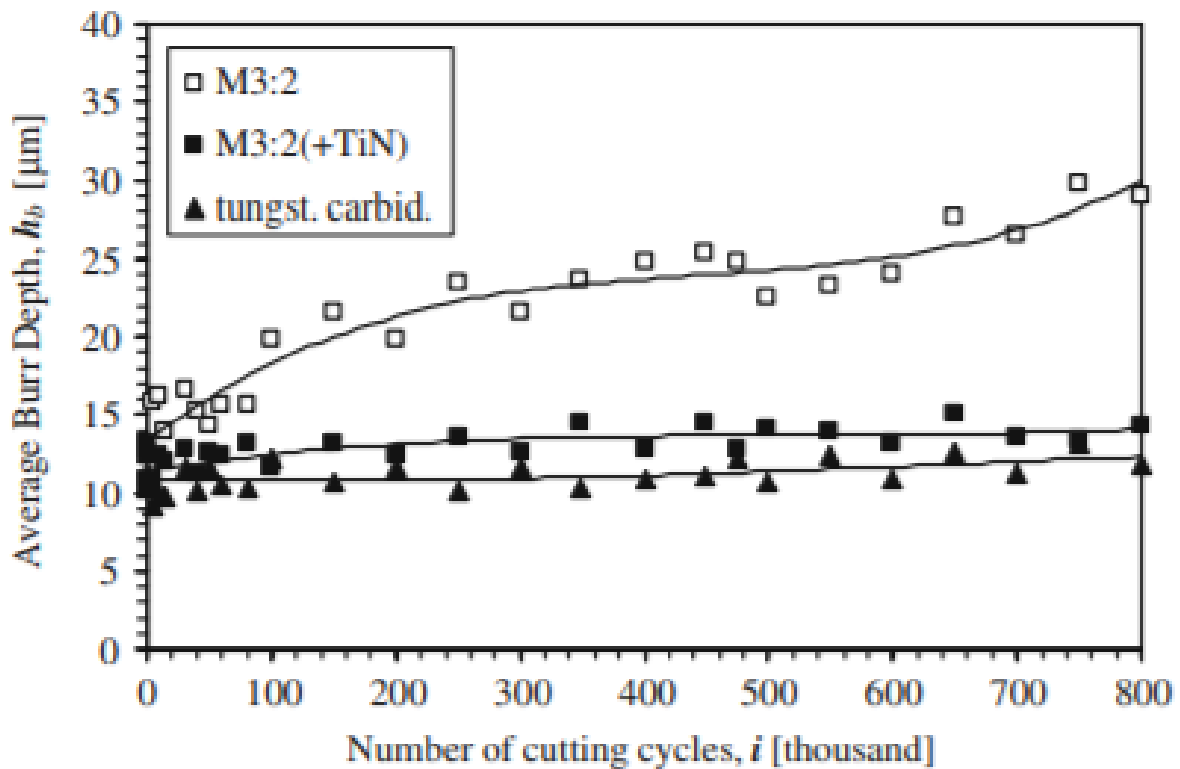


Figure 28 Average burr height across tool life with different tool materials (Mucha, 2010)

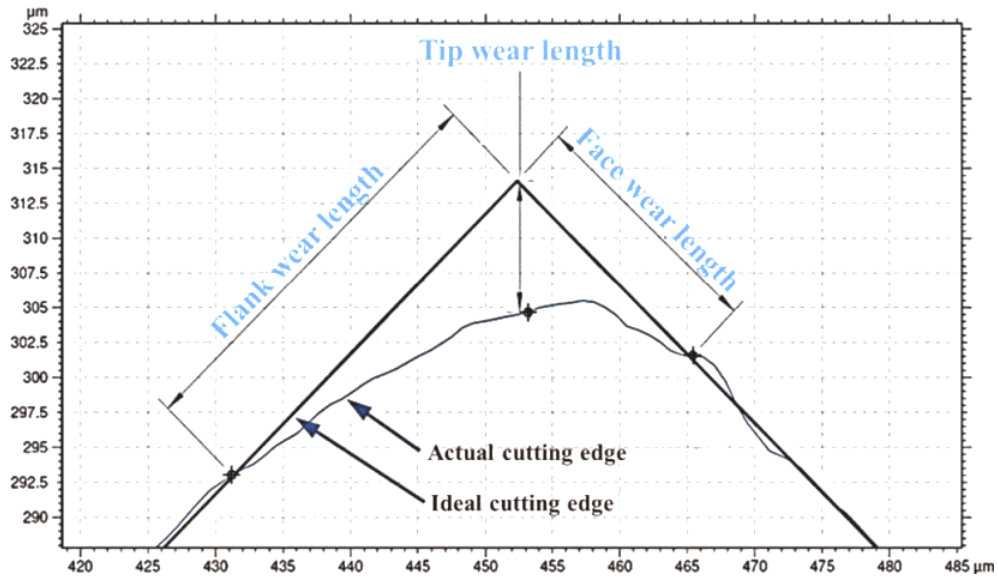


Figure 29 Tool wear nomenclature (Kraemer, et al., 2015)

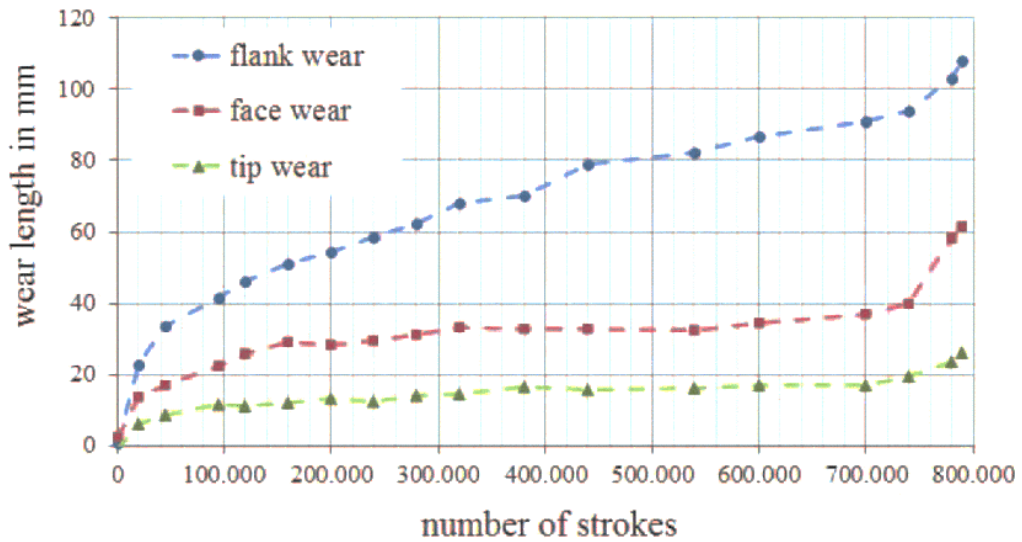


Figure 30 Tool wear over number of strokes (Kraemer, et al., 2015)

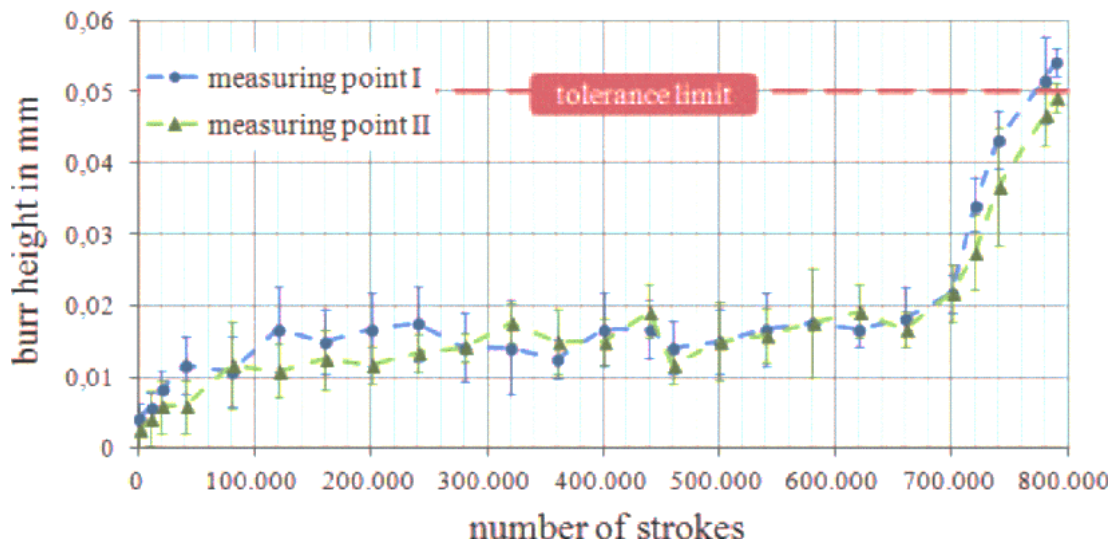


Figure 31 Average burr height over number of strokes. Both 300 SPM (Kraemer, et al., 2015)

### 2.5.2 Laminate performance and cut quality using laser cutting

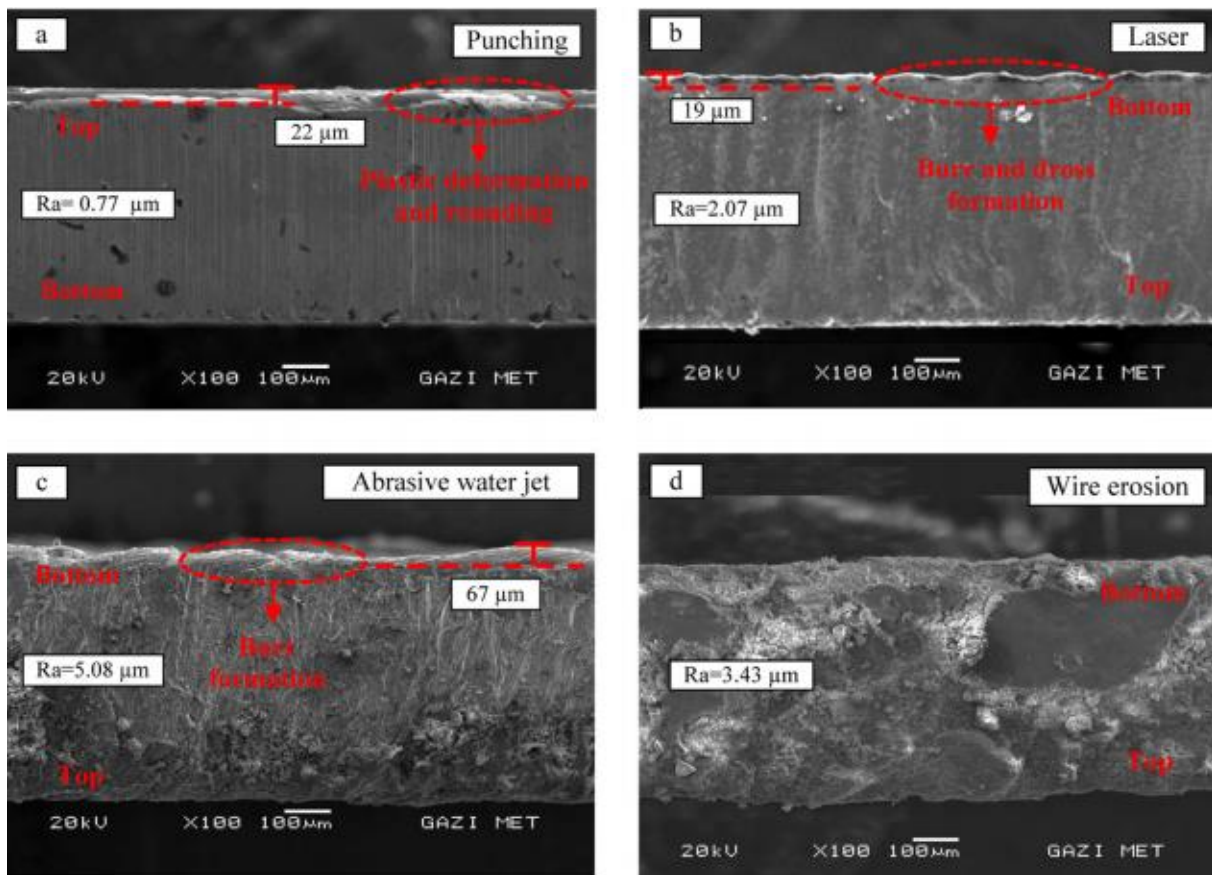


Figure 32 Examples of cut edge by various methods by Bayraktar & Turgut (2018, p. 6)

Kaliudis (2018) recognises the need for new manufacturing technologies in the automotive sector, writing that companies are starting to reconsider some of the slower, traditional, manufacturing methods currently used for electric motors. Stamping is a traditional manufacturing method which is still used because it is considered a cost effective and rapid production method. However, little knowledge exists about alternative production methods at scale. Laser cutting has predominately been studied from a technology and quality perspective.

Gaworska-Koniarek (2011) has studied the effect of using different cutting gases on the electromagnetic performance of electrical steels. Gaworska-Koniarek concluded that the use of compressed air had a more detrimental impact on the magnetic properties of the sheet than cutting with a nitrogen atmosphere. Gaworska-Koniarek proposes that the reduction in electro-magnetic performance may be as a result of iron oxides forming on the cut edge, although it appears unlikely that these would penetrate very deeply into the material. Gaworska-Koniarek also compared laser cut samples with punched samples, with results showing that for 1.5T induction punched samples had total energy losses of 5% whereas the laser cut with air was 20% and laser cut with nitrogen 17% total energy losses. Salvador (2016) has similarly compared the performance of laser cut and guillotined (mechanically very similar to

stamping) samples, again concluding that laser cutting introduces greater losses than stamping-like processes. Bayraktar & Turgut (2018) compare four different cutting methods, as seen in Figure 32. Visually the stamped samples appear slightly better than the laser cut samples. Punched and laser cut samples show much cleaner cuts than those produced by abrasive water jet cutting and wire erosion. The electromagnetic performance was measured, with a punched stator providing 85.16% motor efficiency and laser cutting 83.47%.

Krings (2014) compared the performance of punched and laser cut Nickel Iron samples after the samples had been annealed. The results from that research show similar levels of performance between the stamped and laser cut laminates. Krings writes that the laser cut samples reach a slightly higher saturation flux density at the cost of a slightly larger magnetic coercivity and iron losses. Interestingly, Krings concludes that there is real potential to reduce iron losses by adjusting the manufacturing processes used, suggesting that some form of optimisation can be incorporated into the manufacturing an assembly processes to increase the quality of parts produced. With laser cutting being less established, it may be that there is more potential for optimisation improvement than for stamping. Bali & Muetze (2019) investigated the degradation effects of punching and laser cutting and showed that further research is required to understand effects that laser cutting has on the degradation of cut laminates. Bali & Muetze (2019, p. 9) also note that more research is needed to obtain a better understanding of the mechanisms which occur in the case of laser cutting.

The research consistently demonstrates that laser cutting laminates introduces greater losses in the electric machine than punching laminates. In the best instances, the difference in performance is small, but not negligible. The current research does not consider the economic and wider operations effects of using laser cutting as an alternative manufacturing process. One of the concerns of using laser cutting to produce stators is that the laser cutting process will reduce the quality of electro-magnetic performance of the laminates. Miljavec (2018, p. 23) states that punching (or stamping) is the process which should be used, citing concerns that laser cutting will increase magnetic losses. Miljavec (2018, p. 32) does approve of the use of laser cutting in the production of prototypes . However.

## 2.6 Gap analysis

The research discussed in this review shows that there is a consensus that the market for electric vehicles is set to increase over the next few decades. This transition to electric vehicles creates a need to be able to produce and assemble new parts and components at much greater volume than is currently being done so. New technologies are already emerging and being incorporated into new EVs, such as the hairpin winding technology. Hairpin winding technology is only recently being introduced into EVs, and it appears that the technology remains based on the use of copper. Aluminium has the potential to be an alternative material to copper for hairpin applications, and whilst some research exists in this field, it does not consider the implementation of aluminium hairpin technology from an industrial engineering, mass manufacture perspective.

The slinky style stator method is already used to produce stators. The benefits, namely a reduction in waste material from the cutting process, is well understood. However, the design constraints which define what sizes of stators are producible, and how design changes affect the overall performance of a stator are much less known.

Stators have been produced from stamped electrical steels for many years. However, the knowledge in stamping is mixed. There are multiple different areas of research under consideration as regards stamping electrical steels. Current research has been directed towards identifying the effect of cutting clearances on the electromagnetic performance of laminates. Other research has studied the effect of different parameters on the life of a stamping tool. The decisions and parameters chosen by industry and manufacturers are mostly based on experience rather than specific rules or knowledge. There is also no consideration of how to best create a set of manufacturing parameters which manage the quality of part produced or the rate or costs of production.

Laser cutting is an established alternative to stamping in stator production, but only for small batches or one-offs. Research exists which compares laser cutting to stamping in terms of cut quality and laminate performance. However, no research exists which investigates the potential of laser cutting as a mass manufacturing alternative. Similarly, no research exists which studies the potential of cutting multiple laminates in one operation using laser cutting.

Given these various areas of uncertainty in the manufacturing processes, and how they may most effectively be implemented in production for automotive, this thesis will examine some of the technical aspects of each of them, and with this understanding seek to develop an operational model of production, to make general assessments of the economic viability of different manufacturing strategies.

## 3 Manufacturing implications of a shift from wire winding to hairpin winding

---

### 3.1 Methodology

#### 3.1.1 Knowledge gap

Hairpin winding technology is only recently being introduced into EVs, and it appears that the technology remains based on the use of copper. Aluminium has the potential to be an alternative material to copper for hairpin applications, and whilst some research exists in this field, it does not consider the implementation of aluminium hairpin technology from an industrial engineering, mass manufacture perspective.

The work in this chapter is dedicated to understanding the relative benefits and opportunities which occur from the use of hairpin windings instead of wire winding technology. In this chapter the manufacturing processes have been mapped out visually for both winding technologies. This chapter also contains a study of alternative materials for hairpin windings from a cost, mass, and conductivity perspective. Further research in this chapter identifies joining methods for use in hairpin winding assembly.

#### 3.1.2 Approach

The work in this chapter has been conducted using a modelling approach. Process maps for both winding technologies have been developed using Microsoft Visio software. Using data from various sources, a model has been created comparing the performance of winding materials. An analysis of this model is conducted to provide insight. A further model is created similarly comparing the feasibility and potential performance characteristics of joining technologies for hairpin windings. Details are provided in section 3.6 regarding attempts to perform an experiment using ultrasonic welding between copper and aluminium.

## 3.2 Introduction

Windings are an integral part of an electric machine. Normally, copper wire is wound around tooth sections in a stator to create the electrical circuit which will in turn be responsible for producing magnetic flux during operation. The winding component can add significant mass to the electric machine, and as such, a study is conducted in this report to determine the viability of using alternative materials for windings with a view to reducing the mass of winding material required to produce an electric machine. Another issue with windings is that the manufacturing and assembly processes can be both technical and time consuming. An alternative method of producing windings, known as hairpin windings, is researched in this report, with particular consideration to the necessity to incorporate joining processes into the hairpin assembly process.

### 3.2.1 Process route

The stator winding process can be very time consuming, particularly if done manually. Generally, stators are wound using one of two technologies. Insertion winding or hairpin winding. The two technologies involve using very different processes and machines, as illustrated in Figure 33. Hairpin windings are the more recent technology and offer the potential for a greater slot fill, which in turn can help improve the performance of the electric machine. The hairpin winding is produced from an extruded bar which has an insulation coating on the surface made from resin or varnish. The bar is cut to length and bent into shape. Once shaped the bars are inserted into the slots. Any winding method generally requires the use of a busbar terminal to create the final electrical circuit. The busbars would therefore need to be joined to the hairpin windings, through some welding method typically, before the assembly can continue along the production route. All of these individual processes are unique to the hairpin winding technology. Hairpins are typically made from copper, just as in the wire winding process.

Wire winding can be accomplished using a variety of processes. Hand winding a stator is the slowest method and is only relevant to small order sizes or prototypes. Insertion winding takes advantage of automation to wind stators at much quicker speeds than hand winding.



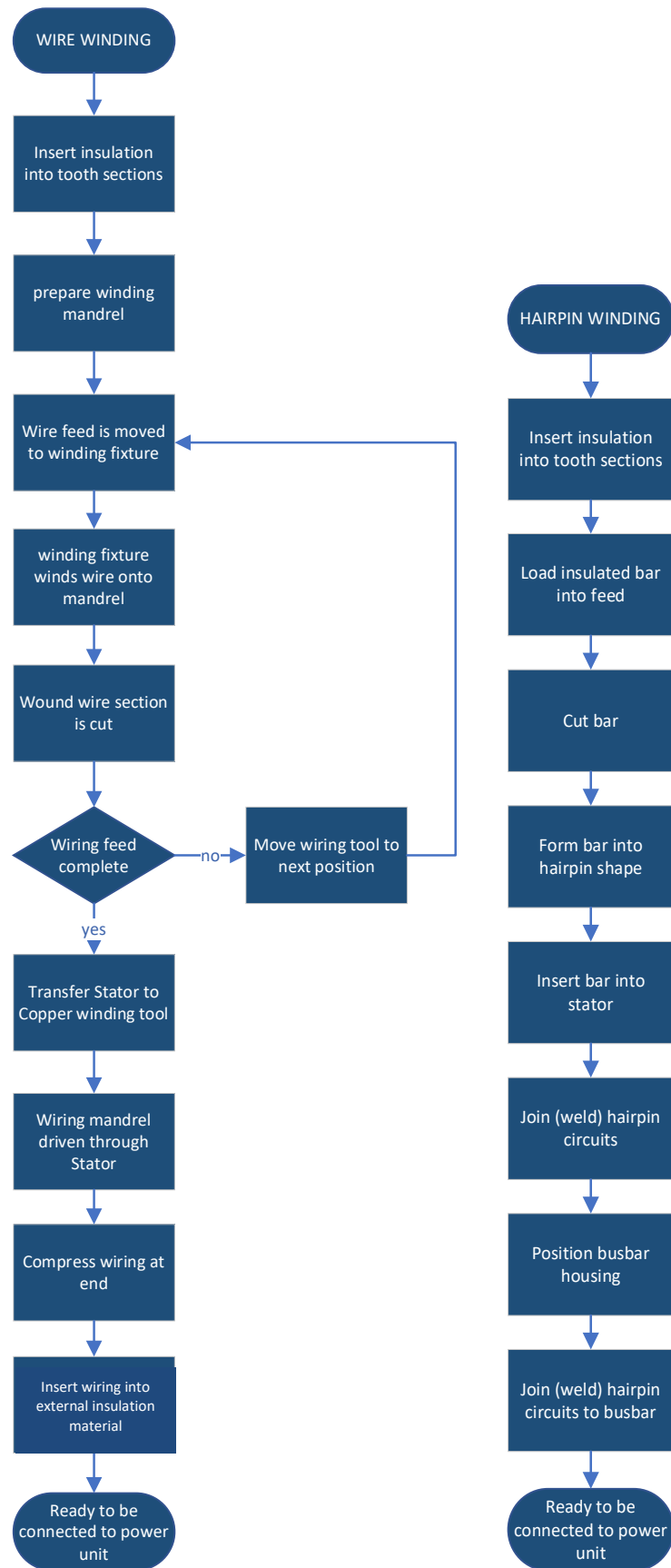


Figure 33 Process route for insertion winding and hairpin winding

### 3.3 Material selection

The main purpose of the winding component is to conduct electricity with low resistance, and thus to generate the field to drive the machine. The winding component also adds weight and costs to the overall electric machine, which creates a trade-off between what makes the best winding component and what makes the best machine. Any winding should also be mechanically and thermally sound. Whilst mechanical stresses on the component are limited as windings are not a structurally integral part, they do exist as a result of the temperatures and magnetic forces involved. Windings are expected to operate at temperatures broadly in the region 100-200°C, and it is hoped that working temperatures of 400 °C can be achieved (as per the original specification in Table 1). There are a number of issues with operating at high temperatures, such as the limitations of the coating material to remain stable, or the hairpin material itself melting. High temperatures can also cause thermal stresses in the component, and the performance of the parts may alter at higher temperatures. The study conducted in this report has been produced under the assumption that the winding components would use the newer hairpin winding technology, which are currently used by VW and BMW (ZEISS, 2020) (Duff, 2018). Winding material alternatives have been gathered based primarily on material conductivity. Materials with reasonable levels of conductivity were considered further, and properties such as density, thermal expansion, and cost were then assessed. Table 3 provides a basic overview of the alternative material properties and Table 4 includes the required volume for each material to be able to supply equal amounts of current, that is to say, that a less conductive material would require the use of more material to provide an equivalent current carrying capability, and vice versa. The initial required volume was based on an arbitrarily sized copper hairpin of 8mmx4mmx200mm. These are feasible dimensions for the type and size of machine under consideration. Materials with less conductivity would require more material, which is to say, a larger hairpin. This method means that scores are based on a relative weighting to each other.

	Electrical conductivity (10.E6 Siemens/m)	Electrical resistivity (10.E-8 Ohm.m)	Thermal Conductivity (W/m.k)	Thermal expansion coef. 10E-6(k-1) from 0 to 100°C	Density (g/cm3)	Melting point or degradation (°C)	Price £/Kg
Silver	62.1	1.6	420	19.1	10.5	961	380
copper	58.5	1.7	401	17	8.9	1083	4
Gold	44.2	2.3	317	14.1	19.4	1064	30000
Aluminium	36.9	2.7	237	23.5	2.7	660	1.3
Molybden	18.7	5.34	138	4.8	10.2	2623	12.5
Zinc	16.6	6	116	31	7.1	419	1.6
Lithium	10.8	9.3	84.7	56	0.54	181	62
Tungsten	8.9	11.2	174	4.5	19.3	3422	54
Brass	15.9	6.3	150	20	8.5	900	3.5
Carbon (ex PAN)	5.9	16.9	129	0.2	1.8	2500	34
Nickel	14.3	7	91	13.3	8.8	1455	6.8
Iron	10.1	9.9	80	12.1	7.9	1528	0.5

Table 3 Alternate hairpin material properties (Tibtech innovations, 2011)

\*based on a 4x8x200 Hairpin

Relative conductance %	Required Volume of hairpin* m3		Mass of hairpin Kg	Cost of Hairpin £	Relative Mass of hairpin	Relative Cost of Hairpin
100.00%	6.40E-06	Silver	0.07	25.54	3.38	675.5
94.20%	6.79E-06	copper	0.06	0.24	3.04	6.4
71.18%	8.99E-06	Gold	0.17	5233.26	8.78	138426.7
59.42%	1.08E-05	Aluminium	0.03	0.04	1.46	1.0
30.11%	2.13E-05	Molybden	0.22	2.71	10.91	71.7
26.73%	2.39E-05	Zinc	0.17	0.27	8.55	7.2
17.39%	3.68E-05	Lithium	0.02	1.23	1.00	32.6
14.33%	4.47E-05	Tungsten	0.86	46.54	43.37	1231.1
25.60%	2.50E-05	Brass	0.21	0.74	10.69	19.7
9.50%	6.74E-05	Carbon (ex PAN)	0.12	4.12	6.10	109.0
23.03%	2.78E-05	Nickel	0.24	1.66	12.31	44.0
16.26%	3.94E-05	Iron	0.31	0.16	15.64	4.1

Table 4 Hairpin considerations

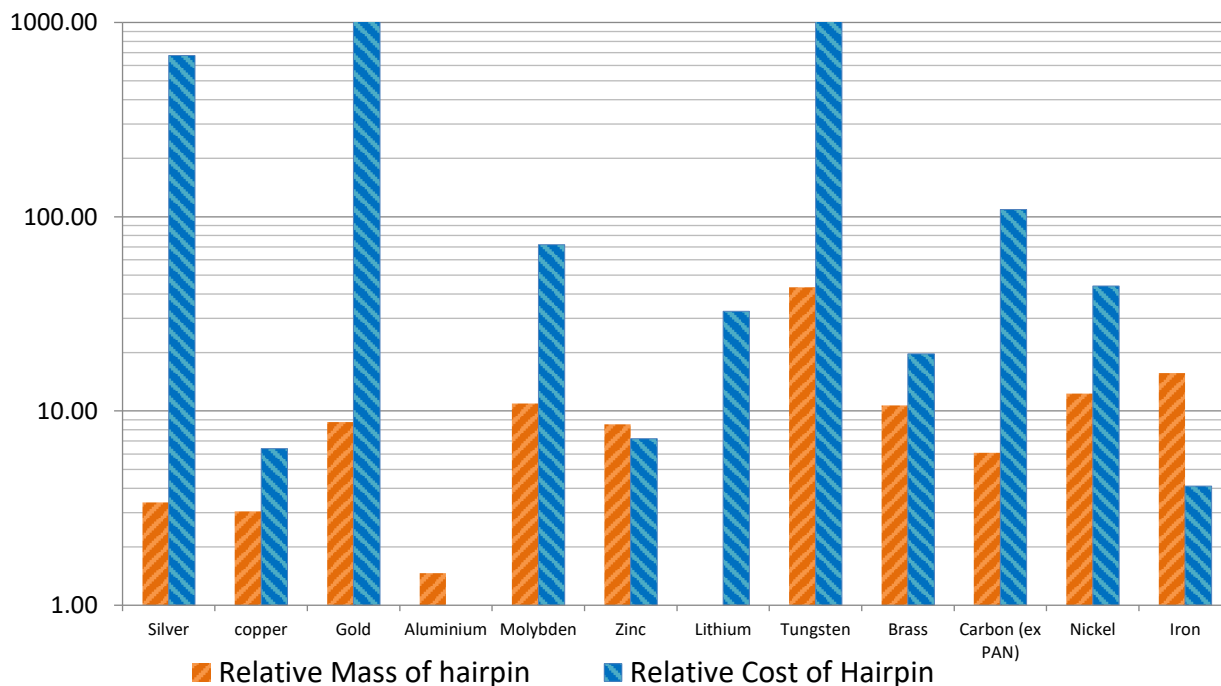


Figure 34 Comparison of alternative winding materials for a hairpin winding

Whilst cost and mass are both key metrics, it is important to consider other parameters when discussing the best possible material for future hairpin windings. As high performance may warrant a premium in these areas. The results in Figure 34 show the performance of a material parameter relative to the best-case alternative for that parameter. Aluminium offers the best performance in terms of cost (thus a relative cost of 1), while simultaneously being the second-best performer in terms of mass (Figure 34). Most Aluminium alloys have a melting point of approximately 600°C, which might make aluminium unsuitable for some electric machine designs that are expected to run at higher temperatures. However, this would not necessarily mean that aluminium is automatically discounted in these instances. Lithium provides the best performance in terms of reducing mass (thus a relative mass of 1). However, this comes at the expense of cost, as lithium windings would cost over 30 times that of an aluminium, and 5 times more expensive than the current standard material copper. Lithium also has a melting point below 200°C, which limits the electric machine designs that would be suitable for lithium windings, and is highly reactive, which could also lead to manufacturing and in-service problems. Copper performs well with regard to an overall cost and mass performance, with similar performances from zinc and iron. Aluminium has a greater thermal expansion than copper (Figure 35), which could potentially cause further issues to both the hairpins windings and stator as the material expands.

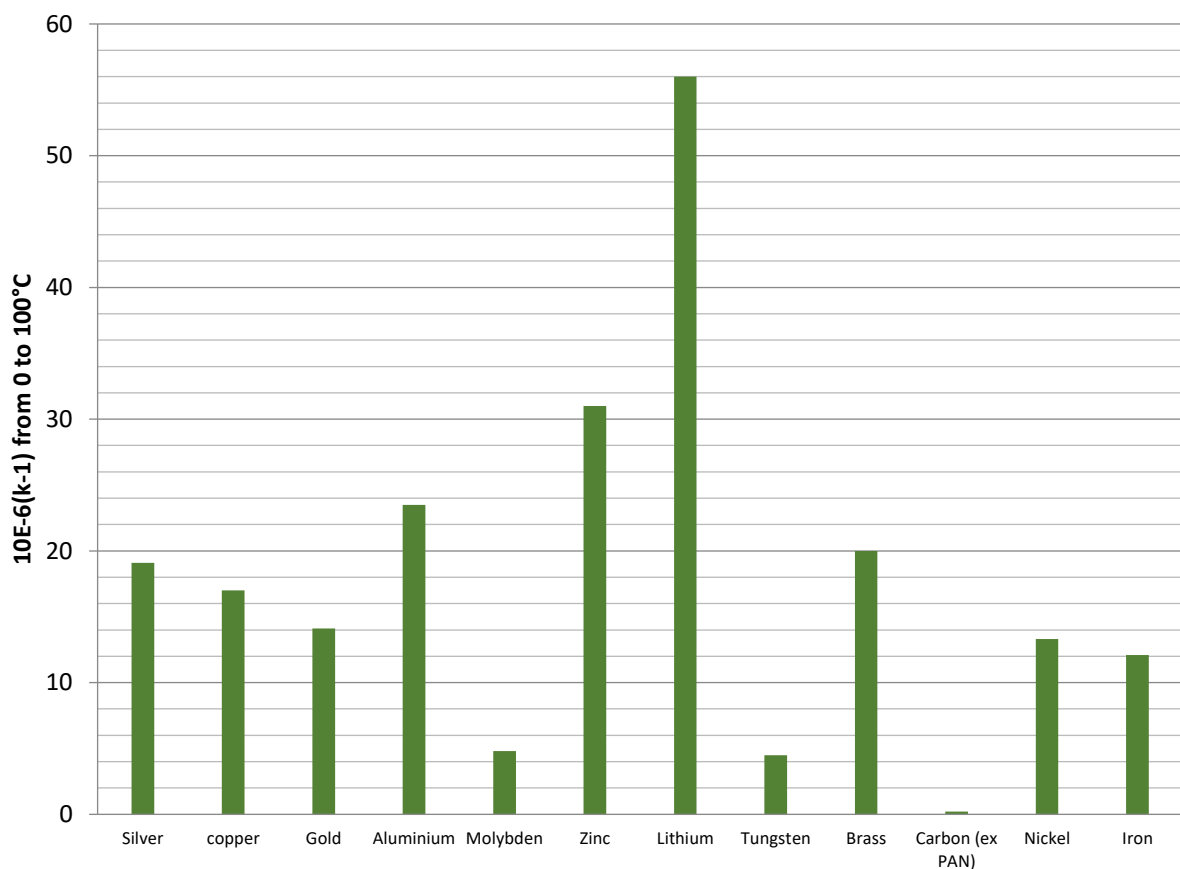


Figure 35 Coefficients of thermal expansion of various pure elements and alloys

### 3.3.1 Aluminium

Producing hairpins from extruded bar is the most sensible approach. It might be possible to cast parts into shape. However, the quality of cast aluminium would likely not be as good as a worked piece of extruded material; castings can contain porosity which would reduce conduction and are likely to have reduced strength over a deformed part. For a simple cross section such as the hairpins require, extrusion is likely to be the best method. It is also possible to extrude non-standard cross sections, such as a hollow piece. If busbars are made from the same material as the hairpin, it would potentially aid the joining and surface treating issues. In this case, the busbar might require a different form of material, such as plate rather than extrusion.

	<u>criteria</u>	<u>importance factor</u>	<u>Property value</u>	<u>suggested score</u>	<u>weighted score</u>	<u>suitability rating</u>
<b>Alloy 1050 'O' Sheet</b> (10% penalty for sheet)	Melting point (*C)	3	650	5	15	72%
	thermal expansion (/K)	3	2.40E-05	3	9	
	Electrical resistivity (Ω .m)	4	2.82E-08	4	16	
	Workability	4	excellent	5	20	
	Machinability	4	poor	1	4	
	Weldability	4	excellent	5	20	
	Anodising	4	excellent	5	20	
	<u>criteria</u>				<u>weighted score</u>	<u>overall rating</u>
<b>Alloy 6005A - T6</b> Extrusion	Melting point (*C)	3	605	5	15	71%
	thermal expansion (/K)	3	2.40E-05	3	9	
	Electrical resistivity (Ω .m)	4	3.40E-08	3	12	
	Workability	4	fair	3	12	
	Machinability	4	fair	3	12	
	Weldability	4	excellent	5	20	
	Anodising	4	good	3	12	
	<u>criteria</u>				<u>weighted score</u>	<u>overall rating</u>
<b>Alloy 6061 - T6</b> Extrusions	Melting point (*C)	3	650	5	15	70%
	thermal expansion (/K)	3	2.34E-05	4	12	
	Electrical resistivity (Ω .m)	4	4.00E-08	2	8	
	Workability	4	good	4	16	
	Machinability	4	acceptable	3	12	
	Weldability	4	good	4	16	
	Anodising	4	good	3	12	
	<u>criteria</u>				<u>weighted score</u>	<u>overall rating</u>
<b>Alloy 6063A - T6</b> Extrusions	Melting point (*C)	3	600	5	15	76%
	thermal expansion (/K)	3	2.35E-05	4	12	
	Electrical resistivity (Ω .m)	4	3.50E-08	3	12	
	Workability	4	average	3	12	
	Machinability	4	average	3	12	
	Weldability	4	excellent	5	20	
	Anodising	4	good	4	16	
	<u>criteria</u>				<u>weighted score</u>	<u>overall rating</u>
<b>Alloy 6063 - T6</b> Extrusions	Melting point (*C)	3	655	5	15	76%
	thermal expansion (/K)	3	2.35E-05	4	12	
	Electrical resistivity (Ω .m)	4	3.30E-08	3	12	
	Workability	4	acceptable	3	12	
	Machinability	4	good	4	16	
	Weldability	4	good	4	16	
	Anodising	4	good	4	16	
	<u>criteria</u>				<u>weighted score</u>	<u>overall rating</u>
<b>Alloy 6082 - T6</b> Extrusions	Melting point (*C)	3	555	3	9	66%
	thermal expansion (/K)	3	2.40E-05	3	9	
	Electrical resistivity (Ω .m)	4	3.80E-08	2	8	
	Workability	4	good	4	16	
	Machinability	4	good	4	16	
	Weldability	4	good	4	16	
	Anodising	4	good	3	12	

Table 5 Hairpin aluminium alloy comparison

Alloy 1050 is the best material in terms of electrical conductivity (Figure 36). The only drawback is that 1050 is not suited to being machined. The benefit of using a machinable material is that features can be added to the hairpin winding, such as holes, which can be used as part of a bus bar assembly process. So long as the overall process is designed to reduce or negate the need for machining on the hairpins, Alloy 1050 would be the best material to use. Alloy 1050 plate would also be a useful material for a busbar assembly. If the busbar were to be produced from a plate, it would then be stamped to produce the correct geometry. It is not known whether the poor machining characteristics of alloy 1050 would also be bad for stamping, though this seems a possibility. Extruded bar would probably be the cheapest way to form the hairpin. However not all forms of aluminium are available in extruded bar form. Alloy 1050, a potentially very good material choice, is readily available in plate form. It may also be available in extruded form. However, further investigation is required.

The three materials selected to investigate further are 1050, 6063 and 6082 and copper c101. It can be seen from Figure 34 that aluminium is the standout alternative to copper. Various aluminium alloys have been considered and following analysis, alloy 1050 (the best electrically) and alloys 6063 and 6082 have been chosen for further experimentation. The expectation is that 1050 should perform best and 6082 worst, as indicated by the ratings in Table 5.

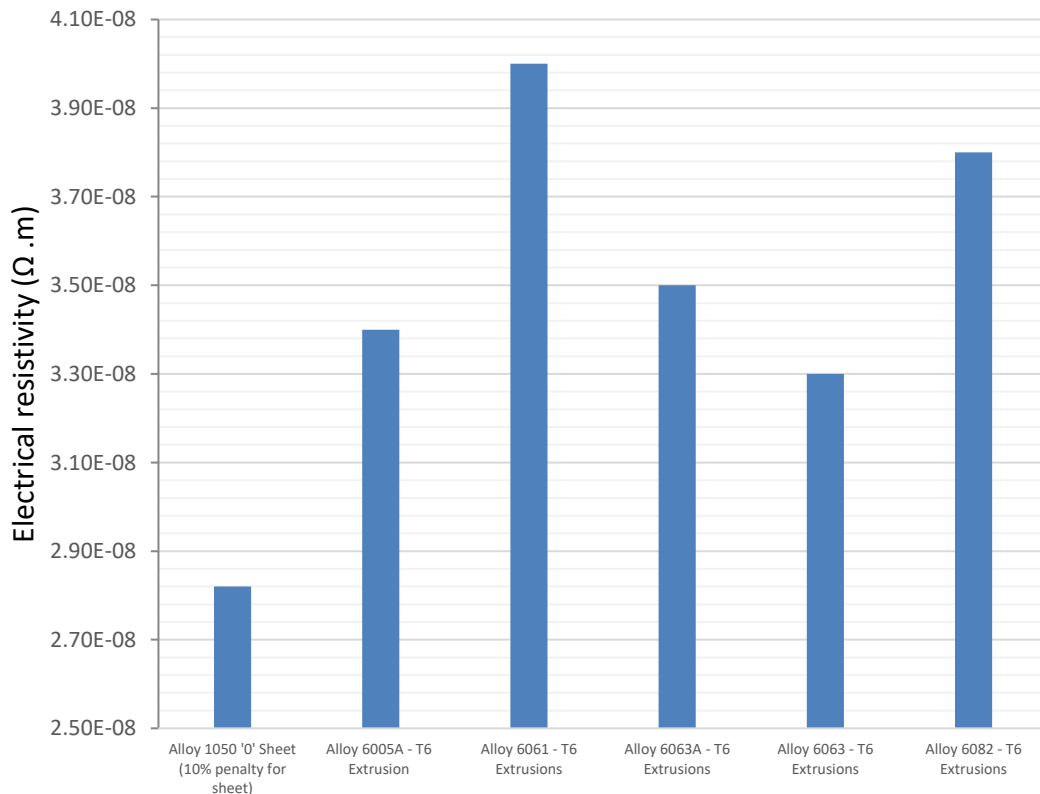


Figure 36 Aluminium alloy electrical resistivity comparison

### 3.4 Temperature effect on resistivity

$$d\rho = \rho \cdot \alpha \cdot dt \tag{3.1}$$

The resistivity of a material changes relative to temperature. As the material gets hotter, its resistivity will generally increase, meaning that it is harder for electrical current to flow through the material. Windings in electric motors are expected to operate at temperatures well above room temperature, naturally effecting the ability of the hairpins to perform. The change in resistivity for many materials can be calculated with a good degree of accuracy as in equation ( 4.1 ) where;  $d\rho$  is the change in resistivity,  $\rho$  resistivity at room temp,  $\alpha$  temperature coefficient of material, and  $dt$  is the change in temperature.

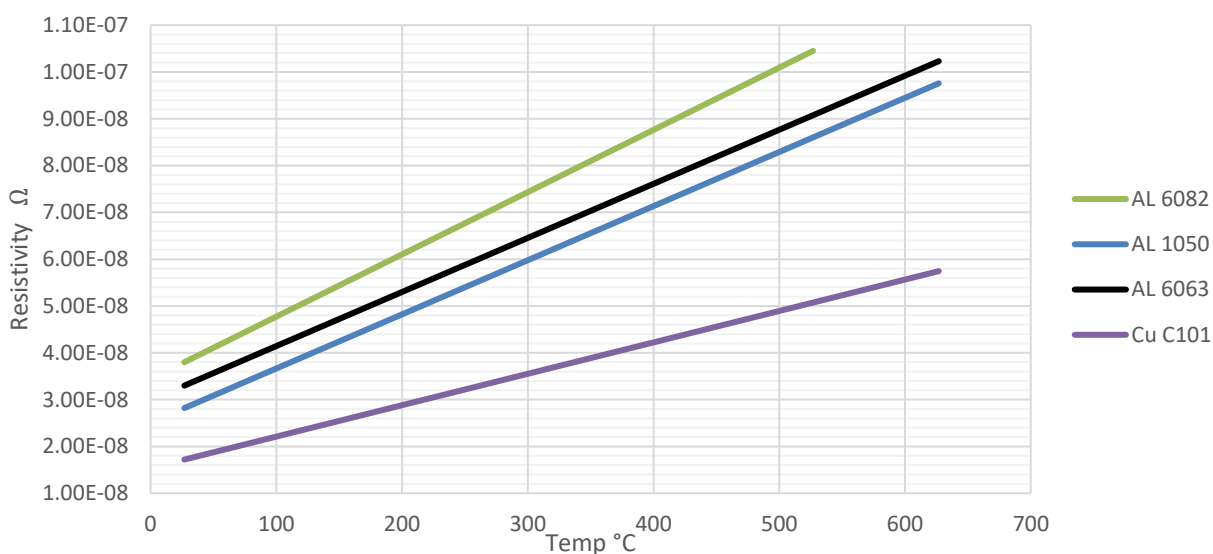


Figure 37 Resistivity at temperature

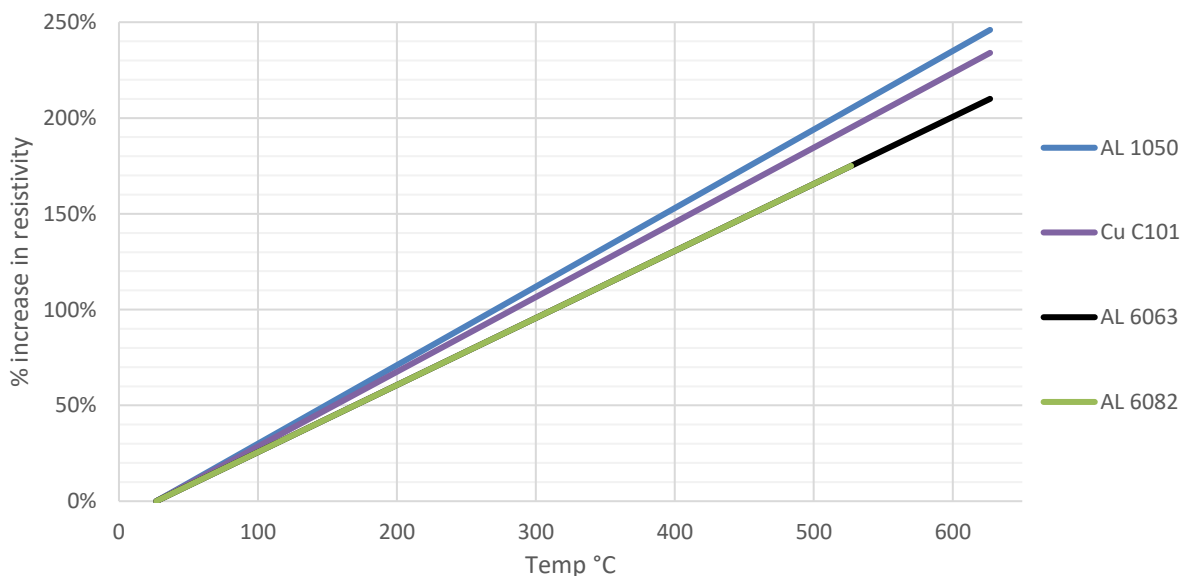


Figure 38 Percentage increase in resistivity for increasing temperatures

Copper is a better conductor of electricity than aluminium and this holds true for all temperatures. Aluminium 6082 only has results to 526.85°C as it would be expected to have melted beyond this temperature. It can be seen that for a projected operating temperature of 400°C, all materials suffer an increase in resistivity of approximately 130%-150%. Taking copper as a baseline, AL 1050 shows the best resistivity results. The performance benefits relative to copper differ dependant on temperature. Figure 39 shows that AL 1050 actually becomes slightly better at as temperatures decrease, whereas AL 6082 and AL 6063 perform gradually worse relative to copper at lower temperatures. This is potentially useful when considering high level system trade-offs, where operating temperature might be a key parameter to be reduced or alternatively unconstrained.

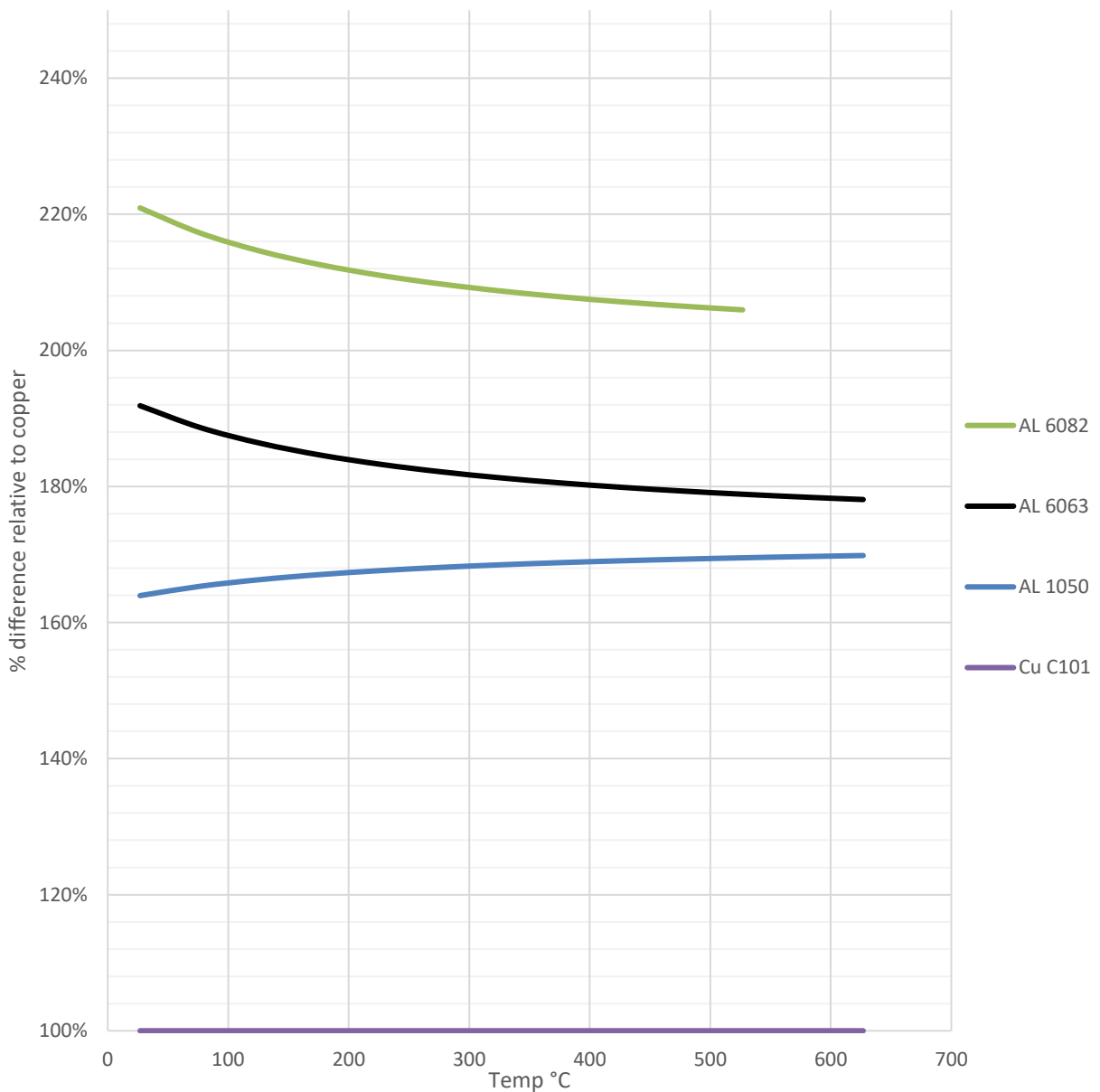


Figure 39 Relative resistivity relative to copper for increasing temperatures



### 3.5 Joining methodology for hairpin to busbar assembly

One of the additional process steps resulting from the incorporation of hairpin windings is the necessity to join the hairpin windings to a busbar assembly. A variety of joining processes have been considered based on the introduction of aluminium hairpins and aluminium busbar, but also a combination of copper and aluminium hairpin/busbar architecture. To evaluate the potential suitability of a given process, there must be some form of criteria by which to judge the process against. These criteria will not only consider the merits of the joint, but also the prospective efficacy of the process in relation to its intended use as a part of a mass manufacture product line. Suggested scores are assigned based on multiple factors. An evaluation is made using previous application history, known capabilities and limitations in literature of a process (as discussed in section 2.2.7) and further input from industrial partners (Ricardo plc, 2017) (Atkins, 2016) and experts (Goodall, 2018) (Cater, 2018) regarding the implementation requirements and concerns for inclusion in a stator assembly process. The final suggested scores are reached based on the culmination of the feedback attained and the perception of the author based on these facts. As such there is an element of considered subjectivity in the results.

The results are based on the indication of performance from previous literature and the suggested importance factors. As such, it should not be taken that these results are a rigorous assessment of joining methods for the application of hairpin windings. Further work should be conducted to further understand the strengths and limitations of these joining methods empirically.

These joining methods have also been considered without fully defining the hairpin design or the type of joint required. It is considered that these choices might be influenced by the choice of joining method, and as such, the suitability of a method is influenced by the ability to incorporate the method into a process route.

#### 3.5.1 Suitability parameter justification

*Conduct electricity / have low resistance*      **IMPORTANCE FACTOR: 5/5**

Owing to the function required from a hairpin winding, it is vitally important that the joint allows electrical current to flow through the circuit unimpeded. As such, joints which have low electrical resistance properties will be preferred.

*Have sufficient mechanical strength*                      *IMPORTANCE FACTOR: 2/5*

Mechanical strength of the joint can refer to a number of characteristics. However, in this case, tensile strength is considered the more important feature. The joints must be strong enough to survive rough handling and life in service. Joints must be able to achieve a certain (currently unquantified) strength as a minimum, with stronger joints being more likely candidates.

*Survive high temperature*                              *IMPORTANCE FACTOR: 5/5*

It is hoped to achieve a working environment for hairpin windings in the region of 400°C. Whilst this is optimistic, it relates to the initial specification for components as provided at the project's commencement (see Table 1 p17). It is clearly vital that the joint remains intact as these temperatures and remains electrically conductive.

*Scope for mass manufacture*                              *IMPORTANCE FACTOR: 3/5*

It is intended to produce these hairpins in vast numbers, as such; the joining process must be one which is quick, scalable, and technically achievable for mass manufacture levels of output.

*Reasonable cost*    *IMPORTANCE FACTOR: 4/5*

Given the proposed level of output, small changes to cost can have a large nominal impact. Therefore, it is important to use a process which is economical. Costs can be associated to high energy requirements, cost of purchasing machinery or the requirement to purchase extra materials such as fluxes.

*Application flexibility*                                      *IMPORTANCE FACTOR: 5/5*

This is a highly important aspect of the joining process. The joining process must be able to form the correct geometry of the parts required. This does not necessarily mean a specific type of joint design must be identified at this stage. However, the flexibility to join both thick and thin parts, flat or bent, sheet or pipe, would allow for further flexibility in the ultimate design of the hairpin, its relation to other components and the overall manufacturing strategy. The joining process must also make sense as a solution for this application. It is considered that the hairpins would require joining "in situ" inside the stator / motor. Joining processes must therefore be flexible enough to accommodate this scenario, whilst also not compromising the integrity of any other components during the joining process.

	<u>criteria</u>	<u>importance factor</u>	<u>suggested score</u>	<u>weighted score</u>	<u>suitability rating</u>
<b>Brazing</b>	electrical conductivity	5	5	25	<b>67%</b>
	mechanical strength	2	3	6	
	thermal adaptiveness	5	3	15	
	mass producable	3	4	12	
	potential cost	4	3	12	
	application flexibility	5	2	10	
<b>Flash welding</b>	<u>criteria</u>	<u>importance factor</u>	<u>suggested score</u>	<u>weighted score</u>	<u>overall rating</u>
	electrical conductivity	5	4	20	<b>70%</b>
	mechanical strength	2	4	8	
	thermal adaptiveness	5	4	20	
	mass producable	3	3	9	
	potential cost	4	3	12	
application flexibility	5	3	15		
<b>Friction welding</b>	<u>criteria</u>	<u>importance factor</u>	<u>suggested score</u>	<u>weighted score</u>	<u>overall rating</u>
	electrical conductivity	5	4	20	<b>73%</b>
	mechanical strength	2	5	10	
	thermal adaptiveness	5	5	25	
	mass producable	3	3	9	
	potential cost	4	2	8	
application flexibility	5	3	15		
<b>Friction stir welding</b>	<u>criteria</u>	<u>importance factor</u>	<u>suggested score</u>	<u>weighted score</u>	<u>overall rating</u>
	electrical conductivity	5	5	25	<b>78%</b>
	mechanical strength	2	4	8	
	thermal adaptiveness	5	5	25	
	mass producable	3	3	9	
	potential cost	4	3	12	
application flexibility	5	3	15		
<b>projection welding</b>	<u>criteria</u>	<u>importance factor</u>	<u>suggested score</u>	<u>weighted score</u>	<u>overall rating</u>
	electrical conductivity	5	4	20	<b>70%</b>
	mechanical strength	2	3	6	
	thermal adaptiveness	5	4	20	
	mass producable	3	4	12	
	potential cost	4	4	16	
application flexibility	5	2	10		
<b>Ultrasonic welding</b>	<u>criteria</u>	<u>importance factor</u>	<u>suggested score</u>	<u>weighted score</u>	<u>overall rating</u>
	electrical conductivity	5	4	20	<b>73%</b>
	mechanical strength	2	3	6	
	thermal adaptiveness	5	4	20	
	mass producable	3	4	12	
	potential cost	4	5	20	
application flexibility	5	2	10		
<b>Laser beam welding</b>	<u>criteria</u>	<u>importance factor</u>	<u>suggested score</u>	<u>weighted score</u>	<u>overall rating</u>
	electrical conductivity	5	4	20	<b>77%</b>
	mechanical strength	2	3	6	
	thermal adaptiveness	5	4	20	
	mass producable	3	3	9	
	potential cost	4	3	12	
application flexibility	5	5	25		
<b>Snap fit</b>	<u>criteria</u>	<u>importance factor</u>	<u>suggested score</u>	<u>weighted score</u>	<u>overall rating</u>
	electrical conductivity	5	2	10	<b>70%</b>
	mechanical strength	2	2	4	
	thermal adaptiveness	5	2	10	
	mass producable	3	5	15	
	potential cost	4	5	20	
application flexibility	5	5	25		
<b>Cold press</b>	<u>criteria</u>	<u>importance factor</u>	<u>suggested score</u>	<u>weighted score</u>	<u>overall rating</u>
	electrical conductivity	5	4	20	<b>76%</b>
	mechanical strength	2	4	8	
	thermal adaptiveness	5	3	15	
	mass producable	3	4	12	
	potential cost	4	4	16	
application flexibility	5	4	20		

Table 6 Joining process suitability rating<sup>2</sup>

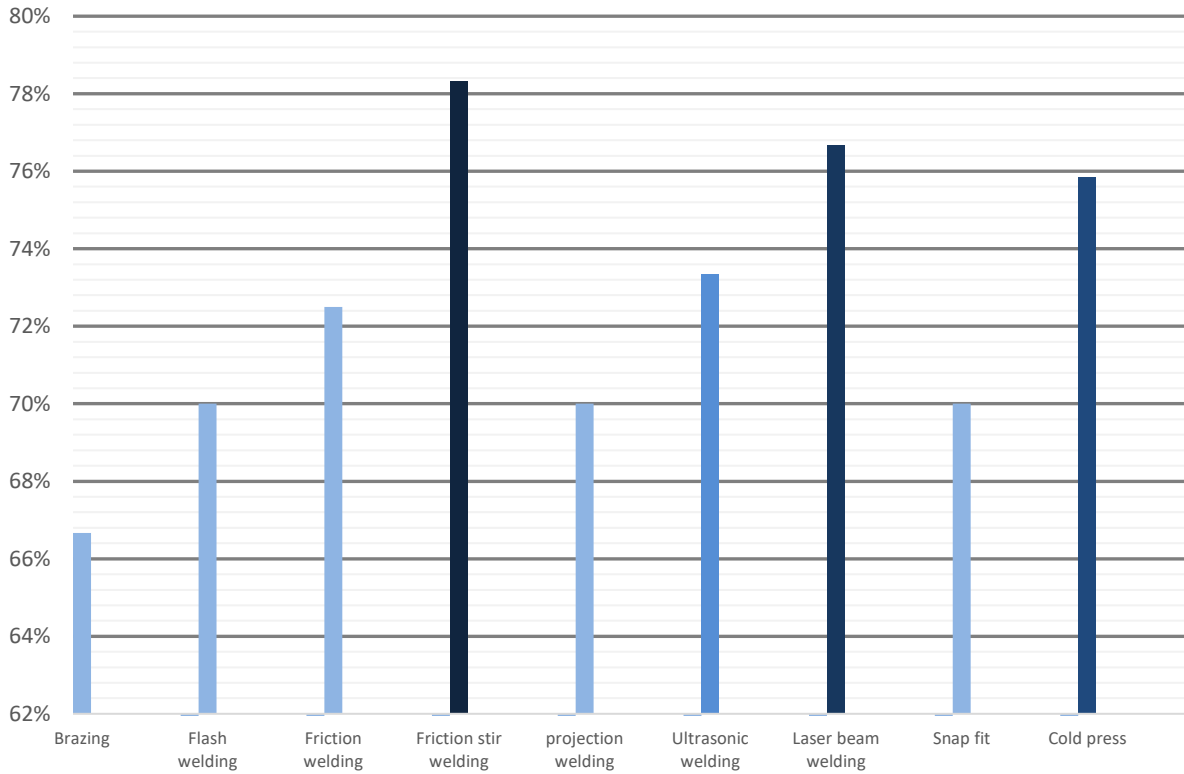


Figure 40 Overall suitability rating of joining methodologies as in Table 6, clearly showing friction stir welding as the most promising joining method relative to the alternative proposed methods

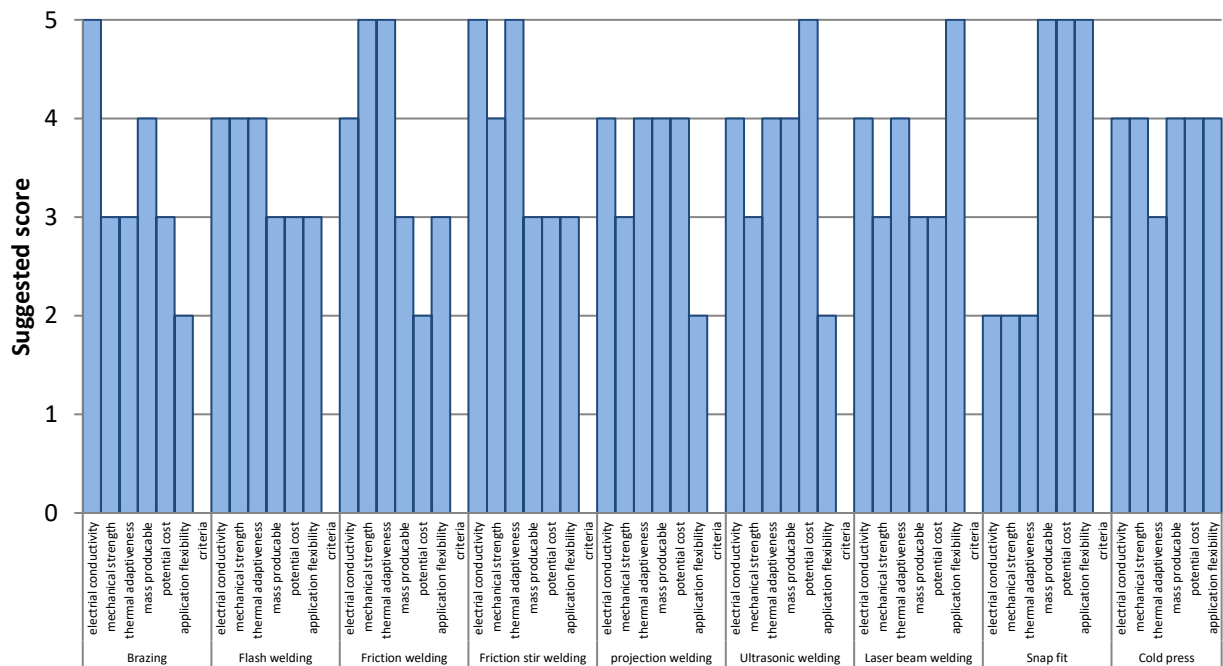


Figure 41 Suggested criteria scores of joining methodologies as in Table 6, signifying areas of strength and weakness for each joining method

<sup>2</sup> These results are based on current understanding and knowledge. Results would need to be revised should further knowledge become available, such as; insulations materials, mechanical forces, or end winding geometry.

### 3.5.2 Assessment of joining methods

The top four scoring joining processes are; friction stir welding, laser beam welding, cold pressure welding and ultra-sonic welding. Friction stir welding comes out of this assessment as an interesting joining process. Nominally it is most useful in joining long sheets of metal. However, the process is surprisingly flexible. Apple has been using friction stir welding to knit together their products since at least 2012 (Dilger, 2012), showing that the process clearly has some value in a mass market, smaller sized product. Unfortunately, the limitations of the process are not wholly understood, and it is hoped that from further investigation and actualisation, the process can be better appreciated. Friction stir welding should be capable of producing a joint with the right characteristics; it is the transition to mass manufacture and the applicableness to the specific manufacturing challenge in this project that remains somewhat unclear. However there appears to be enough flexibility to continue investigation.

Laser beam welding has a high application flexibility. Laser welding offers a good amount of flexibility in terms of materials and geometries of parts to be welded. Laser welding also offers the potential to create welds in difficult to access areas, depending on if a route for the laser beam can be found and parts fixed during the operation. It should also be possible to combine a laser beam welder with a robotic arm, offering further flexibility in designing an assembly process.

Cold pressure welding is a relatively low-tech solution, but non the less offers great potential. The costs involved in cold pressure welding would be concentrated on fixturing and press machines, keeping tooling and consumables costs relatively low compared to other methods. Similar can be said of ultra-sonic welding. Both cold pressure and ultra-sonic rely on creating joins mechanically. Laser beam and friction stir are likely to alter the chemical structure of the materials at the join.

Snap fit, whilst having a weak score, is noteworthy. It is clearly the simplest and cheapest form of joining under consideration. It is also nominally the weakest and least electrically sound. Snap fit may be useful as part of a two-stage joining process. If this were the case, understanding how to incorporate a snap fit into the part and process design would require some thought and potentially investigation. Laser welding might not be suited to this approach as a small clearance between parts is required to achieve a laser weld. Friction stir might benefit from this approach, as there is a requirement to have components fixed in place before applying the friction stir tool. It is unclear whether ultra-sonic welding would be viable in a snap fit, similarly a cold press might be achievable, but the parts would require designing around achieving a snap fit and then surviving the force during the cold pressure operation.

### 3.6 Experimental exploration

Attempts were made to manufacture aluminium-copper test samples using some of the best assessed joining methodologies. A lap joint was chosen as the best join for testing as it represented the closest type of join to that which would likely be used in practice.

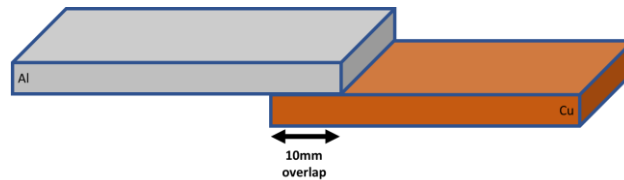


Figure 42 lap joint – 10mm

Samples were sent to *Sonobond ultrasonic* who attempted to join AL 6082, AL 6063 & AL 1050 to copper samples using ultrasonic welding. For each material combination joining failed. *Sonobond* indicated that material transfer had failed to be achieved and as such, the aluminium and copper samples did not join. Whilst research suggests it is possible to produce aluminium-copper welds using ultrasonic welding, the process remains challenging, and in this instance, unachievable by this *Sonobond ultrasonic method*.

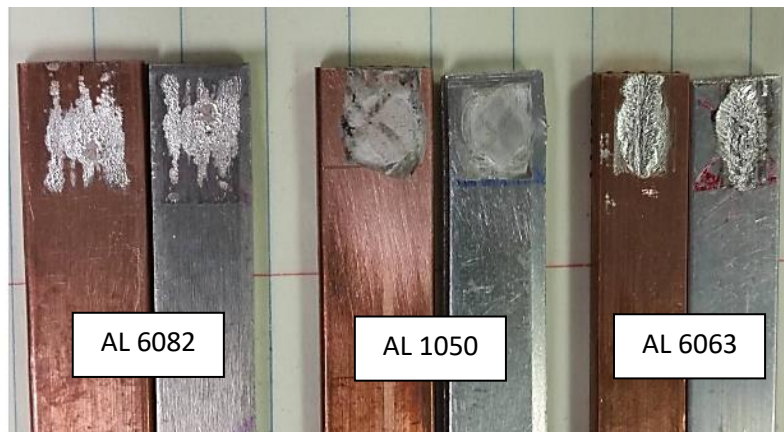


Figure 43 Attempted ultrasonic joining of samples

It had been proposed to use laser welding facilities within the AMRC organisation. However, this was ultimately not viable with the equipment available. In trials performed by Timothy Shelly and Stephen Holt of the AMRC, a relatively “low power laser” (Holt 2018) was used to bond 0.6 mm copper and 1.6 mm aluminium alloy. It was found that even up to times of 1 hour, no flow was seen between the copper and the aluminium, indicating that in these highly conductive materials it is challenging to concentrate enough energy to create a weld pool without high powered laser welding equipment.

### 3.6.1 Thermal expansion issue

A potential issue with using hairpin winding technology is maintaining an effective surface coating under thermal loading, where the hairpin material has expanded as a result of thermal expansion. Aluminium has been considered as a potential alternative to copper. However, aluminium has a greater thermal expansion coefficient than copper, which is the current standard material. A standard surface coating on aluminium would be to create an oxide layer through anodization, but the oxide that would be developed would have a lower coefficient of expansion and very limited ductility, and so could be at risk of cracking off. A finite element model was created to provide an understanding of this issue and the likelihood of an oxide layer failing due to thermal expansion. Two different hairpin designs have been considered. One with a standard cross section as Figure 44 and a design which includes a hollow section in the cross section as Figure 45. The hollow cross section design is considered as a possible method of reducing the external surface expansion of the part. The oxide layer is considered as a separate body which is fixed to the hairpin. Both parts are heated to 400°C, as per the original specification (see Table 1). This is a much higher temperature than would normally be expected (approx. 200°C) in order to check the feasibility this technology as a solution for extreme temperature conditions.

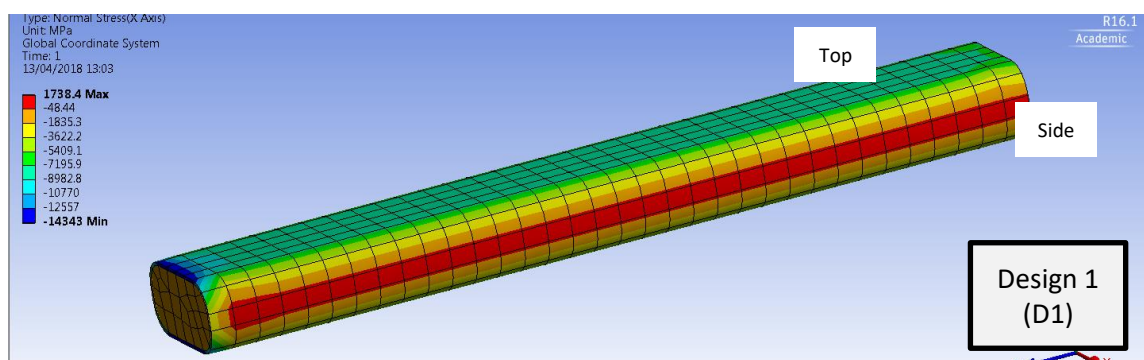


Figure 44 heated hairpin with oxide layer (D1)

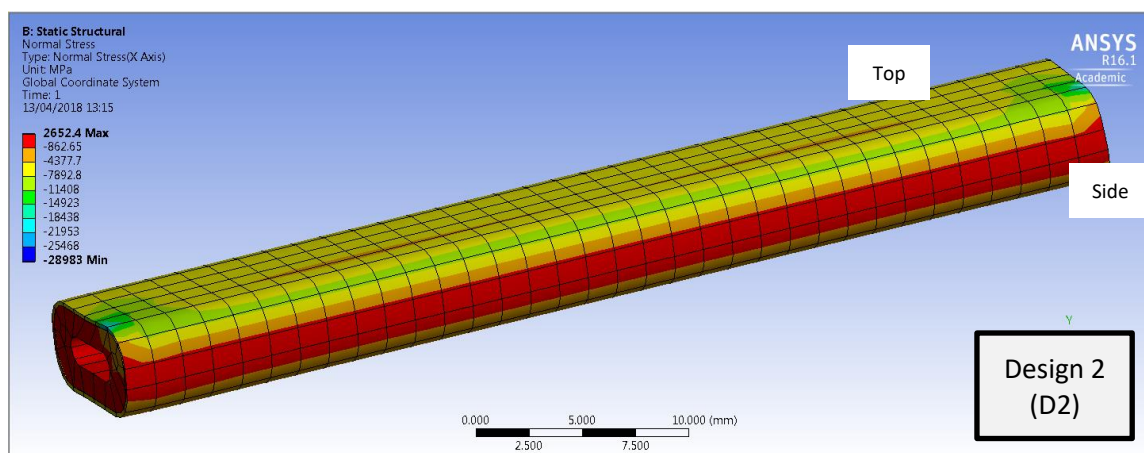
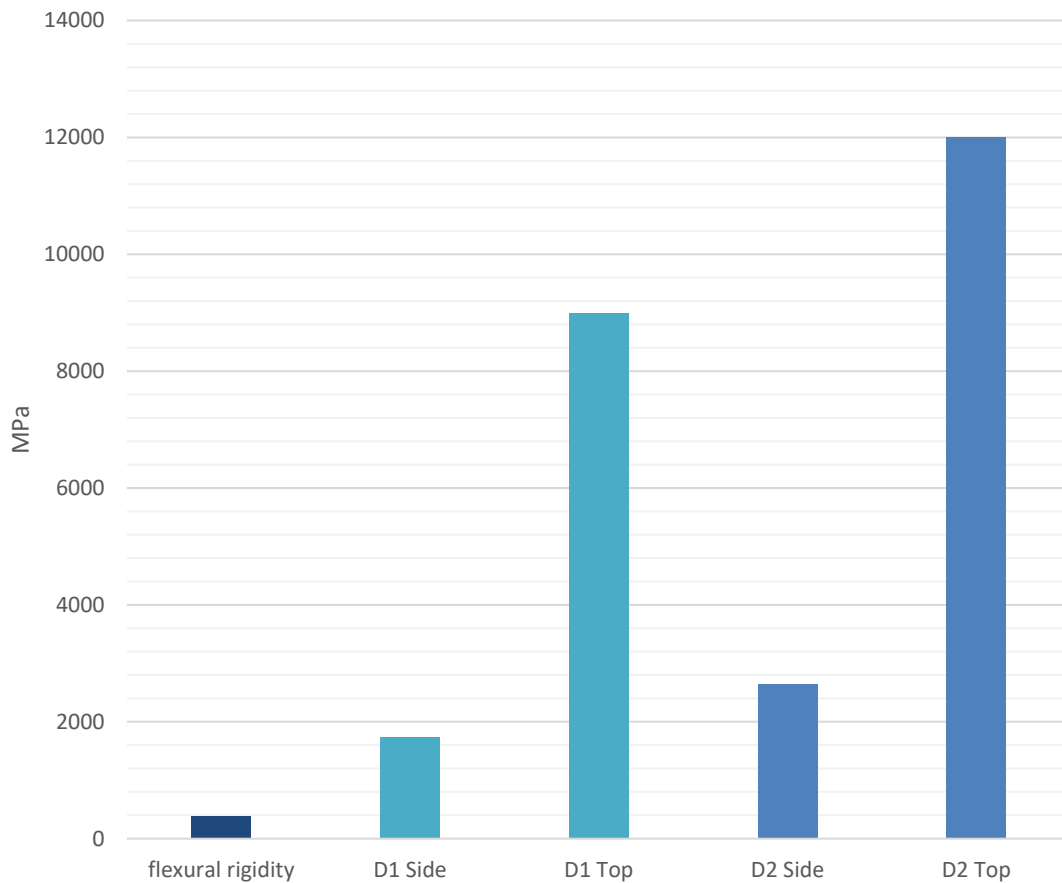


Figure 45 heated Hairpin with hollow cross section and oxide layer (D2)

There are some potential benefits and drawbacks associated with the use of hairpins with hollow sections. In order to produce hairpins with a hollow section would require a special die to be produced. The hollow hairpin section would not conduct electricity as well because there is less material in the part. A potential benefit of the hollow section is that it could potentially be used to supply some coolant into the hairpin windings, further aiding the ability of the part to survive at higher temperatures (Atkins, 2016).



*Figure 46 Stresses in surface as result of thermal expansion of aluminium hairpin at 400°C*

The results of the experiment show that the stresses in the part are well beyond the UTS of the oxide layer, which has a flexural rigidity of 379 MPa (Accuratus, 2013), indicating a high likelihood that the part would fail, 1738 MPa in the side section and approximately 9000 MPa in the side section for design 1. The second hairpin design which includes a hollow section appears to aggravate the issue further, with stresses of approximately 2500 MPa in the narrow side section and approximately 12000 MPa in the wider top section. It was expected that the cavity in the hollow section would provide a space for the material to expand into and thus reduce stress. Perhaps it is the case that as there is less material to resist the effect of thermal stresses, the stresses in the part are greater. Anodization may not be suitable for applications where the machine is expected to reach extreme elevated operating temperatures despite the potential for being an attractive technology to create a non-conductive coating on aluminium hairpins in a cost-effective way.



### 3.7 Conclusions

Hairpin winding technology is already adopted by the automotive industry, as evidenced by VW (ZEISS, 2020). The results of this study show that the best alternative to copper for hairpin windings is aluminium. Aluminium is a cheaper, lighter alternative to copper as a hairpin material. One of the issues of using aluminium as a hairpin compared to copper is the increase in thermal expansion. Whilst in situ during operation, hairpins are tightly packed and have no room for expansion, which would cause a build-up of stress in the material and potentially lead to a failure state in the component. The use of a hollow section was considered to alleviate this issue. However, the stresses on the external faces were greater than with a solid part.

In order to use aluminium hairpins, a joining process must also be found which is capable of joining the hairpins to the busbar architecture. The busbar component should ideally be as small as possible, and in this case a copper busbar assembly would occupy less volume than an aluminium hairpin. It is possible to create a winding assembly using both aluminium hairpins and copper busbar if a suitable joining technology is used. Various joining methodologies were considered in this study, with friction stir, laser beam and cold press being identified as the most feasible joining methods based on a combination of capability and manufacturability with the total winding process. It should be noted that these conclusions are based on the suggested scores in the study which are somewhat subjective, based on the user's perception and weighting of importance of factors. For example, one might argue that the mechanical strength requirement of the join should be scored at 3 or 4, based on the potential issues of vibrations and magnetic flux leak during the service of the component. In this case, the score of 2 was chosen predominately based on an argument of structural integrity in the face of external forces or knocks.

This experiment considered the hairpin sections at a 400°C temperature. Should the experiment be repeated at temperatures closer to expected working temperatures of machine components today (approximately 200°C) the results would show much lower stresses on the surface of the parts and could potentially demonstrate the viability of anodization to coat hairpins for operation at these more normal working temperatures.

## 4 Cost model for stator production

---

### 4.1 Methodology

#### 4.1.1 Knowledge gap

Stators have been produced from stamped electrical steels for many years. However, the knowledge in stamping is mixed. There are multiple different areas of research under consideration as regards stamping electrical steels. Current research has been directed towards identifying the effect of cutting clearances on the electromagnetic performance of laminates. Other research has studied the effect of different parameters on the life of a stamping tool. The decisions and parameters chosen by industry and manufacturers are mostly based on experience rather than specific rules or knowledge. There is also no consideration of how to best create a set of manufacturing parameters which manage the quality of part produced or the rate or costs of production.

#### 4.1.2 Approach

The work in this chapter has been conducted using a modelling approach. Process maps have been developed using Microsoft Visio software for the stamping production process and also the slinky style stamping process. Using data from various sources, a manufacturing cost model has been created which provides manufacturing economics results based on complex interactions of parameters. An analysis of this model is conducted to provide insight.

## 4.2 Introduction

### 4.2.1 Understanding the operation

Using a total quality management approach, as described by Slack (2019), each individual process along the manufacturing route for a stator is considered. This enables a holistic approach to continuous process improvements. This requires developing an understanding of the operation from both the top down and bottom up. A process route analysis has been conducted to understand the individual processes which occur within the operation, and to identify where knowledge gaps might occur. Following this, a working model has been developed which captures the design and process parameters as identified within the process route and operations.

The stamping process route has certain operations which affect all three of the key manufacturing business targets; time, cost, and quality. The first process is a 'goods in' step. The choice of raw material clearly has an impact on the quality of the stator produced and equally the cost those materials will affect the production cost of the stator. The machinability of the material will affect the processing time required, while the delivery and accessibility of material can also cause dramatic changes to the timeliness of production. The choice of material is therefore an important consideration, and so an analysis of the materials used in the stamping process has been conducted in this research.

The most important stage in terms of stamping is the cutting process, and this can be considered from two points of view. Firstly, there is the machine and its set-up, and secondly, there is the component and its design. One of the major cost factors in stamping is the stamping tool. To maximise the use of each tool, it is essential that the correct tool set-ups are used. Standard industry practice relies on the knowledge and expertise of technicians to create a viable tool set-up using best practice principles. An analysis of the process parameters at the cutting stage, and the effect they have on the tool, are considered in this research to develop an understanding of the real-world impact of tool set-up variations.

It is important to ensure that the manufacturing processes and component designs do not produce excessive wastes, in terms of material, energy and production time. A study has been conducted using design for manufacture and assembly techniques to understand how the various design features of the stator impact the manufacturing operation.

It is possible to produce stators using different manufacturing processes, one such is the slinky style process. The slinky style stator still uses stamping technology, but rather than stacking laminates, the

stator is coiled around a mandrel, similar to a slinky. Each process has its benefits and limitations, as outlined in the SWOT analysis (Table 7). A feasibility study was conducted using various stator designs to understand the design limitations of the slinky style production method.

#### 4.2.2 Stamping process route

The stamping process in Figure 48 represents a typical production route for a stator and rotor and assumes that the design of stator is producible by stamping in some form. In this instance, only the stator is considered in the research. The stamping process in Figure 48 is representative of a situation where a manufacturing operation which produces stators from stamping receives a new order. The manufacturer then organises the appropriate tool. The decision to use a current tool or a new tool is primarily determined by the geometry of the cut required by the tool. For more novel stator designs, it is increasingly likely that a new tool would be required. If a new tool is required, this would take much time to design and manufacture, with mistakes at this stage being costly to remedy. If an old tool is to be used, the condition of the tool will need to be monitored with particular attention. Once the tool is set-up and the tool and press have both been inspected, the raw material can be loaded in the system. The raw material will typically be electrical steel sheet, delivered as a roll of sheet. The roll is loaded into a fixture and then fed into the stamping press through a short system of rollers. Once the stamping press is started, the cutting process runs continuously, as indicated by the sub system in Figure 48. The stamped parts are collected onto a mandrel. The mandrel releases the laminate stack once enough laminates have been collected. At this point, the process ceases to be continuous and becomes more similar to a batch process. This means there is not a continuous feed of stator stacks into the next stage of the process. The stacks are then transferred to be seam welded, such that the stack is now one fixed body of laminates, as in Figure 47. The stacks are then sent forward to the winding stage of the production process.

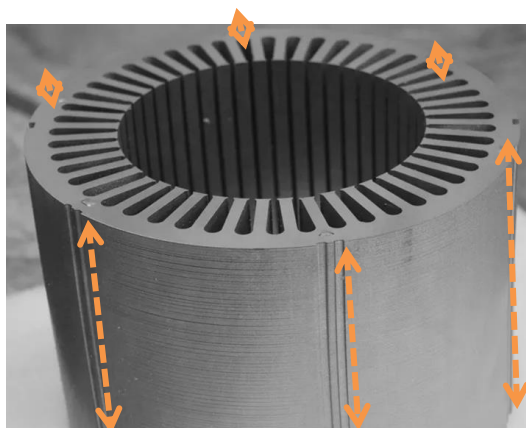


Figure 47 Example of a stator post stacking and welding (weld lines identified by orange arrows)

#### 4.2.3 Slinky style process route

The slinky style process route (Figure 49) is similar to the standard stamping route. In the slinky process, the stamping press and tool are different. It is possible that a press used in the normal stamping method can be used in the slinky method, but the requirements are subtly different. The slinky style stator has a less complex and smaller cutting profile and does not require as much force in the press machine. The cutting process does need to operate at much quicker speeds though as the cutting operations required are now multiplied by the number of teeth in each laminate layer. The two processes have different space requirements also. The slinky style production method requires a longer, narrower footprint to be available, as the material feed must be flattened, straightened, and remain straight through the process until it is coiled around the mandrel. The coiling process is unique to the slinky style stator and is responsible for creating limitations in the types of stator designs which are manufacturable by this method. After coiling, the process runs similar to a standard stamped stator, using roughly the same resources and process steps. There may be some slight changes to fixtures and handling prior to welding (joining) process but otherwise, the same equipment would remain suitable. The welding process for a slinky stator requires only one weld line to be produced, unlike the standard laminated stator seen in Figure 47.

Stamping offers the potential cut parts at a rate of approximately 200-300 SPM (strokes per minute). Operating at a faster cutting rate has disadvantages, as process control limitations widen. Weiss et al (2016) have evidenced how increasing the cutting speed can adversely affect the quality of the cut, noting that cutting at higher velocities increases the size of the deformed zone.

#### 4.2.4 SWOT analysis

A simple SWOT analysis of the slinky style process provides a good overview of the potential benefits and issues. The opportunities and threats are ideal areas for further investigation.

<p style="text-align: center;"><b>Strengths</b></p> <p>Use of similar stamping technology and knowledge (as normal stamping method)</p> <p>Use of similar raw materials</p>	<p style="text-align: center;"><b>Weaknesses</b></p> <p>Requires high level of process control to accurately stamp features</p> <p>Induce mechanical stress due to stamping cut</p>
<p style="text-align: center;"><b>Opportunities</b></p> <p>Potential to reduce waste, depending on part design</p> <p>Rotor can be produced by another method</p>	<p style="text-align: center;"><b>Threats</b></p> <p>Introduction of mechanical stress in stator material through bending / coiling</p> <p>Rotor not produced concurrently in slinky process</p> <p>Raw material is in different form factor / geometry (long strips)</p>

*Table 7 SWOT analysis of slinky style stator production*

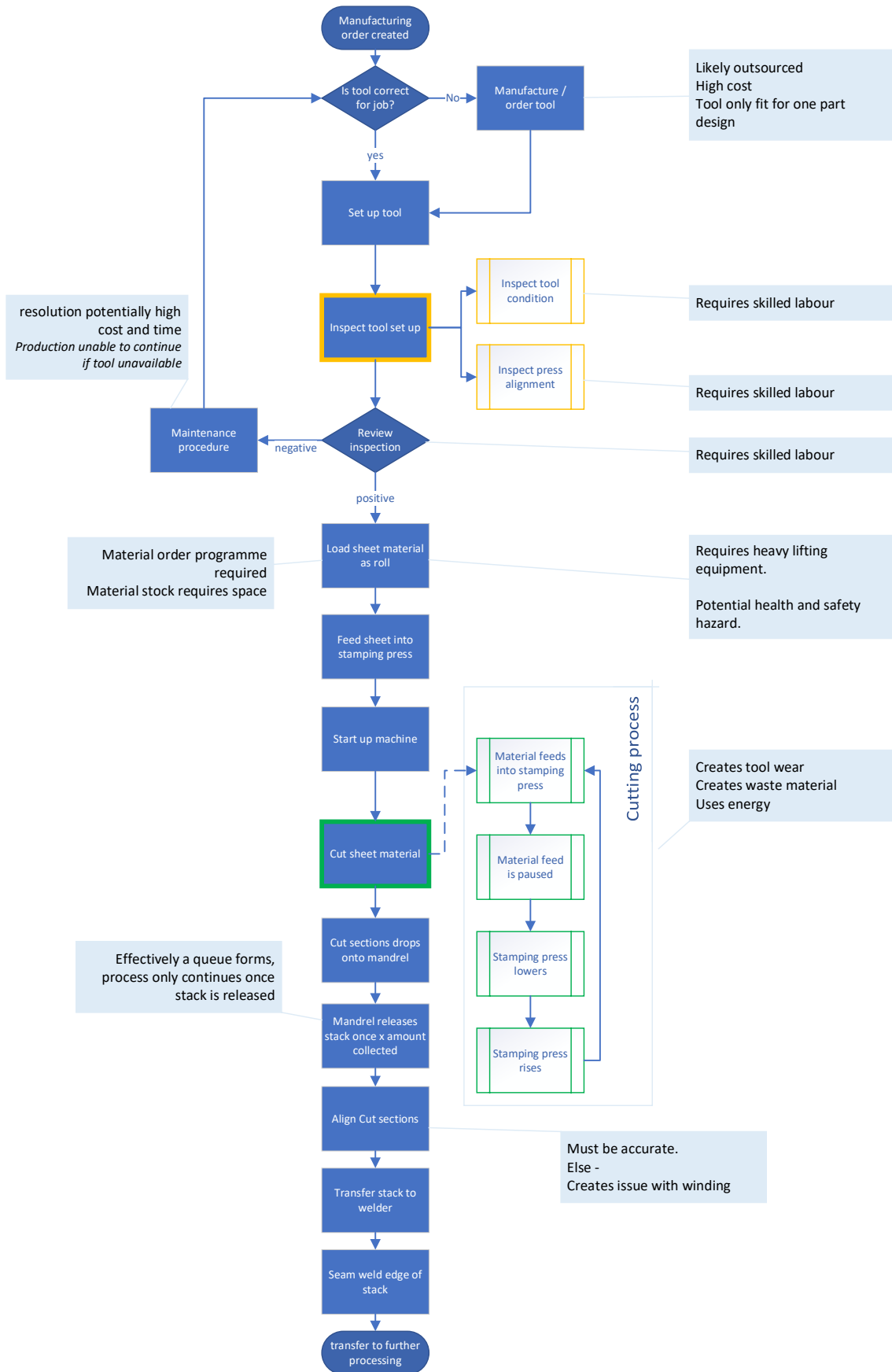


Figure 48 Process map for standard stamping route

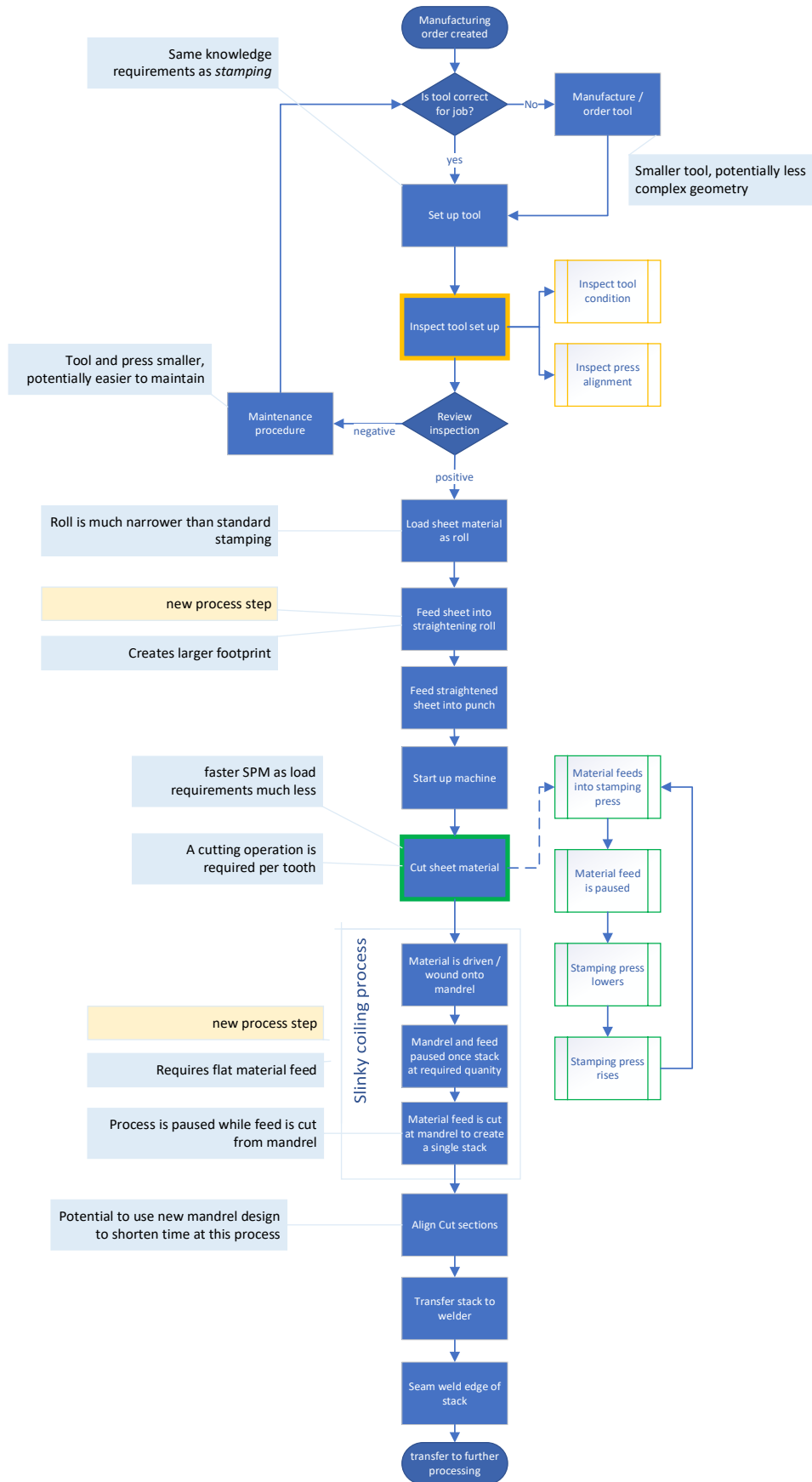


Figure 49 Process map for a slinky style stator

### 4.3 Development of manufacturing cost model for stator stamping activities

The stamping process identified from inspection of Figure 12 (p.36) and interpretation of the Mechler induction motor process (Section 2.2.5) is a four-step cutting process. This has been simplified into a single cutting step within the manufacturing model at this stage. The forces related to each cutting step are accounted for in the model, but they are used to provide an estimate for the simplified 'single cut' version of the cutting process which is considered from this point.

Four design features have been identified; part thickness, inner diameter size,  $L_D$ , number of slots and the length of cut  $L_C$ . Each of these features will be assessed using a tool in order to discover their effect on manufacturing costs, as well as further understand any issues which might arise from the design of these features. The aim of this model is to create a tool which can provide an understanding of how different design and machining decisions will affect the overall performance of the process. Whilst every effort has been made to ensure that all the data is specific and evidenced, there are some parameters that are included using a more general rule of thumb. These parameters were deemed important to include in the model, as this provides a more realistic model of operations, if not 100% accurate. The figures used in the model are from various sources, with some data being based on specific examples or knowledge, and some data estimated, this has been identified in the model by the key provided in Figure 50. The electric machine design is based on the general design specification for a synchronous reluctance electric machine as provided by Ricardo as the commencement of this research project (see Table 1, p17).

<i>Input</i>	<b>Known</b>	specific and evidenced
<i>Reliability</i>	<b>Estimated</b>	backed by evidence or standards
<i>key</i>	<b>Nominal</b>	user expectations

Figure 50 Reliability of data

For each part of the model, there are two sections, key outcomes, and variables / required information. Whilst the main purpose of this is to achieve clarity within the model, it should be noted that some inputs could equally be considered as key outcomes, and this is reflected later as further analysis is conducted.

The simplest part of the model is the *production quantity*. There are two fundamental aspects, how many machines are intended to be produced, and the size / length of each machine. Orders are made in terms of stacks in real life, but it is laminates that are being produced at the cutting stage of the process. The part design and material choice are based on the general requirements for a machine of the prerequisite size. The part design parameters can be altered in the model to better reflect the design of machine being considered, or as in this study, to consider the manufacturing implications of the various design criteria.



A major aspect of manufacturing is the ability to produce goods in a timely manner. This part of the model begins to examine the dynamic relationship between producing laminates at speed and producing laminates at cost. The most complex aspect in this trade off relates to the tool wear and condition. The model includes time lost to maintenance and tool change. These variables are difficult to model accurately, particularly with regards to maintenance, as there is a wide range of times it might take to perform a maintenance operation for any given maintenance issue. Similarly, time lost to tool changes is inconsistent and further affected by other aspects of the model. These variables have been included with values that offer a realistic representation of the effects as opposed to a highly accurate reflection of events. A variable, overhead rate, has also been included to represent the cost of time taken to manufacture goods. The overhead rate is a simple method of capturing the cost of labour, space and other resources that would be used by the process, but not directly attributable. The overhead rate is highly dependent on the specific circumstance of any business but is a useful measure to understand the further effects of manufacturing time.

The model has included various aspects of manufacturing costs, these are split into two main sub-categories, energy costs and machining costs. The cost of a die is directly linked to the quality of the die, which in this case, is proportional to the tool hardness. Stamping tools, not including the stamping press, can cost vast sums. Figures of the region £100,000 - £500,000 are not uncommon for stamping tools, particularly if made from quality materials and with more complex geometries. The parameter 'number of strokes until tool failure' has been considered in much more detail. The benefit of this research is a much greater understanding of how manufacturing parameters affect tool life.

#### 4.3.1 Stamping model assumptions

The model produced in this work represents a simplified version of the stamping process. As such, assumptions have been made to simplify some areas within the stamping processes which would at this stage be difficult to account for individually or specifically.

- The model assumes that the cutting operation is completed in a single cutting stroke.
- The forces in the model are identified for each design feature of the stator, however these are combined to provide a single force. This force is therefore applied to a single tool whereas the tool previously identified in this research (Figure 12 p36) has four separate tools.
- The cutting tools in this model are used only once. They are not re-grinded or re-purposed.
- The maintenance operation is considered towards the tool and stamping press for issues such as set-up, tool alignment and general press maintenance.
- Sheet material costs (£/kg) is constant for all sheet thicknesses.

Production quantity				
key outcomes	Total number of stacks	$n_{stacks}$	100000	
	Laminates per stack	$n_{lps}$	286	
	Total required Laminates	$n_{lams}$	28571429	
variables / required info	m	sheet thickness	$L_d$	
	m	stack length	$L_{stack}$	
				0.00035
				0.10

Table 8 Production quantities

The total number of laminates required to produce the requested number of stacks is defined by equation ( 4.1 ). The number of laminates in each stack is a function of the laminate thickness and proposed stack depth ( 4.2 ).

$$n_{lams} = n_{stacks} \cdot n_{lps} \quad ( 4.1 )$$

$$n_{lps} = \frac{L_{stack}}{L_d} \quad ( 4.2 )$$

(Notation listed in Table 8 - Table 11)

Part design details & material choice			
m	Length of cut	$L_c$	2.0
$m^3$	Material used in n stacks	$V_{ups}$	419
£	Material value in n stacks	$C_{ups}$	£ 1,674,012
$m^3$	Material scrapped	$V_{sps}$	801
£	Material value scrapped	$C_{sps}$	£ 3,203,614
N	NUMBER OF SLOTS PER LAMINATION	$n_{slots}$	20
$m^2$	SHEET SIZE (SQUARE)	$A_{sq}$	0.122
m	INNER DIAMETER	$L_{ID}$	0.17
m	OUTER DIAMETER	$L_{OD}$	0.2910
$m^2$	INNER AREA	$A_I$	0.02270
m	INNER CIRCUMFERENCE	$L_{IC}$	0.5341
$m^2$	OUTER AREA	$A_O$	0.06651
m	OUTER CIRCUMFERENCE	$L_{OC}$	0.9142
m	SINGLE SLOT OUTLINE	$L_{slot}$	0.042
$m^2$	SINGLE SLOT AREA	$A_{slot}$	0.000098
$kg / m^3$	DENSITY	$\rho$	8000
£ / kg	MATERIAL COST / KG	$C_{kg}$	£ 0.50
£ / $m^3$	MATERIAL COST / M3	$C_V$	£ 4,000.00
Pa or $N/m^2$	ULTIMATE TENSILE STRENGTH	$\sigma_{UTS}$	510000000
	CUTTING RESISTANCE	$\sigma_{CR}$	408000000

Table 9 Part design and material choice

The length of cut (*per laminate*) is derived by collecting the various lengths of each cut required ( 4.3 ) to produce each feature (outer diameter, inner diameter, stator slot). The volume of material used is defined by equation ( 4.4 ) and the volume of material scrapped is defined by equation ( 4.5 ). The material costs are estimated based on CES Edupack (2018) results (see also section 4.5.2)

$$L_c = (L_{slot} \cdot n_{slots}) + L_{OC} + L_{IC} \quad (4.3)$$

$$V_{ups} = (A_O - A_I - (A_{slot} \cdot n_{slots})) \cdot n_{lams} \cdot L_d \quad (4.4)$$

$$V_{sps} = (A_{sq} \cdot L_{stack} \cdot n_{stacks}) - V_{ups} \quad (4.5)$$

(Notation listed in Table 8 - Table 11)

Production rates			
			Stamp
hours	Time to produce quantity	$t_{\alpha}$	3099
secs	av. laminate production rate	$t_{lam}$	0.39
secs	av. stack production rate	$t_{stack}$	112
£	Overhead costs	$C_O$	£ 619,860
£/hr	Overhead rate	$C_t$	£ 200.00
Operation per minute		$\alpha_O$	300
laminates cut per operation		$\beta$	1
%	FORCE FACTOR OF SAFETY	F	2
kN	INNER CIRCUMFERENCE	$P_{IC}$	152.53
kN	OUTER CIRCUMFERENCE	$P_{OC}$	261.10
kN	SLOTS	$P_{slots}$	205.63
kN	TOTAL FORCE / STROKE	$P_{\Sigma}$	619.26
mins	Maintenance time	$t_m$	240
mins	die change over	$t_D$	480

Table 10 Production rates for stamping

The time taken to produce the total number of stacks is defined by equation ( 4.6 ). It should be noted that the total force calculation is based on a simplification of the 4-stage progressive die stamping process, in which a single cutting operation is considered rather than four individual cutting operations. This in turn means that the model is considering a single tool, where there would instead be 4 tools (one tool for each of the 4 cutting steps). The overhead rate figure has been estimated following consultation with operations management professors at the University of Sheffield (Ballantyne & Heron, 2020). The overhead rate has been studied further to understand its effect within the system. The force factor of safety represents a how much extra force is used during a stamping operation to ensure the cut is achieved. The force factor of safety, maintenance time and die change over times have been estimated based on conversations with industry (Campbell & Brittle, 2017).

$$t_{\alpha} = \frac{\frac{n_{lams}}{\alpha_O \cdot \beta} + t_m \cdot n_m + (t_D \cdot (n_D - 1))}{60} \quad (4.6)$$

(Notation listed in Table 8 - Table 11)

Costs			
			<b>Stamp</b>
Energy costs	$C_E$		£3,934
Machine & Machining	$C_{\alpha o}$		£11,289,266
Maintenance	$C_{\alpha m}$		£286,000
Consumables & other	$C_c$		
Total costs (Machining)	$C_{\Sigma \alpha}$		£11,579,200
Total costs (inc raw Mats)	$C_{\Sigma^*}$		£17,076,686
Av. Stack Cost	$C_{\bar{x}}$		£170.77
Energy costs			
£ / kWh	RATE	$C_{eW}$	£ 0.25
£ / kJ	RATE	$C_{eJ}$	£ 0.000069
kJ	Inner circumference	$E_{IC}$	0.053
kJ	Outer circumference	$E_{OC}$	0.091
kJ	slots	$E_{slots}$	0.084
kJ	Die position return	$E_m$	1.766
kg	Die Mass	$E_{DM}$	200
m	Die Travel	$L_{DT}$	0.3
Machining & other costs			
	Die cost	$C_D$	£ 240,197
	Tool Hardness	H	62
	Number of strokes until tool failure	$n_{\alpha}$	617672
	Tools required to produce stacks	$n_D$	47
	Cost of performing maintenance	$C_m$	£ 1,000
	Number of strokes until tool maintenance	$n_s$	100000
	Number of tool maintenance occurrences	$n_m$	286.00

Table 11 Production costs for stamping

The cost accounted to energy usage in the stamping process is estimated using equation ( 4.7 ). The cost of purchasing tools for machining is given by equation ( 4.8 ). The cost of maintaining the machines and tools is defined by ( 4.9 ). The total machining costs are then calculated using equation ( 4.10 ).

$$C_E = (E_{IC} + E_{OC} + E_{slots} + E_m) \cdot C_{eJ} \cdot n_{lams} \quad (4.7)$$

$$C_{\alpha o} = C_D \cdot n_D \quad (4.8)$$

$$C_{\alpha m} = C_m \cdot n_m \quad (4.9)$$

$$C_{\Sigma \alpha} = C_E + C_{\alpha o} + C_{\alpha m} \quad (4.10)$$

(Notation listed in Table 8 - Table 11)

## 4.4 Tool failure predictive model

One of the most complex aspects of stamping is understanding the lifecycle of a stamping tool and the variables which effect the rate at which the tool wears. An analysis of various stamping studies has been conducted, though these outcomes should be tempered by the understanding of incomplete knowledge of processes and materials used in all tests and experiments.

### 4.4.1 Methodology

The creation of an evaluative, dynamic tool for understanding how stamping parameters and part design effect the performance of a laminate is a highly complex affair and beyond the scope of this work. The model is structured from two distinct yet highly interactive parts.

The first consideration is the quality or condition of the cutting tool. A link has already been established between tool sharpness and laminate quality. The tool's condition will deteriorate with each cutting operation. The effect of each cutting operation, or the wear rate, is dependent on the circumstance of the cutting operation.

Tool wear mechanisms have been considered. However, as these are complex, dynamic and non-linear, these factors cannot be modelled accurately by such an approach and are not included mathematically within the model.

Kraemer's (2015) tool wear data gives a good indication of a typical wear pattern for a stamping tool. Flank wear shows continuous wear throughout the operation of the tool and is also similar to a typical tool wear curve.

### 4.4.2 Wear parameters

The model attempts to assess the proportional wear or tool life, as opposed to direct calculations. Archard's wear equation ( 2.12 ) shows that tool wear is proportional to; sheet thickness, material strength, tool hardness and length of cut. Cutting speed is considered in a slightly more complex way. Archard's' equation includes a parameter K which is found empirically for a give given set up. This parameter, k, accounts for tool parameters which Archard does not include in his considerations but non the less influence the tool wear. As a result of this gap, it may prove necessary to manipulate the equation somewhat to create a model which works without relying on an empirical input.

#### 4.4.3 Application of Taylor's tool wear to stamping

Using a combination of Kraemer's (2015) results and Taylor's tool wear equation ( 4.11 ) it is possible to generate a prediction of the number of strokes a stamping tool will be able to make and remain useful. For a continuous cutting operation it would be typical that the tool speed would be considered in m/s or mm/s . However, as stamping is not a continuous cutting operation, and given that the stroke rate is more closely linked to the production rate in this case, tool speeds are calculated in strokes per minute (SPM) and tool life as number of strokes.  $v_1$ : 300 SPM,  $T_1$ : 750000 strokes as Kraemer's (2015).

$$\frac{v_2}{v_1} = \left(\frac{T_1}{T_2}\right)^n \quad ( 4.11 )$$

$$v_2 = v_1 \cdot \left(\frac{T_1}{T_2}\right)^n \quad ( 4.12 )$$

$$T_2 = \frac{T_1}{\sqrt[n]{\frac{v_2}{v_1}}} \quad ( 4.13 )$$

The key parameter in the model for this project is the operating speed,  $\alpha$ , measured in strokes per minute. there is a definite relationship between operating speed,  $\alpha$ , and cutting speed,  $v$ , and as such, the terms are used interchangeably ( 4.14 ) for the application of the Taylor tool wear modelling process.

$$\alpha \cong v \quad ( 4.14 )$$

#### 4.4.4 The n problem

It is important that the tool life model is accurate for a wide range of operating speeds. a stamping press can operate at anywhere between 20 SPM and 1500 SPM (efunda, 2020), though higher rates are more likely for thinner and softer materials, such as Stroud Metal Company Limited (2020) production of less than 1mm thick parts at 1200 SPM. Stamping dies for rotor and stator production, such as in this project, are listed on websites such as METs (2020) stating maximum operating speeds of approximately 600 SPM – 800 SPM. These tools also typical state a tool life of 2-4 million strokes.

Despite knowing the tool material used by Kraemer would typically have an n value between 0.1 – 0.2, these values for n provide an unrealistic model of the potential effect of tool speed on tool life. For speeds below 100 SPM the tool life well exceeds 60,000,000 strokes, and at speeds approaching 800 SPM, the tool life would be below 20,000 strokes. These figures are well in above and below (respectively) of those that are being advertised for a standard tool die, and although both are feasible strokes per minute (they

are reported in literature as values used in investigations, and are within the rated capabilities of existing production machines), but the resulting lifetimes are never as high or low, respectively, as the output numbers. Given that Taylor's equation considers a continuous cutting operation, a typical value of  $n$  appears to be no longer suitable to accurately reflect the tool wear dynamics in stamping. The effect of  $n$  on tool life data is plotted in Figure 51.

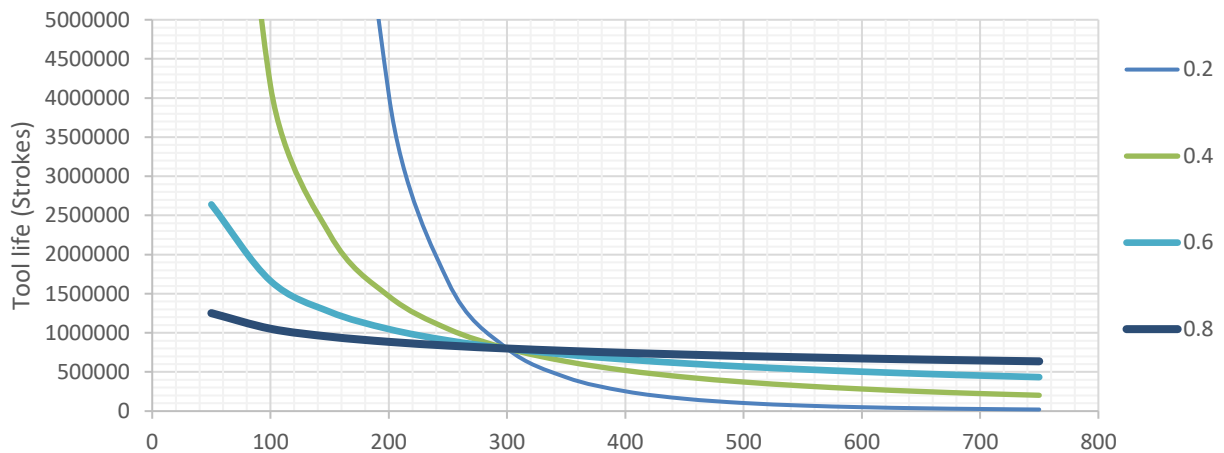


Figure 51 Tool life prediction for various  $n$  values

A further proof of the inadequacy of using standard values for  $n$  is shown in Figure 52. This applies Taylor's equation to four different tools and plots the various predicted tool lives against tool speed. For the types of stamping operations being considered, actual operational tool speeds could reasonably range from 60 SPM to 800 SPM and are shown by a shaded region. In this example, tool lives exceed 10,000,000 strokes for speeds under 100 SPM, well beyond any baseline tool expectancy, and appears to demonstrate that Kraemer's tool (63 HRC) lasts significantly longer than Mucha's tungsten carbide (85 HRC) tool for all speeds. Whilst this is not necessarily impossible, it is not an expected result, as the parameter differences otherwise are reasonably similar.

A further test was modelled using an  $n$  value of 0.8. These results provide a much more realistic view of the potential tool lives. However, there is still an issue. For speeds approaching 0 SPM, the tool life approaches infinity. The model therefore suggests that at 1 SPM any tool would last for an *almost* infinite number of strokes. This is an issue for all values of  $n$ . Instead, in order to obtain a useful output for the model developed here, the idea of a terminal tool life is considered. Any tool can only produce so much work. A tool, unused, fresh off the shelf, does not have 'infinite life,' it has some finite amount of usable working life that it can give. No matter how carefully a tool is used with optimum conditions for life extension, at some point it will break or be degraded to a point where it is no longer useful.



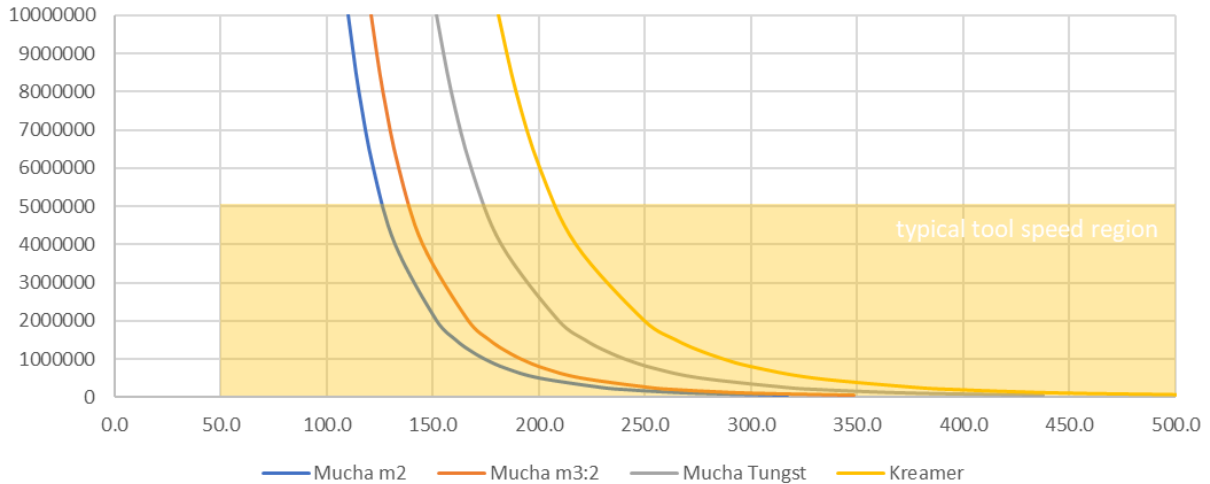


Figure 52  $n$  effect for various tool data  $n$  0.2

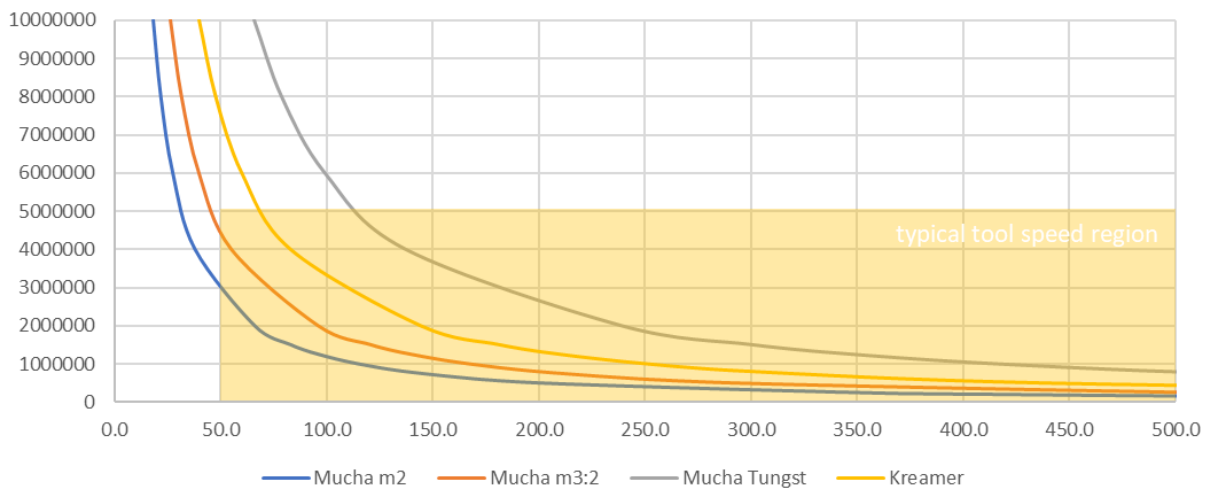


Figure 53  $n$  effect for various tool data  $n$  0.8

The addition of the function  $v_s$  has the effect of moving the asymptotic part of the graph, such that the new graph is asymptotic at  $-v_s$  SPM, instead of 0 SPM. Figure 54 demonstrates this effect, with the various tools being asymptotic at  $-150$  SPM. To maintain accuracy with the known tool life data,  $T_1$  at  $v_1$ ,  $v_s$  has also been added to  $V_1$ . For the purpose of  $v_1$ , the  $v_s$  functions cancel each other out. This can be seen in Figure 54, as each tool data set still passes through its original  $T_1$  and  $v_1$  values. This approach is considered to be suitable for models where the tool parameters are reasonably similar to the original data set. However, the approach works less well where the tool parameters, such as tool type and hardness differ more greatly. A separate approach was taken to incorporate these variances.

$$T_2 = \sqrt[n]{\frac{(v_1 + v_s) T_1^n}{v_2 + v_s}} \quad (4.15)$$

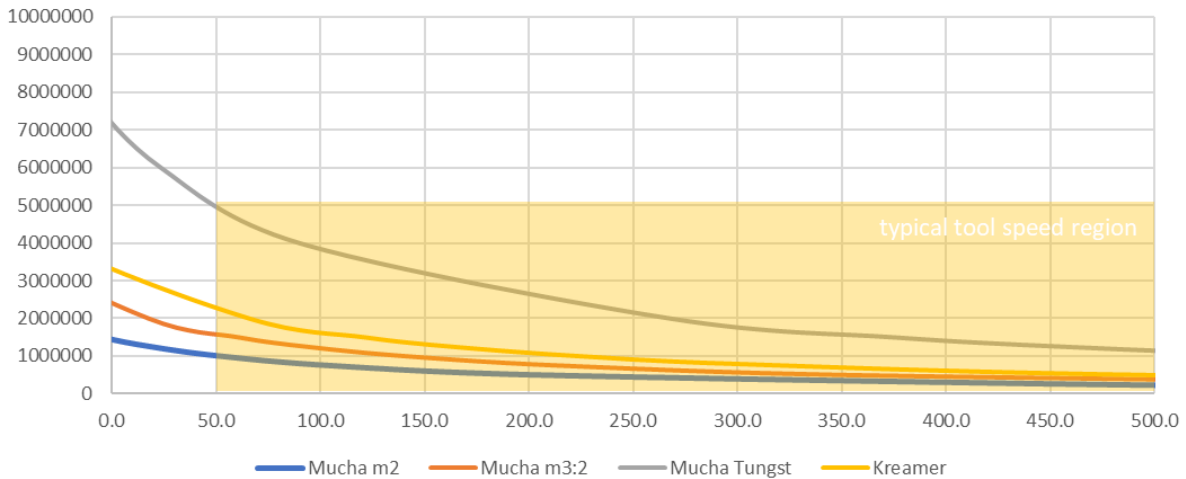


Figure 54 Shifted data (150 shift)

4.4.5 Tool hardness issue and solution

There are a number of issues regards the implementation of tool hardness in the Archard model. Firstly, it is noted that Rockwell hardness (the value most readily available to characterise the mechanical response of most tool materials) is “an inadequate measure of wear resistance” (Syed, 2006, p. 29).

Furthermore, tool hardness is only one tool parameter. The Archard equation does not identify the effects of friction co-efficient or thermal degradation. The effect of these parameters would be captured as part of the all-encompassing k function, which is found empirically, and takes a particular value for a certain temperature, for example. Using the standard Archard equation, the predictive tool life model is only capable of producing accurate results where tool hardness is close to the baseline.

To improve the accuracy of the new tool life model for a much greater range of tool hardness, it was assumed that (as is considered in the Archard equation) tool hardness is an indicative measure of how materials properties will affect tool wear resistance. There are any number of unknown parameters relating to the tool which could also alter the potential tool life. These could be one unknown parameter or hundreds of highly specific ones, as in equation ( 4.16 ). This simplest expression of the hypothetical tool effect,  $T_e$  , is to collect the unknown terms. Given that H is being used as a driving function, such that H is proportional to any given  $T_e$ ,  $T_{e\text{unknown}}$  is substituted with H. This produces an equation ( 4.17 ) which can be fitted empirically to the (limited) data that exists linking tool life in stamping to other variables.

$$T_e = H \times T_{e1\text{ unknown}} \times T_{e2\text{ unknown}} \times T_{e3\text{ unknown}} \times T_{e4\text{ unknown}} \dots \dots \dots \tag{ 4.16 }$$

$$T_e = H \times T_{\text{unknown}}^n \tag{ 4.17 }$$

Various values of n were modelled. Figure 55 (c) shows the effect of using an n power of 5 for the tool effect function ( 4.18 ) compared to a base power 1 (standard Archard) in Figure 55 (b).

$$T_e = H^5 \tag{ 4.18 }$$

The final tool life prediction model provides accurate results across the various data sets and successfully provides a realistic interpretation of how the various stamping parameters effect the tool life. During the development of this solution, it can clearly be seen by comparison of Figure 55 (a) and Figure 55 (d) that the new solution has results which are much more aligned to those in the data by using the various the mathematical tools. Figure 56 and Figure 57 demonstrate this by clearly showing the trend of each solution against the expected result, where a 1:1 relationship is ideal. Though these tools are quite crude, given the objectives of this study to understand the wider economic implications of the machining process, they are well suited to provide a general picture of the tool life.

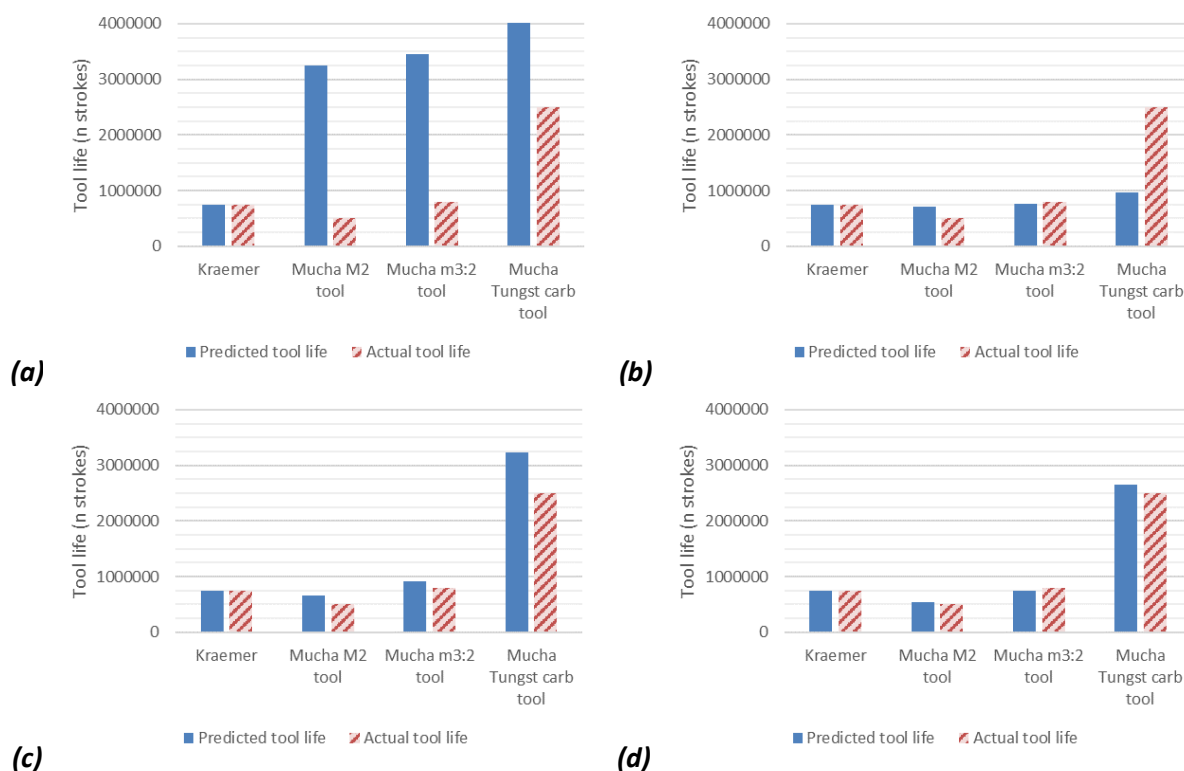


Figure 55 Development of solution where (a) Model with n 0.2 (b) Model with n 0.8 (c) Model with Tool Hardness power 5 (d) Model with shifted axis by 150

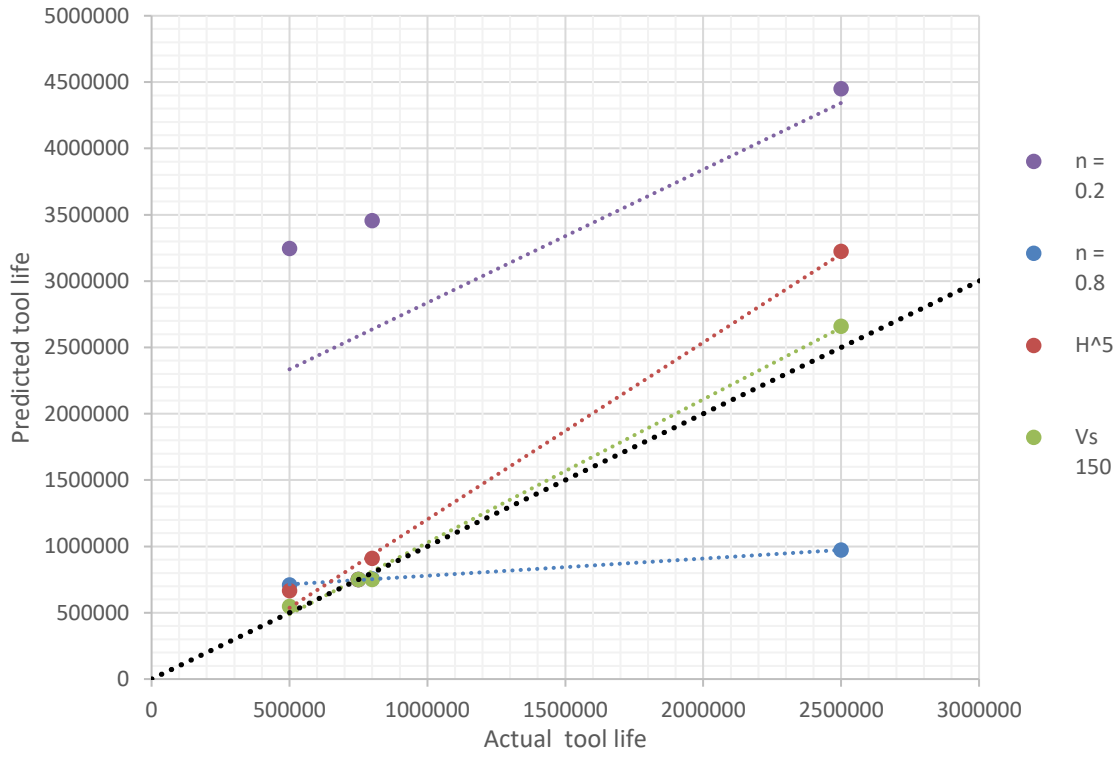


Figure 56 Correlation between actual life and predicted tool life

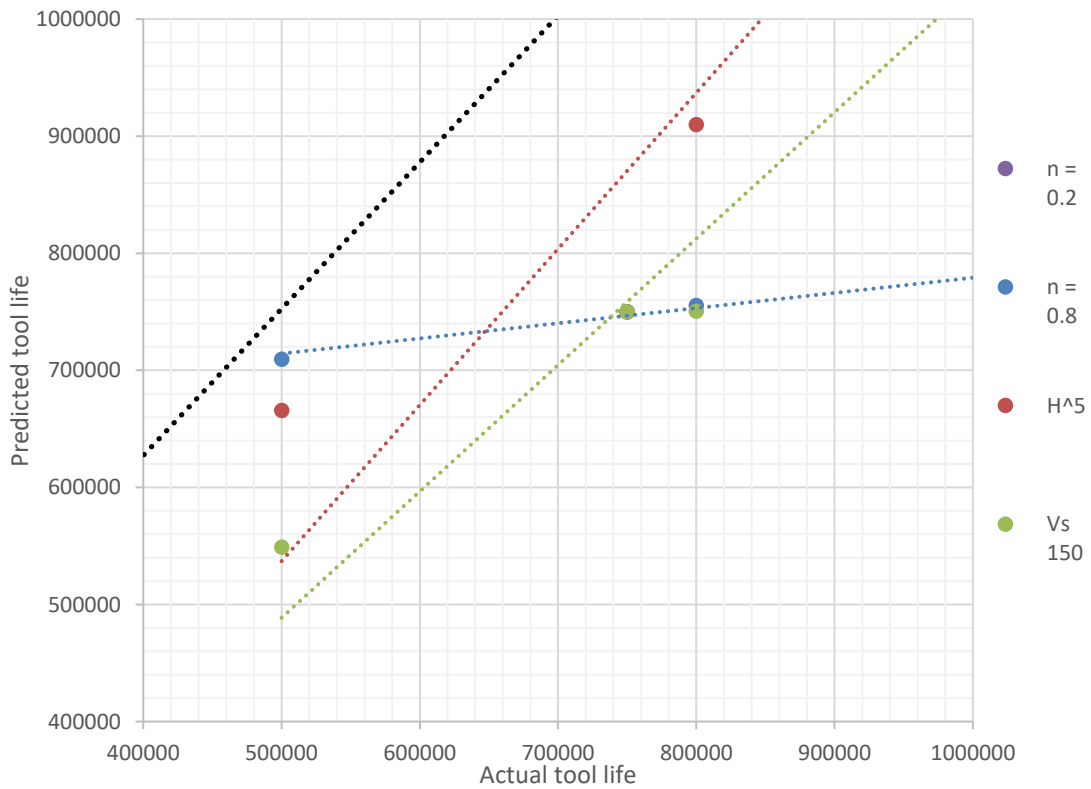


Figure 57 Expanded view of correlation between actual life and predicted tool life

#### 4.4.6 Final tool wear model implementation

The final tool wear model incorporates the various ideas which have been developed within this project to create a model which applies to the stamping of thin laminations. The knowledge derived from Taylors tool wear model has been used to derive equation ( 4.19 ), and this has been combined with the Archard tool equation, using laws of proportionality for the variable of Sheet thickness,  $L_d$ , Sheet cutting resistance,  $\sigma$ , and also tool hardness,  $H$ , which has been considered to be an indicator of further tool parameters as described in section 4.4.5. The combination of these factors is used to produce an estimate for the number of strokes a tool will be capable of producing cuts before it is considered to have reached the end of the tool's life ( 4.23 ). If all parameters are set to the baseline level, the proportionality is 1:1.

$$T_2 = \sqrt[0.8]{\frac{\alpha_1 T_1^{0.8}}{\alpha_0 + \alpha_s}} \quad ( 4.19 )$$

$$H_P = \frac{H^5}{H_{base}} \quad ( 4.20 )$$

$$L_{dP} = \frac{L_d^2}{L_{d\ base}} \quad ( 4.21 )$$

$$\sigma_P = \frac{\sigma}{\sigma_{base}} \quad ( 4.22 )$$

$$n_\alpha = T_2 \times \frac{H_P}{L_{dP} \cdot \sigma_P} \quad ( 4.23 )$$

Kraemer's results (one of few datasets to show wear progression in a tool across several cycles) have been plotted and recorded to generate an empirical baseline. Using proportionality, a new output is recorded as tool condition, where the tool is deemed to be out of condition (>100%) once it has entered the runaway stage of its wear.

TOOL AFFECTING PARAMETERS			INPUT VARIABLE	BASELINE	Proportionality
	SPM	Cutting Speed	<b>300</b>	<i>60-800 Limits</i>	750000
Wear effect	mm	Sheet thickness	<b>0.35</b>	0.35	1.00
Wear effect	MPa	Material Strength UTS	<b>510</b>	455	1.12
Wear effect	HRC	Tool hardness	62	63	0.92
<b>Total Proportionality</b>					<b>0.82</b>
<b>Strokes till worn</b>					<b>617672</b>

Table 12 Tool life extension to manufacturing model

#### 4.5 Analysis of materials used in stamping process

In most stator stamping operations, the stator and rotor are produced simultaneously in the same stamping tool, from the same sheet material. An initial study was conducted into electric machine laminate materials for both rotor and stator application. The data in Table 13 reflects the specification as described by Table 1 (p17).

<b>MAX Density of rotor material</b>		kg/m <sup>3</sup>	
leap		2643	
stretch		5022	
step		9252	
<b>MAX Material cost per kilogram</b>		\$/ kg	£/ kg
leap	\$	8.75	7.00
stretch	\$	10.53	8.42
step	\$	16.67	13.33
<b>MIN Required tensile strength [Tangential]</b>		Pascals	MPa
<i>Factor of safety = 1</i>			
leap		349897000.00	349.90
stretch		295468000.00	295.47
step		241904000.00	241.90

*Table 13 Stator & rotor requirements*

In addition to the values in Table 13, the maximum magnetic permeability of the potential material was considered. The value for maximum permeability (also relative permeability) used in the search was 18000 based on the magnetic properties for 4Si-Fe soft magnetic alloy (section 2.2.2). These value were then entered in the CES software to provide a list of materials which satisfy the requirements in each of the scenarios outlined. CES Edupack (2018) is an academic resource which contains a large database of materials and material properties.

##### 4.5.1 Assumptions in stamping cost model

- It has been assumed that the stator & rotor will be 100mm in length and the rotor is assumed to be manufactured as a solid homogenous part. This is highly unlikely to be the case, for example Figure 7 (p29) shows a rotor with air gaps. For this study, approximating the part as a solid should still present a reasonably accurate output.
- It has been assumed that the material properties are consistent for all temperatures. This is clearly not the case. The potential effect on the properties of material at high temperatures are considered in the discussion.
- The tangential stress is equal to the radial stress for each scenario and as such, only the tangential stress is considered.
- The stator back iron width is constant unless otherwise stated, such that when the inner diameter changes, the out diameter also changes by the same amount.

#### 4.5.2 Results

The CES software was unable to find any materials which satisfied the stretch and leap conditions. Listed below are the materials which satisfied the step conditions. They have been categorised into three distinct types; nickel alloys and cobalt iron, Metglas and electrical steels. These materials are compared graphically Figure 58 and Figure 59.

##### *Nickel alloys and Cobalt Iron*

*Nickel alloys and Cobalt Iron* price ranges from £10-13/kg approximately, which is 20x more expensive than Electrical steels. *Nickel alloys and Cobalt Iron* are also denser than electrical steels without providing any significant increase in tensile strength.

- Nickel-magnetic alloy, 49Ni-Fe, Alloy 2B, soft (annealed)
- Nickel-magnetic alloy, 49Ni-Fe, Alloy 2B, cold rolled, soft
- Nickel-magnetic alloy, 45Ni-Fe, Alloy 1, soft (annealed)
- Nickel-magnetic alloy, 45Ni-Fe, Alloy 1, cold rolled, soft
- Nickel-magnetic alloy, 45Ni-3Mo-Fe, soft
- 2V-49Co-49Fe (high purity) soft magnetic alloy

##### *Metglas*

*Metglas* is the least dense material, whilst simultaneously providing the most strength. *Metglas* . However comes at a cost 10x greater than electrical steels.

- Metglas 2826MB (iron-nickel based)
- Metglas 2605SC (iron based)
- Metglas 2605SA1 (iron based)
- Metglas 2605S3A (iron based)
- Metglas 2605CO (iron based)

##### *Electrical steels*

Electrical steels are the standard use material for stator and rotor production. They are by far the cheapest. However, they are also offer the least tensile strength.

- 4 Si-Fe soft magnetic alloy
- 2.5 Si-Fe soft magnetic alloy

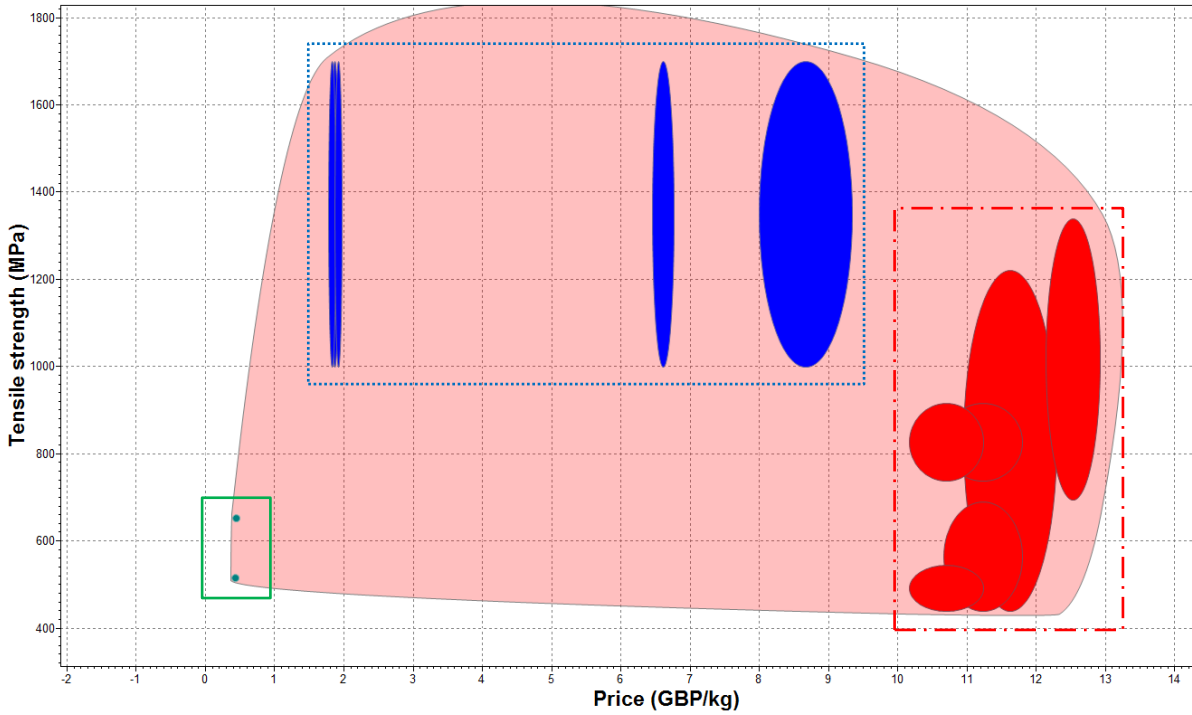


Figure 58 STEP condition results- price against tensile strength (CES Edupack, 2018)

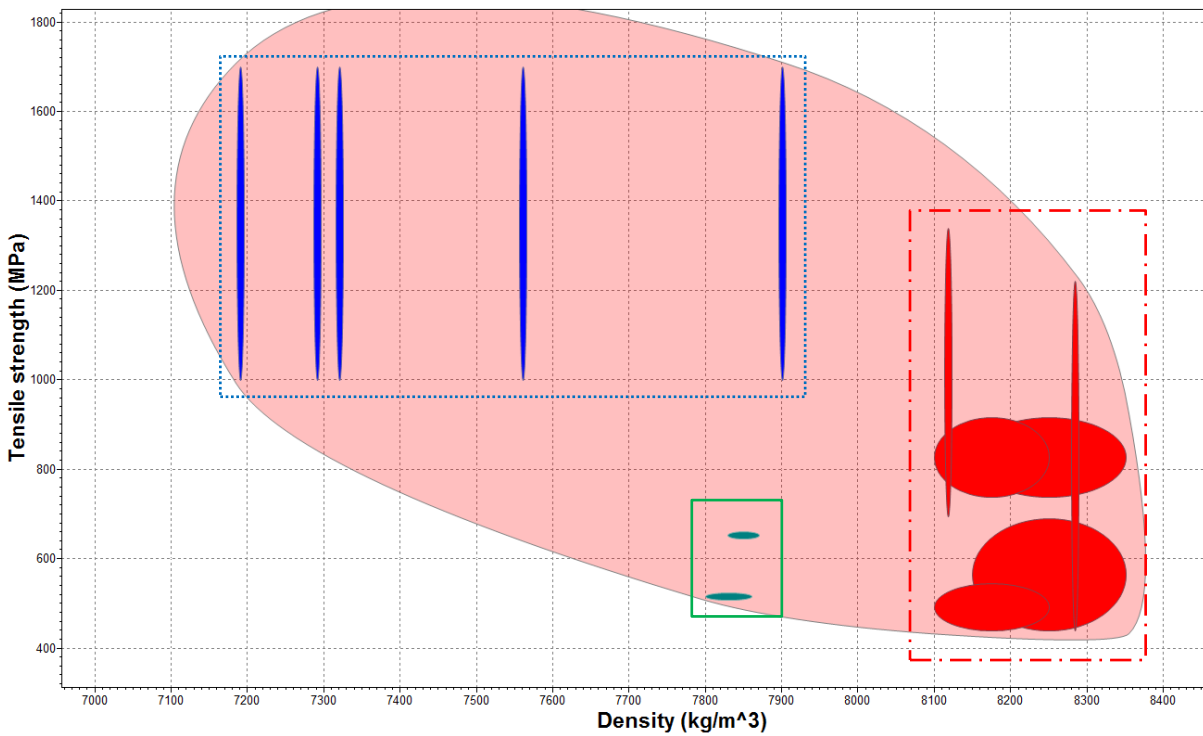


Figure 59 STEP condition results- density against tensile strength (CES Edupack, 2018)



#### 4.5.3 Stator & rotor material alternatives

Three potential material groups emerged in the step condition search on CES. The *Nickel alloys and Cobalt Iron* are the heaviest, most expensive and contain some of the weakest available materials. Whilst the *Nickel alloys and Cobalt Iron* appear to clearly be the worst materials of those considered based on the step conditions search, there is no clearly definitive best material. The lightest material is a form of Metglas. Not only is the Metglas the lightest material, but it is also the strongest available material; . However, this comes at a cost. The cheapest Metglas costs four times the price of silicon steels and is only around 10% lighter than silicon steels. The higher strength and lower density may mean that less material is required in each machine, potentially creating a greater cost benefit relative to electrical steels. Some markets, such as motorsports and high-end sports cars, may be willing to accept the higher costs of a material such as Metglas as the benefits of weight reduction are much more important to these sectors.

These results are based on the assumption of a single solid part. However, will not be the case for the final rotor. A typical rotor for example includes ‘airgaps’ or ‘flux barriers.’ These flux barriers would effectively reduce the volume of material used in the rotor and as such raise the allowable density of a material. The air gaps would also alter the stresses in the rotor, meaning that the material might in fact be required to have a higher tensile strength. Further information is required to be able to adequately understand which materials are the most suitable for use in this project. It is possible that whilst Metglas may be more expensive to purchase, it might also be less expensive to machine than silicon steels.

It is also very important to consider the material’s ability to operate at higher temperatures. It is not known how these materials change with respect to temperature. Should a material lose its magnetic properties at high temperatures, an aspect which is affected by curie temperature, or become less strong at higher temperatures, then the material would cease to be capable of satisfying the step conditions.

There were no results for stretch and leap conditions within CES. This is due to the density requirements for these conditions. Not including density in the search criteria, silicon steels and some Metglas materials would have appeared within the stretch and leap results as they satisfy the price and strength requirements. As previously mentioned, these results are based on the assumption of a single solid part.

This study is considered from a purely mechanical engineering perspective. Further work should be undertaken from an electrical engineering approach to understand how the changes in material will affect the overall performance of the machine. One example is that changes to the stator or rotor materials can affect the parts reluctance and therefore affect the torque capability of the machines.

4.6 Study of manufacturing model for stamping of stator laminations

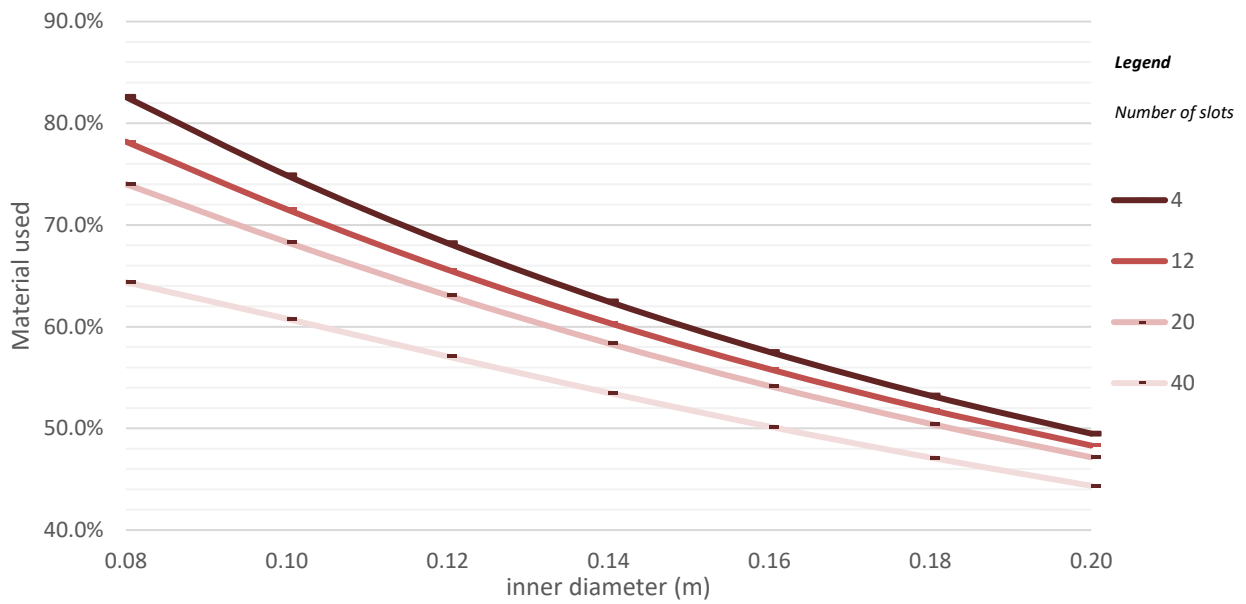


Figure 60 effect of inner diameter size on proportion material scrapped<sup>3</sup>

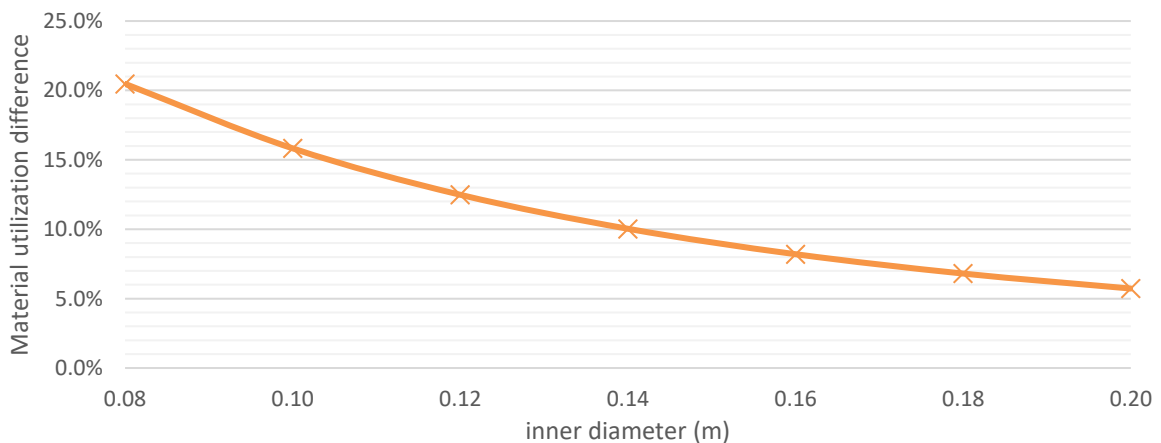
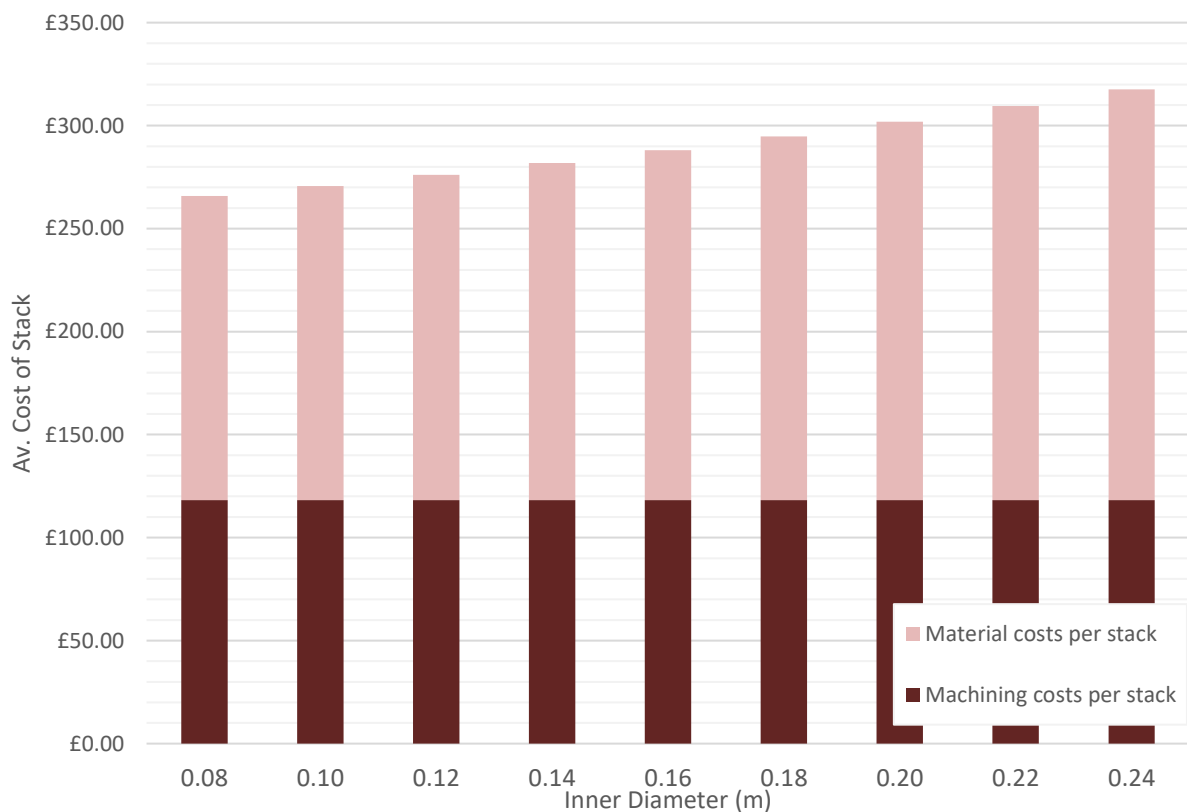


Figure 61 Material utilization difference between 0 slots and 40 slots

As the inner diameter is increased, the proportion of material which is scrapped also increases. There appears to be a linear relationship between the size of the *inner diameter* and the % of material scrapped. For the region of inner diameters considered, there is always more than 50% material scrapped. As the number of slots increases, the proportion of material scrapped increases. as the inner diameter increases, the effect of the number of slots on material utilization diminishes. It should also be noted that the sheet thickness has no effect on the amount of material which is utilized or scrapped. This is expected as the amount of material used to produce a stack remains constant across different lamination thicknesses.

<sup>3</sup> It is not necessarily feasible to change number of slots to 4, 20 or 40 without further stator design alterations. Additionally, the size of slots should remain constant ideally to maintain current carrying capability. The number of slots function provides an indication of material utilization for designs which would use differing numbers of slots.

The most prominent source of material waste occurs because of the *inner diameter* design parameter. (Figure 60). Normally this material would be used to produce a rotor concurrently. However, given that research into new novel rotor technologies is ongoing, it would be a limitation of the application of this research to assume that this material would indeed be utilized in the manufacture of a rotor. Reducing the size of the inner diameter would positively affect material utilization. However, this then reduces the available space to insert a rotor, reducing the potential power / torque capabilities of the machine. Increasing the output does not affect the amount of scrap produced. However, it may increase the value of reverted scrap due to the higher quantities of scrap collected.



*Figure 62 Inner diameter effect on average production cost per stack*

The average cost of producing a stator stack increases as the size of the stack increases. There is the intrinsic use of more material in a larger cross section. This effect might be offset by the value of the stack as a result. However, that can only be determined by studying the performance capabilities of the larger stator stack, and the market value perception of that performance. Where machine sizes are roughly similar, it might be prudent to design a stator which maintains similar levels of performance using a smaller inner diameter.



Figure 63 Sheet thickness effect on average machining costs for various production quantities

The effect of increasing the quantity of laminations produced shows both economies and dis-economies of scale. The cost of producing a laminated part generally falls as output is increased. However, costs rise significantly where new tools (dies) must be purchased to account for the added production. It is interesting that the economies of scale vary based on the design of the component. This is an example of the dynamic relationship between cost, time, and quality. Thinner laminations should theoretically be able to produce similar torque output with lower iron losses. Thinner laminates must be produced in greater quantities to achieve the same stack size. The average machining cost of a stack is less when producing thinner laminates, most likely because the stamping tool has a greater life expectancy when cutting thinner materials. However, there is a cost associated to the time taken to manufacture these laminates, and in extreme cases well beyond the assumed £200/hr overhead rate, the most cost-efficient stator design becomes more complex to derive, changing depending on production quantities. If material costs are also considered further, it is likely the case that for extremely thin sheet material, the cost of purchasing the materials will be greater than for standard sized sheets. The model does not currently account for this and is an area of potential development in the future.

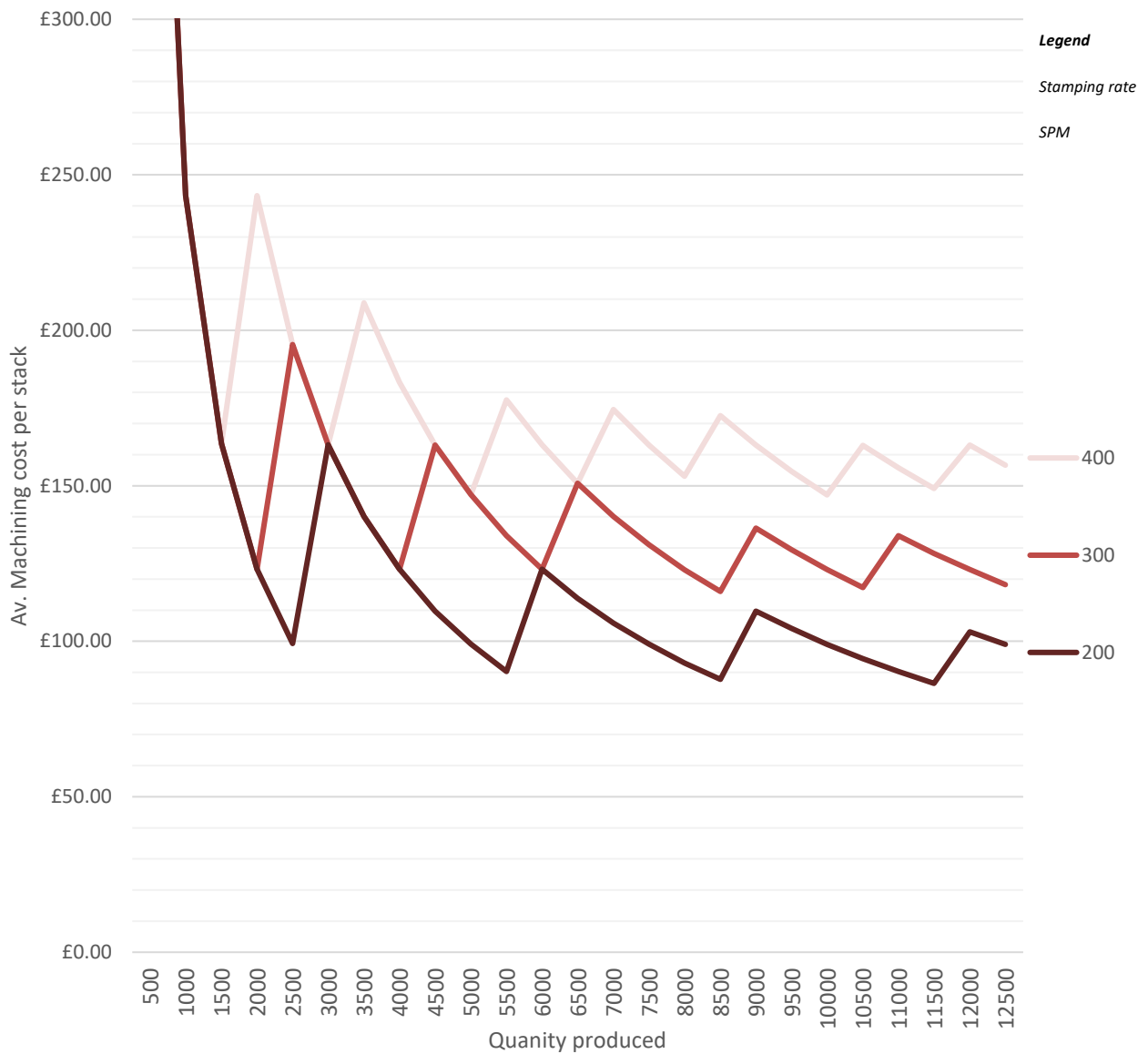


Figure 64 Stamping rate effect on average machining costs for various production quantities

There is visually a difference in the economies of scale that occur between stamping rates (Figure 64) and sheets thickness (Figure 63). The same trade-offs occur as previous, with considerations required into the cost of time taken as result of reducing the machining costs. There appears to be a greater potential for reducing machining costs using slower stamping rates as opposed to thinner laminations.

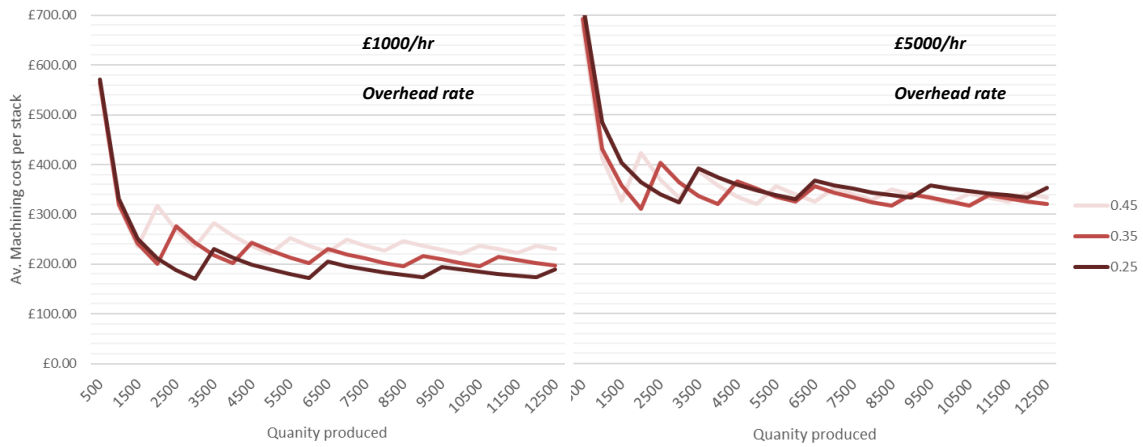


Figure 65 £1000 & £5000 overhead rate example

Overhead costs are directly related to the time it takes to produce goods. The overhead rate is a simple method of capturing the cost of labour, space, and other resources such as administration costs that would be used by the business, but not directly attributable to a specific aspect of the machining process. Figure 66 provides the clearest indication of how the lamination thickness effects the production time. The issue of time is exacerbated by running the stamping machine at a much slower stamping rate. Whilst this is a relatively simple logical step, it is still striking that the effect of changing the stamping rate is more complex than simply performing a uniform calculation.

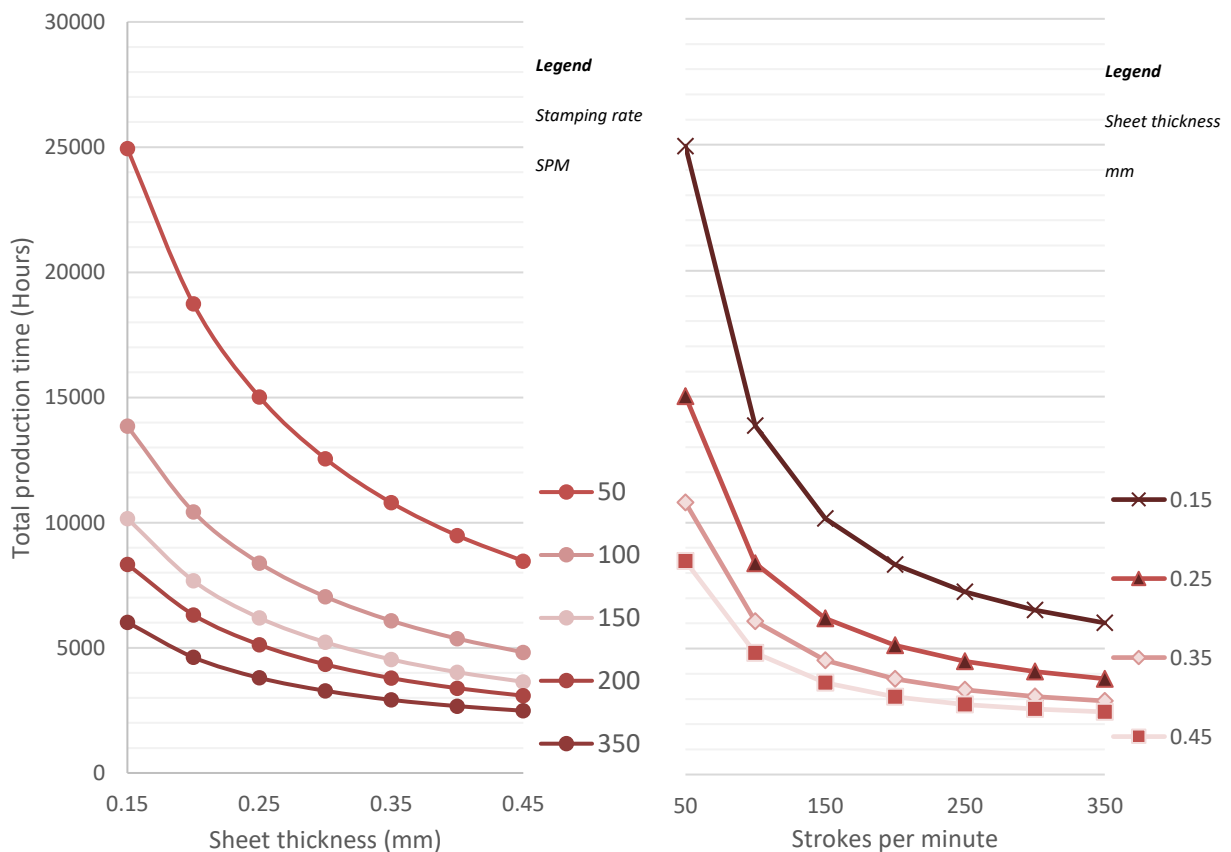


Figure 66 Total production time for various sheet thicknesses and stamping rates

Production time (hrs)	Stamping rate (SPM)							
	50	100	150	200	250	300	350	
Sheet thickness (mm)	0.15	24946	13851	10163	8336	7248	6524	6019
	0.2	18739	10429	7676	6319	5509	4986	4621
	0.25	15021	8387	6196	5125	4491	4086	3801
	0.3	12559	7044	5224	4338	3830	3500	3283
	0.35	10796	6082	4535	3789	3361	3099	2921
	0.4	9485	5367	4026	3387	3027	2805	2670
	0.45	8467	4820	3641	3088	2781	2599	2486

Table 14 Sheet thickness X Stamping rate matrix for production time (hours)

Average machining costs	Stamping rate (SPM)							
	50	100	150	200	250	300	350	
Sheet thickness (mm)	0.15	£ 26	£ 31	£ 36	£ 43	£ 50	£ 55	£ 62
	0.2	£ 29	£ 36	£ 43	£ 53	£ 60	£ 70	£ 80
	0.25	£ 33	£ 42	£ 52	£ 64	£ 74	£ 86	£ 95
	0.3	£ 39	£ 51	£ 61	£ 73	£ 87	£ 99	£ 114
	0.35	£ 44	£ 58	£ 70	£ 85	£ 99	£ 116	£ 130
	0.4	£ 51	£ 65	£ 79	£ 96	£ 113	£ 130	£ 149
	0.45	£ 55	£ 72	£ 89	£ 108	£ 127	£ 146	£ 166

Table 15 Sheet thickness X Stamping rate matrix for average machining costs

Overhead cost per stack	Stamping rate (SPM)							
	50	100	150	200	250	300	350	
Sheet thickness (mm)	0.15	£ 125	£ 69	£ 51	£ 42	£ 36	£ 33	£ 30
	0.2	£ 94	£ 52	£ 38	£ 32	£ 28	£ 25	£ 23
	0.25	£ 75	£ 42	£ 31	£ 26	£ 22	£ 20	£ 19
	0.3	£ 63	£ 35	£ 26	£ 22	£ 19	£ 17	£ 16
	0.35	£ 54	£ 30	£ 23	£ 19	£ 17	£ 15	£ 15
	0.4	£ 47	£ 27	£ 20	£ 17	£ 15	£ 14	£ 13
	0.45	£ 42	£ 24	£ 18	£ 15	£ 14	£ 13	£ 12

Table 16 Sheet thickness X Stamping rate matrix for overhead cost per stack

A simpler way of interpreting the production time and cost data is as a matrix. There is a clear difference between what is the quickest way to produce stacks and what is the cheapest way to produce stacks, occurring in opposite parts of the relevant matrix. However, there is a cost associated with time. Where stacks are produced quickly, the overhead cost per stack is much less than where stacks have been produced more slowly. The overhead rate has a major effect on manufacturing decision making. Table 17 demonstrates how the best set-ups change dramatically as a result of overhead costs. The range of overhead costs represents the unknown range of costs that might be associated with businesses of different sizes and scale.

Total cost inc overhead @ £200/hr		Stamping rate (SPM)						
		50	100	150	200	250	300	350
Sheet thickness (mm)	0.15	£ 7,586,181	£ 5,847,553	£ 5,590,407	£ 5,945,428	£ 6,448,597	£ 6,784,043	£ 7,403,614
	0.2	£ 6,656,082	£ 5,714,807	£ 5,884,643	£ 6,574,053	£ 7,132,778	£ 7,988,856	£ 8,876,679
	0.25	£ 6,291,845	£ 5,925,700	£ 6,448,444	£ 7,435,208	£ 8,269,063	£ 9,389,160	£ 10,292,856
	0.3	£ 6,453,236	£ 6,551,110	£ 7,147,929	£ 8,171,729	£ 9,511,401	£ 10,646,313	£ 12,044,186
	0.35	£ 6,532,447	£ 7,030,849	£ 7,922,375	£ 9,214,427	£ 10,569,972	£ 12,199,060	£ 13,604,492
	0.4	£ 6,954,567	£ 7,572,016	£ 8,745,022	£ 10,298,713	£ 11,907,960	£ 13,544,984	£ 15,439,679
	0.45	£ 7,204,097	£ 8,155,936	£ 9,601,603	£ 11,412,523	£ 13,272,826	£ 15,157,821	£ 17,056,925
Total cost inc overhead @ £500/hr		Stamping rate (SPM)						
		50	100	150	200	250	300	350
Sheet thickness (mm)	0.15	£ 15,070,048	£ 10,002,886	£ 8,639,429	£ 8,446,094	£ 8,623,130	£ 8,741,154	£ 9,209,195
	0.2	£ 12,277,682	£ 8,843,607	£ 8,187,309	£ 8,469,653	£ 8,785,578	£ 9,484,589	£ 10,262,965
	0.25	£ 10,798,245	£ 8,441,700	£ 8,307,377	£ 8,972,808	£ 9,616,263	£ 10,615,027	£ 11,433,085
	0.3	£ 10,220,969	£ 8,664,177	£ 8,715,040	£ 9,473,062	£ 10,660,468	£ 11,696,268	£ 13,029,176
	0.35	£ 9,771,190	£ 8,855,421	£ 9,282,756	£ 10,351,113	£ 11,578,201	£ 13,128,851	£ 14,480,655
	0.4	£ 9,800,167	£ 9,182,016	£ 9,952,755	£ 11,314,913	£ 12,815,960	£ 14,386,451	£ 16,240,822
	0.45	£ 9,744,319	£ 9,601,847	£ 10,693,943	£ 12,338,879	£ 14,107,271	£ 15,937,391	£ 17,802,785
Total cost inc overhead @ £1000/hr		Stamping rate (SPM)						
		50	100	150	200	250	300	350
Sheet thickness (mm)	0.15	£ 27,543,159	£ 16,928,442	£ 13,721,133	£ 12,613,872	£ 12,247,353	£ 12,003,006	£ 12,218,497
	0.2	£ 21,647,015	£ 14,058,273	£ 12,025,087	£ 11,628,987	£ 11,540,245	£ 11,977,478	£ 12,573,441
	0.25	£ 18,308,911	£ 12,635,033	£ 11,405,600	£ 11,535,474	£ 11,861,596	£ 12,658,138	£ 13,333,466
	0.3	£ 16,500,525	£ 12,185,955	£ 11,326,892	£ 11,641,951	£ 12,575,579	£ 13,446,194	£ 14,670,827
	0.35	£ 15,169,095	£ 11,896,373	£ 11,550,057	£ 12,245,589	£ 13,258,582	£ 14,678,501	£ 15,940,927
	0.4	£ 14,542,834	£ 11,865,350	£ 11,965,644	£ 13,008,579	£ 14,329,293	£ 15,788,895	£ 17,576,060
	0.45	£ 13,978,023	£ 12,011,699	£ 12,514,511	£ 13,882,805	£ 15,498,011	£ 17,236,675	£ 19,045,885
Total cost inc overhead @ £2000/hr		Stamping rate (SPM)						
		50	100	150	200	250	300	350
Sheet thickness (mm)	0.15	£ 52,489,381	£ 30,779,553	£ 23,884,540	£ 20,949,428	£ 19,495,797	£ 18,526,710	£ 18,237,100
	0.2	£ 40,385,682	£ 24,487,607	£ 19,700,643	£ 17,947,653	£ 17,049,578	£ 16,963,256	£ 17,194,394
	0.25	£ 33,330,245	£ 21,021,700	£ 17,602,044	£ 16,660,808	£ 16,352,263	£ 16,744,360	£ 17,134,228
	0.3	£ 29,059,636	£ 19,229,510	£ 16,550,595	£ 15,979,729	£ 16,405,801	£ 16,946,046	£ 17,954,128
	0.35	£ 25,964,904	£ 17,978,278	£ 16,084,660	£ 16,034,542	£ 16,619,344	£ 17,777,803	£ 18,861,471
	0.4	£ 24,028,167	£ 17,232,016	£ 15,991,422	£ 16,395,913	£ 17,355,960	£ 18,593,784	£ 20,246,536
	0.45	£ 22,445,430	£ 16,831,403	£ 16,155,647	£ 16,970,656	£ 18,279,493	£ 19,835,243	£ 21,532,087

Table 17 Overhead rate decision making effect



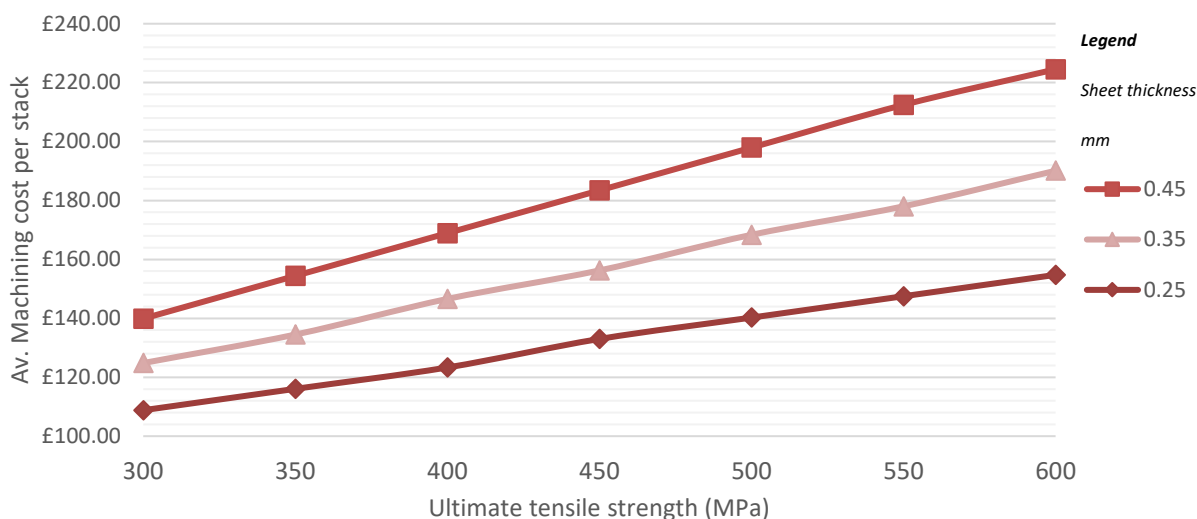


Figure 67 Ultimate tensile strength effect on average production cost per stack

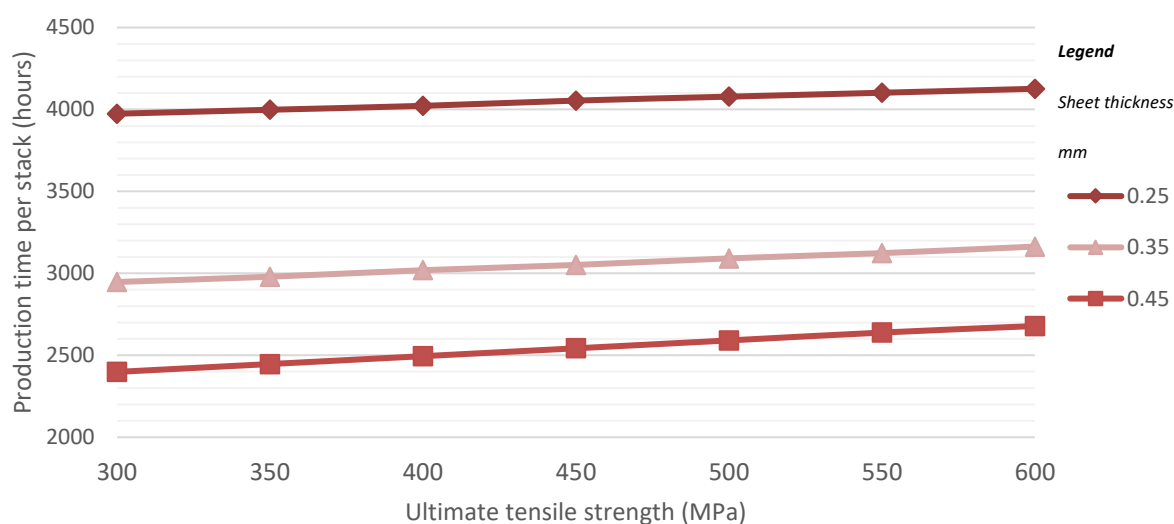


Figure 68 Ultimate tensile strength effect on production time of stacks

One of the key aspects of material selection is the material's ability to be cut, or more specifically in this case, stamped. Ultimate tensile strength is directly proportional to the cutting resistance. Materials that are more difficult to cut, having higher cutting resistance, create more tool wear and negatively impact on tool life. As a result, more tools are required to produce stacks, and more tool change occurrences cause the manufacturing to become slower. Increases in machining costs could potentially be recouped through a change in material costs, or by an increase in stator quality resulting from the use of a different material. Other quality issues might arise too. The ductility of a material could create an excessive burr, which has a negative impact on the quality of a stator lamination. Excessive burring on laminates can create inter lamination short circuits (as Figure 21 p45) and allow eddy currents to flow more easily in the unwanted axial directions between lamination layers, resulting in a loss of performance.

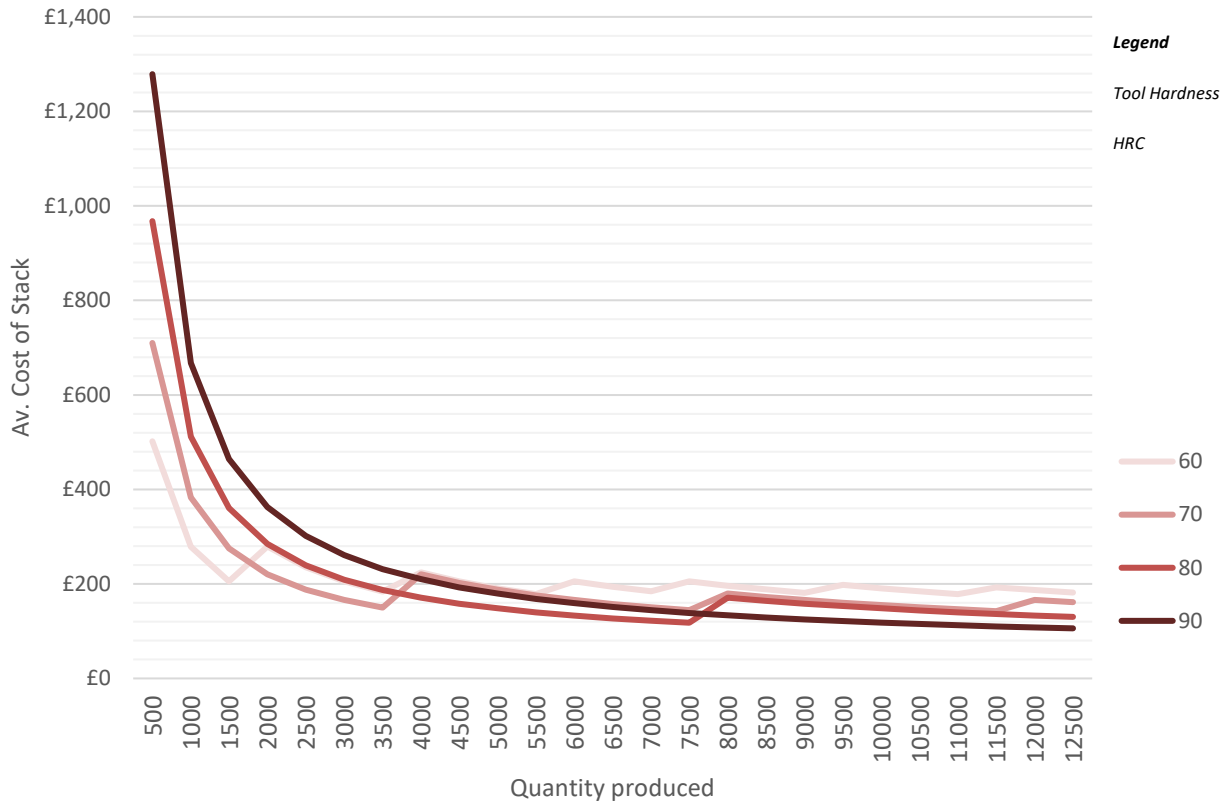


Figure 69 Tool hardness effect on Average stack cost (including £200 overhead rate)

Tool selection is naturally an important aspect of the manufacturing process. There are different tool materials available, which offer different tool hardness, amongst other variables. The most prominent tool materials are tool steels and tungsten carbide, with tool hardness approximately 60 HRC and 90 HRC, respectively. There is an intrinsic cost of procuring tools which have higher degrees of tool hardness, but these costs can be overcome by needing less tools, or the time saved using less tools. There is also the potential to perform maintenance activities on worn tools to increase the life of the tool, such as re-grinding. The benefits of using different tools change depending on the quantity of stacks being produced. For very large orders, 10000 stacks and more, it is generally considered that the harder the tool, the better.

## 4.7 Conclusions

The manufacturing model shows that stamping has much higher costs for smaller production quantities. This might not necessarily be a problem for OEMs in the automotive sector but given the electric vehicle market is still relatively new and consumer adoption of the technology is still in its infancy, the scales of production expected for a single EV machine design at this time might not create the most cost-efficient manufacturing set-ups. There are various ways of affecting the production cost of a stator. If production quantities are expected to be of less than 10000 stacks, it is worth considering tools which are less durable but lower cost. Overhead rates have a major impact on the cost effectiveness of any manufacturing set-up and must be considered alongside machining costs. Generally, the research indicates that where manufacturing times are reduced, machining costs are increased, but when overhead rates are considered, the trade-off becomes much more complex. Each decision, whether relating to part design or manufacturing set-up, trades between the three key business aims of time, cost, and quality. It is possible to use the model created in this research to create a more suitable manufacturing process depending on the specific aim of the product or production.

The current model has been developed on the basis on some simplifying assumptions for the stamping process. In the future, the model should be developed to consider the effect of using a 4-stage progressive die instead of a single stage tool. The model can be developed to include extra activities such as tool maintenance activities, like tool re-grinding.

This cost model has been produced from a perspective of mechanical engineering and operations management. In the future, the parameters in the model could be developed with a specific electric machine design, further establishing the relationship between the manufacturing costs with the implications on electric machine performance and quality.

## 5 Feasibility study for a slinky style stator

---

### 5.1 Methodology

#### 5.1.1 Knowledge gap

The slinky style stator method is already used to produce stators. The benefits, namely a reduction in waste material from the cutting process, is well understood. However, the design constraints which define what sizes of stators are producible, and how design changes affect the overall performance of a stator are much less known.

#### 5.1.2 Approach

A finite element analysis (FEA) was conducted in section 5 to assess the manufacturability of various slinky style stator designs. ANSYS workbench V16.1 was used to perform the FEA analysis. The FEA model is constructed from four parts; a spindle, coiler, slinky guide, and slinky strip (see Figure 70). The spindle is used to rotate the coiler around, whilst also constraining the coiler from moving laterally. The slinky guide similarly ensures that the slinky strip is only able to move in the x axis. The coiler and slinky strip are 'bonded' to each other, this means that as the coiler is turned around the spindle, and the slinky is dragged around simultaneously, being forced to conform to the shape of the coiler. This method of coiling slinky strips has a few potential issues. Firstly, if the back iron is too thick so as to not be very bendable, the slinky strip may buckle or deform. Secondly, ensuring that the stator teeth remain flat is a potential issue. A variety of stator designs have been considered for this simulation. For each design, the length of stator strip and gap between each tooth is constant. The two key variables being considered are the tooth length and the back iron width. The back iron width plays a major role in the electrical efficiency of the component, whilst similarly the tooth length also effects the space available for winding material. In creating an FEA model which runs satisfactorily, several hurdles had to be overcome. Because of the complexity of the model, and the non-linear nature of the problem, it was found that a fine mesh is essential. Initial models which used a coarse mesh failed to converge on a solution and often crashed. The interactions between the various bodies are also an important factor. All contacts between bodies have been set to be frictionless, except for where the slinky strip attaches to the coiler. At this point the contact is bonded. It was recommended to set the contact formulation to 'augmented LaGrange,' and to use a stiffness factor of 0.001. A number of constraints have also been included. The slinky guide has been fixed in place, such that it cannot move in any direction. The slinky strip has been fixed in the Z axis (out of page). This ensures the strip can pass through the slinky guide.

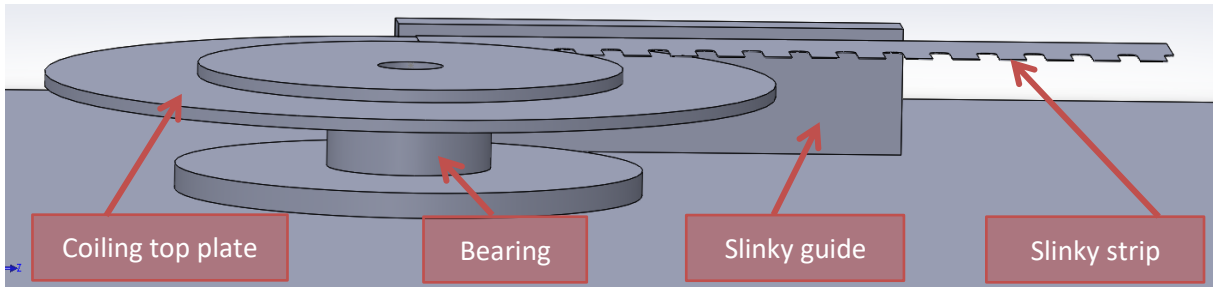


Figure 70 Final design proposed set-up

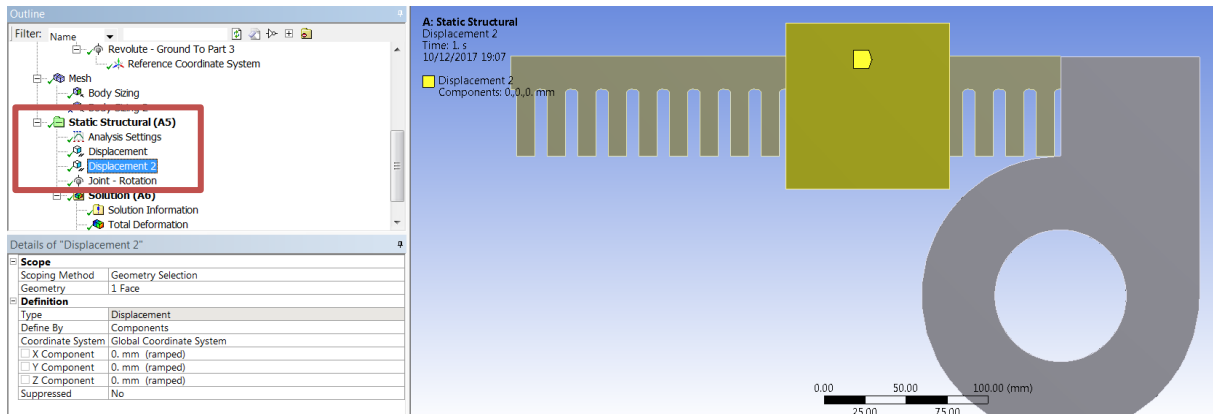


Figure 71 Constraints used in FEA model, where slinky guide has fixed displacement

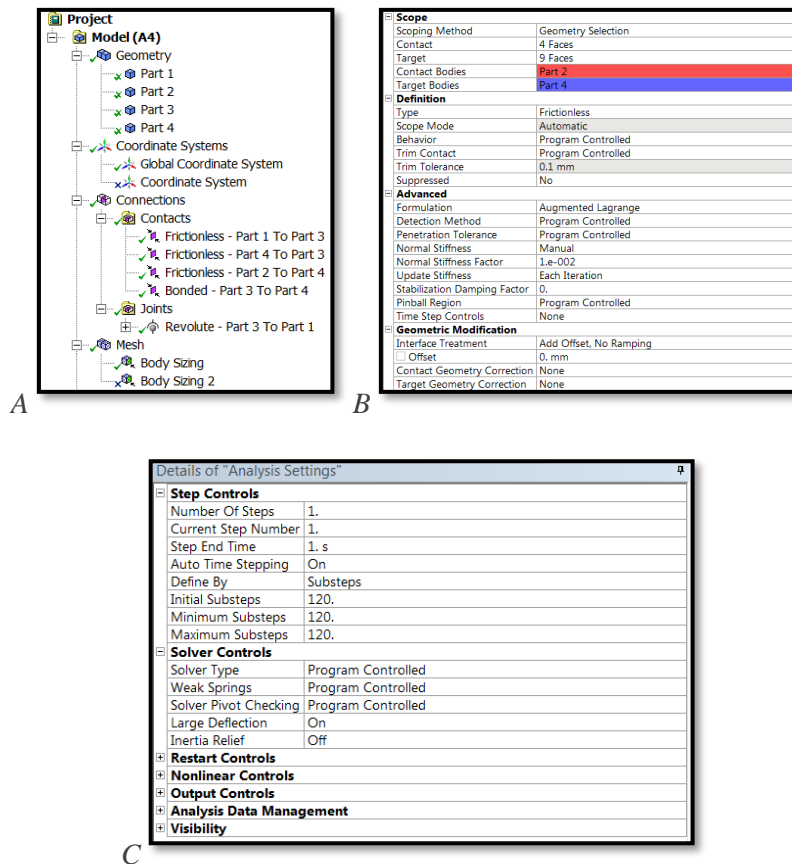


Figure 72 (A) Overview of set-up showing four bodies, four contacts and a revolute joint about the spindle. (B) Contact set-up between slinky guide and slinky strip. (C) Analysis set-up conditions

## 5.2 Slinky coiling trial

A method of coiling slinky style stator strips was devised to understand how the slinky strips deform when being coiled. A number of concepts were explored and modelled using Solidworks 2018 V26 CAD software. One of the key questions that arose from the visualisation of attempting to create a coiling mechanism was how to effectively attach the slinky to the coiling element. It was proposed to use G-Clamps to affix the slinky to the coiling plate, and then apply a torque to the plate. In this set-up, it is necessary to have some form of guide or channel for the slinky to create a bending moment. The final design is an assembly which consists of; a coiling top plate, which has been designed to fit into a *UCFC211 Medway bearing*, a slinky guide or channel, the slinky strip, several G-clamps and an MDF base. The proposed set-up works by feeding the slinky strip onto the coiling plate and clamping the strip to the plate. The plate is turned in the bearing, causing the slinky strip to bend, and another clamp is used to affix the bearing to the top plate. This process is repeated until the desired bend is achieved. The slinky strips have been laser cut from a sheet of 0.35mm thick Cogent M250-35A. Figure 74 shows each of the parts and gives a clear indication as to the difference in sizes between each design of stator strip. In the assembled rig set up (Figure 75), the slinky guide has been fashioned using some spare aluminium bar sections and is held in place with G clamps. An extra guide was used during the experiment to constrain the part vertically. A torque wrench was used to apply force manually through the Allen bolt, found centrally in the coiling plate. Slinky stator internal diameter 170mm, external diameter 170mm + tooth width as per original specification in Table 1 (p17).

Back iron width	Tooth length	Total width
10	10.5	20.5
10	30.5	40.5
10	50.5	60.5
20	20.5	40.5
20	40.5	60.5
30	10.5	40.5
30	30.5	60.5
40	20.5	60.5

Table 18 slinky stators to be made and tested (all measurements in mm)

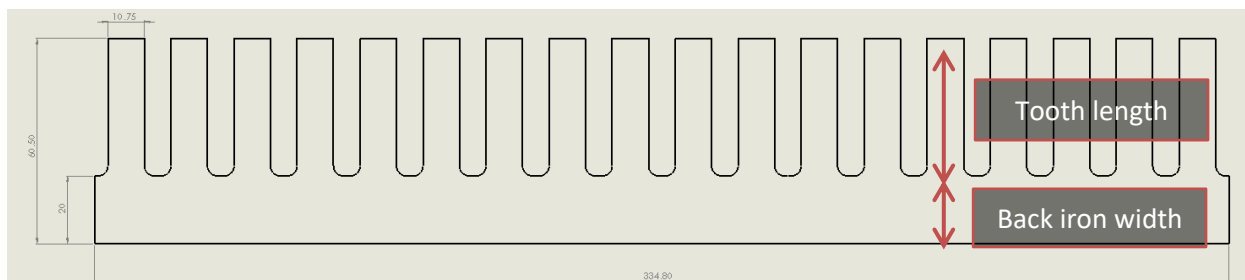


Figure 73 Slinky stator design

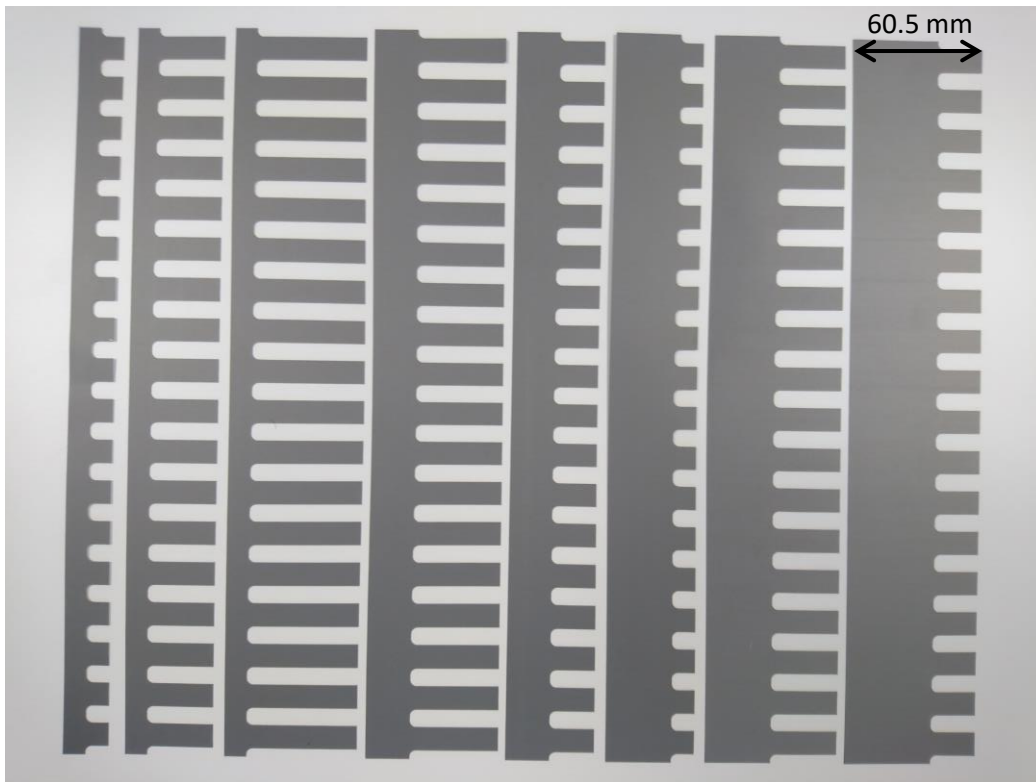


Figure 74 Laser cut slinky stator strips using Cogent M250-35A

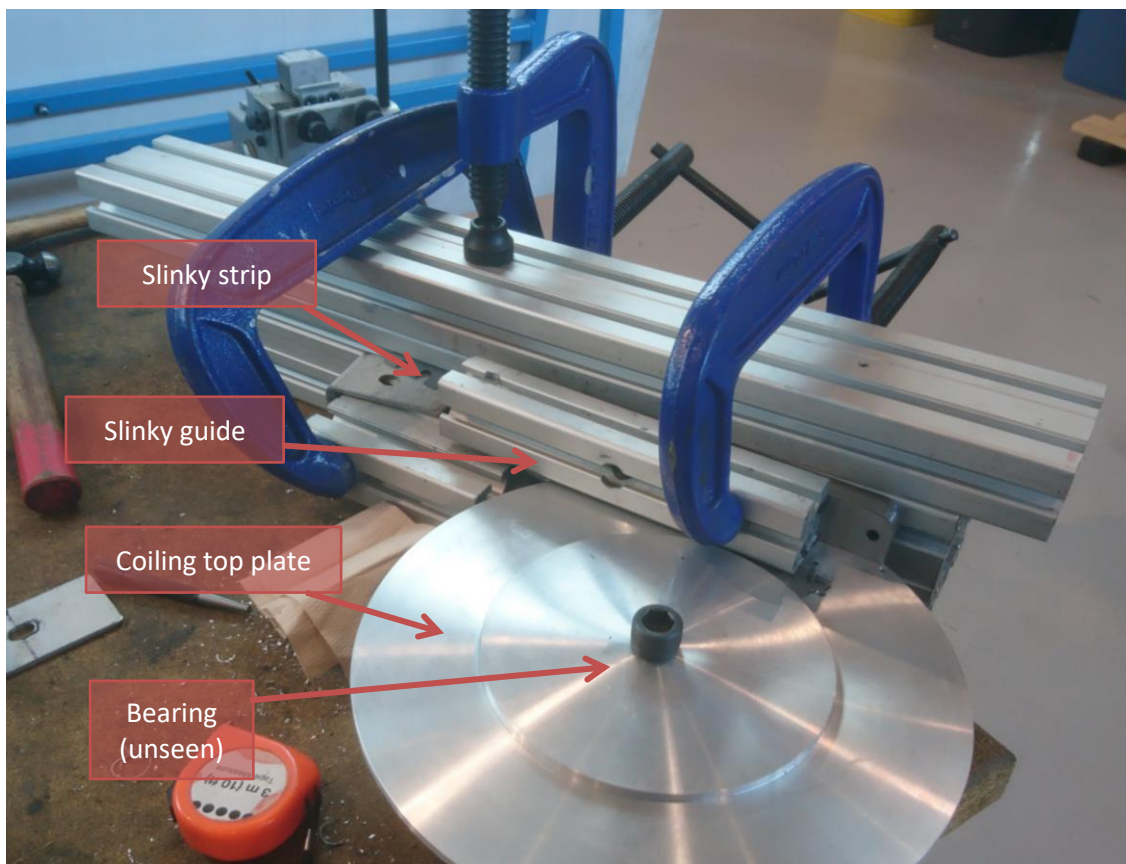


Figure 75 Assembled rig for coiling trial

### 5.3 Introduction

The normal method for producing stator laminations is most efficient when used as part of a holistic manufacturing approach in which the rotor is also manufactured from the same sheet material. The design of the rotor in this project is likely to be non-standard and as such, require a non-standard manufacturing process. The new rotor process also influences the efficiency of the standard stator manufacturing process, as much more material is now wasted and scrapped. An alternative method of manufacturing stator laminations has been discovered, in which long strips of material are stamped and then wound into a stack. This method would reduce the scrappage issue considerably. However, in order to be able to bend the strips into shape; further research would need to be considered in order to understand the dynamics of this alternative method, and how this might affect the design of both the stator and rotor laminations. This project aims to construct a rig which is capable of coiling prototype strips, such that it is possible to evaluate the stator strip design and recommend revisions. Alongside this, a finite element model will be created with the view to being able to validate a stator designs ability to be coiled. The aim of this study is to produce a variety of designs for a slinky style stator lamination. These designs will then be prototyped with a view to understanding the design constraints of a slinky style lamination. This will be done by comparing the resulting prototype to the design in terms of tolerances, concentricity, fit, etc. To achieve this aim, a winding rig will also need to be designed and manufactured.

Slinky style stators are manufactured by coiling long strips of material around a mandrel. This process imparts a bending stress in the stator slinky element and can potentially be the cause of faults during the manufacture. In order to understand the process of coiling a slinky style stator more clearly, an FEA model has been produced. This model allows for both a numerical and visual understanding of the process, whilst also providing insight into how the part deforms and allowing for an evaluation of the design constraints which are required in order to create a producible part.



## 5.4 Slinky coiling finite element analysis results

Readings have been taken from the FEA simulation to find where the minimum and maximum stresses occur in the part. These stresses can then be compared against the ultimate tensile stress (UTS) of the material. For parts where stresses exceed the UTS of the material, they are deemed to be uncoil-able. It is not known whether this is in fact the case and is used merely as a guide to refer to. However, stresses exceeding the UTS are unlikely to be supported without inconsistent deformation in the material, rendering it unusable in a stator.

back iron width	total width	bending radius	max stress	min stress	% Difference	Coilable
<i>mm</i>	<i>mm</i>	<i>mm</i>	<i>MPa</i>			
10	20.5	183.5	327	432	24%	YES
10	40.5	203.5	309	423	27%	YES
10	60.5	223.5	296	409	28%	YES
20	40.5	198.5	346	567	39%	YES
20	60.5	218.5	324	538	40%	YES
30	40.5	193.5	426	697	39%	NO
30	60.5	213.5	391	680	43%	NO
40	60.5	208.5	1106	1991	44%	NO
<i>UTS OF MATERIAL:</i>			<i>575</i>	<i>MPa</i>		

Table 19 Structural analysis results showing peak stresses occurring in coiling of slinky strip using FEA

Initial results showed that five designs are coil-able, and that three designs are uncoil-able. The three uncoil-able designs have back irons of 30mm or greater. These designs would fail due to the stress which occurs between the teeth of the part. This is where the largest stresses occur consistently for all designs. The Max stresses are positive, and the Min stresses are negative. This is due to the stress on the top of the part being a tensile stress, whereas the stress in the lower area of the part is compressive.

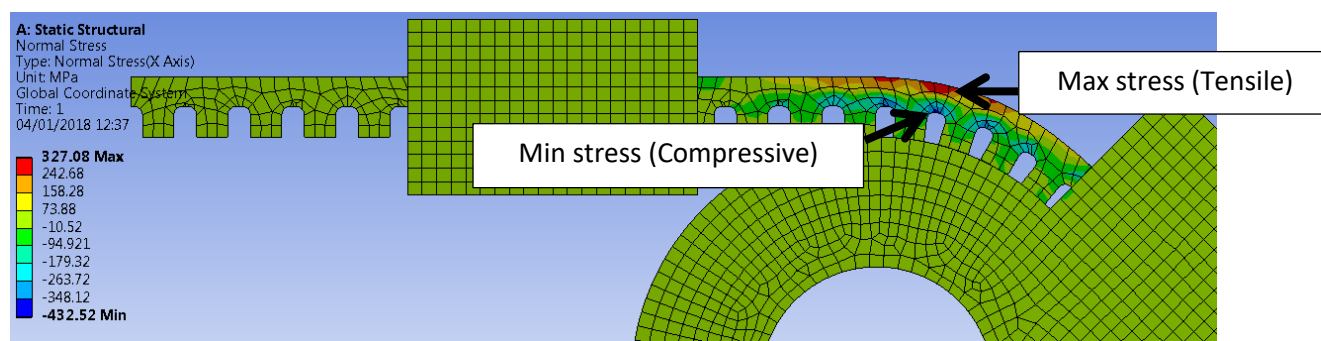


Figure 76 Stress gradient for 10 Back iron, 20.5 Tooth length

There is a clear trend that increasing the size of the back iron means that more work is required to bend the part. Bending a 10mm wide back iron part should be a relatively simple task. However, a 20mm back iron, whilst appearing possible, may be much more difficult. The compressive stress induced in the 30mm back iron design appears to inhibit its ability to be coiled. If the compressive stress could be reduced

without greatly increasing the tensile stress, then it may be possible to design a stator with a 30mm wide back iron. Results for a 60.5mm wide stator (Figure 77) are very similar to the 40.5mm wide stator designs. There is a clear jump in stresses from a 30mm back iron to a 40mm back iron. This is the only result which has a tensile stress above the UTS of the material.

It can clearly be seen that for all 10mm back iron sized designs (Figure 78) the stresses in the part are well below the UTS of the material, suggesting that these parts should all be easily coil-able. The effect of increasing the tooth length reduces the stresses. However, this effect is only small, whereas the effect of changing the size of the back iron can be seen have a much greater impact. It may be possible to manufacture slinky stator strips which have 20mm wide back irons (Table 19) . However, small variations in the material or processes, which could occur from sources such as tool wear, would make the bending process much more difficult owing to the limited scope for error.

The results in Table 19 appear to show that for 30mm wide back irons, the compressive stress would make the designs unfeasible. As the tooth length, and thus bending radius increases, a greater proportion of the stress in the part occurs between the teeth. It is already observed that increasing the bending radius creates a small reduction in both the compressive and tensile stresses that occur in the part. It is not understood why there is a greater proportion of stress between the teeth at larger bending radii but it may be that the larger radius gives a greater length of material that is allowed to bend, and produces a larger bending moment.

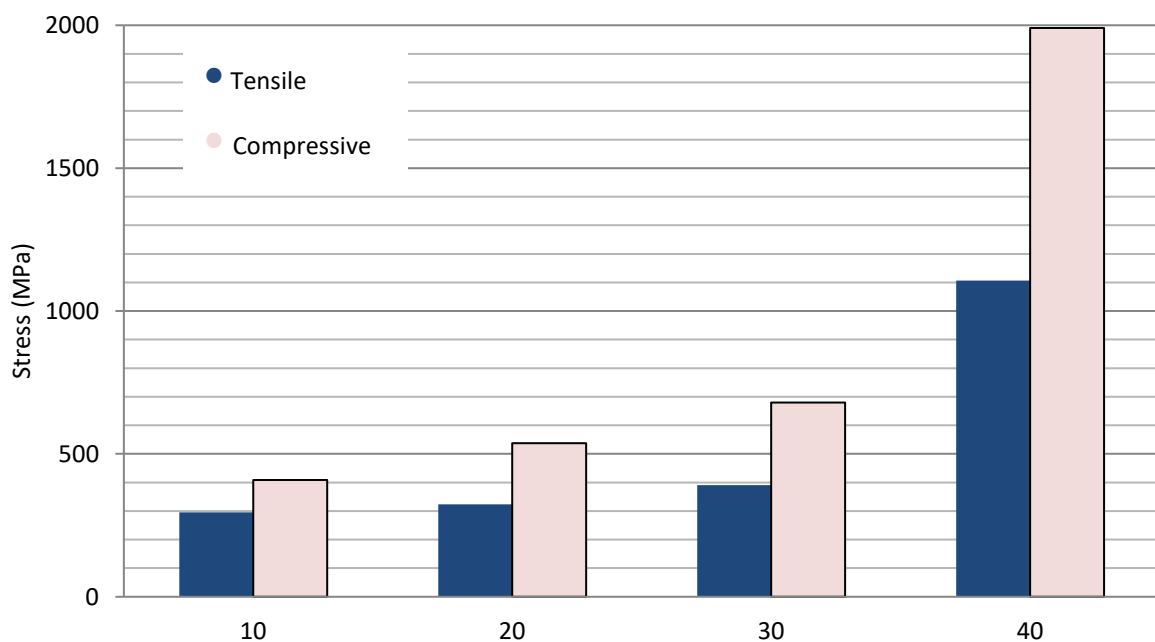


Figure 77 Stress results for different back iron sizes for samples with total Stator width 60.5mm

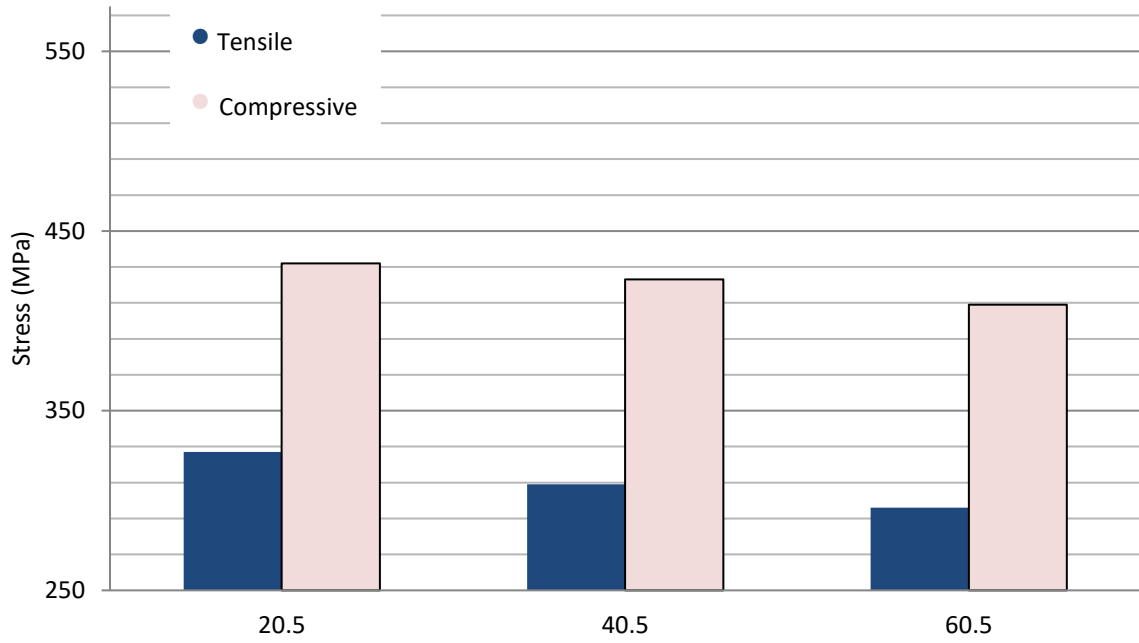


Figure 78 Stress results comparison for different sized stator width samples with back iron 10mm

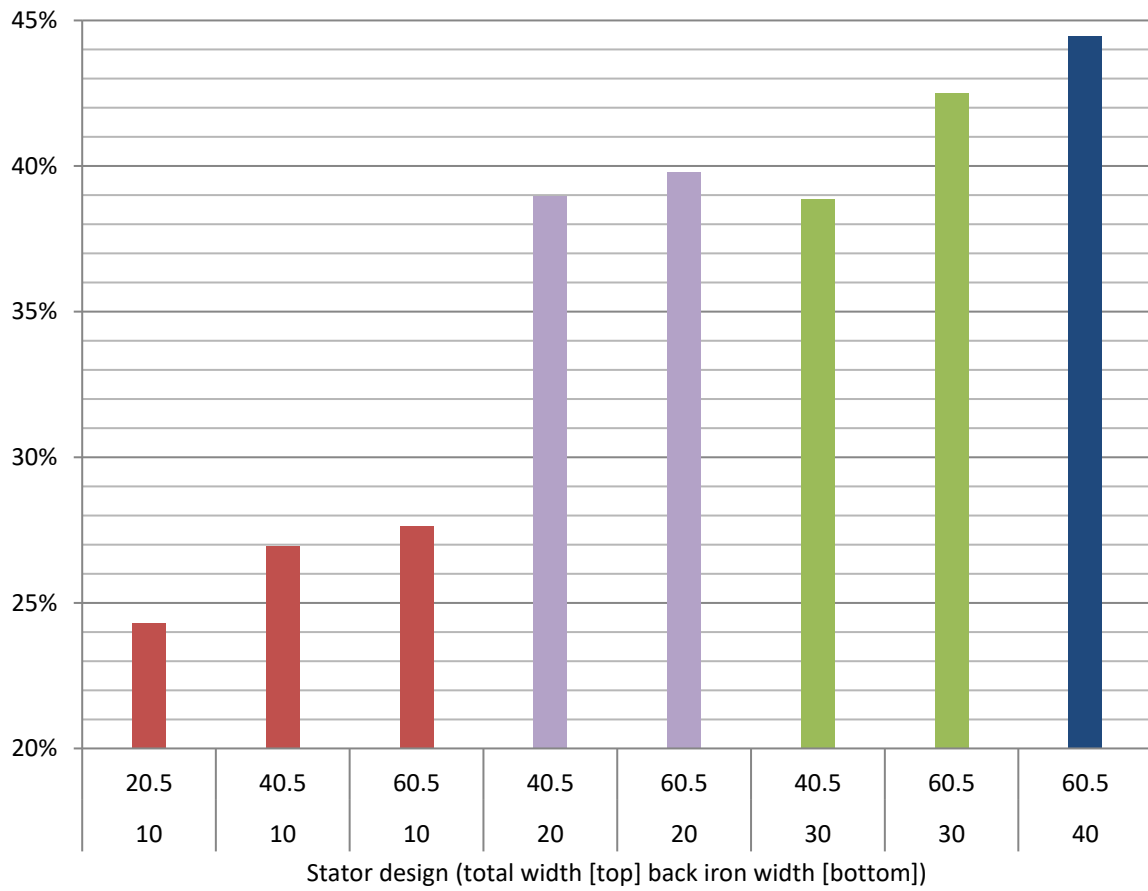
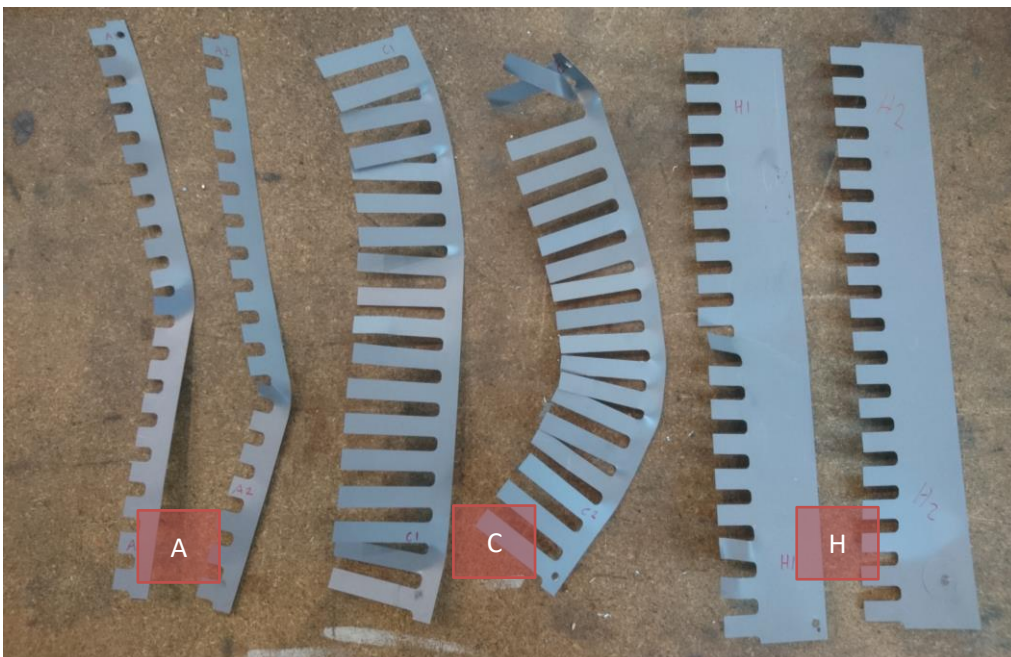


Figure 79 Percentage difference between tensile and compressive stresses

## 5.5 Slinky coiling trial experimental results

Three different cross sections were ultimately tested during the experimentation process. There was enough evidence to suggest that testing the further designs would have only resulted in the same issues and outcomes. The three tested designs were; **(A)** 10 Back iron 20 Total width **(C)** 10 Back iron 60 Total width and **(H)** 40 Back iron 60 Total width. The FEA suggested that designs A and C should have been coil-able. The results of this experiment contradict the FEA in this regard. However, it may be that the designs are coil-able but require a different process to be successfully coiled. Figure 80 clearly shows that no one design has been coiled. There are several shared flaws between designs. Some issues are shared because of limitations in the process which was developed for this experiment. Design C shows the most sign of being coil-able, as is suggested by the FEA model.

Design C shows the clearest examples of the part buckling under compression. It can be seen how a wave like form appears between the teeth. The FEA model showed that the largest stresses occurred between the teeth and this appears to be consistent with the resulting parts. It can also be seen where one of the teeth has been caught on something during the coiling process and been dragged out position. A better feed system, or guiding system would help to stop this occurring. For the larger design (H), the back iron section has remained largely unmoved, resulting in some buckling in the teeth. Figure 83 shows how the part tries to bend along the cross section. It is for this reason that a guide was then placed above the slinky strips to attempt to keep the parts flat during the coiling process.



*Figure 80 top view of tested slinky strips*



*Figure 81 slinky strip C2*



*Figure 82 slinky strip H1*



*Figure 83 Slinky strip H2 twisting during bending*

## 5.6 Discussion of results for slinky coiling process

The FEA model shows that increasing the size of the back iron makes the part less coil-able. The current model suggests not exceeding 20mm thickness in the back iron. The FEA shows that the largest stresses occur between the teeth. This is supported somewhat by the experimental results, which show buckling on the inner radius between the teeth, but the outer radius remains relatively untroubled. There are some key differences between the FEA model and the set up for the experiment. The FEA model has the slinky constrained in the Y axis, which is to say that it cannot deform vertically. The experiment set up initially did not have a guide for the Y axis and so that slinky was free to deform in the Y axis. This was remedied somewhat by the crude implementation of using an aluminium bar over the top of the slinky. Unfortunately, this guide, whilst proving beneficial, did not entirely solve the issue. In the future, a bespoke guide should be designed to hold the part in all axis. The slinky strips will always try to find the easiest way out, and so it is important to keep them constrained as much as possible. One possible solution might be to implement rollers into the process. This would enable forces to be applied to the part without reducing the ability to move or turn the part around the system.

Design improvements can be made to the stator to ease the bending problem. Further designs could seek to reduce the stress occurring between the teeth, using the FEA model as a guide to the potential effectiveness of the proposed new design. It is entirely possible to manufacture a stator using the slinky strip methodology. However, the process created in this report would not be the one to use. Should further improvements be made to this process, particularly in the feed mechanism, then there might be some potential to the current idea. The slinky designs should also be improved, with particular attention to the space between the teeth. The slinky designs used in this report were fairly basic, but still show the difficulties encountered when trying to coil them. New designs could include selectively reducing the material in the back iron or using different geometries between the teeth to encourage bending. The three designs proposed in Figure 84 have been tested within the FEA simulation and the results plotted against the original designs. The compressive (min) forces which are concentrated between the teeth are improved from the best-case original design, with Design A showing the greatest improvement. The tensile stresses (max) which occur, and the outer region of the back iron remain at similar levels, with Design C being slightly worse in this regard to the best-case original design. All three new designs show more consistent stress profiles with Design A particularly having a much more consistent stress profile across the face of the laminate. It is assumed that this would affect the deformation mechanisms during winding, and potentially help to solve the issue of buckling between the teeth.

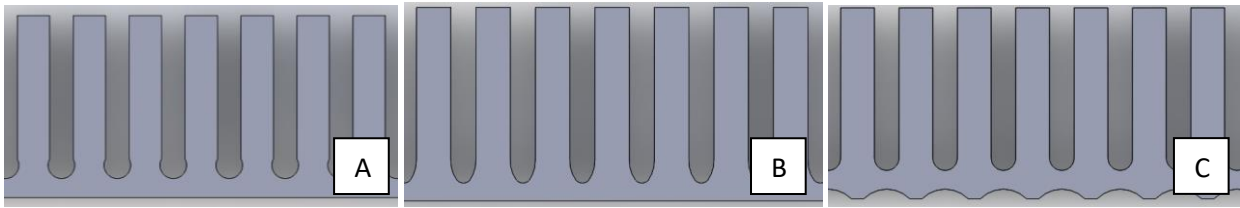


Figure 84 possible design changes to slinky (A,B,C)

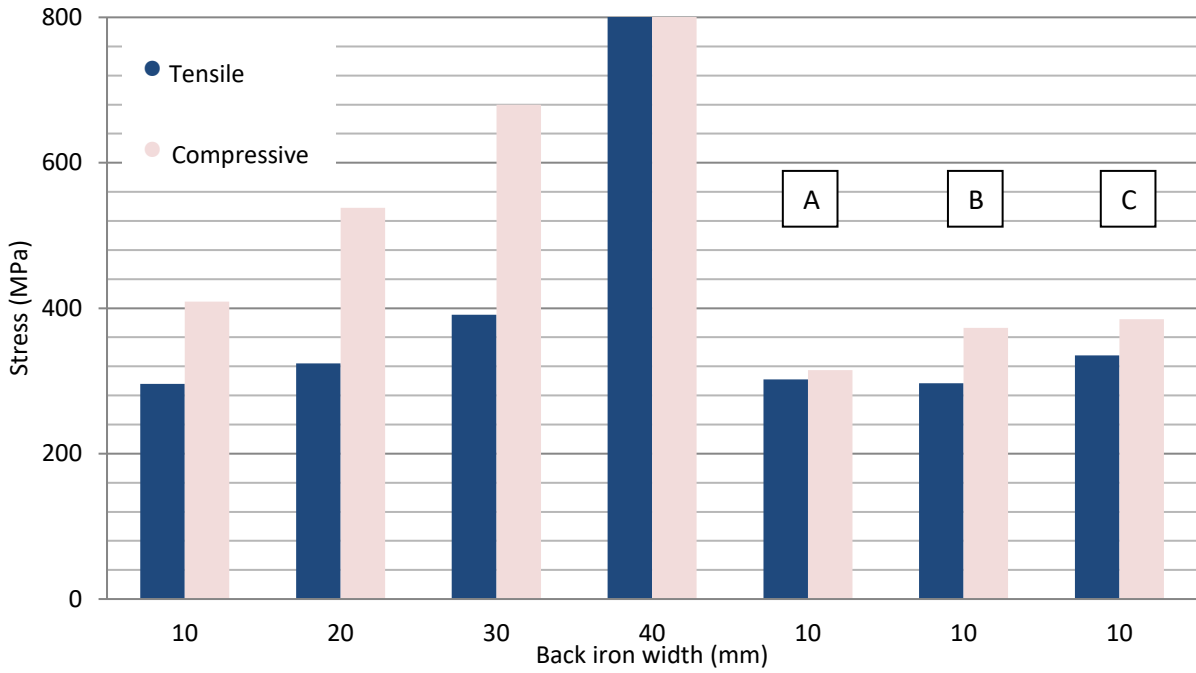


Figure 85 Comparison of new designs

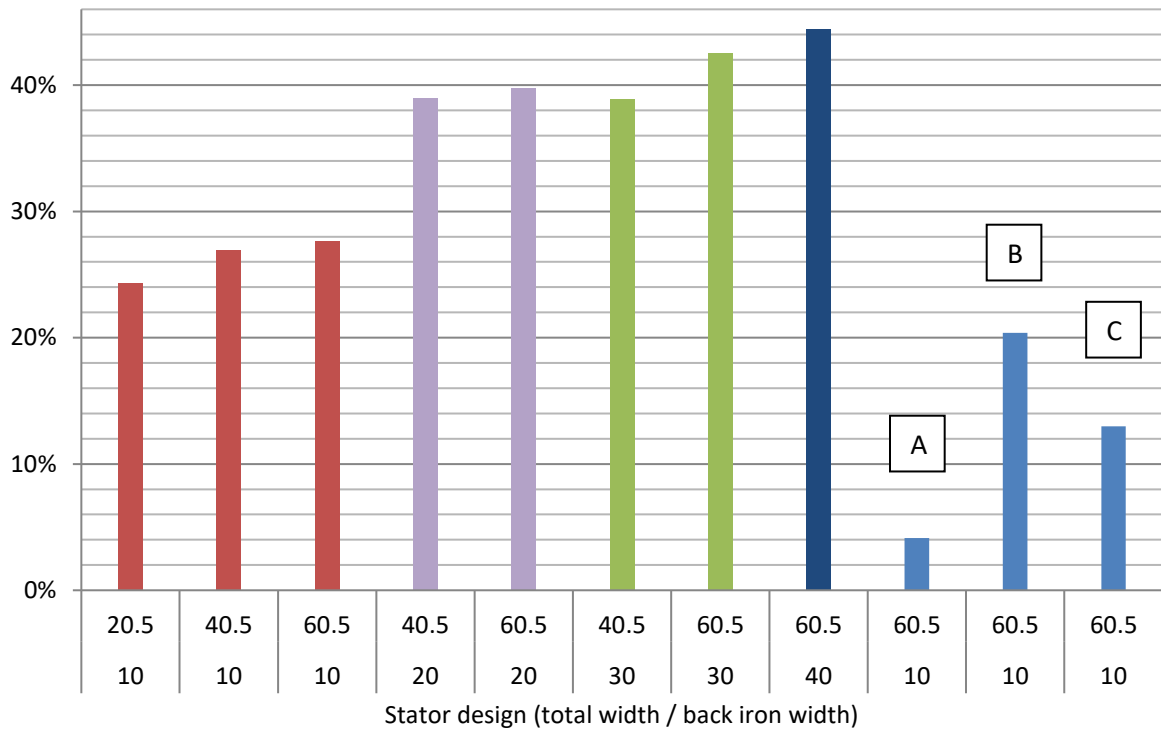


Figure 86 Comparison of new designs

## 5.7 Conclusions

There are three classes of material which satisfy the step specification conditions, these are silicon steels, Metglas and Nickel alloys and Cobalt Iron. The Nickel alloys and Cobalt Iron appear to be the weakest option based on the search criteria currently. No materials were found which satisfy the stretch and leap goals, which appear to be as a result of the density required from the materials in these step conditions.

The FEA model shows the correct areas of high stress and appears to correctly identify the relative coil-ability of the various slinky designs. Further work to the FEA model would be beneficial, such as taking away the Y axis constraint on the slinky strip to achieve a more realistic modelling of the process. The coiling process for the experiment also requires further work and refinement. One key area of improvement is the guiding mechanism for the slinky. The slinky part is all too ready to deform axially and as such, needs to be restrained so that it can be bent into the correct shape. The use of rollers would no doubt be beneficial to the process. It is possible to reduce bending stresses by using alternative design criteria. Whilst the new designs (A B & C) have successfully reduced stress and created more balanced stress profiles across the back iron, each design introduces new issues. The first issue is particular to designs A & C, which remove material from the back iron, reducing the available material for flux to travel through. The second issue regards winding. In the case of standard coil winding, the slot fill factor might be affected, as would the actual room available to pack wiring. In the alternative scenario that hairpin winding is used, the cross sections of the new designs might create difficulties winding with hairpin structures.

One of the challenges with developing slinky coiling processes is that currently there is only limited knowledge publicly available. Whilst there exists some techniques for the coiling process, these are patented and as such, it is difficult to develop an evidenced understanding of the process without attempting experiments such as conducted in this research (Lee, 2005) (Mitsuhiro, 1989) (Mitsuhiro, et al., 1990) (Yasuo & Toshihiko, 2004).



## 6 Laser cutting model and evaluation as an alternative approach

---

### 6.1 Methodology

#### 6.1.1 Knowledge gap

Laser cutting is an established alternative to stamping in stator production, but only for small batches or one-offs. Research exists which compares laser cutting to stamping in terms of cut quality and laminate performance. However, no research exists which investigates the potential of laser cutting as a mass manufacturing alternative. Similarly, no research exists which studies the potential of cutting multiple laminates in one operation using laser cutting.

#### 6.1.2 Approach

The work in this chapter has been conducted using a modelling approach. Process maps have been developed using Microsoft Visio software for a laser cutting production process. A process map has also been developed for a proposed improved laser cutting process. Using data from various sources, and developing on the stamping manufacturing cost model, an expanded cost model has been devised to consider laser cutting operations. This cost model provides manufacturing economics results based on complex interactions of parameters. An analysis of this model is conducted to provide insight.

## 6.2 Introduction

Stators are generally produced using a stamping manufacturing process, as this is considered the most economically viable production method. Often laser cutting is used as a way to produce very small batches, typically for prototype applications or similar. Whilst there appears to be a limited amount of research relating to technical aspects such as the quality of cut produced by laser, it is not always in relation to stator manufacturing and its application in the production of electric vehicles. There is an even smaller amount of research which considers the economic viability of laser cutting, particularly in conjunction with consideration of the quality of stator produced. Using an expanded version of the stamping economic model, the feasibility of laser cutting is assessed, and trials conducted using representative materials to measure the performance of laser cut parts as described in sections 0, 0, 0. In standard laser cutting, a laser cuts a single sheet of material. This will be referred to hence as a '*monostroma*'<sup>4</sup> cut, where a single sheet is cut during the cutting operation.

Laser cutting carries the greatest economic potential if the cutting of 'stacks' of sheets is considered particularly in combination with an optimisation of laser cutting parameters to maximise the operational performance of the process. The cutting of multiple layers during a single operation shall be referred to hence as '*polystromata*'<sup>5</sup> cut. Current laser cutting systems are capable of machining through mild steel up to approximately 40mm depth, and so theoretically it would be possible to stack sheets to around 40mm thickness and cut through them all at once. Including this theoretical manufacturing scenario in the economic model has required developing a system which is able to dynamically provide a 'best case' laser cutting route. As with stamping, a study of the various manufacturing process parameters is conducted, with the main consideration focussed on production time and costs.

### 6.2.1 Process

With these factors in mind, the laser cutting process route is considered as an alternative to stamping. It is assumed that material would enter the process in much the same manner as for a stamping process route (this allows the current production of electrical steel strip to be unaltered, and so this does not need to be explicitly considered in this planning scenario). Figure 87 illustrates how a laser cutting process path would look, where the first stage of the process is that large rolls of sheet material would be received

---

<sup>4</sup> *Monostroma* – from Greek where; *mono* - single and *stroma* – layer. Used to refer to cutting a single sheet of material in a single operation.

<sup>5</sup> *Polystromata* – from Greek where; *poly* – many and *stromata* – layers. Used to refer to cutting multiple sheets of material in a single operation.

and stored. The roll would be loaded onto a spindle so that it could be unwound. The sheet would feed into a simple cutting process, such as a guillotine, which would be capable of producing cuts quickly, if not with great precision and quality. The cut sheets would then be collected and stacked. Sheets would continue to be collected in the stack until the stack has the correct amount of material. The stack is then transferred to the laser, where it would join a queue if necessary. The stack would then be transferred from the queue into the laser cutting machine, and fixed into position, potentially requiring provision for a bespoke fixture to be manufactured in the initial setup of the process line. The laser would then be set up to begin cutting. The precise parameters used in the laser set-up, such as power, cutting speed, cutting gas, etc. would be found in a pre-trial and/or following the laser manufactures guidelines. Once cutting is initiated, the laser head would move into the start position, engage the laser, cut along the prescribed path, disengage the laser, and return to the home position. The fixture would release the stack and the cut stack would then be transferred to be seam welded.

### 6.2.2 Process improvements

One major improvement to the laser cutting process would be changing how the material is received. If the material could be received as pre-cut sheets, this would shorten the process route, reduce handling, and reduce the equipment required in the overall process. Figure 88 illustrates how the process path becomes shorter, reducing complexity in the operation through a reduction in required actions. Ideally the sheets would be sourced directly from the supplier. However, it might still be worthwhile using a third party to pre-cut sheets. This would create a much more complex supply chain, and as such increase both cost and risk, and so it is not a simple decision to make.

Another improvement to the process would be to create an automated, in situ, manufacturing line. It could be possible to use the laser for both cutting and welding operations, though it would be necessary to have a way of changing tool heads, and the provision to operate in a 3D space, with a robotic arm for instance, as the cutting operation typically occurs from the above plane, and the seam weld from a side plane. This type of approach would offer manufacturing flexibility as the tools could be easily re-programmed to operate around different stator sizes.

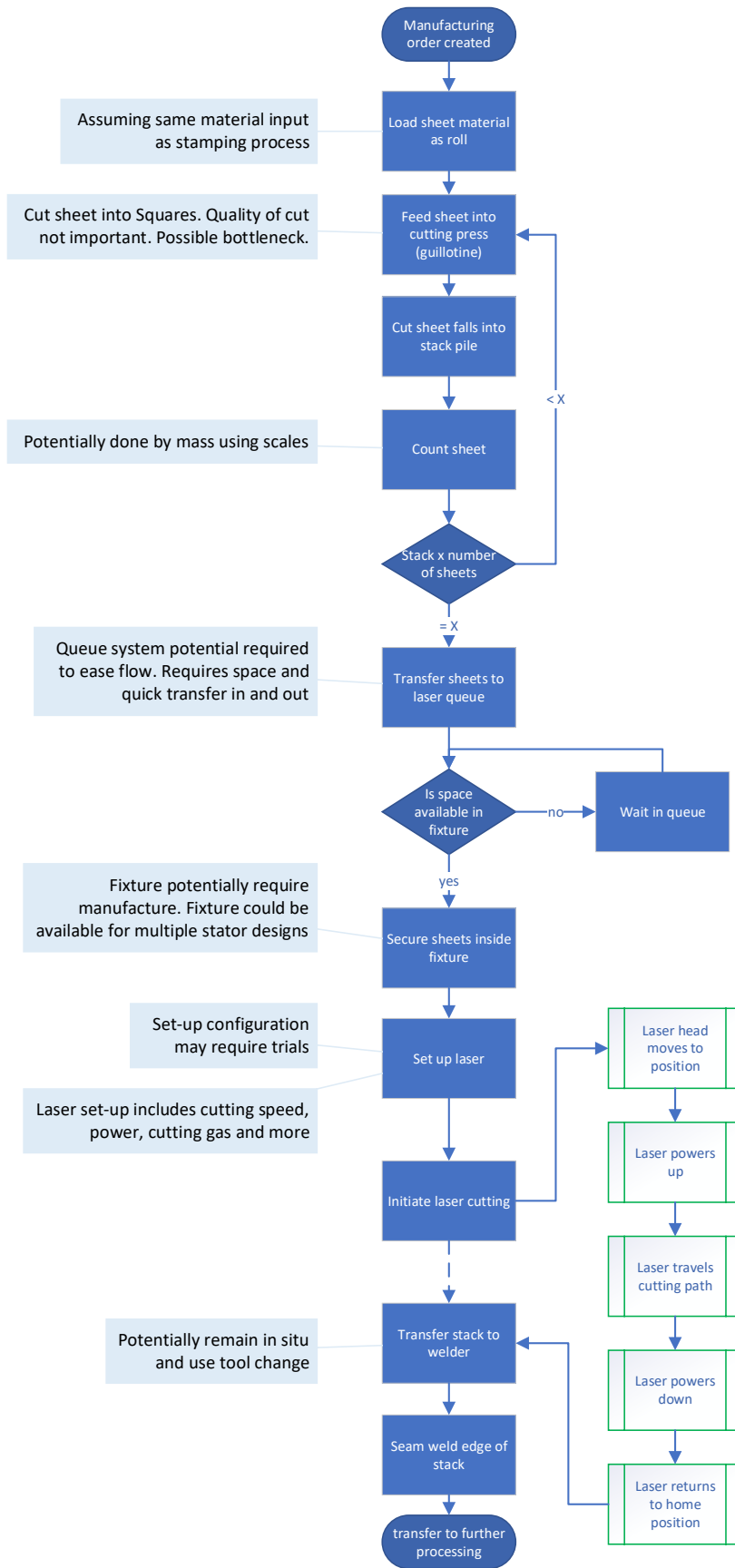


Figure 87 Flow diagram representing a general case of a laser cutting process route

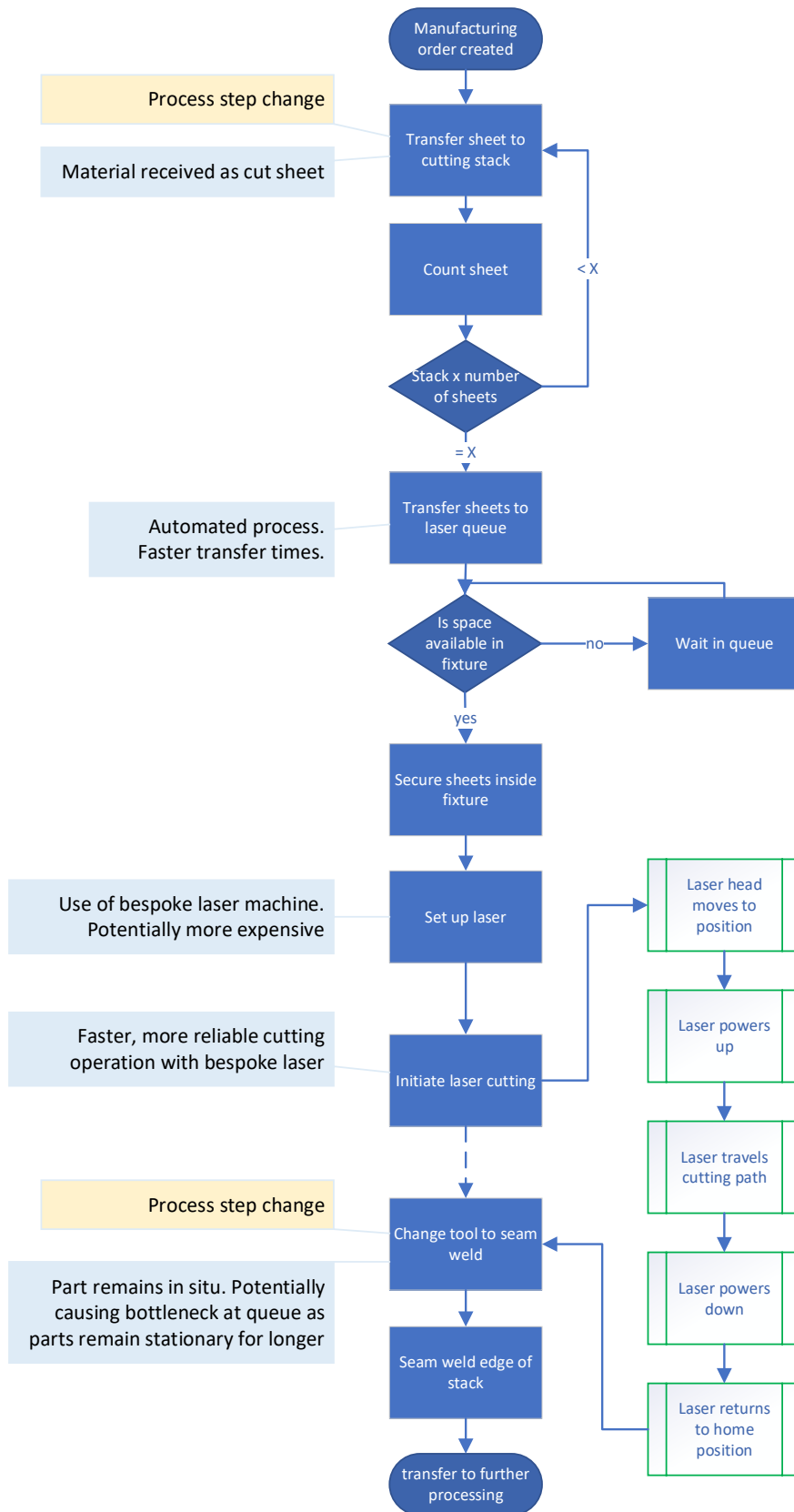


Figure 88 Flow diagram representing a possible improved laser cutting process route

### 6.3 Development of laser cutting model

The laser cutting model uses the same starting parameters for the part design as in the model developed in section 4.3. The laser cutting model requires its own bespoke cost and production modelling, as the considerations and parameters considered are entirely different to those required for stamping.

The first consideration for laser cutting is the speed at which the laser travels through the material. To complete a successful cut the laser will need to travel more slowly through thicker materials and so this must be taken into account when calculating the production rates possible with laser cutting. The laser cutting speed used in this model is based on typical cutting rates achieved by the 3kW Trumpf laser at the AMRC Sheffield for cutting mild steel. Previous cuts of mild steel had been performed by the operator. The historical data provided was for mild steel with thickness of 20mm where the cutting speed was found to be 916 mm/minute, and mild steel thickness of 3mm where the cutting speed was found to be 5245 mm/minute (AMRC, 2019). These points have been plotted in Figure 89. A simple line of best fit was used to create an approximation of the cutting speed trade-off for the AMRC laser. In actuality the line would be curved and asymptotic to the X-axis. However, there was insufficient data to develop an equation on this basis.

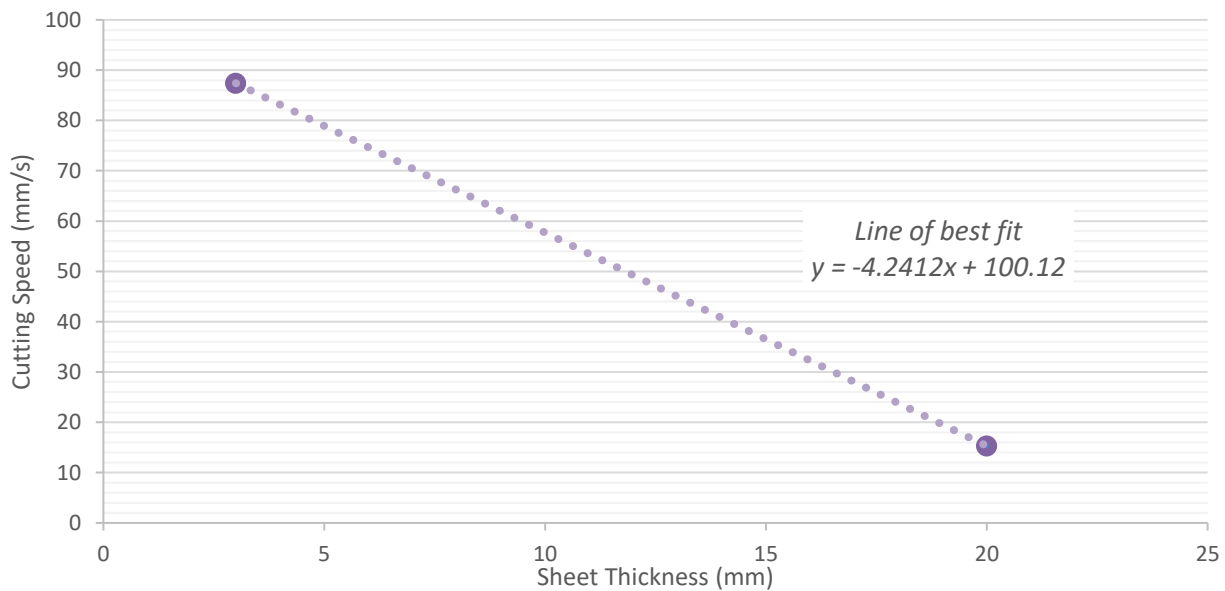


Figure 89 Trumpf 3kW AMRC laser cutting speed for mild steels

The time taken to perform a cutting operation (equation ( 6.1 )) is a function of the cutting distance (which is determined by the design of the stator and teeth) and the cutting speed. The cutting speed is a function of the cutting depth. The cutting depth is a function of the number of laminates being cut,  $n_{LC}$ , and the thickness of each laminate, with the assumption of no distance between layers.  $n_{LC}$  is derived from  $L_D$  & minimum expected cutting time using the laser model optimisation (Table 23).

$$U_L = \frac{100 - (4.241 \cdot L_L \cdot 1000)}{1000} \quad (6.1)$$

Change over time considers the time between cutting operations, where either the tool or material is moved from point to point to begin the next cutting operation. A variety of plausible change over times have been considered, showing the importance of having quick change over.

The cost of purchasing a laser cutting machine is considered within the model. One note is that stamping considers the cost of a die and not the cost of a press; it could be expected that while most laminate manufacturers already have power press facility, they would be much less likely to have laser cutting facilities.

Laser cutting uses a variety of consumables. During the process of laser cutting, gas is used. The model considers the cost of gas used per cutting operation. There are also other consumables which relate to parts such as nozzles and parts relating to the cutting bed. These have been considered as cost per 100 hours of operation. Maintenance costs are estimated and occur per maintenance occurrence. Maintenance is considered to be required after a certain number of operating hours have been completed.

### 6.3.1 Assumptions in laser cutting cost model

The models in this chapter represent a simplified version of the laser cutting and assembly processes.

- Sheet material costs (£/kg) is constant for all sheet thicknesses.
- stacking factor effect is not considered for different laminate thicknesses

### 6.3.2 Parameter sets

Parameter set 1 represents the original data set which the model has been developed with. This includes the stator design parameters used in the previous chapter (see Table 9). The laser cutting data set can be seen in full in Table 21 & Table 22. Parameter set 2 uses the same data, except for those changes listed in Table 20.

	Parameter	Units	Parameter set 1	Parameter set 2
L	Maintenance Cost	£	2000	5000
L	Gas cost	£	0.05	2.00

*Table 20 Parameter sets used in laser cutting study*

## 6.3.3 Laser cutting model

Production rates			
			Laser
hours	Time to produce quantity	$t_\alpha$	5340
secs	av. laminate production rate	$t_{lam}$	0.67
secs	av. stack production rate	$t_{stack}$	192
	Operation per minute	$\alpha_O$	1.0767
	laminates cut per operation	$\beta$	43
m/sec	laser cutting speed	$U_L$	0.036
	laminates cut (best case)	$n_{LC}$	43
m	actual cutting stack depth	$L_L$	0.01505
mins	change over time	$t_L$	1
	total operations required	$n_O$	664452
mins	Laser maintenance	$t_j$	120

Table 21 Production rates for laser cutting

The time taken to produce the total quantity of stacks by laser cutting is given by equation ( 6.2 ). The number of operations per minute ( 2.2 ) is a function of the cutting speed and length of cut. The laser cutting speed ( 6.1 ) is derived from the data in Figure 89. The cutting stack depth is found using equation ( 6.4 ). The laminates cut per operation is found using an optimisation process, laminates cut (best case). This optimisation process is explained and studied in section 6.4.

$$t_\alpha = \frac{\frac{n_{lams}}{\alpha_O \cdot \beta} + t_L \cdot n_O + t_j \cdot \frac{n_O}{n_j}}{60 \cdot n_L} \quad (6.2)$$

$$\alpha_O = 60 \cdot \frac{U_L}{L_C} \quad (6.3)$$

$$L_L = n_{LC} \times L_D \quad (6.4)$$

(Notation listed in Table 21 - Table 22)



Costs			
			<b>Laser</b>
Energy costs	$C_E$		£447
Machine & Machining	$C_{\alpha o}$		£1,200,000
Maintenance	$C_{\alpha m}$		£14,833
Consumables & other	$C_c$		£59,922
Total costs (Machining)	$C_{\Sigma \alpha}$		£1,275,203
Total costs (inc raw Mats)	$C_{\Sigma^*}$		£6,152,828
Av. Stack Cost	$C_x$		£61.53
Energy costs			
£ / kWh	RATE	$C_{eW}$	£ 0.25
£ / kJ	RATE	$C_{eJ}$	£ 0.000069
kW	Laser power rating	$E_L$	3
kW	Laser Power usage	$E_P$	9
Machining & other costs			
	Number of machines purchased	$n_L$	4
	Laser cutter	$C_L$	£300,000
/operator	Gas	$C_G$	£0.05
/100 hours	other consumables	$C_C$	£500
	Maintenance costs	$C_J$	£2,000
operations	Operations until maintenance	$n_J$	10000

Table 22 Production costs for laser cutting

Energy costs ( 6.5 ) are found by considering the cost rate of energy, the energy usage rate and the time that energy is used for. Machining costs ( 6.6 ) are predicated on the cost of purchasing laser cutting machines. Maintenance costs ( 6.7 ) are predicted based on numbers of operations conducted.

$$C_E = C_{eW} \cdot E_P \cdot t_{\alpha} \quad (6.5)$$

$$C_{\alpha o} = n_L \cdot C_L \quad (6.6)$$

$$C_{\alpha m} = C_J \cdot \frac{n_o}{n_j} \quad (6.7)$$

(Notation listed in Table 21 - Table 22)



The data provided by the first lookup table is used to define a more specific search criterion, and helpfully, this is automatically adapted to changes in the model elsewhere. For parameter set 1, the best production times occur when there is a cutting depth somewhere in the region of 15mm-16mm (Figure 90). Using this knowledge, a more defined search is conducted, where given a sheet thickness, results are only considered where the number of laminates cut per operation equate to cutting depths in the search region, as demonstrated by the example in Figure 91.

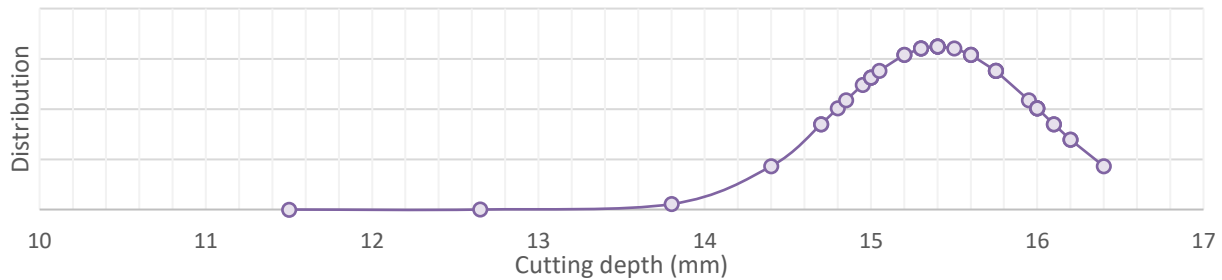


Figure 90 Cutting depth distribution

Sheet thickness (mm)	Number of laminates									MIN	N Lams	
	40	41	42	43	44	45	46	47	48			49
0.35	5668	5628	5598	5578	5568	5569	5581	5606	5644	5697	5568	44

Figure 91 Example of final lookup in model

The model can either be optimised to provide the most efficient production times for a given set of parameters, or alternatively, to provide the most cost-efficient production set-up. Using the same optimisation process as before, results were obtained across a range of sheet thicknesses to assess the differences in optimisation choice. Results for costs have been obtained using a variety of overhead rates. Overhead rates are directly proportional to time, and so it is useful to understand how they might affect the optimisation decision process as a result. A further study was conducted using a different set of parameters, considering the effect of a much greater gas cost per operation and increased maintenance costs. These parameters are considered here because they are directly related to costs per operation, and both parameters are included in the model with assumed cost rates, it is not necessarily that gas costs and maintenance costs specifically are expected to be much higher, but that their implementation in the model allows them to effectively be used as a way of manipulating 'operations costs'.

The results in Figure 92 show that the difference in production settings is small, but noticeable between each data set. Differences are more pronounced when sheet thickness is thinner, which is expected as more sheets are required to create the same changes in cutting depth. It can be seen that as overhead rates increase, the optimisation results become synchronised. This makes sense, as with increased overhead rates, there is increased cost associated with time, and as such, optimising costs tends towards optimising time as overhead rates increase.

6.4.1 Parameter set 1

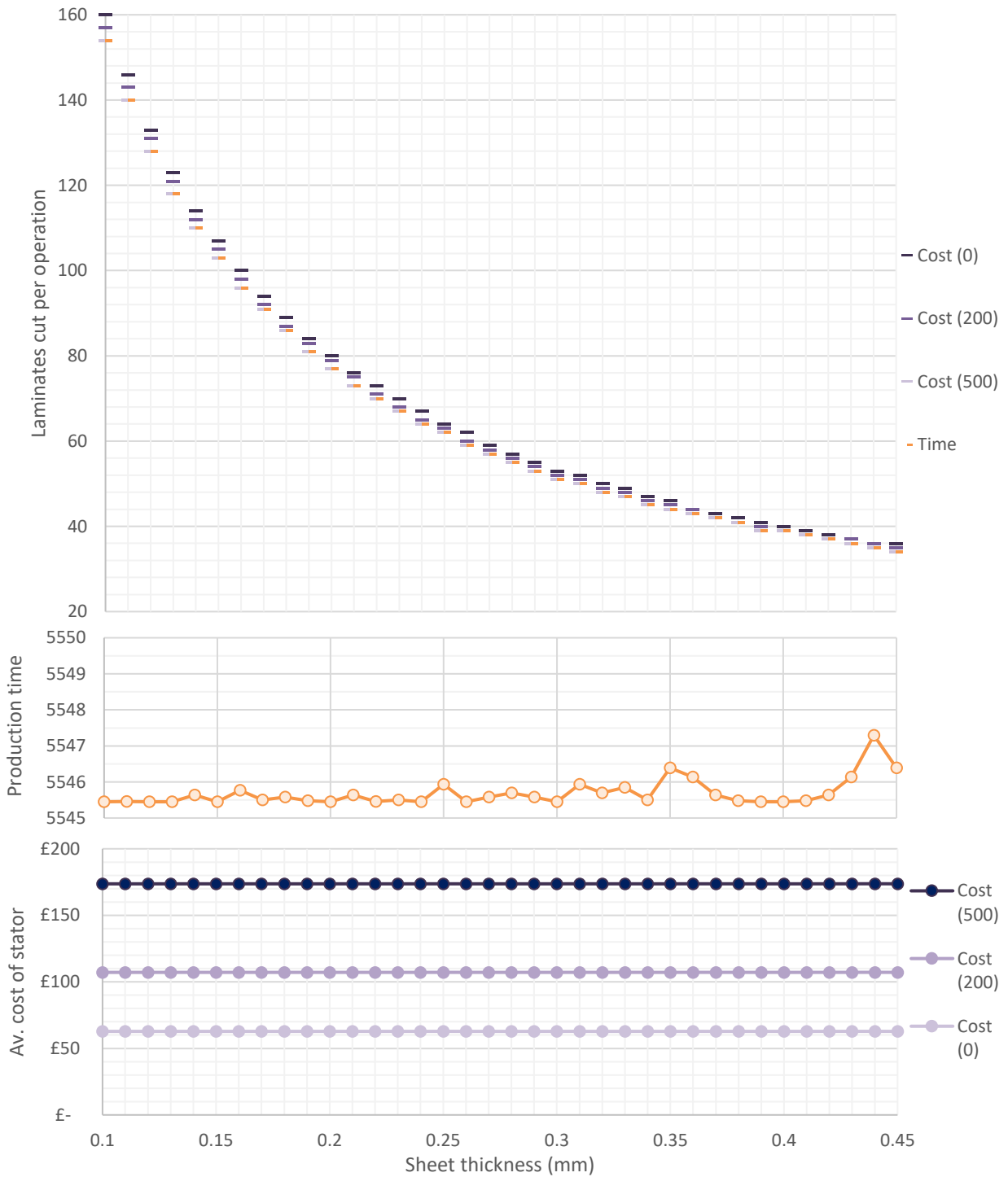


Figure 92 Comparison of optimisation processes, where gas price is £0.05 and maintenance costs £2000 (material costs included in Av. cost of stator)

It is important to recognise that because the model is using an optimisation procedure, the variations in time and costs are very small, regardless of whether the model is optimised for minimum cost or time. It may be the case that with a different set of parameters, most likely relating to the laser cutting machine, there may be much more variation in results across the range of possible cutting set-ups.

## 6.4.2 Parameter set 2

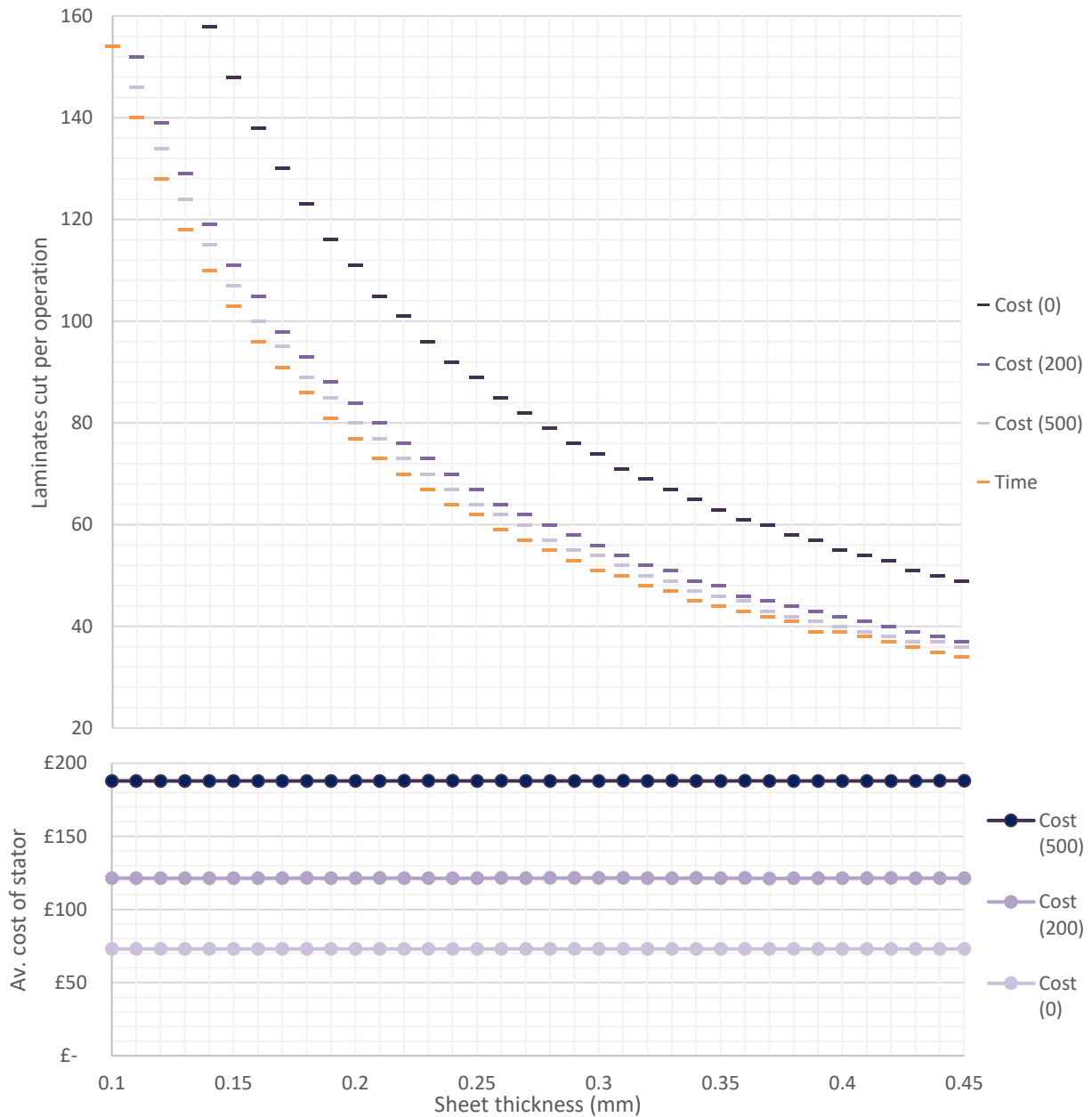


Figure 93 Comparison of optimisation processes, where gas price is £2.00 and maintenance costs £5000 (material costs included in Av. cost of stator)

The alternative parameter set shows results with a much greater spread (Figure 93) than those initially gained from the starting set of assumptions (Figure 92). The time optimised results are exactly the same, which is expected as the parameters which have been changed relate to cost functions only. The same trend occurs where increased overhead rates cause the cost optimised results to tend towards the time optimised results. However, in this case a much greater overhead rate is required to create parity with the time optimised results. It remains true that for any cutting set-up, there are only very small deviations between set ups regarding the optimised output.

The greatest differences can be seen when the overhead rate is set to £0. Whilst an overhead rate of £0 is unrealistic in real terms, it provides the absolute maximum case and is a useful baseline for comparison where actual overhead rates are unknown. In this case, there the two different optimisation processes provide very different outcomes. Optimising for minimal production time results in an increase of average stator costs by approximately 6% compared to the cost optimised set-up. Alternatively, optimising the model to reduce costs dramatically increases production times by approximately 100% in the best case. Interestingly, there is also an increased production time variation across the various cutting set-ups when the model is cost optimised.

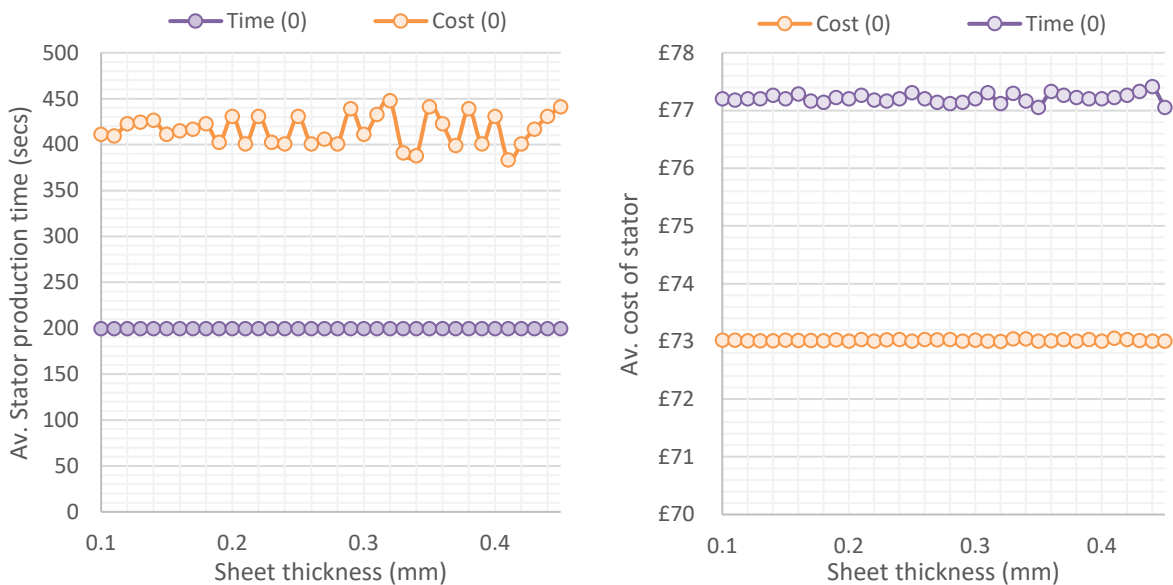


Figure 94 Comparison of time optimisation and cost optimisation for overhead rate £0

This study shows the importance of having a statistical process control system in place for the implementation and use of a laser cutting production process, particularly if the process is expected to perform cuts of multiple sheets per cutting operation, as is examined here. As well as the cost and time aspects of this process, there is of course a question of changes to the quality of the cut occurring when a stack is used. To provide an initial answer to this a study has been conducted here for a limited range of set-ups, with particular attention to the suitability of parts for use in electric machines. For a full consideration of how cut quality might vary with detailed shapes and different potential products, an extensive production trial would be needed.

As the model is further used to study the effectiveness of laser cutting laminations, it will be time optimised using parameter set 1 and an overhead rate of £200 as a default. In this set-up, there are only small differences in the optimised outputs, allowing for a study of individual parameters without the results being dominated by other factors.

## 6.5 Laser cutter variation

One of the major determining factors of time and cost efficiency is the laser cutting speed. The laser cutting speed used in this model is derived from known cutting speeds of mild steel (similar to lamination material) which have been performed using a 3kW Trumpf laser that can be found at the AMRC design & Prototyping centre. It is possible to use laser cutting machines which have different cutting speed profiles, as proposed in Figure 95. The profiles for the alternative lasers are based on a laser cutting speed reference chart (Table 35). Three laser profiles have been selected; 1kW, 3kW and 10kW. It is expected that the 3kW laser from the chart should provide similar results to the AMRC laser. The costs of each laser alternative are not considered in the model at this stage, though it should be expected that the higher power machines are more expensive to purchase and to operate. Each laser has an ideal cutting depth due to the optimisation procedure (Figure 96).

A trend appears present which shows that more powerful lasers can produce stators at a faster rate. Part of the reason for this is the ability of the laser to penetrate through deeper stacks. The more powerful lasers also cut through the same cutting depths at faster rates, as evidenced in Figure 95. The 10kW laser also represents a more cost-effective way of producing stators. However, this does not include the cost of purchasing the more expensive machine. The results for parameter set 1 and set 2 both show that the 10kW laser has cost savings of approximately £9 per stack over the AMRC laser. The long-term production quantity considered in this research is 100,000 stators. This equates to a potential £900,000 cost difference, which would potentially be more than the extra machine costs. Whilst further work is required, particularly with consideration to the lifetime costs of the machines, it appears possible to produce stators more cost-effectively by using more powerful laser cutting machines. It should also be noted that the 1kW laser cutter performs by far the weakest on both time and cost metrics. Interestingly, the 1kW laser cutter also sees a greater increase in cost when considering the effect of Parameter set 1 and Parameter set 2, probably as a result of requiring performing more operations.

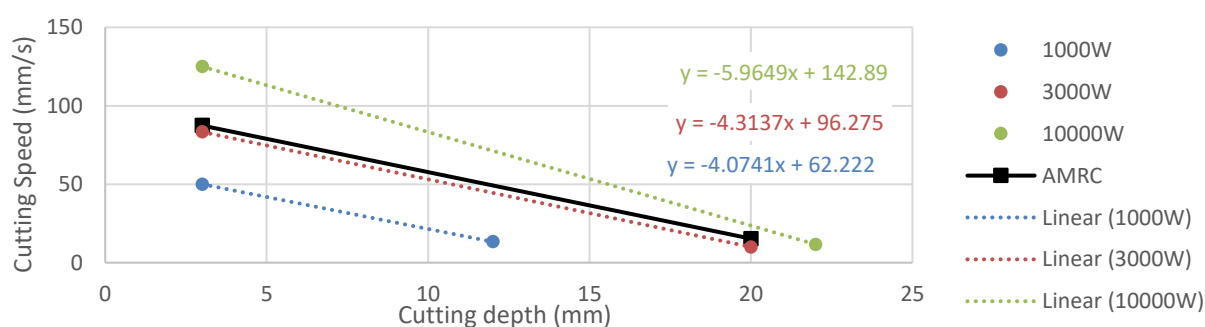


Figure 95 Examples of laser cutting speed alternatives

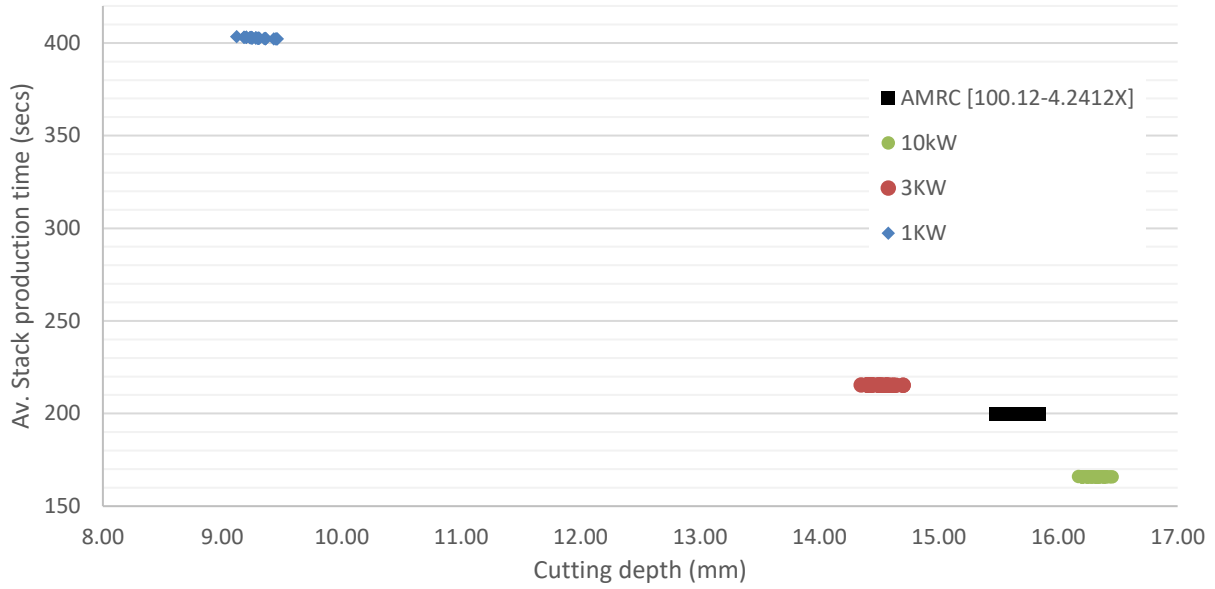


Figure 96 Production times for alternative laser cutting speed profiles using parameter set 1

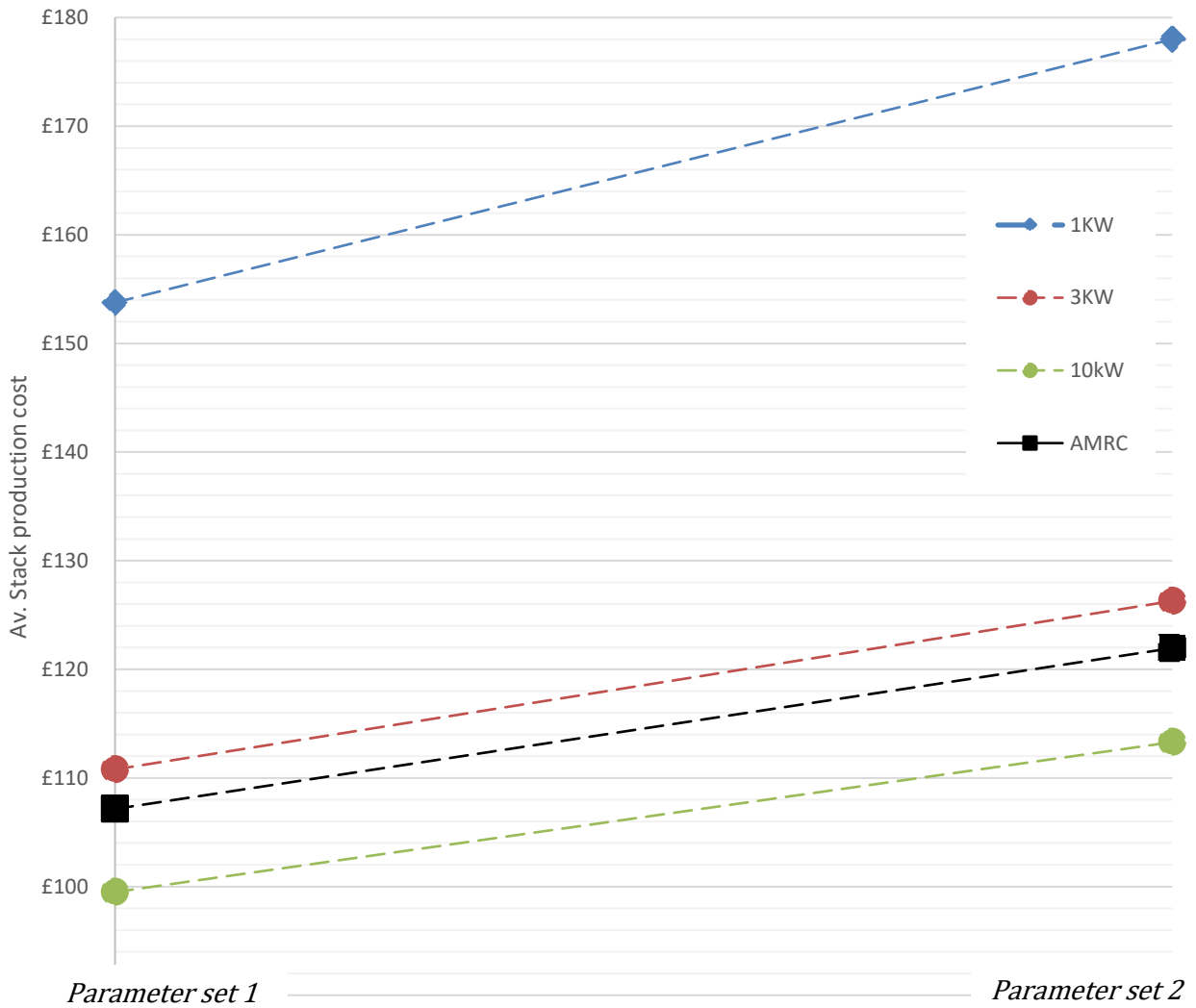


Figure 97 Stator production costs for different lasers using parameter set 1 and set 2



## 6.6 Laser cutting model analysis

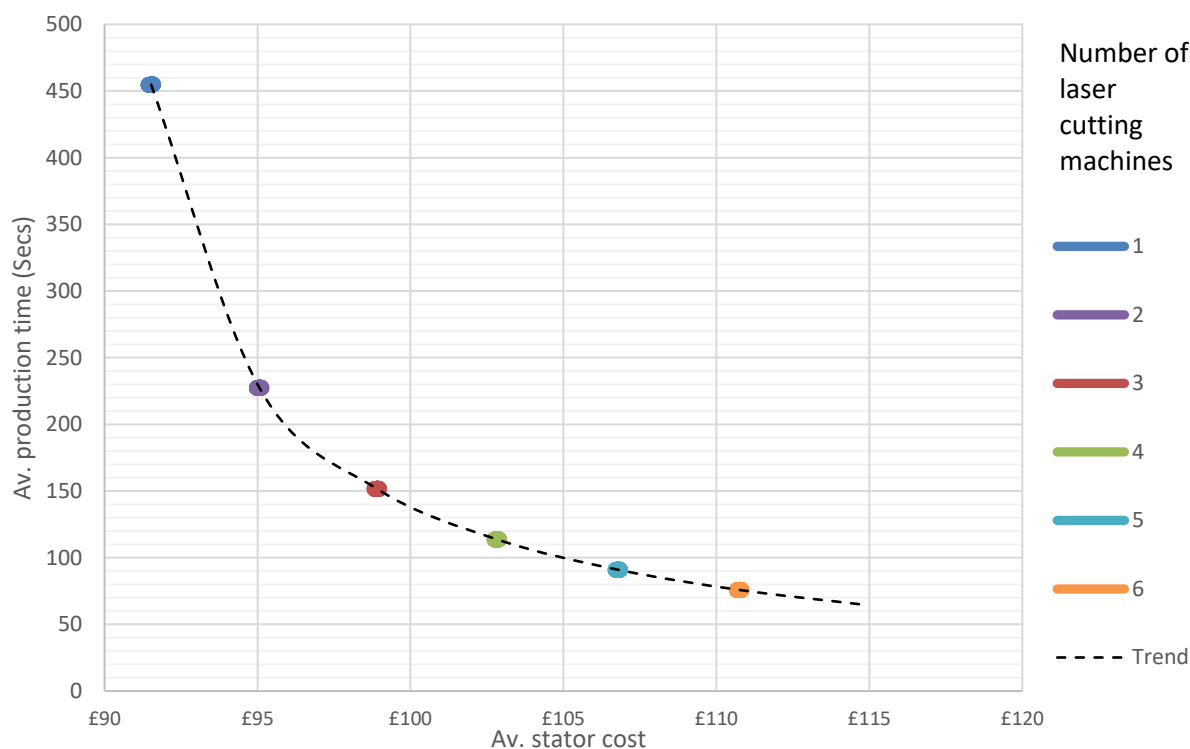


Figure 98 Effect of extra laser cutting machines

The model used in this study uses 4 identical laser cutting machines. Each additional machine adds to the overall initial costs of stator production as the cost of investment for each machine is considered. The model does not account for the added complexity introduced by having more machines and resources in motion, meaning that benefits in production time are effectively overestimated. Another factor that should be considered is risk. Investing in many laser cutting machines has risks, as the large capital investment would effectively be a sunk cost. The machinery would cease to add value should production quantities reduce, and capital would be locked into the value of the laser cutters as opposed to a more easily accessible form as asset, such as cash. There is also the potential that a technology leap occurs, meaning the purchased machines become redundant and lose value. Time would be lost removing old machines and installing new ones, as well as the cost of this process. Given the possible risks, it would be advisable to use as few machines as are necessary to be economically viable. In this case, 3-4 machines balance the benefits of greatly reducing production time, though an argument could be made that 2 machines is sufficient for smaller enterprises as this would balance the need for capital investment whilst gaining the benefits of production time and cost. Whilst these risk factors, and the lowest costs, suggest that 1 machine alone would be the best option, a single machine limits the potential for growth as the manufacturer would be limited to smaller order quantities due to capacity issues and the time required to produce stacks. There is also the risk should a machine breakdown or failure occur at some point, there is no ability to produce stacks otherwise, which would bring the whole operation to a stand.

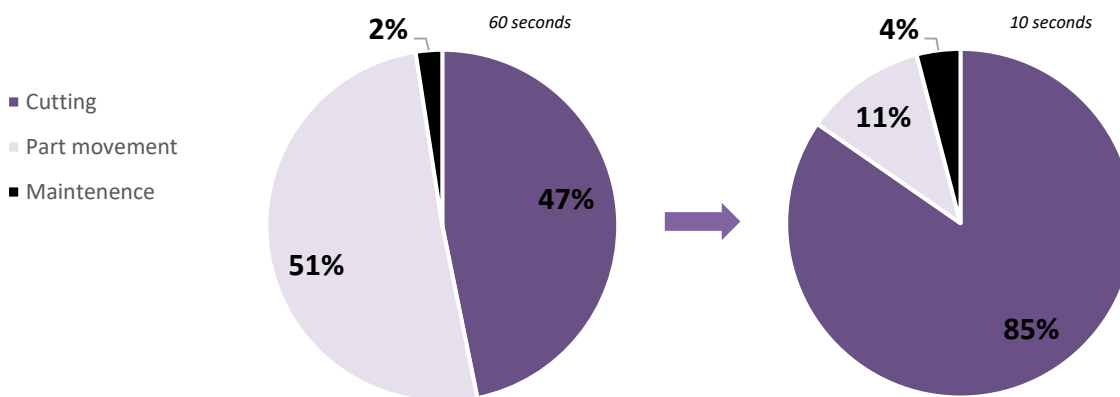


Figure 99 Time spent performing activities where change-over activity takes 60 seconds and 10 seconds

The change over time reflects the time it takes between completing one cutting operation and beginning another, where the stacks are moved into and from the laser cutting machine. The changeover operation does not add any value to the product and is simply a necessity of the process. Change over time has a significant influence on the overall production time, accounting for the majority of time spent producing stator laminations where change-over times are 60 seconds. Given that there is an accountable cost for every hour of production, as defined by the overhead rate, the change-over process has a time and financial costs associated with it. For a production quantity of 100,000 the change-over process is directly responsible for over £500,000 of overhead costs. One method of reducing the time between operations is potentially investing in a fast, automated loading and discharge system to reduce the time lost in change over. These types of systems can be expensive to purchase, and so is only suitable where the improvement to times, and order quantities are sufficient to create real savings. This is a similar argument to the proposal of using an alternative laser cutting machine. Both improvement processes require substantial investment, and they are directly linked in the production process. It would be prudent to consider any process improvement initiative holistically to ensure that the overall system, laser cutting and transition, works without issue otherwise it is possible that the systems may be incompatible, resulting in an increase work and processing as a result of added complexity in the manufacturing system.

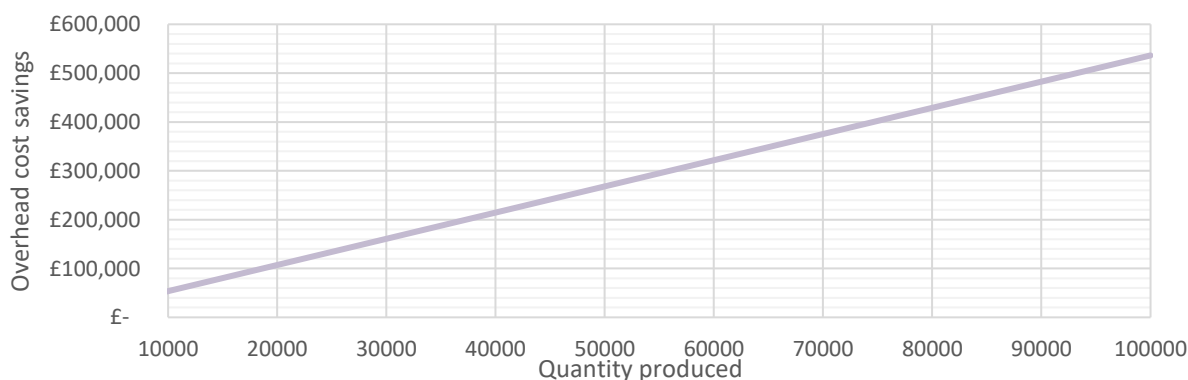


Figure 100 Potential overhead savings of improving change over time from 60 seconds to 10 seconds

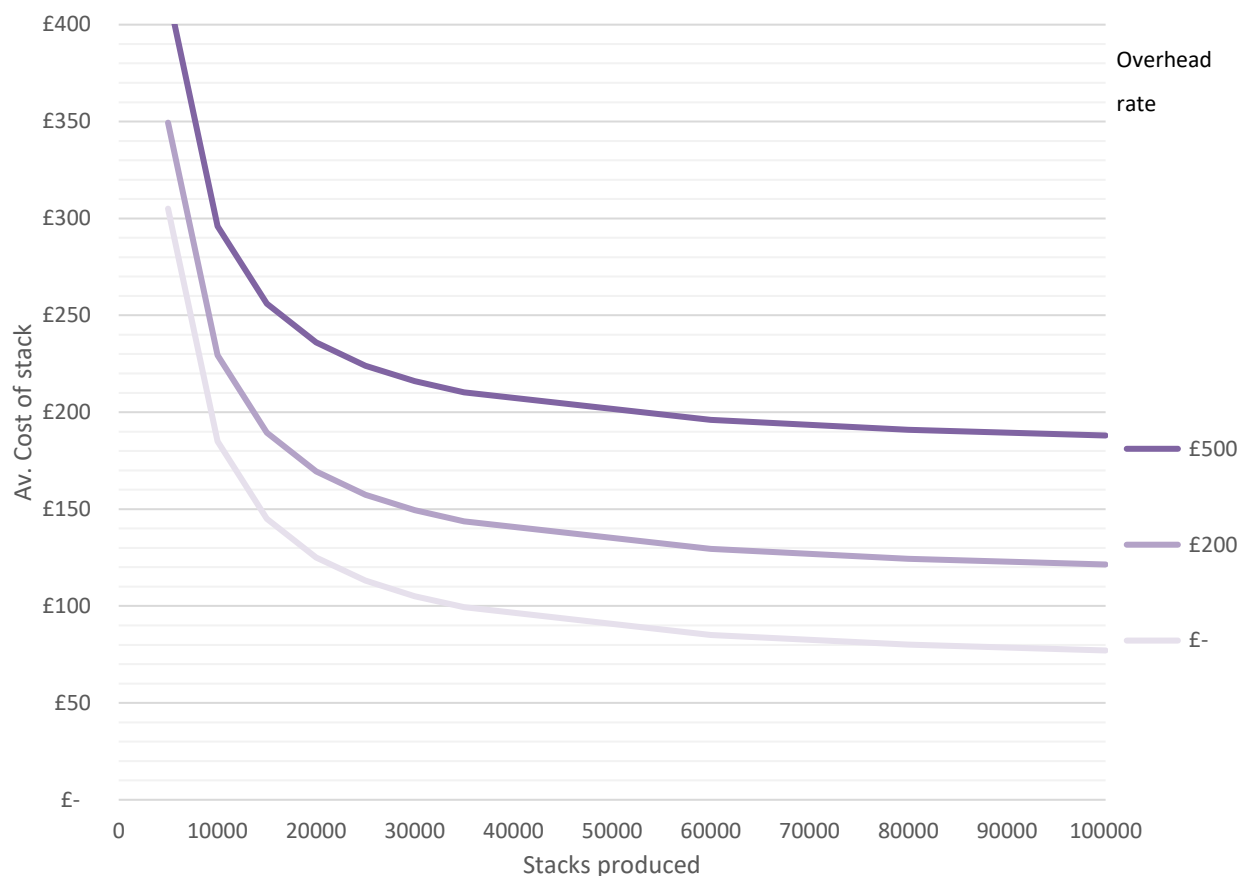
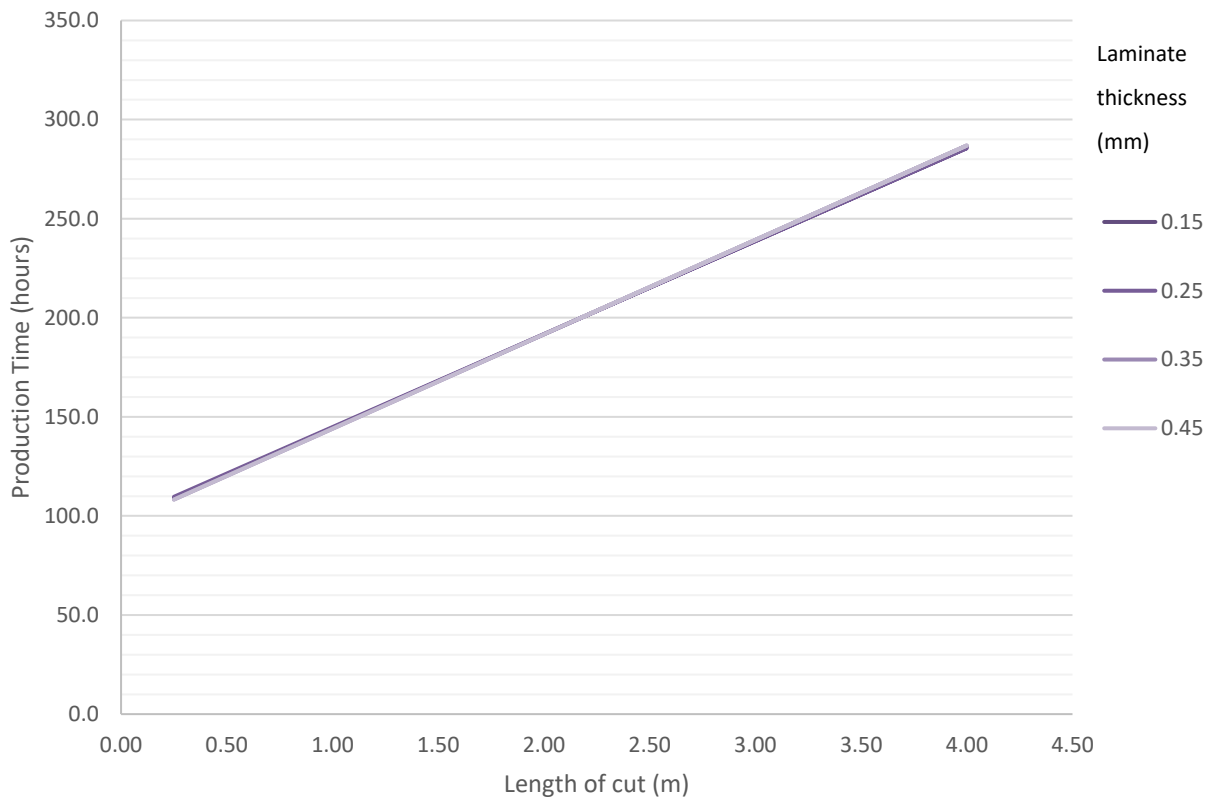


Figure 101 Overhead rate effect for different production quantities

The overhead rate can have a large impact on the decision to invest in new machines and fixtures. In the previous example of investing in an automated loading machine, an increased overhead rate would create greater need to reduce production times and further incentivise the purchase. However, the new machine would also incur some alteration to overhead rates, as its factory footprint, labour & skills requirements and other factors would need to be taken into consideration. The skills required to operate the more advanced technology may not be readily available or difficult to source, which creates greater costs and risks in transitioning towards more advanced processes. It is also possible to use the introduction of new manufacturing facility as an opportunity to optimise the current work spacing and layout design. Additional benefits may exist in terms of the effect on the work force, as a reduction in manual handling stresses may see improvements to both morale and performance.

Small production quantities are very expensive in the considerations of the present work as the model includes the high investment costs for purchasing laser cutting machines, which would likely be required given that stamping is the current standard production process. Once production output has reached 30,000 stacks, the average stack cost steadily reduces regardless of the overhead rate considered (Figure 101).



*Figure 102 effect of length of cut on production time for different sheet thickness*

Given the fixed speed of the laser there is a linear relationship between the length of cut and production time. There is a very small, negligible effect caused by using different sheet thicknesses, which may be seen in the small deviations seen previously Figure 92, suggesting that there is no relationship between the length of cut and sheet thickness.

One of the benefits of using a laser cutter is the ability to produce more complex cutting geometries, where a standard stamping process is limited. It might be possible that if parts are designed for manufacture by laser cutting, that the length of cut can be reduced slightly compared to the standard design, presenting an opportunity to save production time in the laser cutting process.



Figure 103 Effect of gas price on laser cutting cost

Trials in this study showed how different shielding gases can be used during the cutting operation (see section 6.7). It is difficult to quantify the amount of gas used in any cutting operation, and as such, it is only possible to estimate the cost of the gas used in the process. Discussions with technicians indicated that costs are relatively low, with the probability being that gas costs are in numbers of pence rather than pounds sterling per cutting operation. The optimisation study demonstrated that the total cost of consumables used per operation, inclusive of gas, can have a major factor on the design of the process and the selection of process parameters. Excessive consumable costs can have a major impact on the overall cost of producing a stator, as demonstrated by Figure 103, where gas (a consumable per operation) directly increases the average stator cost by approximately £7 for every £1 increase in the cost of the consumable (gas in this case). One method of reducing this effect is to switch to a cost optimised model. However, the results presented earlier (Section 6.4.2) indicates that this can have a negative effect on the productions times as a result.

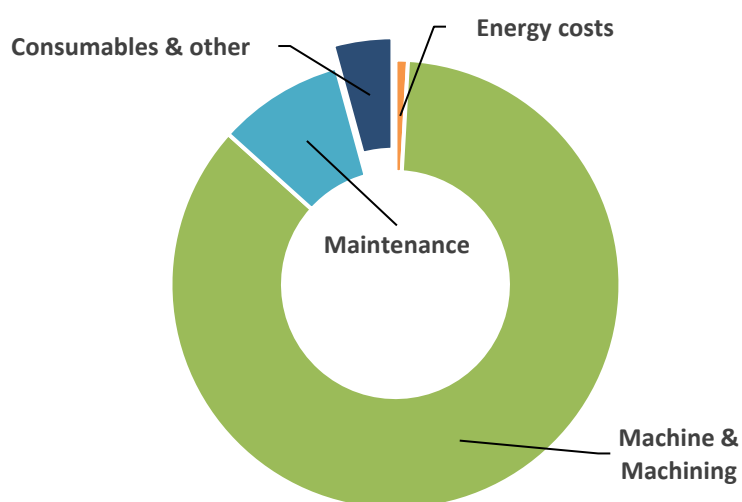


Figure 104 Proportion of cost associated to activity

## 6.7 Conclusions

Laser cutting is currently used primarily as a method of producing prototype laminations for stators. The viability of laser cutting laminations for mass manufacture relies on the ability to improve the process, mostly in terms of reducing production times. This can be tackled from both a technical machining perspective and an operations management perspective. Laser cutting has been demonstrated to have the capability to perform the required task, namely cutting electrical steel laminates, and further work can be conducted to find an optimal set of parameters for a given laser cutting machine. The effect of cutting parameters on the quality of part produced are explored in section 7. From an operational perspective, the introduction of laser cutting as an alternative manufacturing process may create opportunities in the total manufacturing system, such as opportunities to reduce wastes using lean manufacturing principles. The flexibility of a laser cutting machine fits in well with this type of approach, especially compared to stamping where a new tool must be designed and manufactured for each new design of stator.

Laser cutting has relatively low tooling costs, but laser cutting machines require large sums of investment. The model used in this study recommends that multiple laser cutting machines are used in combination with other process improvements. Laser cutting has the potential to reduce process times immensely. However, this is at a cost to the performance of parts produced, and also may be limited by the depth of stack which can feasibly be cut. It may be possible to identify a laser cutting machine, and laser cutting parameters, which are capable of cutting through large stacks without introducing bending or joining issues.

The laser cutting trials in this study involved a manual part change over. This was reflected in the model by the change over time being 60 seconds. An automated system should be possible in combination with a tailored laser cutting machine selection. This would enable parts to be changed over much more quickly and also reduce the time spent manually handling goods, but again requires investment.

## 7 Polystromata laser cutting experiment

### 7.1 Methodology

#### 7.1.1 Knowledge gap

Laser cutting is an established alternative to stamping in stator production, but only for small batches or one-offs. No research exists which studies the potential of cutting multiple laminates in one operation using laser cutting.

#### 7.1.2 Approach

An initial laser cutting trial was conducted using the AMRC's 3kW Trumpf laser. The trial was used to identify settings for further cutting trials. The initial cuttings settings were chosen based on consultation with the machine operator. The machine settings tested in this trial are listed in Table 24. The machine settings were used in combination with manufacturers recommended (default) set-up based on sheet thickness and sheet material. The sheet material which was sourced for this trial was Cogent M250-35A.

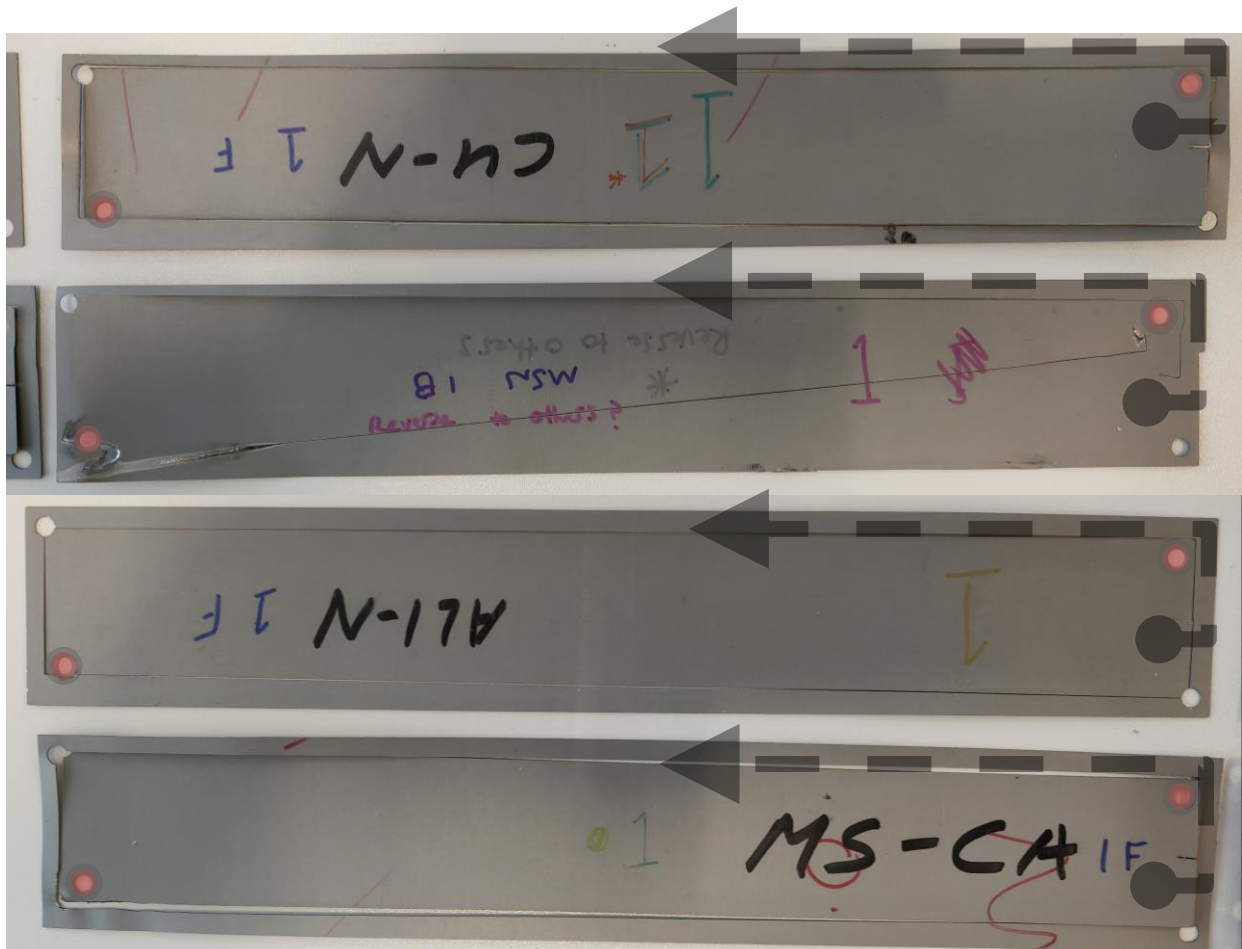


Figure 105 Samples from initial single sheet cutting trial



Figure 106 CAD used in first trial

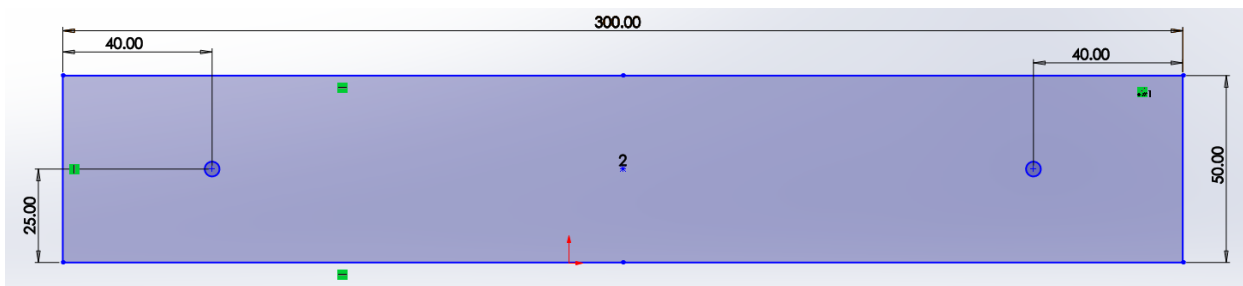
Cutting settings			
settings material	cutting gas	Name	Nozzle
copper	nitrogen	CU N	1.2
Aluminium	nitrogen	ALI N	1.4
Mild Steel	nitrogen	MS N	1.4
copper	oxygen	CU O	1.2
Aluminium	oxygen	ALI O	1.4
Mild Steel	oxygen	MS O	1
Mild Steel	Compressed air	MS CA	1.7

Table 24 Settings entered into Trumpf 3kW laser to create samples



### *Polystromata laser cutting*

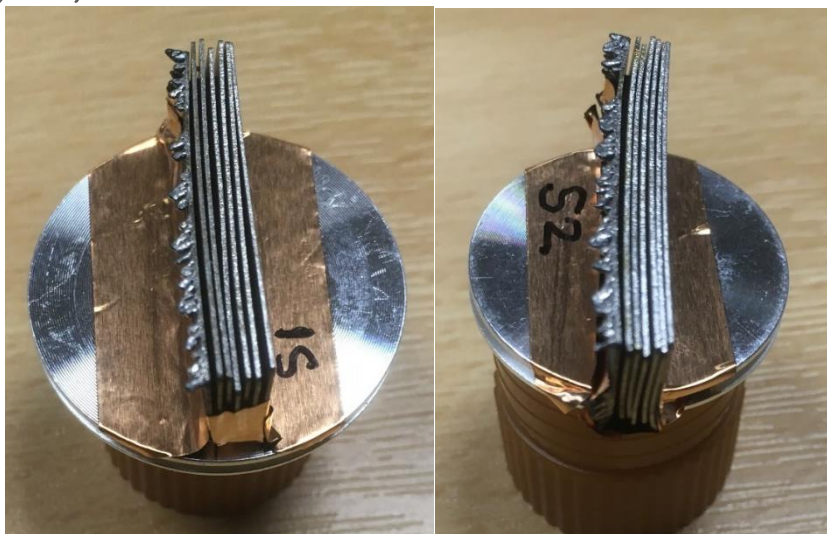
Lessons were learned from the initial single sheet cutting trial. The laser starting position was changed so that the laser begins in the bottom left corner, offset into the scrap material such that the start of the cutting process does not influence the samples. A preliminary polystromata cut trial was also conducted using the CAD design from Figure 106. This revealed that the position of the screws was too close to the laser cutting path. A new CAD design was developed and used, incorporating smaller screws with shorter screw heads. There were 2 x 4mm diameter bolts per stack of 7 laminates. The holes for the bolts are within the strips cut, but are positioned near the ends, in an identical position for all samples, so that they will not interfere with an eventual magnetic measurement by Epstein frame. The laser settings used were identified from the analysis of results from the previous laser cutting trials in section (7)



*Figure 107 Revised CAD used in laser cutting of Epstein samples*



*Figure 108 Side view of stack with new bolt arrangement prior to cutting*

*SEM Microscopy study*

*Figure 109 Mounted samples for SEM trial 1*

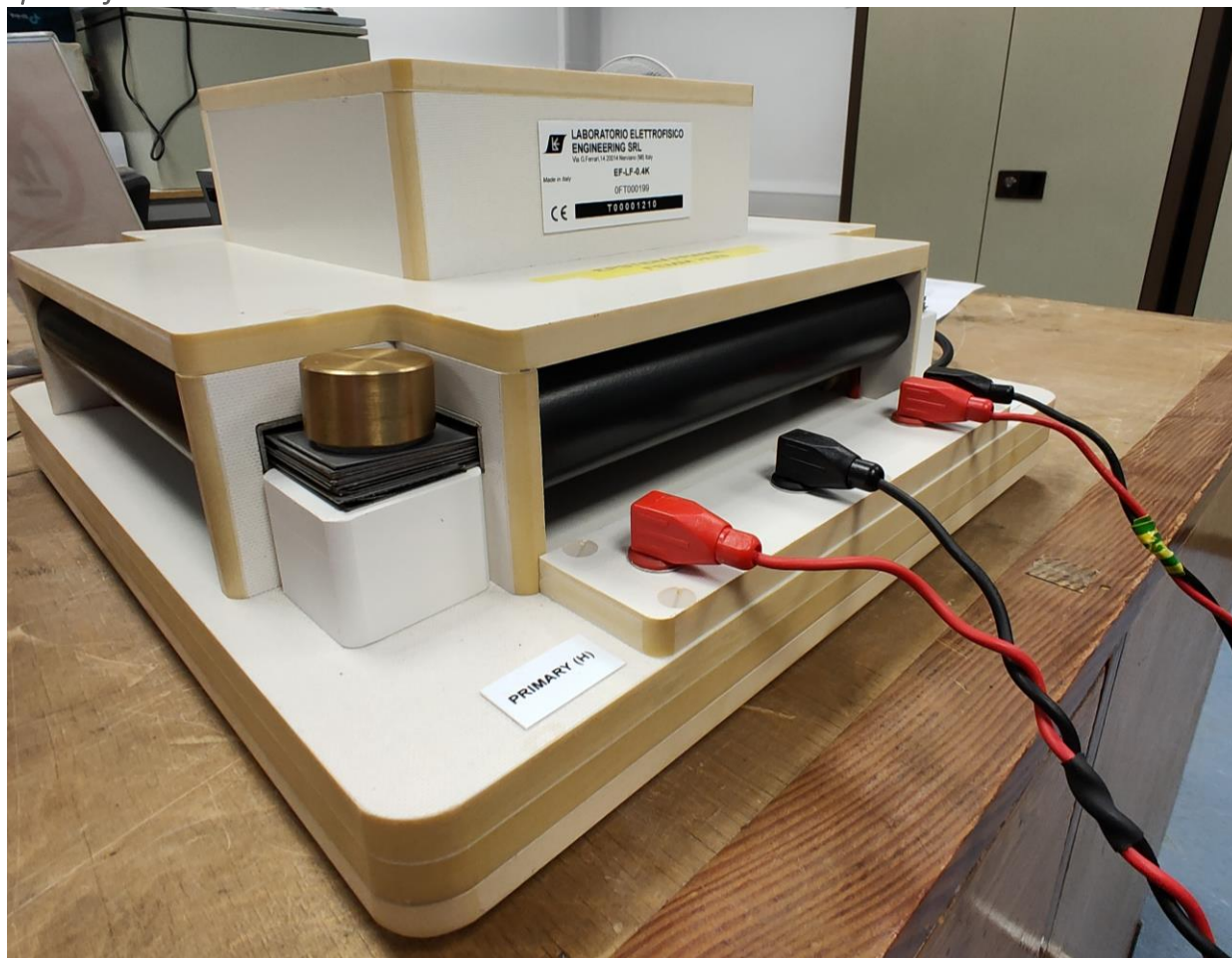
An initial Scanning electron microscope (SEM) trial was conducted to view the quality of the cut edge with greater detail. Sections were taken from the laser cut samples and the laser cut edge viewed under an SEM microscope. Two full stacks were chosen at random for testing. Sections were taken from one end of each stack, and manually cut so that the samples would adhere to the mounting protocols. The samples were mounted and viewed by University of Sheffield electron microscopy technicians following standard procedures. To prepare the samples for microscopic examination slices adhered to each other using double sided conductive carbon tape and further wrapped in conductive copper tape. The assembly was held on aluminium SEM stub with copper tape, providing a conductive pathway for the imaging electrons. The cut edge of samples was examined in an FEI Inspect F FEG-SEM at 15kV, recording images at magnifications x100 and x250 in secondary electron (SE) mode, using a spot size of 3.5 and aperture of 4. Where indicated backscattered electron (BSE) images were also obtained to enhance contrast in regions of topographical and compositional difference.

### *Further SEM Microscopy study*



*Figure 110 Mounted samples for SEM trial 2*

A further study was conducted to understand how the microstructure of the material had been affected as a result of the Polystromata laser cutting process. Further examination was carried out to examine the interior of the samples, using an FEI Inspect F FEG SEM at 15kV, Spot size 3/3.5 and objective aperture 5. The specimens were mounted edge-on in conductive Bakelite and ground and polished to a mirror finish. The exposed surface, which showed the cut edge on one side and then the section through the sheet, was imaged at  $\times 500$  magnification using both SE and BSE imaging, examining the edge of the sample and a region roughly in the middle of each strip. The imaging mode allowed contrast between grains to be seen as predominantly channelling contrast, enhanced by a light etch (Nital) prior to examination to reveal the grain structure.

*Epstein frame trial*

*Figure 111 Epstein frame used in trials*

A trial was conducted using Polystromata laser cut samples. The samples were 300mm x 50mm, as in Figure 107, including the small hole sections. It was determined following consultation with Professor Jewell of the electric machines and drives research group (2019) that these holes should only have a negligible effect on the results of the Epstein trial. Samples were separated into those from layers 1-2, 3-4 and 5-6. Layer 7 samples were not used as a result of non-conformance. Results were obtained based on these groupings of layers. The trial was conducted under the supervision of a trained University of Sheffield technician following the instructions as outlined by Laboratorio Elettrofisico (2019). The Epstein frame was set up with, Frequency 50 Hz and approximately  $B_v$  0.303 T,  $J_v$  0.3 T for all trials.

## 7.2 Introduction

Laser cutting has the potential to be an alternative to stamping in the production of stators and rotors for electric machines. Laser cutting is generally only used to produce prototypes and small batch quantities as the process is considered too slow and costly to be used at scale relative to stamping. One method of increasing the economic efficiency of laser cutting is to perform multiple cuts per cutting operation. As noted before this can potentially be done by stacking laminates prior to laser cutting. However, this type of process has not been verified for electrical steels. Work conducted in section 0 of this research demonstrates how this method can be used to reduce production time and costs. However, it is unclear how the quality of parts produced might be affected. A further problem is understanding the technical hurdles which affect the manufacturability of stators due to the multiple laminate cutting process.

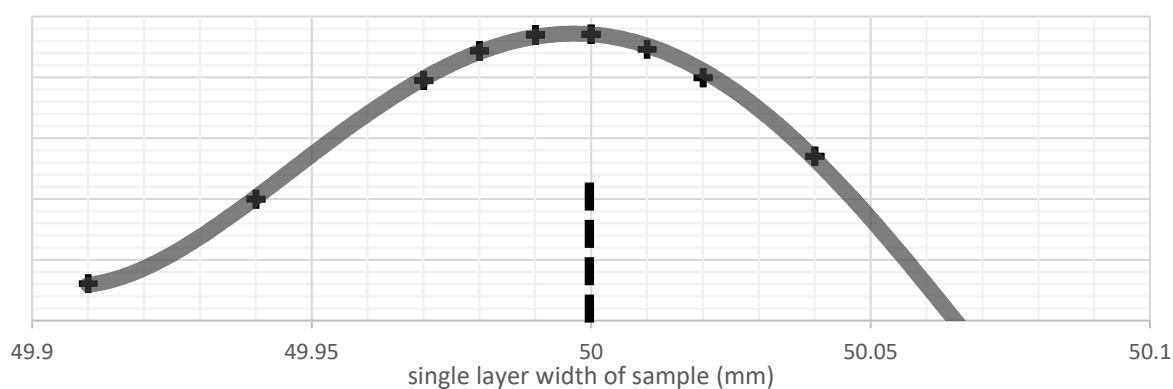
An initial trial study was conducted with single sheets of electrical steel to better understand the interaction between the material and the laser. Multiple laser setting parameters were used, with the best resulting laminate samples settings being used in further studies.

The main trial in this study was conducted using stacks constructed of 7 laminations. These samples were assessed in multiple ways. The geometric accuracy and consistency were measured, as was the size of burrs and defects. The samples were tested using an Epstein frame to measure the electro-magnetic performance of the samples, and further SEM tests were conducted to attempt to identify any meaningful differences in the samples based on the position of the sample in a stack during cutting.

### 7.3 Cutting of single sheet laminates

#### 7.3.1 Single sheet laminate cutting variation

Laser cutting is considered to be an accurate and precise method. A simple rectangular cut was produced on 28 single sheets. The cuts were performed with the same laser settings on each cutting operation. The width of each sample was designed to be 50mm, as described by the CAD (see section 7.1). Measurements were taken using a Vernier calliper to measure the 50mm feature dimension. Figure 112 shows a high level of accuracy for cutting single sheet samples. All samples were cut within a tolerance of better than 1% accuracy.



*Figure 112 Variation of width of sample after single cut operation*

#### 7.3.2 Laser settings effect on part quality

Samples were produced using various laser cutting settings (see Table 25 - Table 27). Different shielding gas settings were used, ranging from; oxygen, nitrogen, and compressed air. Different material settings were selected in the laser cutting machine set-up; ranging from mild steel to aluminium and copper.

All cuts performed with oxygen as a cutting gas exhibited signs of discolouration and burning. This was a particular problem around hole geometries at the point of entry and exit of the laser beam. Samples cut using nitrogen had much less discoloration and edges were both smoother and more conforming to the expected shape as described by the CAD. The quality of laser cut smaller features such as the holes created during the first cutting operation often had discolouration at the entry / exit points of the laser. Settings which used less powerful laser settings appeared to show less discolouration around the holes.

Full results are displayed in Table 25 - Table 27. The different cutting settings are ranked based on the quality of samples produced from this trial. The four best performing cutting settings were then used in a polystromata cutting trial.

Identifier	Cutting settings			Review of cut					Pictures					Ranking		
	settings material	cutting gas	Name	Rating /5	Colour notes	Edges notes /5	Holes notes /5	Front	back	close up	close up	close up				
3.50	1	copper	nitrogen	CU N	1.2	3.67	4	some discolouration on back of holes	5	clean edges, consistent	2	2 holes good, 1 with burrs, 1 very messy				4
	2	copper	nitrogen	CU N	1.2	4.00	3	small dark marks at holes	5	clean edges, consistent	4	all holes no burr, but discoloration at holes				
	3	copper	nitrogen	CU N	1.2	3.00	3	small dark marks at holes	4	some burring on one edge	2	2 holes good, 1 with burrs, 1 very messy				
	4	copper	nitrogen	CU N	1.2	3.33	3	small dark marks at holes	5	clean edges, consistent	2	2 holes good, 1 with burrs, 1 very messy				
4.75	1	Aluminum	nitrogen	ALI N	1.4	5.00	5	tiny amount of burn on 1 hole	5	smooth edges, rounded corners. Couple of slight scuffs, no burrs	5	few very small scuffs				1
	2	Aluminum	nitrogen	ALI N	1.4	5.00	5	tiny amount of burn on 1 hole	5	smooth edges, rounded corners. Couple of slight scuffs, no burrs	5	few very small scuffs				
	3	Aluminum	nitrogen	ALI N	1.4	4.33	5	very small discolouration	4	few scuffs and burrs	4	1 hole not smooth				
	4	Aluminum	nitrogen	ALI N	1.4	4.67	5	slight burr near 1 hole	5	smooth edges, rounded corners. Couple of slight scuffs, no burrs	4	1 hole with many small chips. Rest good				
4.50	1	Mild Steel	nitrogen	MS N	1.4	4.33	5	no colour around holes. One small mark on edge	3	jagged edges in places	5	no burr, very round				2
	2	Mild Steel	nitrogen	MS N	1.4	4.67	4	couple of colour marks	5		5					
	3	Mild Steel	nitrogen	MS N	1.4	4.00	4	colour at edge burr and two other small marks	3	one part of long edge very burred	5					
	4	Mild Steel	nitrogen	MS N	1.4	5.00	5	one small mark by hole	5		5					

Table 25 Laser cutting single laminate trial results part 1<sup>6</sup>

<sup>6</sup> Specific settings were not made available by manufacturer. Indicative settings have been sourced which provide a reasonable estimation of the specific settings which have been used to produce these cuts. (Appendix 11.5 p199)

3.33	1	copper	oxygen	CU O	1.2	3.33	5		2	corners are chipped, not rounded	3	one hole not very circular	
	2	copper	oxygen	CU O	1.2	3.00	5		2	corners are chipped, not rounded	2	one hole not very circular, other holes slight burrs	
	3	copper	oxygen	CU O	1.2	3.33	4	some colour spatter on edges	2	corners are chipped, not rounded	4	very light jagged edge on holes	
	4	copper	oxygen	CU O	1.2	3.67	5		2	corners are chipped, not rounded	4		
2.92	1	Aluminium	oxygen	ALI O	1.4	3.00	1	dark discolouration on edges	3	jagged edges in places	5		
	2	Aluminium	oxygen	ALI O	1.4	2.67	1		2	jagged edges in places, chipped in one corner	5		
	3	Aluminium	oxygen	ALI O	1.4	2.67	3		3		2	one hole not very circular	
	4	Aluminium	oxygen	ALI O	1.4	3.33	2	dark discolouration on edges	3	slight burring on edges	5		

Table 26 Laser cutting single laminate trial results part 2








2.42	1	Mild Steel	Compressed air	MS O	1	2.33	5	light colour marking	1	shape conformity bad, not rectangular, edges also poor	1	two holes are awful				
	2	Mild Steel	oxygen	MS O	1	2.33	5		1	shape conformity bad, not rectangular, edges also poor	1	3 holes awful				
	3	Mild Steel	oxygen	MS O	1	2.00	3	one hole very colours and spattered	2	jagged edges and chips	1					
	4	Mild Steel	oxygen	MS O	1	3.00	5		3	jagged and not rounded corners	1	holes not circular				
4.50	1	Mild Steel	Compressed air	MS CA	1.7	4.67	4	couple of small colour marks by holes	5	very smooth, one edge light burr	5					
	2	Mild Steel	Compressed air	MS CA	1.7	4.33	3	6 separate colour marks around holes	5		5					
	3	Mild Steel	Compressed air	MS CA	1.7	4.67	4		5		5					
	4	Mild Steel	Compressed air	MS CA	1.7	4.33	5		3	one part of long edge very burred and deformed	5					

Table 27 Laser cutting single laminate trial results part 3

## 7.4 polystromata laser cutting

### 7.4.1 polystromata cutting trial 1

The four best laser settings from the single cut trial were carried into a polystromata cutting trial. The purpose of this trial was to begin to understand the challenges around laminate polystromata cutting, and to identify an appropriate method of producing samples for further electro-magnetic trials. The samples were evaluated in the same way as with the single sheet cutting trial. Full results are given in appendix 11.7.

Issues were encountered during the planning for these cutting trials regarding the need to affix parts within the laser cutting machine. The shielding gases used during cutting produce a force capable of moving laminates if they are not properly secured. This issue had occurred during the cutting of single sheets and had only affected one sample which has blown out of position. Stacks were held together using small screws to reduce the potential of parts moving during cutting. During the cutting of stack 2, the stack was shifted from its position. This occurred through a combination of the laser cutting nozzle colliding with a protruding screw and the force of the cutting gases being ejected from the nozzle. As a result, stack 2 has not achieved the desired cut. The laminates in stack 4 are stuck together at the cutting edge. The laminates are less separable as the depth of cut increases. Stack 3 failed to be completely separated from the off cut. There was a small section on a corner which the laser had not passed through. This would appear to be another situation created by the laser nozzle crashing into protruding screws and requiring the operator to restart the operation. The offcut was manually removed after the laser process was completed. The laser was set to cut a thickness of 2.5mm material in each case.

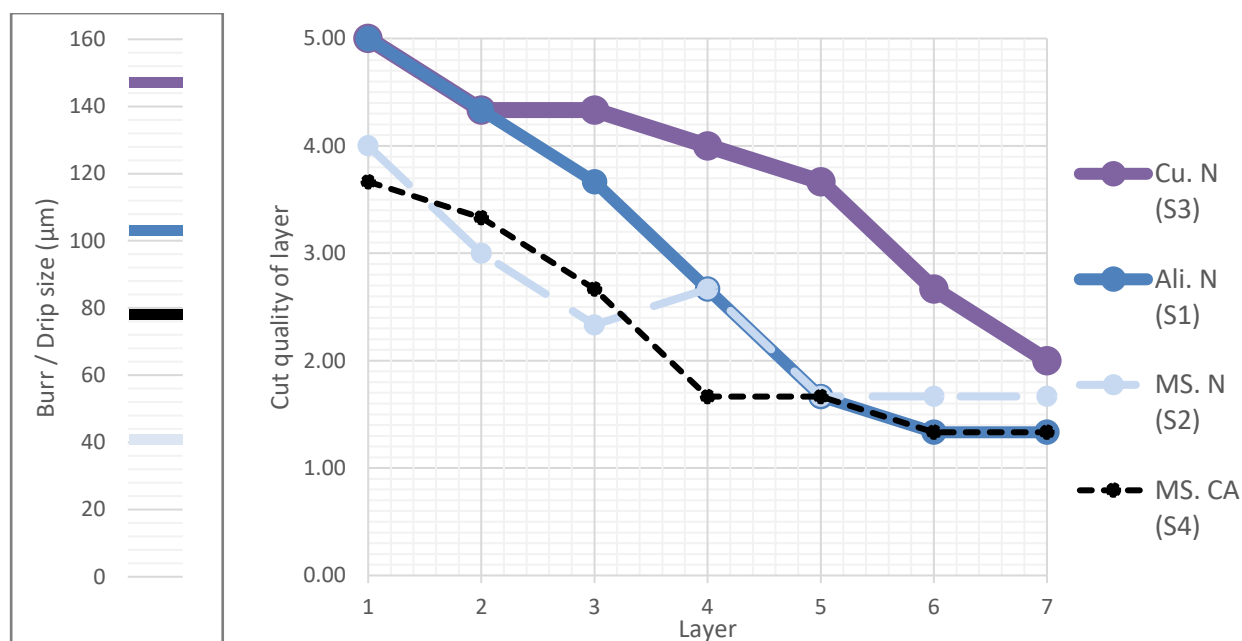


Figure 113 Burr / droplet size on bottom layers of stacks & stack layer quality results

The results for this trial are shown in Figure 113, with each layer of the stack evaluated for quality. The best polystromata cut appeared to have been achieved using the pre-existing 'Copper Nitrogen' laser settings. However, the best single laminate cuts were achieved using 'Aluminium nitrogen' laser settings. The single sheet and stack cutting studies both appear to show that nitrogen as a cutting gas provides greater quality cuts for the material being tested. This confirms the suggestion by Gaworska-Koniarek (2011). Nitrogen cut samples tend to have much less discolouration around the cutting edge, particularly in comparison to samples cut with oxygen. Layer 7 for each stack had an issue with material collecting along the cutting edge in a dripping effect. This effectively created a burr on layer 7. Whilst the copper nitrogen settings appeared to demonstrate the best cut, it was also the settings with the greatest burr on layer 7.

#### 7.4.2 Polystromata trial 2 - geometric variance

An alternative design was developed, moving the screw positions to centre of the part. Samples were produced using copper nitrogen cutting settings. During the laser cutting operation there were no issues with the laser head colliding with screws, as had previously occurred. The geometric variation was measured, just as measurements were taken in section 7.3.1. Measurements were taken at two positions in this case; edge A and edge B (see Figure 114). Both edge features are designed to be 30mm in length.

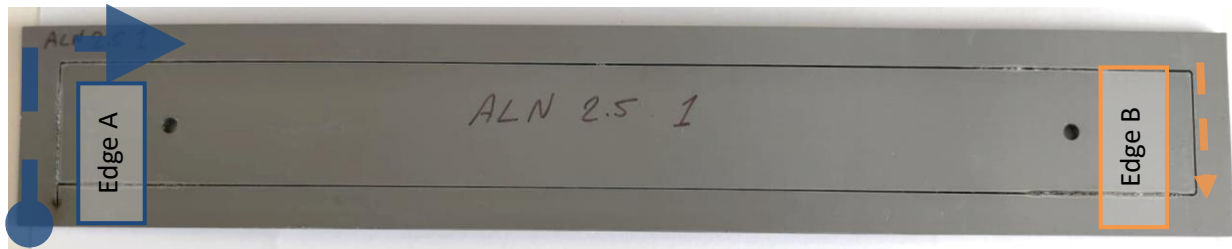


Figure 114 Laser route and identification of Cuts A & B

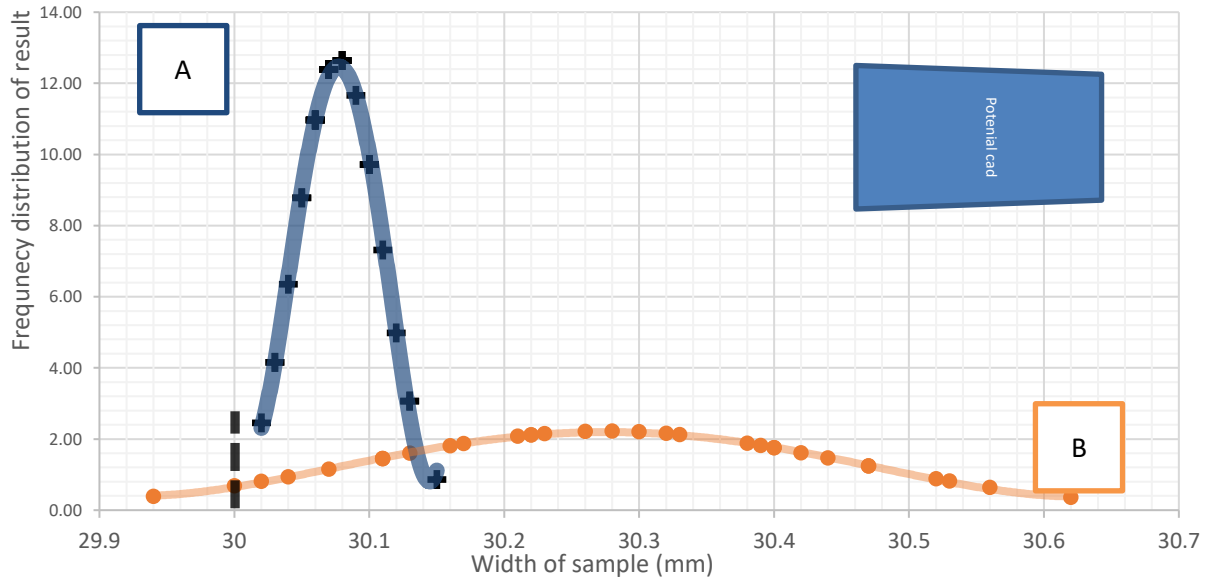


Figure 115 Variation of width of sample after polystromata cut operation

The results in Figure 115 show that at edge A, a similar level of precision as in the single sheet measurements is achieved. However, the cut is less accurate, with the median result being approximately 30.8mm instead of the specified 30mm. The cut at edge B has much more variability in the results, showing a reduction in the precision of the cut performed in this location. The cut is generally less accurate too, with the median cut being 30.27mm instead of the specified 30mm. The cut performed at edge A is along the line of the lasers first action. This means that this cut is performed while the part is firmly fixed in place, as it is still attached to the outer part of the sample. Edge B occurs when the sample is less fixed in place, and this means there is more potential for the part to move, even only very small movements. This is one reason why the cut at edge B is less precise than the cut at edge A. Both cuts were less accurate than cutting single sheet laminates. Part of the reason for this is due to the laser focal point. The laser beam is wider as the distance from the focal point increases. Because these cuts were performed using stacks, different layers in the stack have been cut by a beam which has a variation in beam thickness between layers. A combination of these effects reduces the accuracy and precision of polystromata cutting. However, it may be possible to use a fixture set-up and more developed laser settings to produce more accurate polystromata cuts.

Another solution is to design the CAD geometry with an offset which is equal and opposite to the deviation caused by laser cutting, in this case a slightly undersized trapezoidal geometry might produce more accurate cuts which better reflect the intended specification. It is. However difficult to determine a general rule for how cut geometries should be manipulated to achieve this, rather it could be something that would be determined through the trial of particular geometries.

#### 7.4.3 SEM stack results

Samples were studied using SEM microscopy. Two stacks were studied to confirm a consistency in results between stacks. The resulting images are listed in Table 28. The results show a consistent cutting pattern in layers 1-6 for both stacks. In these layers, there is negligible burring on the edges. Layer 7 in each stack clearly shows excess material on the underside of the layer. This is considered to be as a result of molten material which has collected either through dripping or being blown downwards between layers. Layer 7 is not in a useable state to be included into a stator or rotor lamination stack without further processing to remove the excess material. one solution is to simply scrap layer 7. This would mean scrapping 14.3% of material based on a 7-layer cutting stack. Assuming that only the bottom layer ever needs to be scrapped, the percentage of layers scrapped would be reduced by increasing the number of layers in the cutting stack.

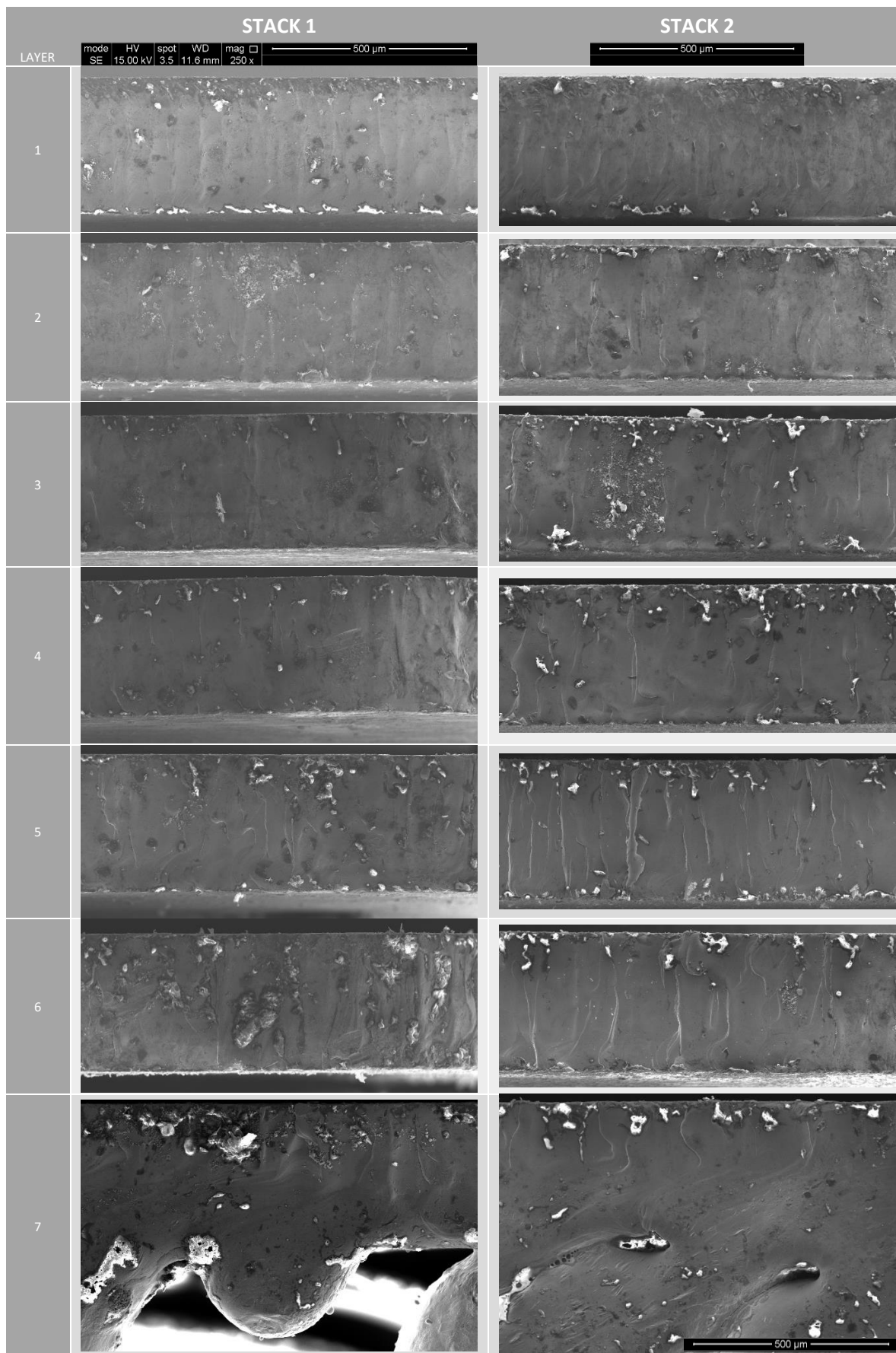
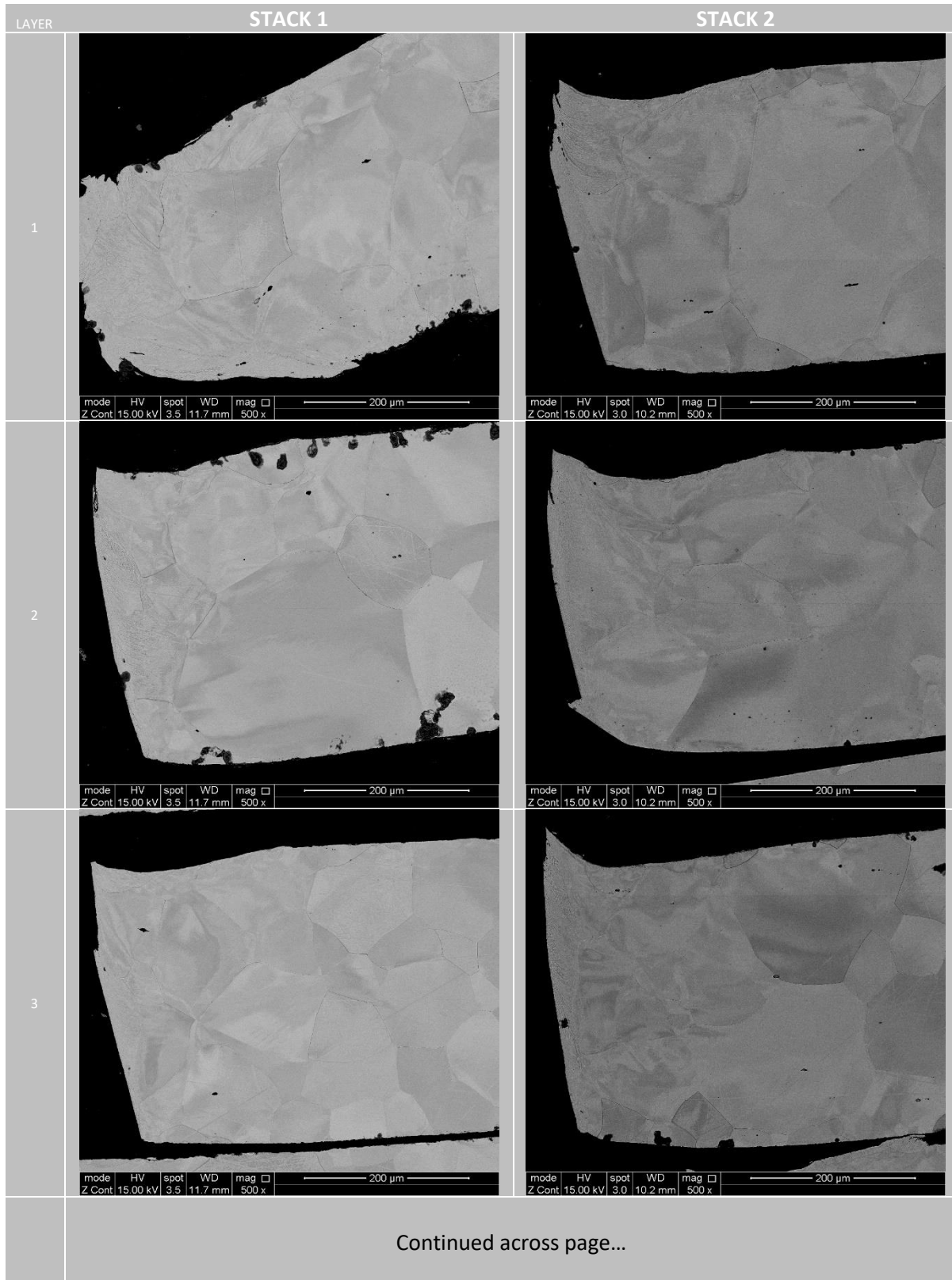


Table 28 SEM results (x250 magnification) secondary electron 15kV

A further investigation into the grain structure of the samples was performed with results shown in Table 29 & Table 30. In all samples the area at the cutting edge shows a different material structure to the rest of the sample.



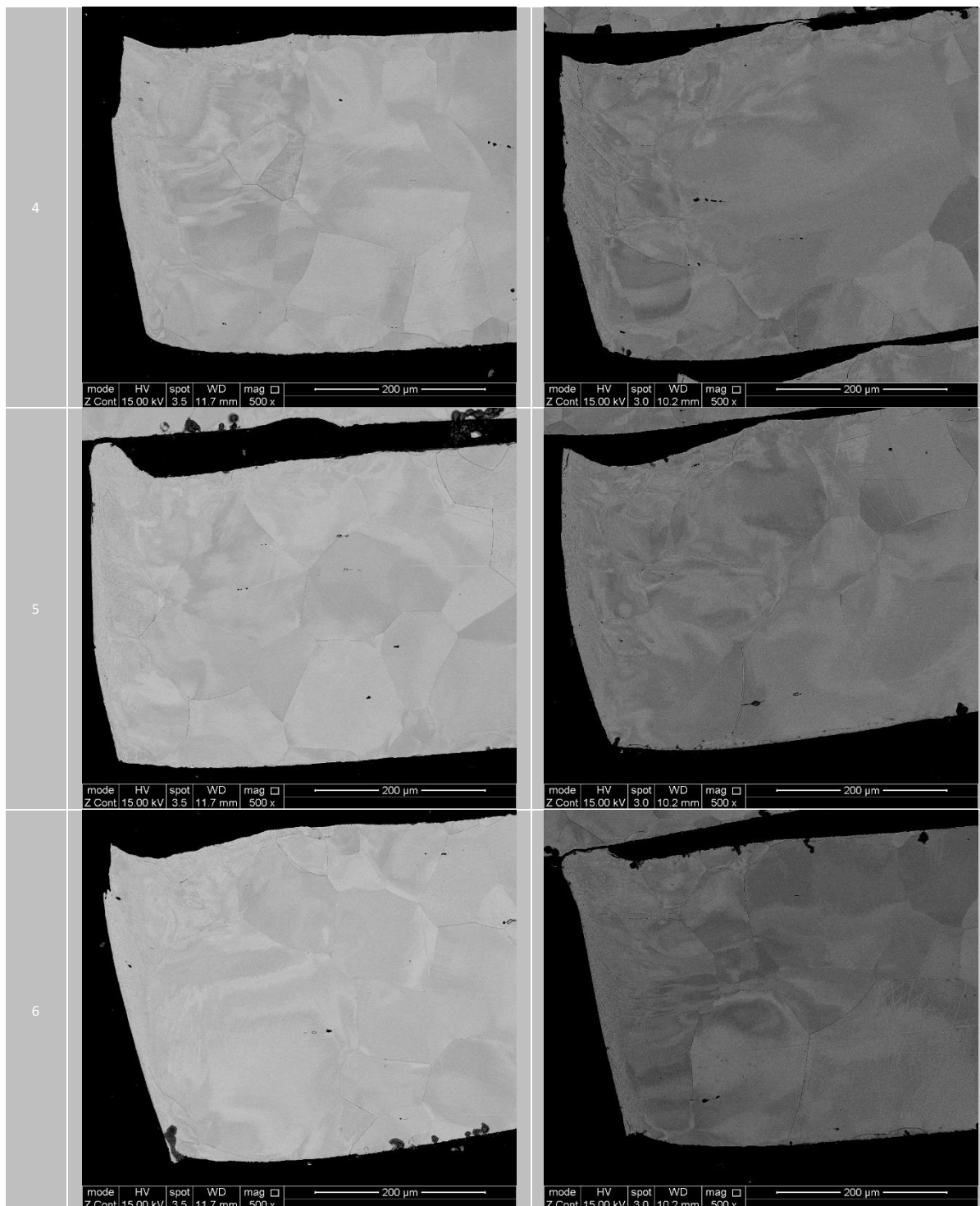
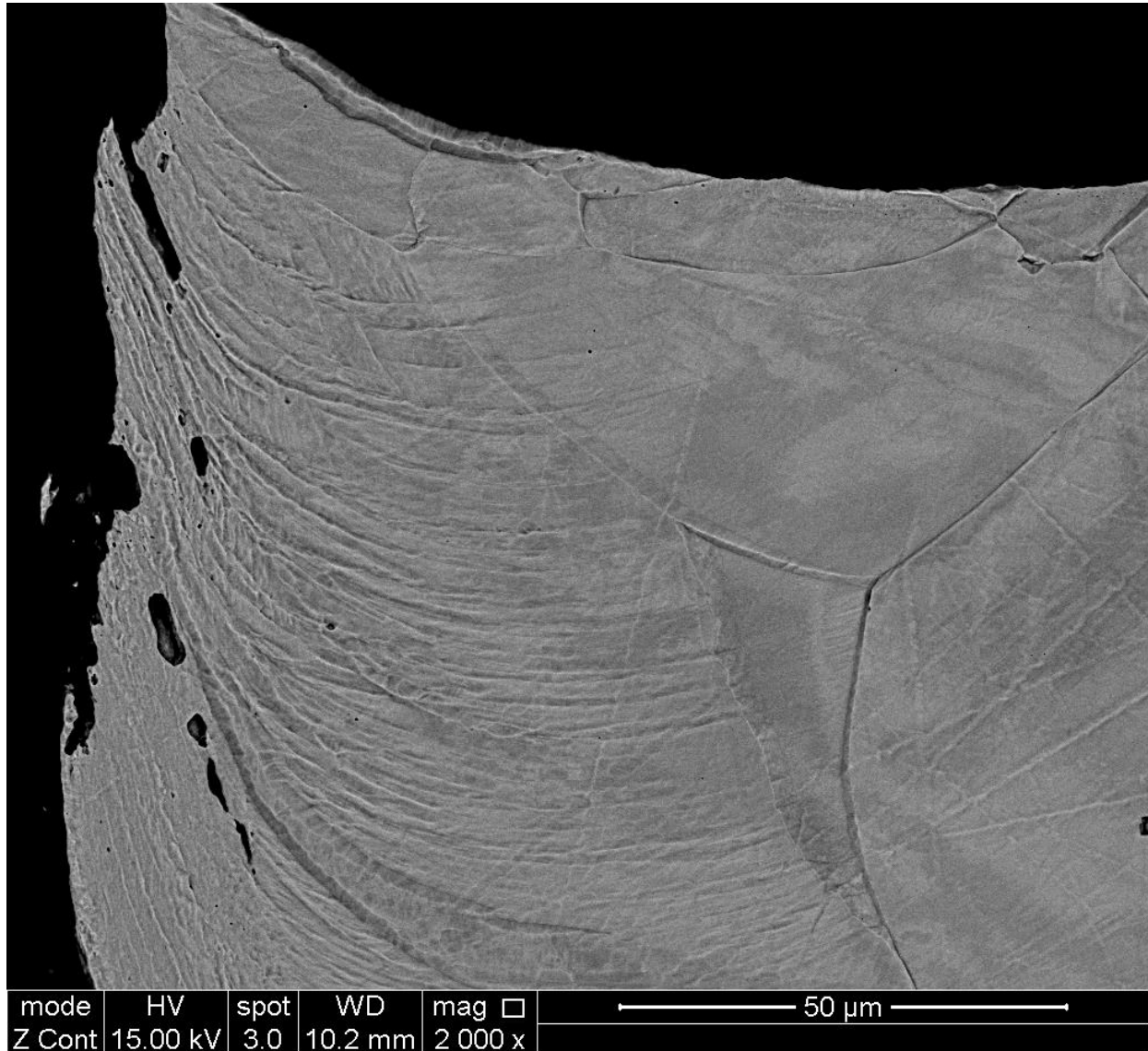


Table 29 SEM results of cut edge (x500 magnification) secondary electron 15kV

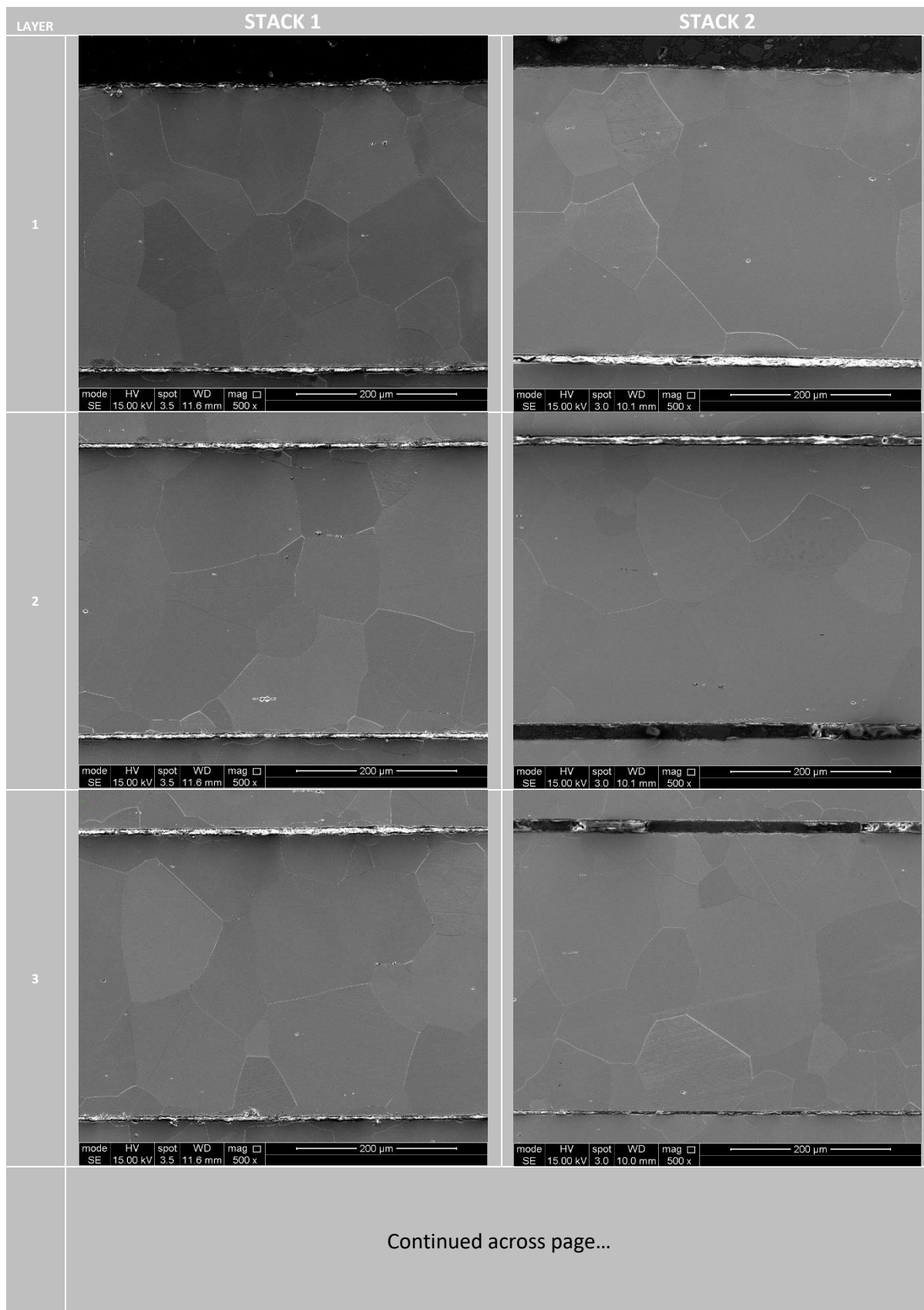


Figure 116 shows a laminar material flow which penetrates into the material by approximately 50  $\mu\text{m}$  on the upper section of the sample and 100  $\mu\text{m}$  on the lower sections of the visible image. There is also consistent evidence that the cut edge is not 'straight' with a small burr occurring on most samples, and the cut receding into the material on the lower sections.



*Figure 116 Stack 1, Layer 1. SEM 2000x Zoom at cut edge*

The mid-section images (Table 30) show a largely consistent grain size through the material and between the layers. There is also little apparent distortion to the grain size in the regions close to the cut, with grains of similar size to the bulk being found within 200  $\mu\text{m}$  of the cut surface.



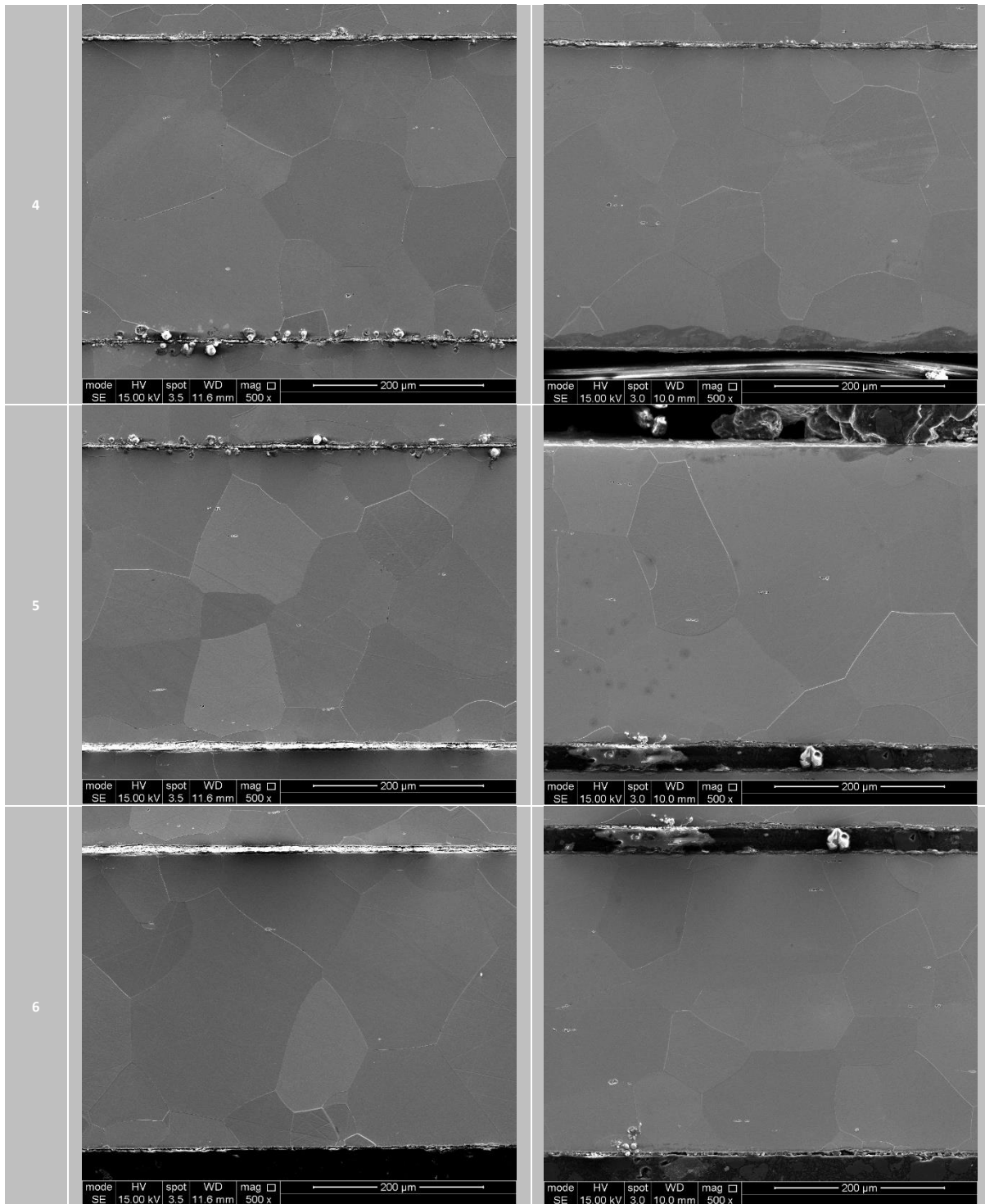


Table 30 SEM results of mid-section (away from cut) (x500 magnification) secondary electron 15kV

## 7.4.4 Joined layers during polystromata cutting

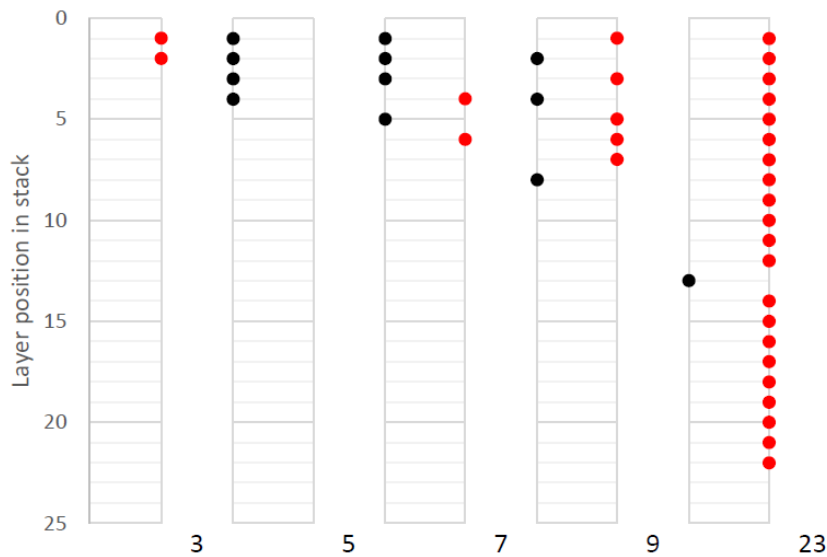


Figure 117 Layers joined in various laser cutting stack sizes (**Black** loose, **Red** joined to layer beneath)

During the stack cutting trials, it was seen that some layers within the stacks can become joined. A small trial was conducted to understand how this joining effect is influenced by stack size. The results of this trial are shown in Figure 117. The smallest stack tested containing 3 layers was quite loosely joined together between each layer. A visual inspection appears to show where small droplets have collected along the length of the cut. These droplets have solidified in the gap between layers and effectively created a small weld. Separating these layers was easily manageable by hand and did not require the use of force.

The 5-stack layer had no issues with layers being joined. However, there was evidence of a similar droplet pattern on the top of the cutting line of layer 3. Despite this, the layer was not joined to layer 2 (layer above). Stacks of 7, from the initial cutting trial, and 9, were very similar. Some layers were joined, but the joins were easily separated by hand. The position of joins appears somewhat random, as some layers were joined close the laser start position, some along the length and some towards the laser end position. That said, there does appear to be a higher likelihood of joining occurring at positions where the laser speed changes, such as when starting, finishing, or turning a corner.

The 23-layer stack was a poor performer in all respects examined. The stack was highly deformed, with a high degree of bending in the stack. The cut stack was delivered in two parts, as layer 13 was the only layer to not be joined the layer beneath. This appeared to be due to some of the bending deformation which had occurred in the middle layers of the stack. The joins are incredibly difficult to separate, such that doing so by hand requires excessive force and would likely cause an injury to be sustained.

## 7.5 Polystromata laser cutting issues

An attempt was made to cut a 7-layer stack using a more powerful laser set-up. This was done by altering the laser machine settings to cut 3mm of copper material instead of 2.5mm. The laser cutting machine is limited by default to only use nitrogen shielding gas up to sheet thicknesses of 2.5mm. As such, oxygen was used instead. The resulting cutting operation had catastrophic consequences for the material. The operation was halted shortly after starting. During the cutting process, vast amounts of sparks shot away from the material, which was unlike the other samples which were produced. Figure 118 shows the damage to the material, which has been melted, forming a solid section at the melt point. The presence of the oxygen gas with the molten metal will have led to extensive oxidation, an exothermic process and the additional heat introduced has led to large amounts of metal being melted.

Figure 119 shows how samples are bent by the laser cutting process. This is most likely as a result a thin layer of material at the cutting edge being melted by the laser and solidifying again, undergoing shrinkage as it does. It is suggested that the edge suffers an overall contraction by this process, and residual stresses are introduced. Because of the edge contracting, the centre of the part deflects, creating a bend in the sample. The cut-off strips demonstrate equal and opposite bending action, which supports this hypothesis.



*Figure 118 Cutting failure*



*Figure 119 Samples bending after being cut*

## 7.6 Electro-magnetic performance measurement using Epstein frame

One of the major factors dictating the quality of a stator is the ability of the material to be magnetised and as such, create torque in an electric machine. An experiment was conducted to evaluate the effect of stack cutting on the performance of laminate materials used in stator stacks. Samples were created by laser cutting 7-laminate thick stacks. An Epstein frame was used to evaluate the performance of the samples. The samples are separated into stack position, where position 1 is the top layer (the first layer penetrated by the laser) and 7 is the bottom layer. The Layers from position 7 (at the bottom of the stack during cutting) are not used in this test as the samples contain burrs (from the dripping effect) and are therefore unsuitable for use in an Epstein frame.

The results show a reduction in performance for all samples. The results show a clear trend, where samples in lower layers have worse performance than samples in higher layers. In Figure 120 magnetic flux,  $H$ , is a desirable feature which directly relates to the torque performance of an electric machine. Figure 120 clearly shows that more magnetising force,  $B$ , is required to create the same levels of magnetic flux for samples in layers 3-4, and more so again for layers 5-6.

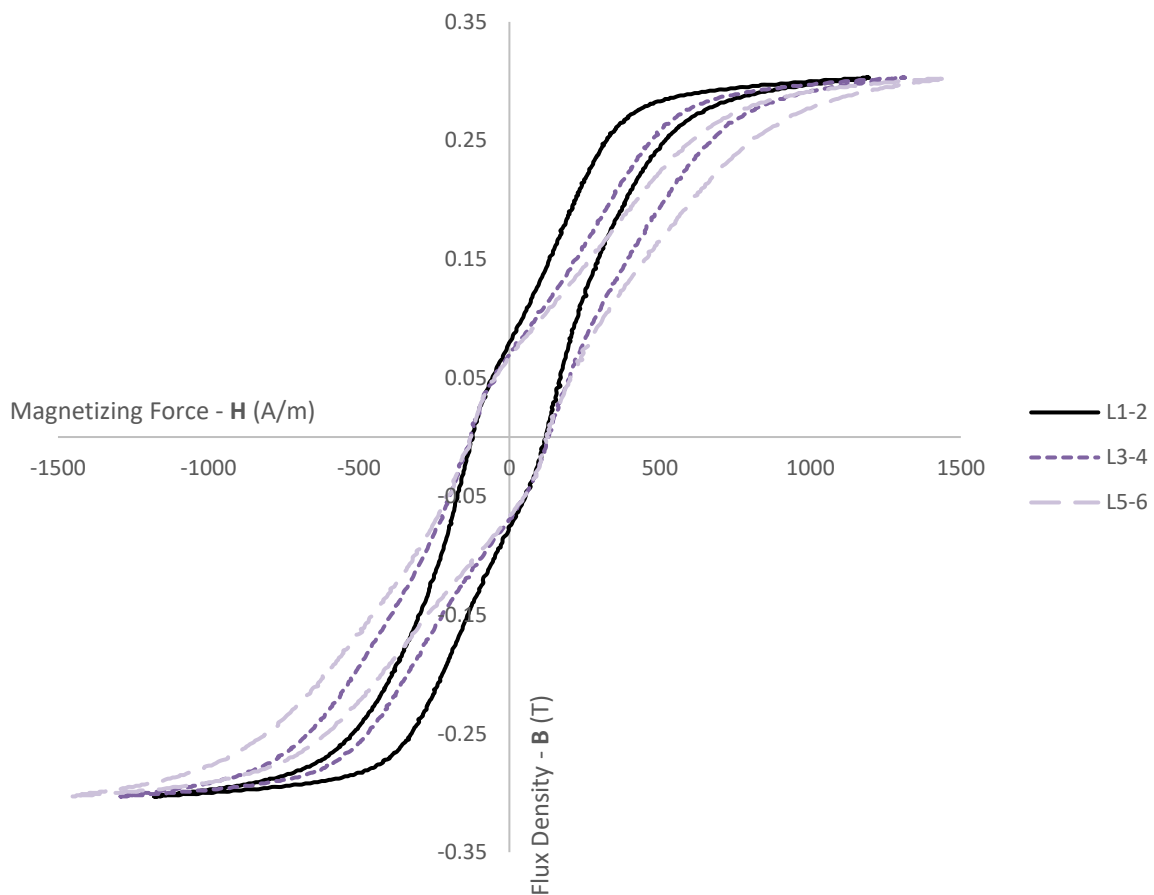
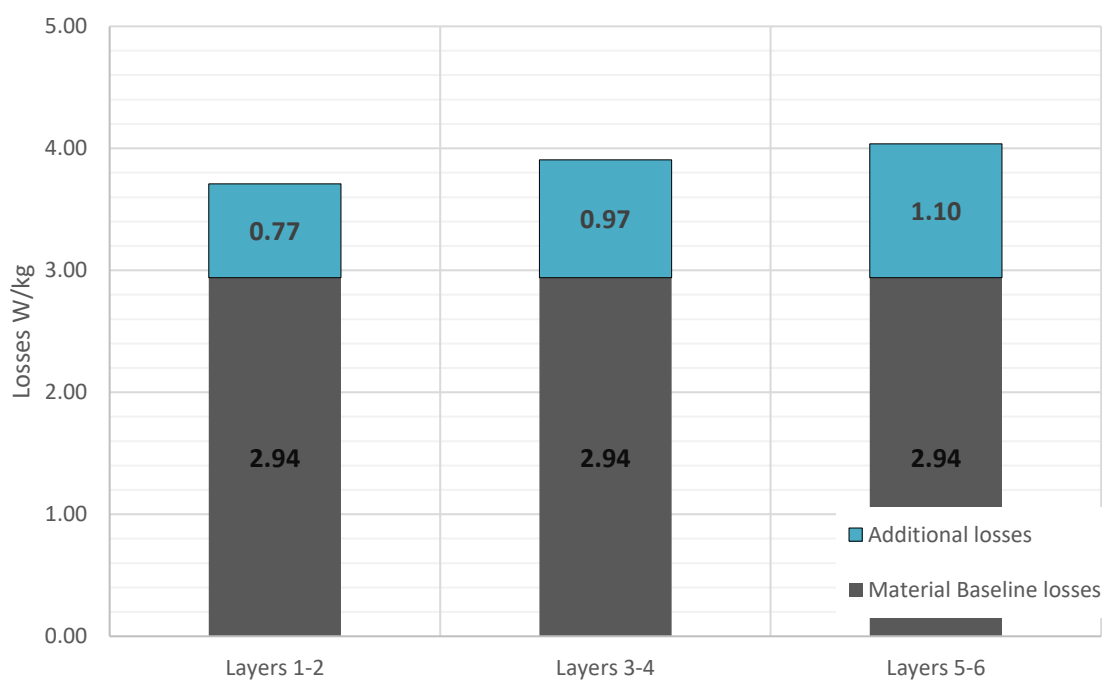
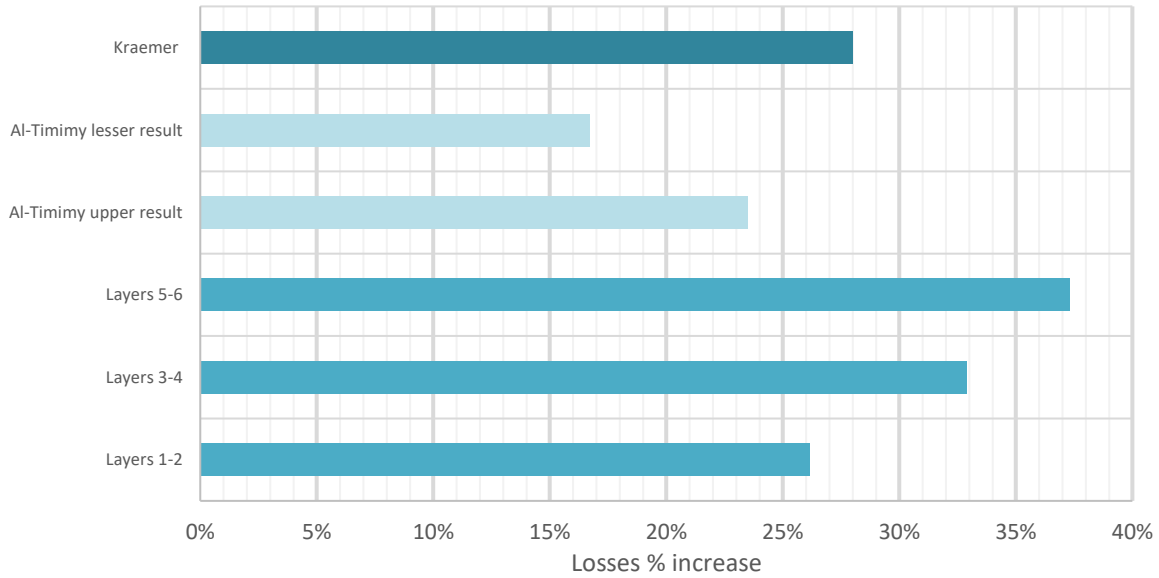


Figure 120 B-H (Flux Density & Magnetizing Force) curve for samples produced by laser cutting stacks

The core losses in the samples are summarised in Figure 121, which shows the total losses as a combination of baseline material losses and additional losses. Additional losses occur in all layers. The additional losses are greater in layers 3-4 and then again in layers 5-6. As the data is limited, it is difficult to know whether further losses continue to increase, or if there is a tailing off of losses through further layers. While the apparent effect on the material as a result of laser cutting (through the change in grain structure investigated earlier) appears relatively small, it is likely that there is a modification of the magnetic domain structure or quality due to the heat introduced by the laser, or by the presence of residual stresses after cutting, which all act to reduce the magnetic performance of the strips cut. In order to fully validate the use of laser cutting in electric machines, the amelioration of these increased losses by further refinement of the processing would need to be investigated. Figure 122 shows additional losses as a percentage increase from the baseline material losses. The data previously identified from Al-Timimy (2018) shows that the increase in losses is comparable to stamping, even though slightly greater losses appear to occur. Kraemer's (2016) research indicated overall losses incurred through stamping were 10% - 18%. Kraemer's results include further loss factors, and isolating for the effect of stamping as an increase against material losses shows that stamping increases losses by 28% (relative to material baseline) in Kraemer's results. The current results would suggest that some optimisation of the laser cutting parameters is required from a quality and performance perspective. Given that these results for laser cut samples are based on a new, innovative approach, the comparability of performance in this instance should provide confidence that with further work, greater levels of quality can be produced, exceeding the current standards of stamping.



*Figure 121 Absolute losses of laminations*



*Figure 122 Percentage increase in losses of laminations*

## 7.7 Conclusions

Laser cutting laminates causes a reduction in laminate performance. Processes which cut or shape laminate material cause a reduction in the electro-magnetic performance of the laminate, either as a result of mechanical, chemical, or thermochemical changes in the material. The core losses seen in this study are comparable to those found in stamped samples in this study. Stamped stators generally have increases in losses as a result of manufacturing in the region 10% - 28% (Al-Timimy, 2018) (Kraemer, et al., 2016) (Bayraktar & Turgut, 2018) whereas the results of this study indicate additional losses as a result of laser cutting in the region 26%-37%. These results for laser cut samples are based on an innovative manufacturing method of polystromata cutting. The comparability of performance in this instance should provide confidence that with further work, greater levels of quality can be produced, potentially exceeding the current standards of stamping.

The joining issues which were identified in this study could potentially be rectified by the use of proper bespoke fixtures and/or an additional process. This relies on the laminates only being joined slightly as was seen throughout this study, with the exception of the 23-layer stack which was much more strongly joined.



## 8 An economic and operational comparison of stamping and laser cutting

---

### 8.1 Methodology

#### 8.1.1 Knowledge gap

The work in this chapter further adds to the industrial manufacturing knowledge which has been developed throughout this thesis. No research currently exists which compares the manufacturing of stators by means of stamping and laser cutting from a perspective of manufacturing economics. In this chapter a comparison is made between stamping and laser cutting in the production of stators.

#### 8.1.2 Approach

This chapter builds on the cost models which have been developed in prior chapters for stamping and laser cutting. A further model is created to study the supply of materials into the manufacturing system using an economic order quantity approach. An analysis is performed across both cost models to develop an understanding of the relative competitiveness of each manufacturing method.

## 8.2 Introduction

The production of laminates for stators and rotors is a key process in the manufacture of an electric machine. The most commonly used production process is to stamp sheets creating individual laminate layers which are then stacked to create a stator stack. The research conducted in this project thus far has identified the challenges and opportunities which currently exist in the stamping processes. An alternative method of producing stators was also studied. The potential benefits of laser cutting laminates as stacks were modelled, requiring the implementation of an optimisation procedure to define the manufacturing set-up. Experiments were conducted to measure the effect of laser cutting stacks on the quality and performance of parts produced this way. So far, the two processes have been studied individually, which has allowed for a deeper understanding of each individual process. This knowledge has been developed further to compare the two processes on the basis of cost, time and quality performance metrics using an operations management approach. It is important to perform a trade study in this way for the two cutting processes. This study provides the case for laser cutting as an alternative for the mass manufacture of laminations. The results of this study can be used by manufacturers to make long term investment decisions regarding the processes and technologies they might choose to use, and also the implementation of these technologies with greater understanding of the effect of different machine design decisions.

An economic order quantity (EOQ) approach has been used to study the inventory management aspects of the stator manufacturing process. The study provides and insight into the supply of raw electrical steel sheet into the manufacturing process based on the manufacturing knowledge in parameter set 1. A further two studies have been performed using the models which were developed for stamping and laser cutting in sections 4 & 0. The first study is conducted on the basis of current knowledge and expectations. The second study uses a new parameter set (parameter set 3), which is designed to reflect the realistic, real-world potential of both processes.

## 8.3 Economic order quantity

In order to achieve the thesis aims of providing both a technical machining review and an operations impact analysis, an understanding of some industrial management techniques is required. The vision of mass manufacturing is a continuous stream of products rolling into and out of a factory. This is rarely the case. There is an element of batching which occurs as a result of supply constraints, such as physical limitations on space or the availability of resources to facilitate delivery. The main concern in this study is maintaining appropriate levels of sheet material such that production is not adversely affected. Using the process model previously developed in chapter 2, it is possible to know how much material is

required, and within what timeframe the material is required. This is achieved by performing an economic order quantity study as laid out in Table 31. The cost of holding material is determined to be approximately £2 per m<sup>3</sup> per day. This cost represents the space, security, handling, and costs associated with storing and maintaining the material prior to use. The order process costs have been estimated to be £100. The order process costs account for administration fees, delivery, order processing time, resource allocation and other order processing costs. The sub total holding costs,  $\Sigma C_H$ , are calculated as in equation ( 8.1 ). This is a similar to the equation given by Slack (2019) in section 2.1.1. The sub-total order process costs are calculated by equation ( 8.2 ).

STATOR EOQ				Number of orders $n_{ord}$	20
				Time interval (days) $t_I$	6.46
	Total number of stacks	$n_{Stacks}$	100000	Stacks per order $n_{StackO}$	5000
	Laminates per stack	$n_{lps}$	286		
	Total required Laminates	$n_{lams}$	28571429 >		1428571
£	Material value in n stacks	$C_{ups}$	£1,674,012 >		£ 83,701
£	Material value scrapped	$C_{sps}$	£3,203,614 >		£ 160,181
£	Total material costs	$C_{ps}$	£4,877,626 >		£ 243,881
m <sup>3</sup>	Material used in n stacks	$V_{ups}$	419 >		21
m <sup>3</sup>	Material scrapped	$V_{sps}$	801 >		40
m <sup>3</sup>	Total material volume	$V_{ps}$	1219 >		61
hours	Time to produce quantity	$t_{\alpha}$	3099 >		155
days	Time to produce quantity	$t_{\alpha^*}$	129.1 >		6.5
weeks	Time to produce quantity	$t_{\alpha^{**}}$	18.4 >		0.9
ADDITIONAL ORDER COSTS					
£/m3/da	Holding cost	$C_H$	£ 2.00	Sub total holding $\Sigma C_H$	£ 7,874
£/order	Order process costs	$C_{ord}$	£ 100.00	Sub total order $\Sigma C_{ord}$	£ 2,000
£	Total order costs	$C_{OC}$	>>> >		£ 9,874

Table 31 Economic order quantity set-up

$$\Sigma C_H = n_{ord} \cdot \frac{C_H \cdot V_{pd} \cdot t_I}{2} \quad ( 8.1 )$$

$$\Sigma C_{ord} = n_{ord} \cdot C_{ord} \quad ( 8.2 )$$

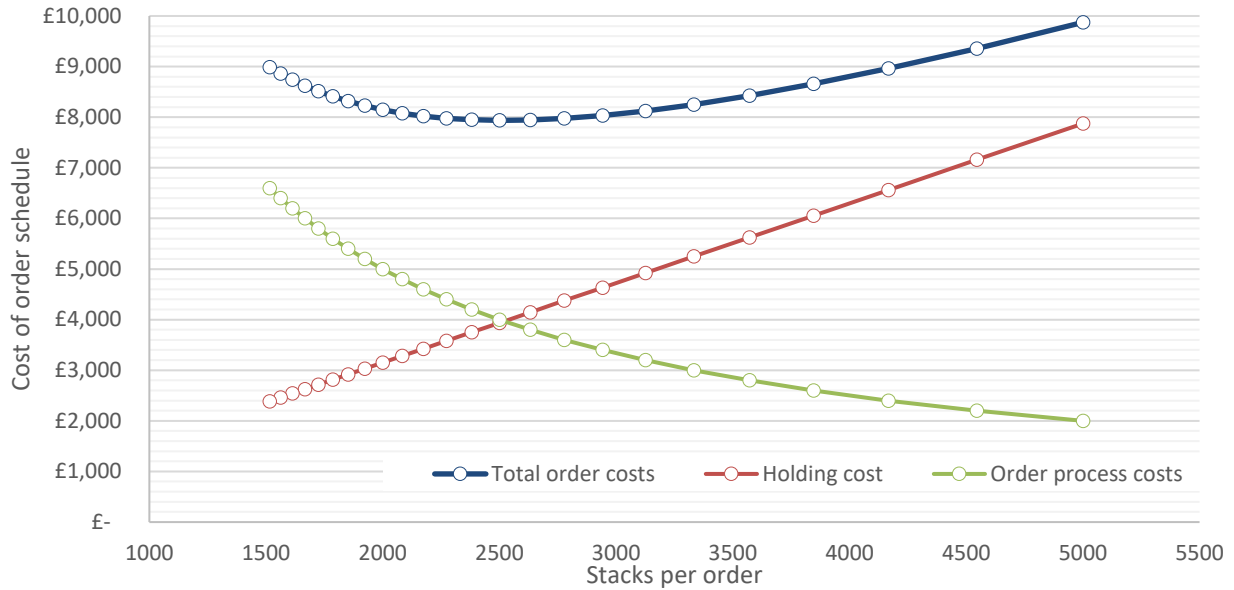


Figure 123 Economic Order Quantity (EOQ)

Based on the estimated cost variables, the most cost-effective order size is approximately 2500 stators worth of sheet material (Figure 123). Based on the production times from the stamping model, these orders would have to be delivered every 3.24 days to maintain a 24-hour production cycle. Clearly, if the factory does not operate a 24-hour continuous production cycle, the time between orders is increased proportionally. A sensitivity analysis was conducted in Figure 124, and results were produced using holding costs £0.50 to £3.50 and order costs £25 to £175. The most frequent result was an order quantity of approximately 2500 stacks worth of material. This result is in line with the original proposal of holding costs £2 & order costs £100. The largest deviations occurred when holding costs were £0.50 and order costs £175, and similarly when holding costs were £3.50 and order costs £25. As mentioned in section 2.1.1, EOQ has limitations owing to the number of assumptions that are required. The results of this study are based on the manufacturing model developed within this research and as such they provide a reasonable estimate of the process as defined by the model. It is expected that there would be some variation in the EOQ for any given specific manufacturer. However, as a first pass these results provide a useful insight and baseline estimate.

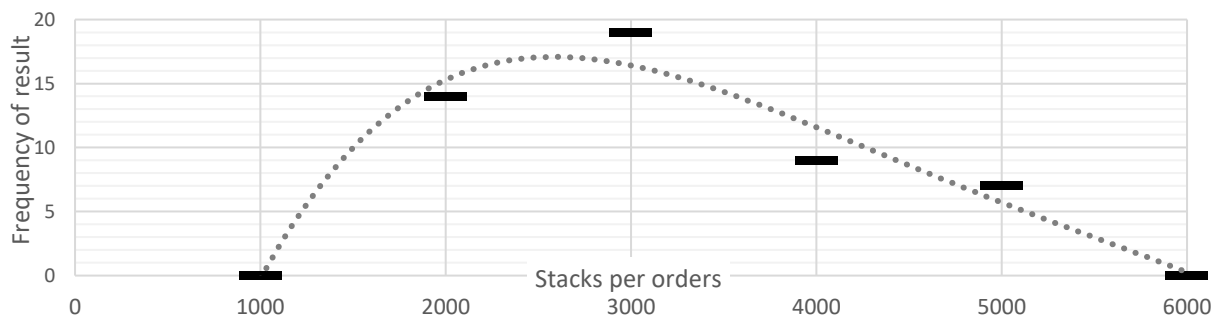


Figure 124 Sensitivity analysis of best order size results

## 8.4 Assessment and evaluation of alternative technologies

The data used in the original stamping and laser cutting models, parameter set 1, was based on current working knowledge and available data. As a result of the research conducted in this thesis, further knowledge was gained and opportunities for process improvements discovered. A new parameter set 3 has been used to represent an improved manufacturing case for both stamping and laser cutting.

### 8.4.1 Parameter sets

	Parameter	Units	Parameter set 1	Parameter set 3
	Quantity produced		100,000	100,000
S	Tool hardness	HRC	62	86
S	Stamping rate	SPM	300	300
S	Maintenance costs	£	1000	5000
L	Laser cutting machines		4	5
L	Change over time	Secs	60	10
L	Purchase cost	£	300,000	400,000
L	Overhead rate		200	250
L	Maintenance costs	£	2000	3000
L	Maintenance time	Mins	120	150
L	Gas cost	£	0.05	0.50

*Table 32 Parameter sets used in trade-off study*

It is possible to design stators with an unlimited number of geometric profiles, sizes, materials and so on. Two of the main properties which relate to stator design in the model are sheet thickness and length of cut. The length of cut is directly related to the size of a stator and the design of the stator profile. As it is not possible to systematically compare stator profile designs, the size of the stator is used here as the main point of comparison for different types of stator design. The size of the stators ranges from inner diameters of 0.07m to 0.37m. The stator proposed previously in the study was designed to be 0.17m.

8.4.2 Scale / quantity

Stamping and laser cutting both have economies of scale, and these are considered in Figure 125 & Figure 126. In this study laser cutting is considered as using an optimised polystromata operation. The average cost of producing a stator using a monostroma operation is approximately £1457, further demonstrating the need to consider polystromata laser cutting to achieve more competitive costs with stamping.

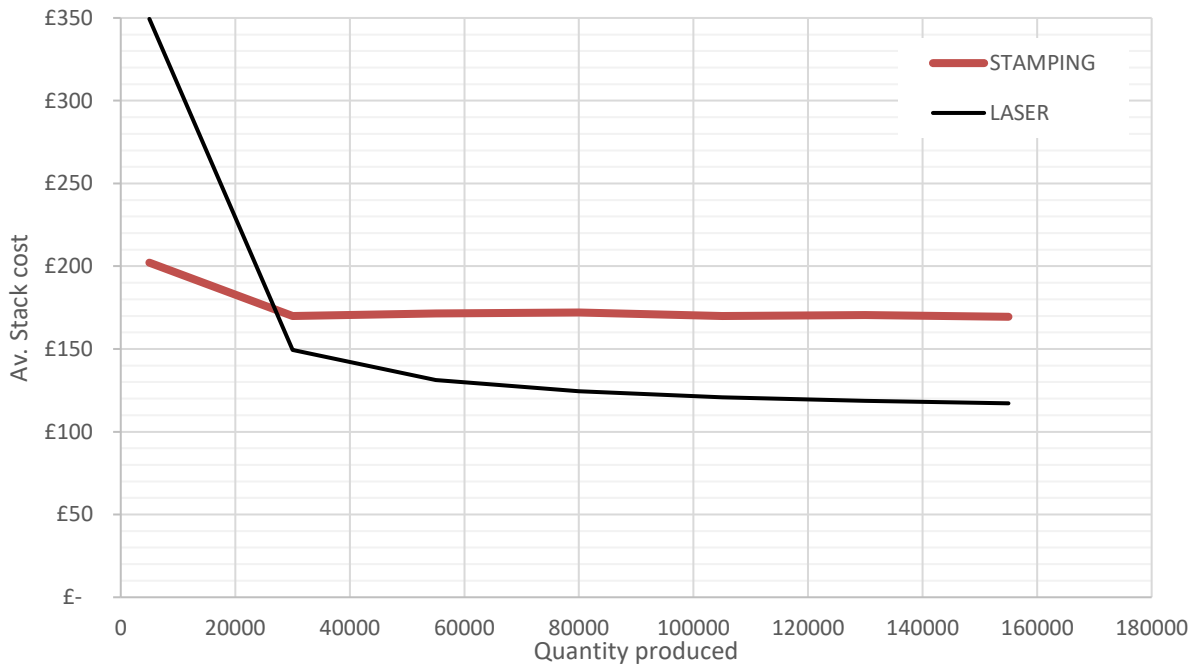


Figure 125 Economies of scale for stamping and laser cutting using parameter set 1

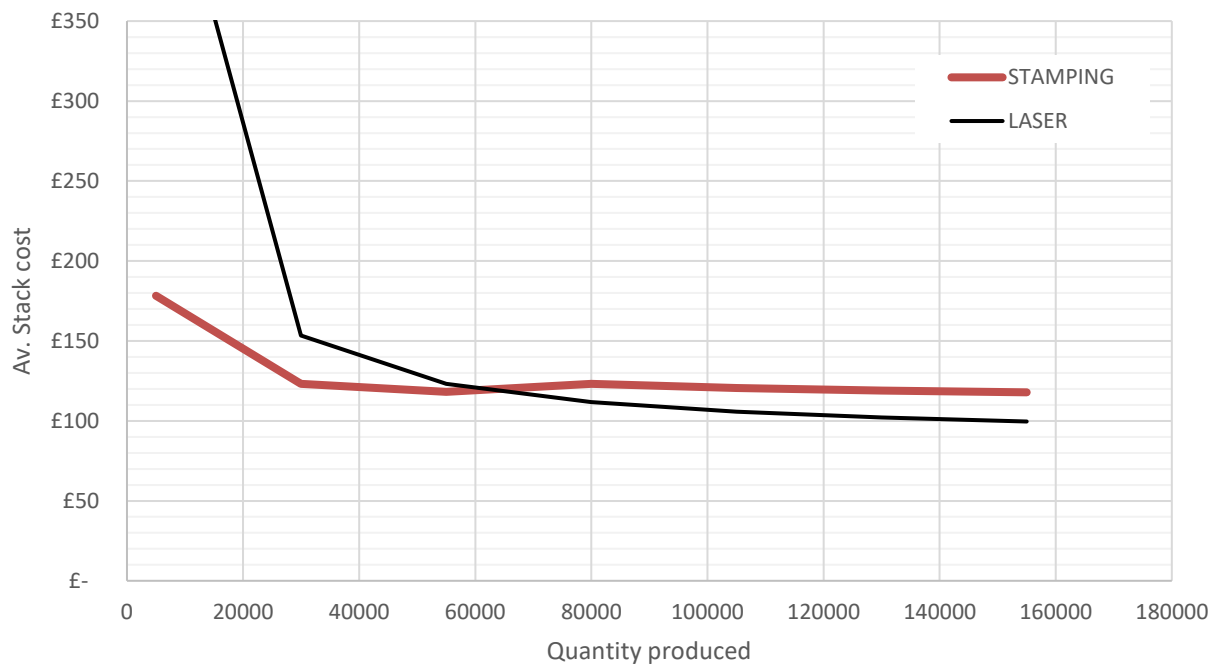


Figure 126 Economies of scale for stamping and laser cutting using parameter set 3

Laser cutting is generally much more expensive than stamping for quantities which are less than 30,000 stacks. The laser cutting costs include the purchase of 5 laser cutting machines and additional automation equipment. These costs are fixed costs and are reduced as the quantity of parts produced increases. Laser cutting can be more cost competitive to stamping if less machines are purchased. However, this has a direct impact on the production times. The best recommendation for businesses which are only likely to produce stacks in quantities up to 30,000/40,000 stacks would be to continue using stamping the stamping technology that is available. A single laser cutting machine might still be worth investment for the production of prototypes and small batches. Both technologies reach a steady state of manufacturing performance in the long term. Figure 126 indicates that a break-even cost point exists between stamping and laser cutting. Given that the long-term average stator cost is similar, and that there are many different stator designs which effect the cost profile for both manufacturing methods, it may not always be the case that a break-even cost point exists.

#### 8.4.3 comparison of cost and time performance for different motor sizes

Stators can be designed and manufactured in many sizes, affecting both the time and cost of production. The following time X cost matrices in Figure 127 & Figure 128 demonstrate the manufacturing capability of both stamping and laser cutting simultaneously for different stator designs based on inner diameter size. Further results are provided in appendix (11.7) for different lamination sheet thicknesses.

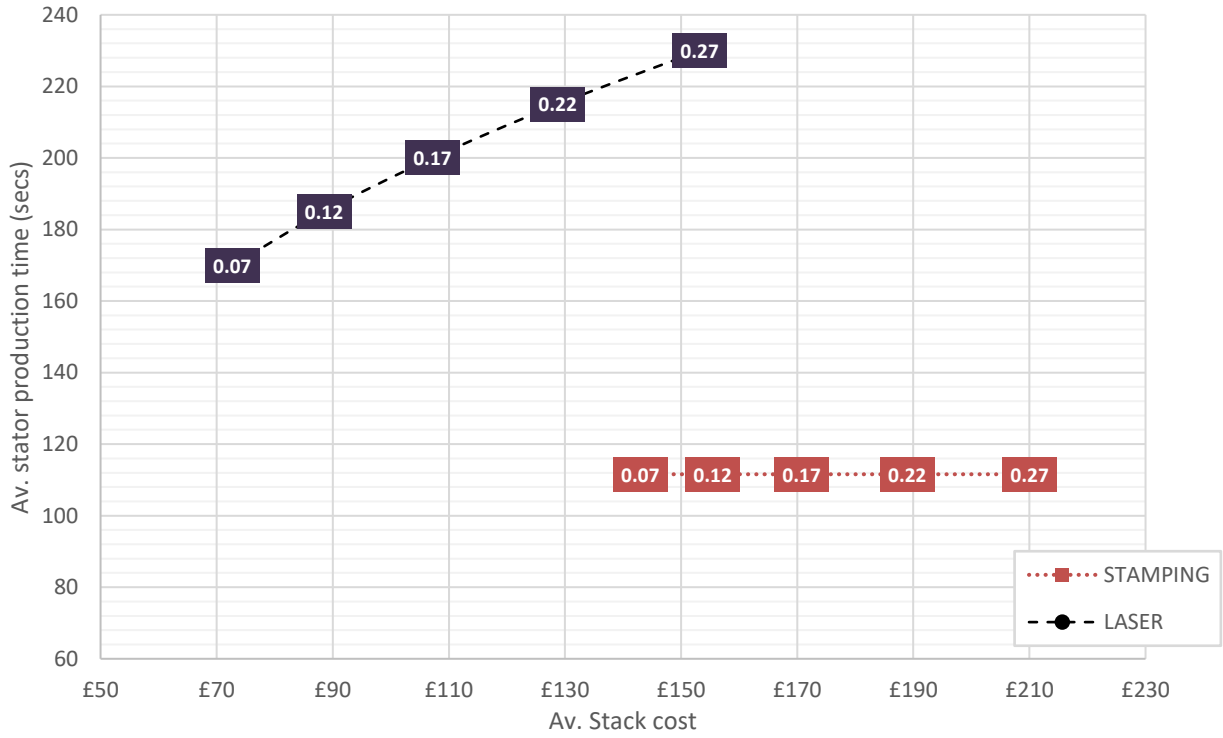


Figure 127 Process performance for various motor sizes using parameter set 1 & sheet thickness 0.35mm

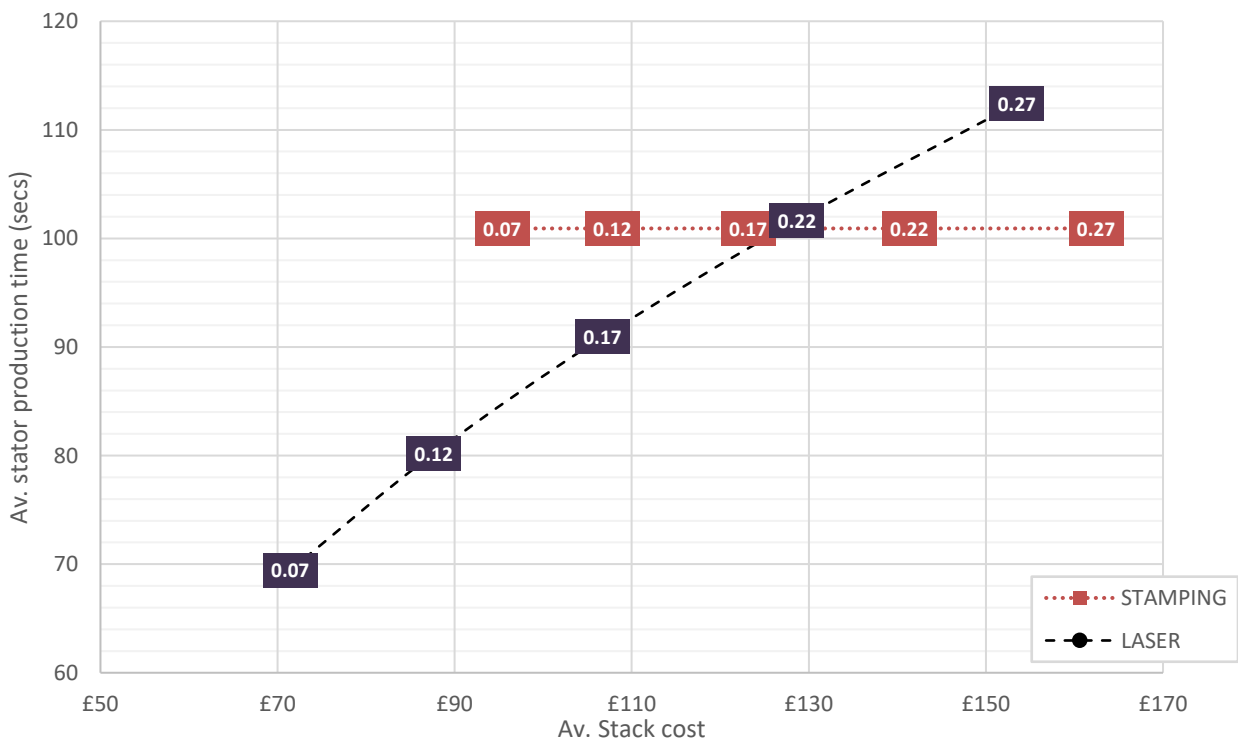


Figure 128 Process performance for various motor sizes using parameter set 3 & sheet thickness 0.35mm



#### 8.4.4 Key points of interest

Points have been chosen from Figure 127 and Figure 128 to highlight the comparisons between stamping (**red**) and laser cutting (**black**). Where Figure 127 and Figure 128 demonstrate the overall performance trend, the table shows a clear comparison of the process performances for a given point in the figure. The graphs used are very similar to bar chart and are used to best illustrates the comparisons visually.

Inner diameter (m)	Av. Stator cost	Av. Stator production time (secs)
0.07	<p>£143</p> <p>£73</p>	<p>112</p> <p>170</p>
0.17	<p>£171</p> <p>£107</p>	<p>112</p> <p>200</p>
0.27	<p>£210</p> <p>£153</p>	<p>112</p> <p>230</p>

Table 33 Cost and time results using Parameter set 1 & sheet thickness 0.35mm

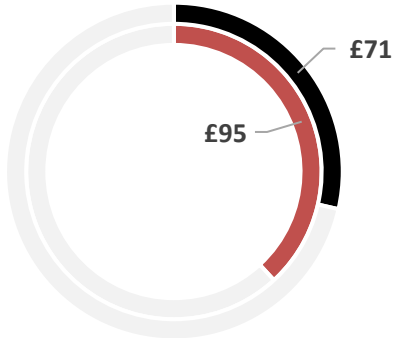
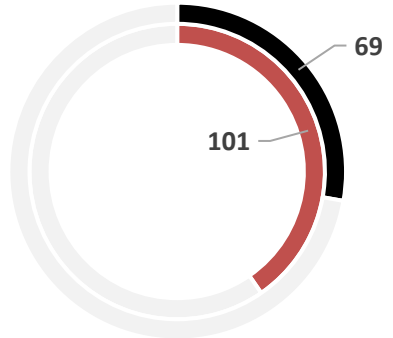
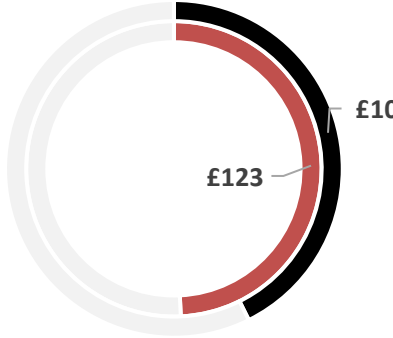
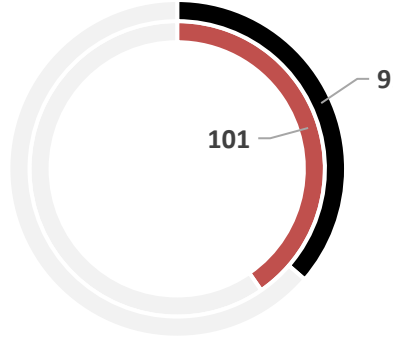

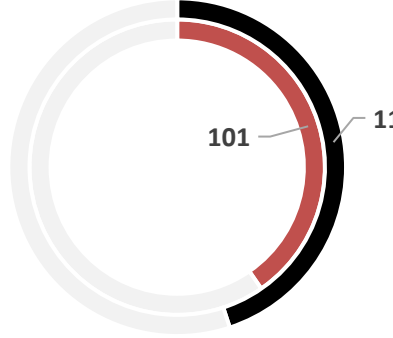
Inner diameter (m)	Av. Stator cost	Av. Stator production time (secs)
0.07	 <p>A circular diagram showing a stator with a red inner ring and a black outer ring. A grey ring is shown in the background. Labels indicate a cost of £71 for the black ring and £95 for the red ring.</p>	 <p>A circular diagram showing a stator with a red inner ring and a black outer ring. A grey ring is shown in the background. Labels indicate a production time of 69 seconds for the black ring and 101 seconds for the red ring.</p>
0.17	 <p>A circular diagram showing a stator with a red inner ring and a black outer ring. A grey ring is shown in the background. Labels indicate a cost of £107 for the black ring and £123 for the red ring.</p>	 <p>A circular diagram showing a stator with a red inner ring and a black outer ring. A grey ring is shown in the background. Labels indicate a production time of 91 seconds for the black ring and 101 seconds for the red ring.</p>
0.27	 <p>A circular diagram showing a stator with a red inner ring and a black outer ring. A grey ring is shown in the background. Labels indicate a cost of £153 for the black ring and £162 for the red ring.</p>	 <p>A circular diagram showing a stator with a red inner ring and a black outer ring. A grey ring is shown in the background. Labels indicate a production time of 112 seconds for the black ring and 101 seconds for the red ring.</p>

Table 34 Cost and time results using Parameter set 3 & sheet thickness 0.35mm

8.4.5 Sheet thickness effect on results

The laminate sheet thickness is another design consideration which directly effects the manufacturing performance of stamping and laser cutting. A comparison is made between the costs and production times of both production methods.

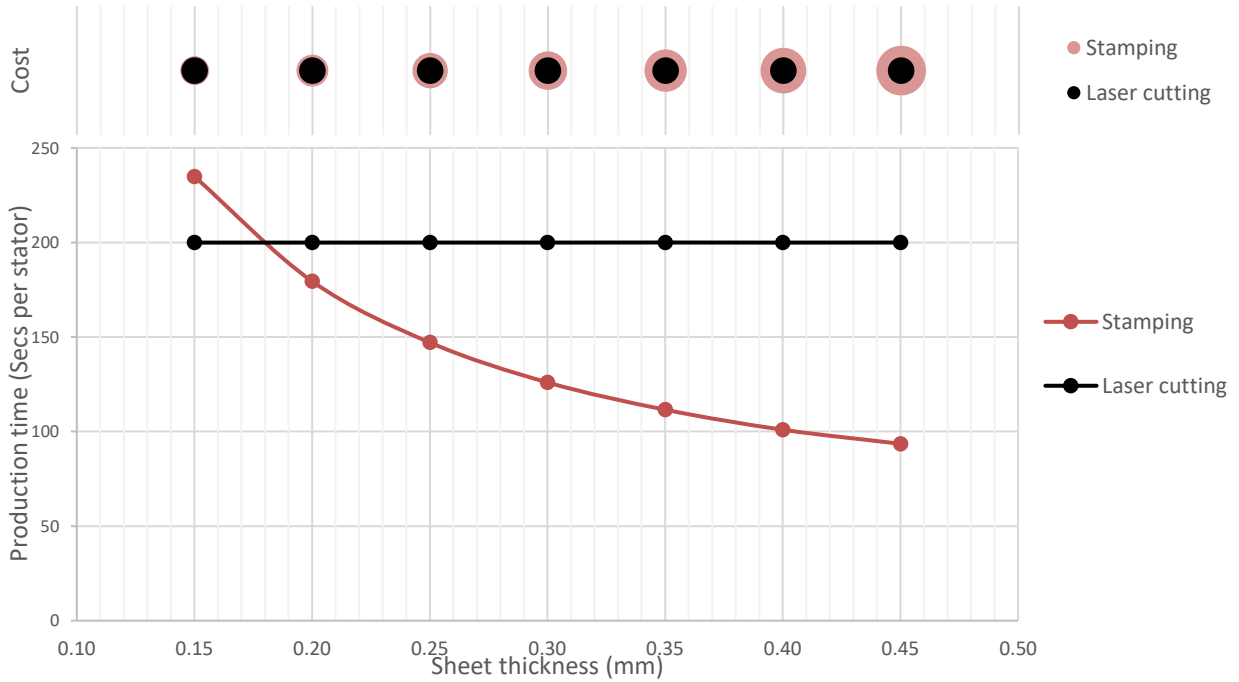


Figure 129 Sheet thickness effect on results using parameter set 1 and inner diameter 0.17m

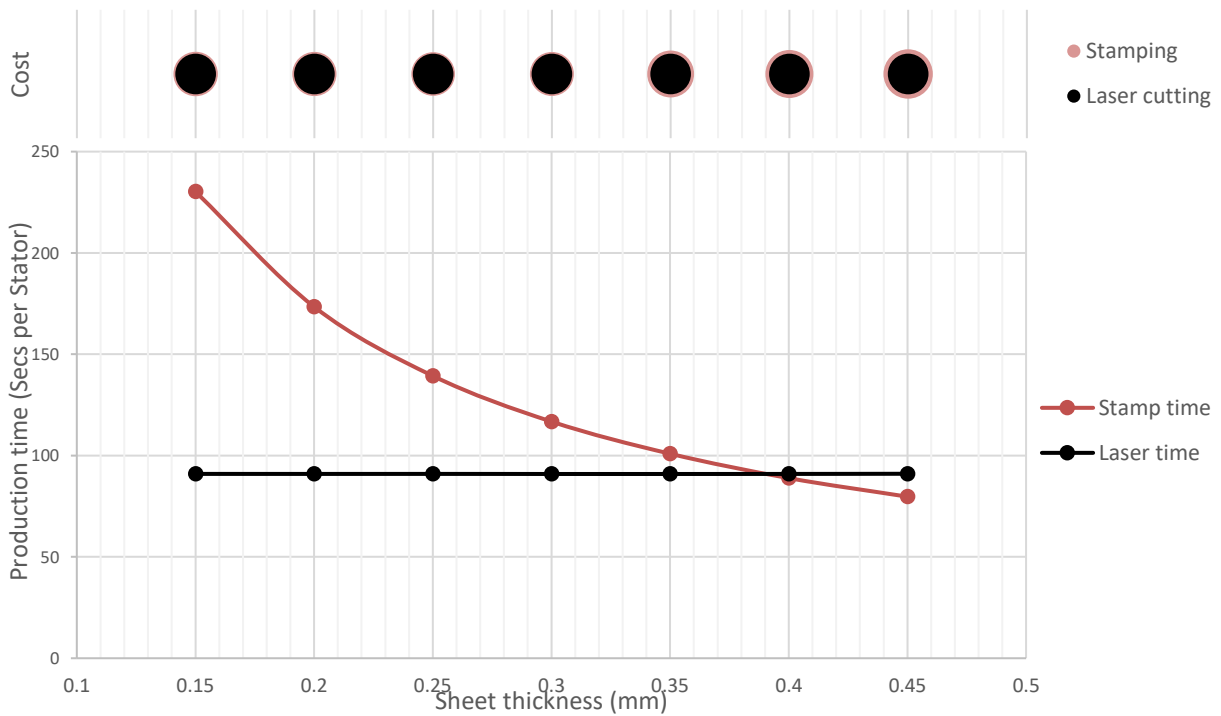


Figure 130 Sheet thickness effect on results using parameter set 3 and inner diameter 0.17m

## 8.5 Discussion & Conclusions

The results for parameter set 1 consistently show that laser cutting is a potentially more cost-effective method of production. However, laser cutting in most cases is a much slower method of production. The only case where laser cutting is quicker than stamping occurs when lamination sheet thickness is  $<0.18\text{mm}$  (Figure 129). The default sheet thickness considered throughout this study, and used in experimental trials, was  $0.35\text{m}$ . Laser cutting could be considered therefore to only be preferential in niche circumstances. Conclusions based purely on parameter set 1 would suggest that laser cutting is not a suitable mass-manufacture process, as the production times are simply not competitive with stamping. Whilst an argument exists about reducing production costs, the cost benefits for laser cutting are generally longer term, as the cost of investment in machines is upfront. This would make the decision to change from one production method to another very difficult for small to medium enterprises, particularly as the knowledge base is different between the technologies, meaning any benefits of know-how are diminished.

Parameter set 3, which proposes a better case for both technologies based on the research conducted throughout this project, is a more ideal comparative measure of the two technologies, particularly for large enterprises where investment decisions are made at greater scale. Laser cutting is a much more cost and time efficient process than stamping for machines designed with inner diameters up to  $0.17\text{mm}$  (Figure 128). The benefits of laser cutting reduce for larger sized machines. In Table 34, the machine size 0.27 demonstrates clearly how laser cutting becomes the more time-consuming process. It can also be noticed in both Table 34 & Figure 128 that the benefits of laser cutting for both time and cost diminish as the size of the machine increases. Laser cutting is also much more competitive across a range of sheet thicknesses (Figure 130), including the  $0.35\text{mm}$  used throughout this project. The cost competitiveness of both technologies is similar regardless of sheet thickness.

The results generally show that laser cutting has the potential to offer real value as an alternative to stamping for manufacturers who are looking to reduce production times, particularly in the production of smaller sized machines. However, at this current time, the potential benefits rely on technology aspects which are not yet proven. Laser cutting has a reliance on stack cutting to be competitive. It has been shown that it is possible to cut stacks, and that the quality of parts produced in a polystromata cut are comparable to those produced by stamping, but it is not known whether it is possible to create similar or better-quality results from stacks of the sufficient size for laser cutting to be a competitive alternative.

## 9 Thesis conclusions and further work

---

The research conducted in this thesis has aimed to analyse the current manufacturing methods used in the production of a synchronous reluctance machine for an automotive application, inclusive of materials and processes. The core components considered in the research are the stator (which shares manufacturing processes with the rotor) and winding assembly. As a result of the work conducted in this research, further opportunities for research and development have been identified, along with a further appreciation for the gaps that exist in the current knowledge of manufacturing processes for electric machines.

The winding architecture in electric machines has already seen a recent technology change, with modern electric cars incorporating the hairpin winding technology as a replacement for copper wire winding. Research has been conducted in this thesis to assess whether there is an opportunity to use alternative winding materials in combination with the transition to hairpin winding technology. The most attractive alternative material is aluminium, as this provides the greatest cost and mass saving, though at a greater size, in an electrically equivalent hairpin. It is possible that a combination of aluminium hairpin and copper busbar may be an ideal solution. However, this requires the capability to join the two components. A range of joining methods were assessed based on their known capability and potentially manufacturability, with friction stir, laser beam and cold press being identified as the most attractive methods. Trials of ultrasonic welding were unable to produce joints between aluminium and copper for the process used here.

The stator and rotor components are manufactured from electrical steel laminations. A study was conducted to identify if any potential alternatives existed which could outperform standard silicon based electrical steel. Two alternatives were found, Metglas and *Nickel alloys / Cobalt Iron electrical steels*. However, both are more expensive than silicon electrical steels. Silicon electrical steels remain the most suitable material for electric machine applications.

One of the major processes used in producing a stator and rotor is stamping. A manufacturing model was created, incorporating manufacturing cost, tool parameters and operational factors to create a more holistic view of the stamping process. A new tool life function was developed using previous research and first principles. The stamping manufacturing model showed how stamping is inefficient for small production quantities, mostly as a result of the cost of tooling. The model demonstrates instances where it is worth considering tools which are less durable but lower cost as a method of reducing costs for smaller quantities. One of the outcomes of the model is to recognise how much material is wasted when

the rotor is not being manufactured in conjunction with the stator. An alternative manufacturing method was identified which reduces the waste material created during the stator manufacture.

The stamping tool life model created in section 4.4 can be developed further. It is possible to perform further experimentation using stamping apparatus to confirm or adjust some of the assumptions. One of the issues encountered in this research was the cost and availability of stamping tools, and so the tool life model was developed based on prior empirical data. A bespoke study into the operational factors which affect tool life, particularly stroke speed, should be conducted to further knowledge in this area.

A study was conducted to understand the feasibility and constraints of manufacturing a slinky style stator. A finite element model was developed in combination and the results measured against a representative experiment. The study demonstrated the challenges in manufacturing a slinky style stator, with large stresses leading to buckling of the stator strip as it is coiled. Stresses in the strip can be reduced by creating bespoke stator designs, as demonstrated by the revised slinky designs created in this study.

Laser cutting is another method of producing stators and rotors from electrical steels. However, laser cutting is currently used primarily as a method of producing prototypes and small batches. The viability of laser cutting laminations for mass manufacture relies on the ability to improve the process, mostly in terms of reducing production times. This can be tackled from both a technical machining perspective and an operations management perspective. Laser cutting has been demonstrated to have the capability to perform the required task, namely cutting electrical steel laminates. From an operational perspective, the introduction of laser cutting as an alternative manufacturing process may create opportunities in the total manufacturing system, such as opportunities to reduce wastes using lean manufacturing principles. The laser cutting trials in this study involved a manual part change over. An automated system should be possible in combination with a tailored laser cutting machine selection. The flexibility of a laser cutting machine fits in well with this type of approach, especially compared to stamping where a new tool must be designed and manufactured for each new design of stator.

Polystromata cutting has the potential to reduce process times immensely. However, this is at a cost to the performance of parts produced and is also limited by the depth of stack which can feasibly be cut. Laser cutting laminates causes a reduction in laminate performance, just as stamping does. Any process cutting/ shaping laminate material is likely to cause a reduction in the electro-magnetic performance of the laminate, either as a result of mechanical, chemical, or thermochemical changes in the material. The core losses seen in this study are comparable to those found in stamped samples (see section 2.5.1).

The laser cutting trials conducted in this research found interesting and novel results whilst being limited to one laser cutting machine. Further trials should be conducted, with a number of areas open to further research. Further studies should be conducted to identify and optimise laser cutting of stacks, with the aim of producing as large a stack cut as possible. Studies should also be conducted to further explore the effect of different laser cutting settings on the electromagnetic performance of laminations.

Laser cutting has the potential to offer real value as an alternative to stamping for manufacturers who are looking to reduce production times, particularly in the production of smaller sized machines. However, at this current time, the potential benefits rely on technology aspects which are not yet proven. Laser cutting has a reliance on stack cutting to be competitive. It has been shown that it is possible to cut stacks, and that the quality of parts produced in a polystromata cut are comparable to those produced by stamping.

The implementation of laser cutting into the total manufacturing system should be explored further, developing on the manufacturing process routes developed in this research and the further laser cutting operations research, it should be possible to create a simulation of the manufacturing operation for both stamped and laser cut parts. Ideally this would be considered in partnership with a real-life manufacturers' operation. A simulation, such as a discrete event analysis, would be able to identify areas for operational improvement of the laser cutting process, and provide a measure of the potential benefits of laser cutting over stamping in a more realised context.

## 10 References

---

ABB, 2015. *A guide to preventing failure*, s.l.: ABB.com.

Accuratus, 2013. *Aluminum Oxide, Al<sub>2</sub>O<sub>3</sub> Ceramic Properties*. [Online]  
Available at: <http://accuratus.com/alumox.html>  
[Accessed 03 2018].

Advanced Propulsion Centre UK, 2020. *Electric Machines Roadmap: 2020 - Narrative Report*, s.l.: automotive council UK.

Al-Timimy, A., 2018. Considerations on the Effects That Core Material Machining Has on an Electrical Machine's Performance. *IEEE TRANSACTIONS ON ENERGY CONVERSION*, 33(3), pp. 1154-1163.

AMRC, 2019. *Discussion with laser cutting operative* [Interview] (10 2019).

Ashwood Electric Motors, 2017. *Update on our new automated production line*, s.l.: Ashwood Electric Motors.

Association of Electrical and Mechanical Trades, 2018. *Nestech laminations stack up for the aftermarket*. [Online]  
Available at: <https://www.theaemt.com/DB/news-webpage/nestech-laminations-stack-up-for-the-aftermarket>  
[Accessed 04 2021].

Atkins, A., 2016. *Ricardo SyncRel electric drive project initialisation specification* [Interview] 2016.

Bali, M. & Metze, A., 2019. The degradation depth of non-grain oriented electrical steel sheets of electric machines due mechanical and laser cutting: a-state-of-the-art review. *IEEE transactions on industry applications*, 55(1), pp. 366-375.

Bali, M. & Muetze, A., 2019. The degradation depth of non-grain oriented electrical steel sheets of electric machines due mechanical and laser cutting: a-state-of-the-art review. *IEEE transactions on industry applications*, 55(1), pp. 366-375.

Ballantyne, E. & Heron, G., 2020. *Operations management knowledge support for EngD thesis* [Interview] 2020.

Bayraktar, S. & Turgut, Y., 2018. Effects of different cutting methods for electrical steel sheets on performance of induction motors. *Proceedings of the Institution of Mechanical Engineers, Part B: Journal of Engineering Manufacture*, 232(7), p. 1287-1294.

Beckley, P., 2011. *Electrical steels for rotating machines*. s.l.:Institution of Electrical Engineers.

Bhamji, I. et al., 2012. Linear friction welding of aluminium to copper. *Science and Technology of Welding and Joining*, 17(4), pp. 314-320.



- BOC, 2021. *Laser cutting. LASERLINE®Technical.* [Online]  
Available at: [https://www.boconline.co.uk/en/images/laser-cutting\\_tcm410-39553.pdf](https://www.boconline.co.uk/en/images/laser-cutting_tcm410-39553.pdf)  
[Accessed 2021].
- Boothroyd, G., 1987. Design for assembly—The key to design for manufacture. *The International Journal of Advanced Manufacturing Technology*, Volume 2, pp. 3-11.
- Boothroyd, G., 1994. Product design for manufacture and assembly. *computer-aided design*, Volume 26, pp. 505-520.
- Boubaker, N., Matt, D. & Enrici, P., 2019. measurements of iron loss in PMSM stator cores based on CoFe SiFe lamination sheets and stemmed from different manufacturing processes. *IEEE Transactions on magnetics*, 55(1).
- Brown, A. S., 2008. Custom Motor? give us two weeks.. *Mechanical Engineering*, 130(9), pp. 52-55.
- Cakal, G. & Keysan, O., 2021. Flat winding made of aluminum or copper sheet for axial flux machines. *IET Electric Power Applications*, Volume 15, pp. 429-440.
- Campbell, S. & Brittle, N., 2017. *MTD LTD Factory visit Q&A* [Interview] (10 08 2017).
- Cater, S., 2018. *Discussion with Stephen Cator - TWI Engineer in joining processes* [Interview] 2018.
- Cavallo, C., 2021. *All About Synchronous Motors - What They Are and How They Work.* [Online]  
Available at: <https://www.thomasnet.com/articles/machinery-tools-supplies/synchronous-motors/>  
[Accessed 10 2021].
- CES EduPack, 2018. *CES EduPack*, Cambridge: Granta.
- Chapman, S. J., 2012. *Electric Machinery Fundamentals*. 5th ed. New York: McGraw Hill.
- Cogent, 2008. *Typical data for SURA® M250-35A.* [Online]  
Available at: <https://cogent-power.com/cms-data/downloads/m250-35a.pdf>  
[Accessed November 2017].
- Cremer, A. & Schwartz, J., 2017. *Volkswagen accelerates push into electric cars with \$40 billion spending plan*, s.l.: Reuters.
- Crosse, J., 2019. *Under the skin: the hierarchy of EV motor technology: Autocar.* [Online]  
Available at: <https://www.autocar.co.uk/car-news/technology/under-skin-hierarchy-ev-motor-technology>  
[Accessed 10 2021].
- Dayton Progress Corp, 2003. *Stamping Basics: Fundamentals & Terminology.* [Online]  
Available at: [https://www.daytonlamina.com/tech/dayton\\_tech-stamping.pdf](https://www.daytonlamina.com/tech/dayton_tech-stamping.pdf)  
[Accessed 04 2021].
- Desai, C., Mehta, H. R. & Pillay, P., 2018. Fabrication and Assembly Method for Synchronous Reluctance Machines. *IEEE TRANSACTIONS ON INDUSTRY APPLICATIONS*, 54(5), pp. 4227-4235.

Dilger, D. E., 2012. *Apple slims down iMac 40% with 'friction-stir welding' & ditching the disc drive.* [Online]

Available at: <http://appleinsider.com/articles/12/10/24/apple-slims-down-imac-40-with-friction-stir-welding-ditching-the-disc-drive>

[Accessed 12 03 2018].

Duff, M., 2018. *BMW Brings the Electric HEAT.* [Online]

Available at: <https://www.caranddriver.com/news/a22656237/bmw-simplifies-ev-production/>

[Accessed October 2021].

Edwards, K. L., 2002. Towards more strategic product design for manufacture and assembly: priorities for concurrent engineering. *materials and design*, Volume 23, pp. 651-656.

ee.co.za, 2016. *The advantages of the synchronous reluctance motor.* [Online]

Available at: <http://www.ee.co.za/wp-content/uploads/2016/05/ABB-FIG-1.jpg>

[Accessed February 2017].

efunda, 2020. *Sheet metal: stamping.* [Online]

Available at: [https://www.efunda.com/processes/metal\\_processing/stamping.cfm](https://www.efunda.com/processes/metal_processing/stamping.cfm)

[Accessed 07 2020].

Engineering Solutions, 2021. *Permanent magnet synchronous motor.* [Online]

Available at: <https://en.engineering-solutions.ru/motorcontrol/pmsm/>

[Accessed April 2021].

enrapps.com, 2017. *Burst and Collapse - Pressure Vessel Design.* [Online]

Available at: <http://enrapps.com/mechanical-systems-and-materials/mechanical-components/pressure-vessels/burst-collapse-analysis.php>

[Accessed February 2017].

ESI, 2021. *Metal stamping design guide: Basic design concepts that improve quality and cut costs.* [Online]

Available at: <https://info.esict.com/lp-metal-stamping-design-guide>

[Accessed 04 2021].

Finken, T., Felden, M. & Kay, H., 2008. *Comparison and design of different electrical machine types regarding their applicability in hybrid electrical vehicles.* Aachen, Institute of Electrical Machines: PROCEEDINGS OF THE 2008 INTERNATIONAL CONFERENCE ON ELECTRICAL MACHINES.

Fonger, N., 2021. *Larson Tool & Stamping Company: Metal Stamping Design Guidelines.* [Online]

Available at: [http://larsontool.com/wp-content/uploads/2015/06/larson\\_design\\_guide.pdf](http://larsontool.com/wp-content/uploads/2015/06/larson_design_guide.pdf)

[Accessed 04 2021].

Franke, J., Dobroschke, A., Tremel, J. & Kühl, A., 2011. *Innovative Processes and Systems for the Automated Manufacture, Assembly and Test of Magnetic Components for Electric Motors.* Nuremberg, IEEE.

Fyhr, P., 2018. *Electromobility: Materials and Manufacturing Economics Lund: Division of Production and, s.l.: Lund University.*

Gaworska-Koniarek, D., 2011. The influence of assist gas on magnetic properties of electrotechnical steel sheets cut with laser. *Journal of Physics: Conference Series*, Volume 303.

General Carbide, 2019. *APPLICATION DATA SHEET*. [Online]  
Available at: <https://www.generalcarbide.com/assets/pdf/GCStamping.pdf>  
[Accessed May 2019].

Genna, S., Menna, E., Rubino, G. & Tagliaferri, V., 2020. Experimental Investigation of Industrial Laser Cutting: The Effect of the Material Selection and the Process Parameters on the Kerf Quality. *Applied sciences*, 10(4956).

Giffi, C., Vitale, J., Schiller, T. & Robinson, R., 2018. *A reality check on advanced vehicle technologies*, s.l.: Deloitte.

Gmyrek, Z. & Lefik, M., 2017. Influence of Geometry and Assembly Processes on the Building Factor of the Stator Core of the Synchronous Reluctance Motor. *IEEE TRANSACTIONS ON INDUSTRIAL ELECTRONICS*, 64(3), pp. 2443-2450.

Goodall, R., 2018. *Discussions with Professor Goodall - Materials Sciences lecturer at the University of Sheffield* [Interview] 2018.

Goss, J. et al., 2017. Electrical Vehicles – Practical Solutions for Power Traction Drive Systems. *IEEE*, Volume 17, pp. 80-88.

Gragger, J., Zanon, A. & De Gennaro, M., 2016. *Design Features of an Innovative Synchronous Reluctance Machine for Battery Electric Vehicles Applications*, s.l.: SAE Technical Paper.

Grimm, A., 2015. Friction stir welding of light metals for industrial applications. *Materials Today: Proceedings*, pp. 169-178.

GROB, 2019. *Successful Production Start-Up of the MEB Project for VW in Salzgitter, Germany*. [Online]  
Available at: <https://www.grobgroup.com/en/news-media/detail/article/successful-production-start-up-of-the-meb-project-for-vw-in-salzgitter-germany/>  
[Accessed 10 10 2020].

Hanselman, D., 2003. *Brushless permanent magnet motor design*. Rhode Island: The Writers' Collective.

Hedrick, A., 2016. Die Science: How many hits does it take to get to the end of a tool's life?. *STAMPING JOURNAL*, pp. (accessed - <https://www.thefabricator.com/article/stamping/how-many-hits-does-it-take-to-get-to-the-end-of-a-tool-s-life->).

Heidari, H. et al., 2021. A Review of Synchronous Reluctance Motor-Drive Advancements. *Sustainability*, 13(729).

Hernandez, M. et al., 2015. Environmental impact of traction electric motors for electric vehicles applications. *ASSESSING AND MANAGING LIFE CYCLES OF ELECTRIC VEHICLES*, Volume 22, pp. 54-65.

Hilinski, E. & Johnston, G., 2014. *Annealing of electrical steel*. Chicago, 2014 4th International Electric Drives Production Conference (EDPC).

Hill, T., 2000. *Manufacturing strategy*. 2nd ed. Hampshire: Palgrave.

Hirsch, M. D. P. G. R. & H. H., 2011. Light Metal in High-Speed Stamping Tools. *Key Engineering Materials*, Volume 473, pp. 259-266.

Hong, K.-M. & Shin, Y. C., 2017. Prospects of laser welding technology in the automotive industry: A review. *Journal of Materials Processing Technology*, Volume 245, pp. 46-69.

Hummel, M. et al., 2020. New approaches on laser micro welding of copper by using a laser beam source with a wavelength of 450 nm. *Journal of Advanced Joining Processes*, Volume 1.

hydraulicspneumatics.com, 2015. *Hydraulic-Electric Analogies: Power Sources, Part 3*. [Online] Available at: <http://hydraulicspneumatics.com/hydraulic-pumps-motors/hydraulic-electric-analogies-power-sources-part-3> [Accessed February 2017].

Idaho National Laboratory, 2016. *History of Electric Cars*, Idaho: Idaho National Laboratory.

Jana, P., Graves, S. C. & Grunow, M., 2018. *Balancing benefits and flexibility losses in platform planning*, s.l.: Available at [https://papers.ssrn.com/sol3/papers.cfm?abstract\\_id=3134037](https://papers.ssrn.com/sol3/papers.cfm?abstract_id=3134037).

Jayarama, T. V., 2015. Effect of Processing of HIPERCO 50 Alloy Laminates on Their Magnetic Properties. *Journal of ELECTRONIC MATERIALS*, 44(11), pp. 4379-4386.

Jewell, G., 2019. *Discussion with Professor Jewell about epstein frame experiment* [Interview] 2019.

Johansson, D., Hagglund, S., Bushlya, V. & Stahl, J.-E., 2017. *Assessment of Commonly Used Tool Life Models in Metal Cutting*. Modena, 27th International Conference on Flexible Automation and Intelligent Manufacturing.

Jones, T., 1997. *New Product Development*. Oxford: Butterworth-Heinemann.

Jung, D. S., Kim, Y. H., Lee, U. H. & Lee, H. D., 2012. *Optimum Design of the Electric Vehicle Traction Motor using the Hairpin Winding*, s.l.: IEEE.

Kaliudis, A., 2018. *It's heading this way*, s.l.: Trumpf.

Kharagpur, n.d. *Lesson 14 Failure of cutting tools and tool life*. [Online] Available at: <https://nptel.ac.in/courses/112105127/pdf/LM-14.pdf> [Accessed 06 2019].

Kim, J.-H. & Hong, J.-P., 2015. Efficiency Improvement of an Automotive Alternator by Heat Treatment. *Journal of Magnetism*, 20(2), pp. 155-160.

Klocke, F., 2005. *Blanking and Fineblanking*. [Online] Available at: [http://www.wzl.rwth-aachen.de/en/f786439a4c53fb78c125709f0055702f/I05\\_blanking\\_and\\_fine\\_blanking.pdf](http://www.wzl.rwth-aachen.de/en/f786439a4c53fb78c125709f0055702f/I05_blanking_and_fine_blanking.pdf) [Accessed June 2017].

- Kraemer, A., Stoll, J., Blickle, D. & Lanza, G., 2015. Analysis of wear behavior of stamping tools in the production of electrical steel sheets. *2015 5th International Electric Drives Production Conference (EDPC)*, pp. 1-7.
- Kraemer, A., Veigel, M. & Pontner, P., 2016. Investigation of the Impact of Production Processes on Iron Losses of Laminated Stator Cores for Electric Machines. *Electric Drives Production Conference (EDPC) 2016 6th International*, pp. 178-185.
- Krings, A., 2014. *Iron Losses in Electrical Machines — Influence of Material Properties, Manufacturing Processes, and Inverter Operation*, Stockholm: KTH School of Electrical Engineering.
- Kuo Tsai-C, S. H. H. Z. H.-C., 2001. Design for manufacture and design for 'x': concepts, applications and perspectives. *computers & industrial engineering* 41, pp. 241-260.
- Laboratorio Elettrofisico, 2019. *Magnetizing & Measuring Equipment: Instruction manual*. 00 ed. s.l.:Laboratorio Elettrofisico.
- Lan, S., 2010. *Optimization of Electric Motor Assembly Operation with Work Study*. Harbin, IEEE.
- Leader, M. E., 2001. Understanding Journal Bearings. *Vibration Institute: Twenty-Fifth Annual Meeting*, pp. 43-55.
- Lee, S. W., 2005. "Laminated Body of Motor and Manufacturing Method Thereof". United States, Patent No. 20050073211.
- lenaleestore, 2018. *Compression Force. The Outside Surface Is In Tension And Inside Compression..* [Online]  
Available at: <http://lenaleestore.com/compression-force/the-outside-surface-is-in-tension-and-the-inside-compression-somewhere-between-two-a-neutral-axis-which-neither-nor-o/>  
[Accessed January 2018].
- Liang, Z., 2002. *Cutting Speed Sensitivity of Tool Life*. Purdue University Fort Wayne, American Society for Engineering Education.
- Libert, F. & Soulard, J., 2006. *Manufacturing Methods of Stator Cores with Concentrated Windings*. Dublin, IET.
- Lubis, D. Z. & Ristiawan, I., 2017. Blanking Clearance and Punch Velocity Effects on The Sheared Edge Characteristic in Micro-Blanking of Commercially Pure Copper Sheet. *Journal of Mechanical Engineering Science and Technology*, 1(2), pp. 53-60.
- MachineMFG, 2019. *Laser cutting thickness and speed chart*. [Online]  
Available at: <https://www.machinemfg.com/laser-cutting-thickness-speed-chart/>  
[Accessed 12 2020].
- McGee, P., 2018. *Carmakers take electric fight to the factory floor*, Frankfurt: Financial Times.
- Mechler, G. C., 2010. *Manufacturing and Cost Analysis for Aluminum and Copper Die Cast Induction Motors for GM's Powertrain and R&D Divisions*, Massachusetts : Massachusetts Institute of Technology.

METs, 2020. *Interlocked Lamination Stator Core Laminations Iron Progressive Stamping Dies*. [Online] Available at: <http://www.metal-stampingdies.com/sale-10491333-interlocked-lamination-stator-core-laminations-iron-progressive-stamping-dies.html> [Accessed 07 2020].

Miljavec, D., 2018. *Report on considered electrical motor technologies, evaluation matrix, concept*, s.l.: European Union's Horizon 2020 research and innovation programme.

Mitsuhiro, T., 1989. *Manufacturing Device for Spiral Laminated Core*. s.l. Patent No. JP1148046.

Mitsuhiro, T., Hiroshi, A., Noriyuki, D. & Izumi, O., 1990. *Manufacture of Spiral Lamination Core*. s.l. Patent No. JP2231943.

Moses, A., Anderson, P., Jenkins, K. & Stanbury, H., 2019. *Electrical Steels Volume 2: Performance and applications*. 1st ed. s.l.:IET.

Moultrie, J. & Maier, A. M., 2014. A simplified approach to design for assembly. *Journal of Engineering Design*, 25(1-3), pp. 44-63.

Mucha, J., 2010. An experimental analysis of effects of various material tool's wear on burr during generator sheets blanking. *The International Journal of Advanced Manufacturing Technology*, 50(5-8), p. 495–507.

Muffatto, M., 1999. Introducing a platform strategy in product development. *International Journal of Production Economics*, Volume 60-61, pp. 145-153.

Muniz, S. T. G. & Belzowski, B. M., 2016. *CARMAKERS ELECTRIC VEHICLES' STRATEGIES: PLATFORMS, MARKETING AND CHARGING*, s.l.: University of Michigan.

Niazi, P., 2007. A Low-Cost and Efficient Permanent-Magnet-Assisted Synchronous Reluctance Motor Drive. *IEEE TRANSACTIONS ON INDUSTRY APPLICATIONS*, 43(2), pp. 542-550.

Ni, Z. L. & Ye, F. X., 2016. Dissimilar Joining of Aluminum to Copper Using Ultrasonic Welding. *Materials and Manufacturing Processes*, Volume 31, pp. 2091-2100.

O'Driscoll, M., 2001. Design for manufacture. *Journal of materials processing technology*, Volume 122, pp. 318-321.

Pham, T., Kwon, P. & Foster, S., 2021. Additive Manufacturing and Topology Optimization of Magnetic Materials for Electrical Machines—A Review. *Energies*, 14(283).

Pitron, G., 2021. *The Rare Metals War: the dark side of clean energy and digital technologies*. s.l.:Scribe.

Polaris Laser Laminations, 2012. *What Are Laminations?*. [Online] Available at: <http://www.polarislaserlaminations.com/motor-laminations.html> [Accessed 04 2021].

Rahman, K. M. et al., 2014. Design and Performance of Electrical Propulsion System of Extended Range Electric Vehicle (EREV) Chevrolet Volt. *IEEE TRANSACTIONS ON INDUSTRY APPLICATIONS*, 51(3), pp. 2479-2488.

Randall, T. & Watanabe, C., 2017. "Tesla's battery revolution just reached critical mass" & "Why battery cost could put the brakes on electric car sales", s.l.: Bloomberg.

Ricardo plc, 2017. *Driving automotive electrification*, Shoreham-by-Sea : Ricardo.

Sahdev, S. K., 2018. *Electrical Machines*. 1 ed. Cambridge: Cambridge University Press.

Saleh, B., 2015. *Cold pressure welding - read only*. [Online]  
Available at: <https://www.slideshare.net/BaselSalehSelim/cold-pressure-welding-read-only>  
[Accessed 08 03 2018].

Salvador, L., 2016. *Influence of Cutting Process on Magnetic Properties of Electrical Steel*, Espoo: aalto university - school of electrical engineering.

Schmitt, B., 2013. Building cars from Legos. *MOBILITY ENGINEERING*, Issue 1, pp. 56-59.

Sculpteo, 2016. *LASER CUTTING: THE ULTIMATE GUIDE*. [Online]  
Available at: [https://www.sculpteo.com/media/ebook/Sculpteo\\_ultimate\\_guide\\_laser\\_cutting.pdf](https://www.sculpteo.com/media/ebook/Sculpteo_ultimate_guide_laser_cutting.pdf)  
[Accessed 04 2021].

Sharma, N., Khan, Z. A. & Siddiquee, A. N., 2017. Friction stir welding of aluminum to copper—An overview. *Non ferrous metal soc*, Volume 27, pp. 2113-2136.

Slack, N., 2019. *Operations management*. 9th ed. Harlow: Pearson.

SMT Winding Equipment, 2017. *Motor Stator Aluminum / Copper Wire Coil and Wedge Inserting Machine With Robot*. [Online]  
Available at: <https://www.youtube.com/watch?v=Xjb9JFXEjkw>  
[Accessed 04 2021].

Soares, J. A., Gipiela & Lajarin , 2012. Study of the punch–die clearance influence on the sheared edge quality of thick sheets. *The International Journal of Advanced Manufacturing Technology*, Volume 65, pp. 451-457.

Sołtysiak, R. et al., 2019. *The Analysis of Fiber and CO2 Laser Cutting Accuracy*. s.l., MATEC Web of Conferences.

Soong, W. L., 2008. Sizing of Electrical Machines. *Power Engineering Briefing Note Series*, pp. 17-18.

Stone, E., 2021. *Private communications* [Interview] 2021.

Stroud Metal Company Limited, 2020. *Progressive Die Pressings*. [Online]  
Available at: <https://www.stroudmetal.co.uk/manufacturing/progressive-die>  
[Accessed 07 2020].

Subramonian, S., 2013. *Improvement of Punch and Die Life and Part Quality in Blanking of Miniature Parts*, Ohio: The Ohio State University.

Syed, A., 2006. *A NEW ANALYTICAL MODEL FOR TOOL LIFE IN METAL STAMPING*, Hamilton, Ontario : McMaster University .

Tang, D. & Gao, B., 2007. Feature-based metal stamping part and process design. Part I.: *International Journal of Production Research*, 45(12), p. 2673–2695.

Taylor, F. W., 1906. *On the Art of Cutting Metals*. 3rd ed. New York: The American Society of Mechanical Engineers.

Thakker, J., Kanda, A. & Deshmukh, S., 2012. Supply chain issues in Indian manufacturing SMEs: insights from six case studies. *Journal of Manufacturing Technology Management*, 23(5), pp. 634-664.

Tibtech innovations, 2011. *Properties table of Stainless steel, Metals and other Conductive materials*. [Online]

Available at: <http://www.tibtech.com/conductivity.php>

[Accessed June 2018].

Tucci, C., 1994. A Simulator of the Manufacturing of Induction Motors. *IEEE TRANSACTIONS ON INDUSTRY APPLICATIONS*, 30(3), pp. 578-584.

Vandenbossche, L., 2015. *Impact of Mechanical Stresses on the Magnetic Performance of Non-Oriented Electrical Steels and its Relation to Electric Machine Efficiency*, s.l.: ArcelorMittal.

Vazquez, M., Hallack, M. & Perez, Y., 2018. The dynamics of institutional and organisational change in emergent industries: the case of electric vehicles. *International Journal of Automotive Technology and Management*, 18(3).

Volkswagen AG, 2021. *From old to new – Battery recycling in Salzgitter*. [Online]

Available at: <https://www.volkswagenag.com/en/news/stories/2021/01/from-old-to-new-battery-recycling-in-salzgitter.html>

[Accessed 04 2021].

Volkswagen, 2019. *From springs and dampers to rotors and stators*. [Online]

Available at: <https://www.volkswagen-newsroom.com/en/stories/from-springs-and-dampers-to-rotors-and-stators-5177>

[Accessed 10 10 2020].

von Pfingsten, G. & Hameyer,, K., 2016. *Influence of Axial Mechanical Stress on the Magnetic Properties of Non-Oriented Electrical Steel*. Nuremberg, 2016 6th International Electric Drives Production Conference.

Weiss, H. A., Leuning, N., Steentjes, S. & Hameyer, K., 2016. Influence of shear cutting parameters on the electromagnetic properties of non-oriented electrical steel sheets. *Journal of Magnetism and Magnetic Materials*, Volume 421, pp. 250-259.



- Weiss, H. A., Trober, P. & Golle, R., 2018. Impact of punching parameter variations on magnetic properties of nongrain-oriented electrical steel. *IEEE Transactions on industry applications*, 54(6), pp. 5869-5877.
- Weman, K., 2012. *Welding processes handbook*. 2nd ed. Oxford: Woodhead Publishing.
- Wu, Q., 2019. Achieving automotive suppliers' mass customization through modularity. *Journal of Manufacturing Technology Management*, 31(2), pp. 306-329.
- Yang, R., 2016. *ELECTRIFIED VEHICLE TRACTION MACHINE DESIGN WITH MANUFACTURING CONSIDERATIONS*, Ontario: McMaster University.
- Yasuo, A. & Toshihiko, F., 2004. *Method and Apparatus for Rolling Up Stator Core*. s.l. Patent No. JP2004159417.
- Young, W. C. & Budynas, R. G., 2002. *Roark's Formulas for stress and strain*. 7th Edition ed. New York: McGraw-Hill.
- Youssef, M. E., 2017. Slinky stator: The impact of manufacturing process on the magnetic properties. *IEEE International Electric Machines and Drives Conference (IEMDC)*, pp. 1-8.
- ZEISS, 2020. *eMobility: Measuring technology from ZEISS provides the key for series production*. [Online] Available at: <https://www.zeiss.co.uk/metrology/magazine/vw-salzgitter.html> [Accessed 09 2020].
- Ziegler, M., Schneider, M., Hubert, M. & Franke, J., 2018. *Potentials of the Rotary Cutting Process for Electrical Steel Strip*. Schweinfurt, IEEE.

## 11 Appendices

### 11.1 Appendix A

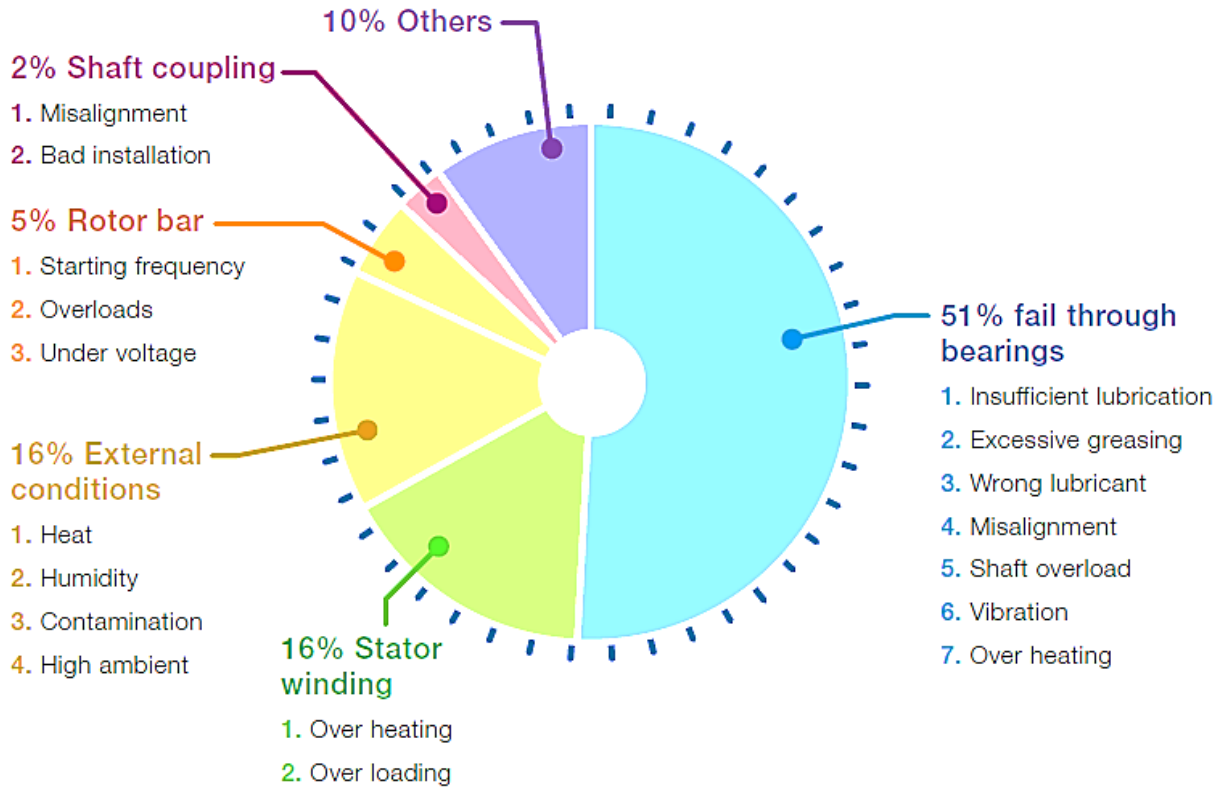


Figure 131 why motors fail chart (ABB, 2015, p. 2)

## 11.2 Appendix B

### FEA results for Slinky coiling of stator

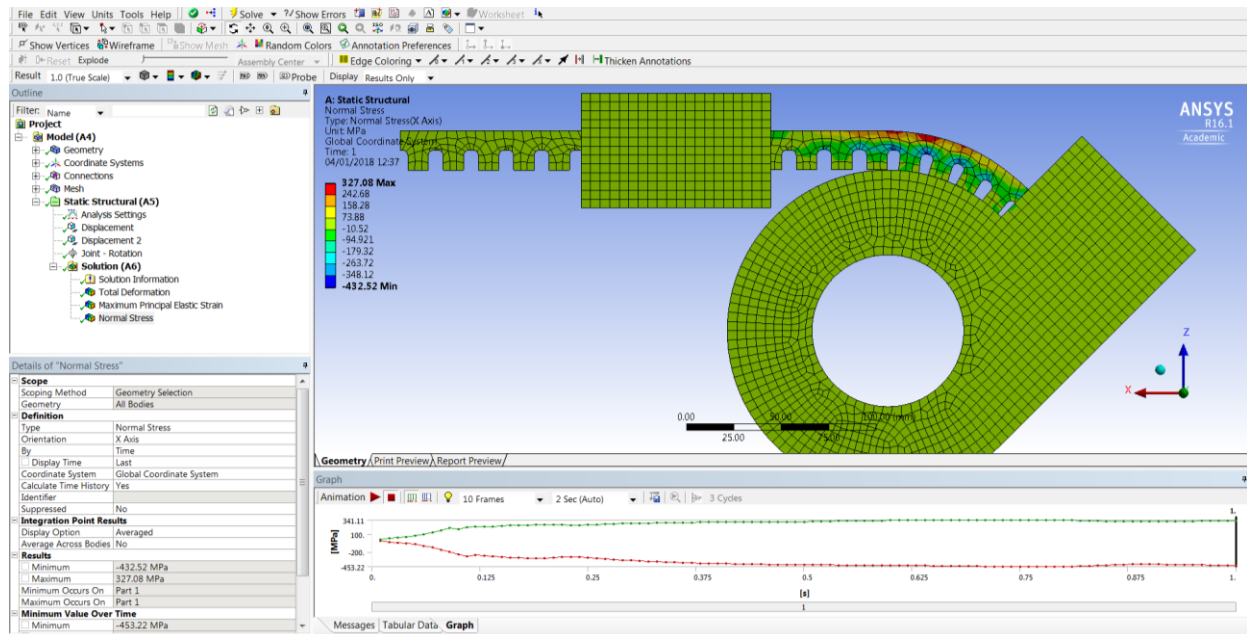


Figure 132 10mm back iron, 20.5mm total width

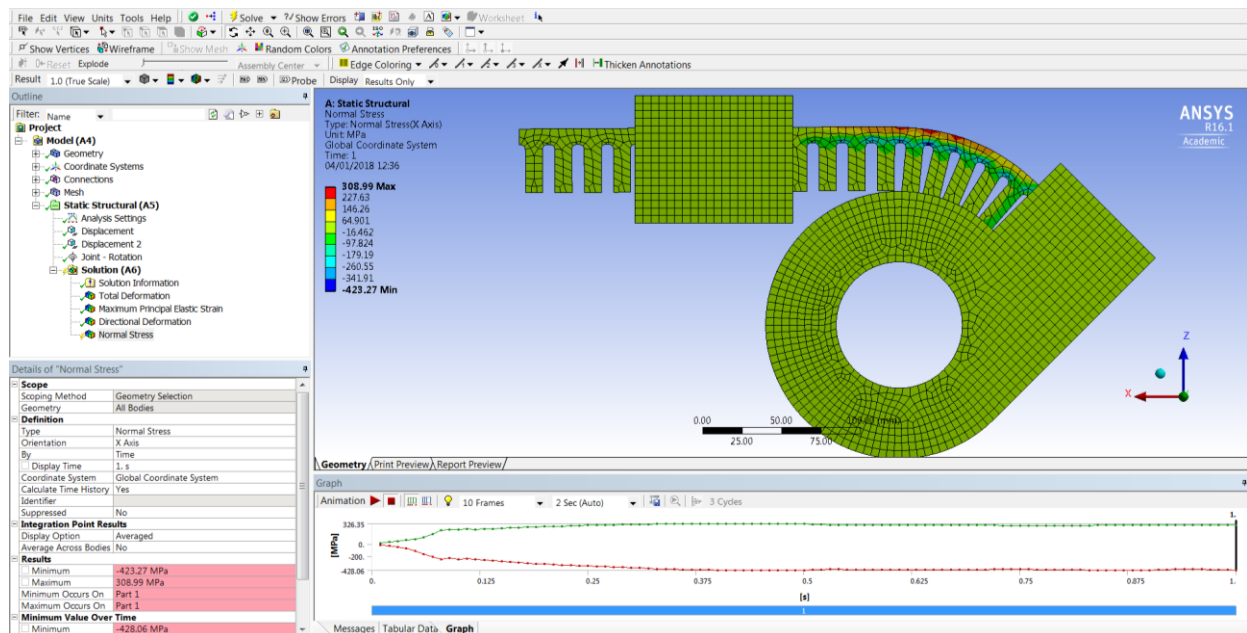


Figure 133 10mm back iron, 40.5mm total width

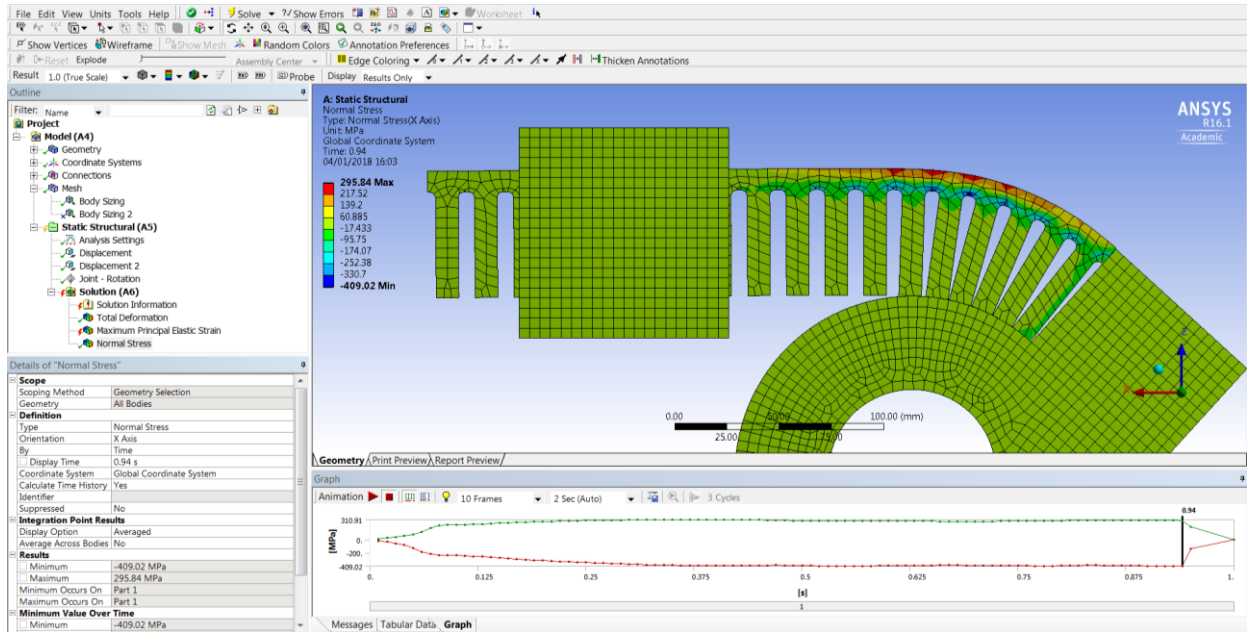


Figure 134 10mm back iron, 60.5mm total width

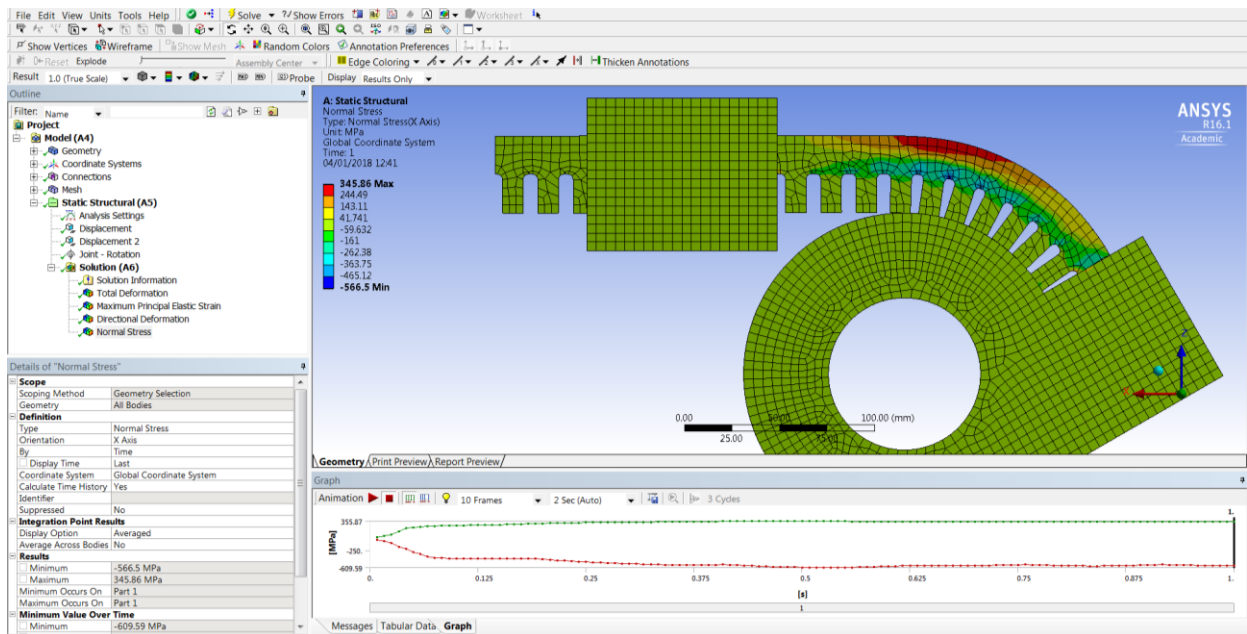


Figure 135 20mm back iron, 40.5mm total width

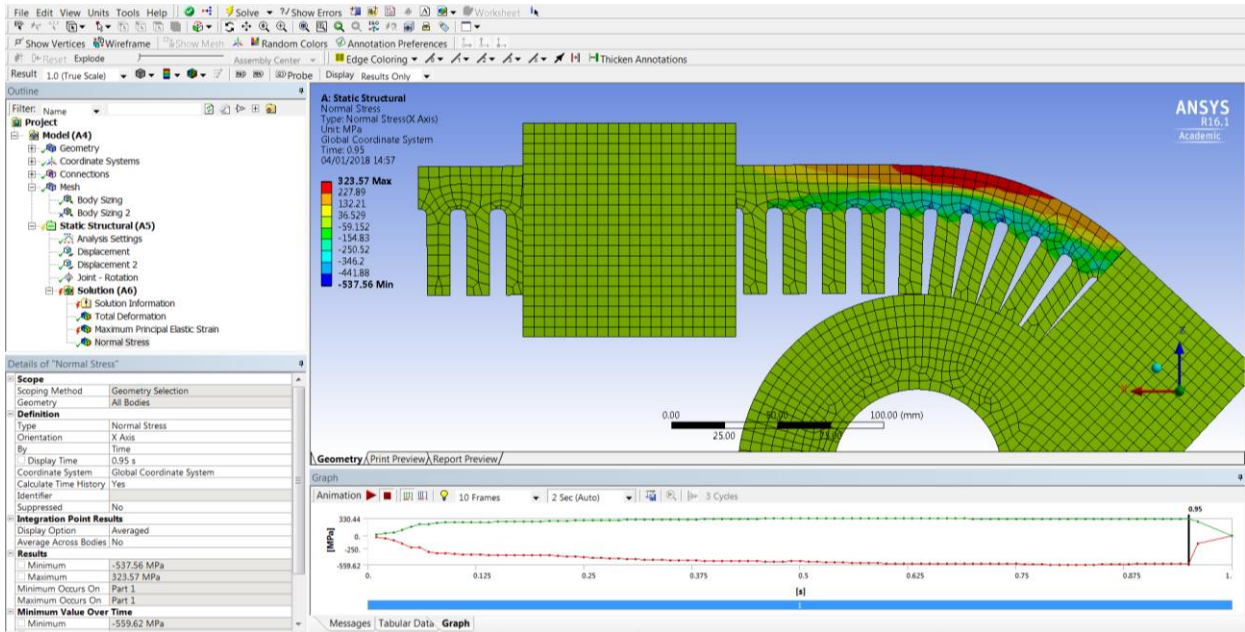


Figure 136 20mm back iron, 60.5mm total width

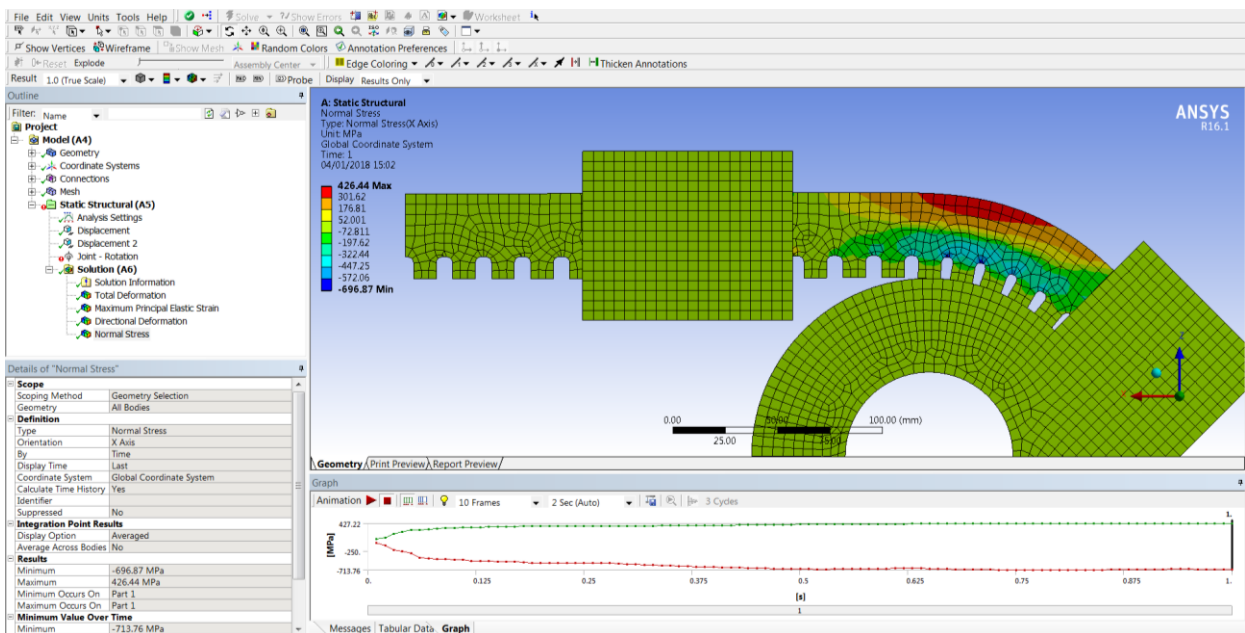


Figure 137 30mm back iron, 40.5mm total width

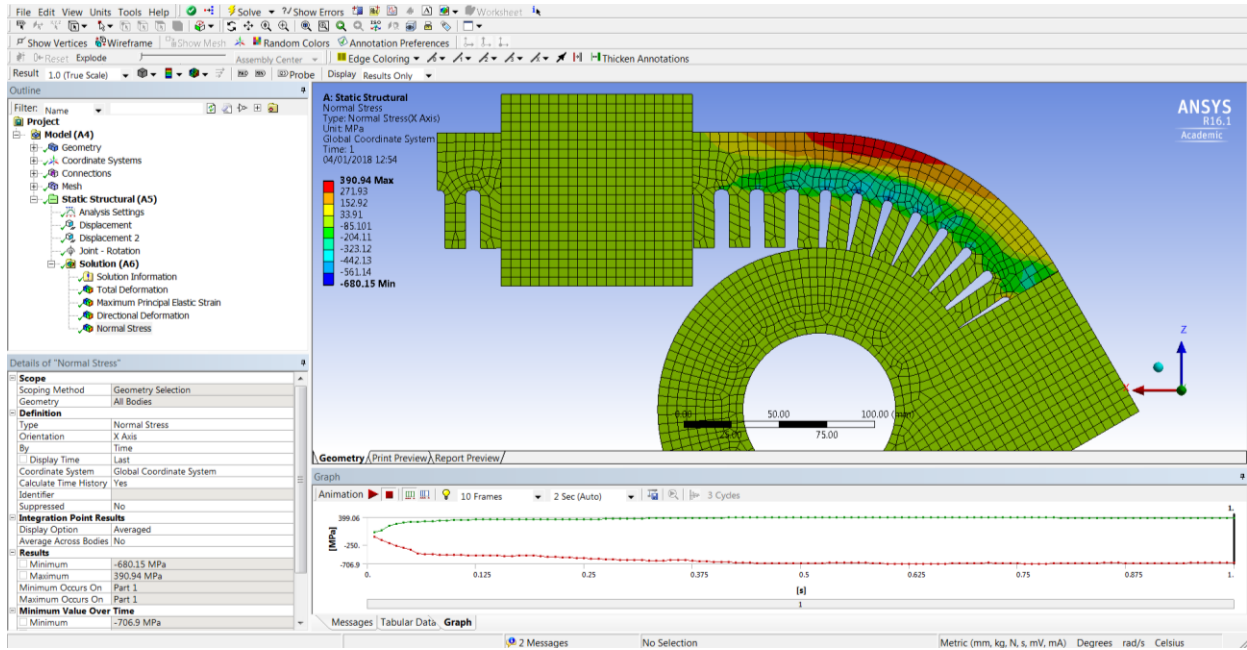


Figure 138 30mm back iron, 60.5mm total width

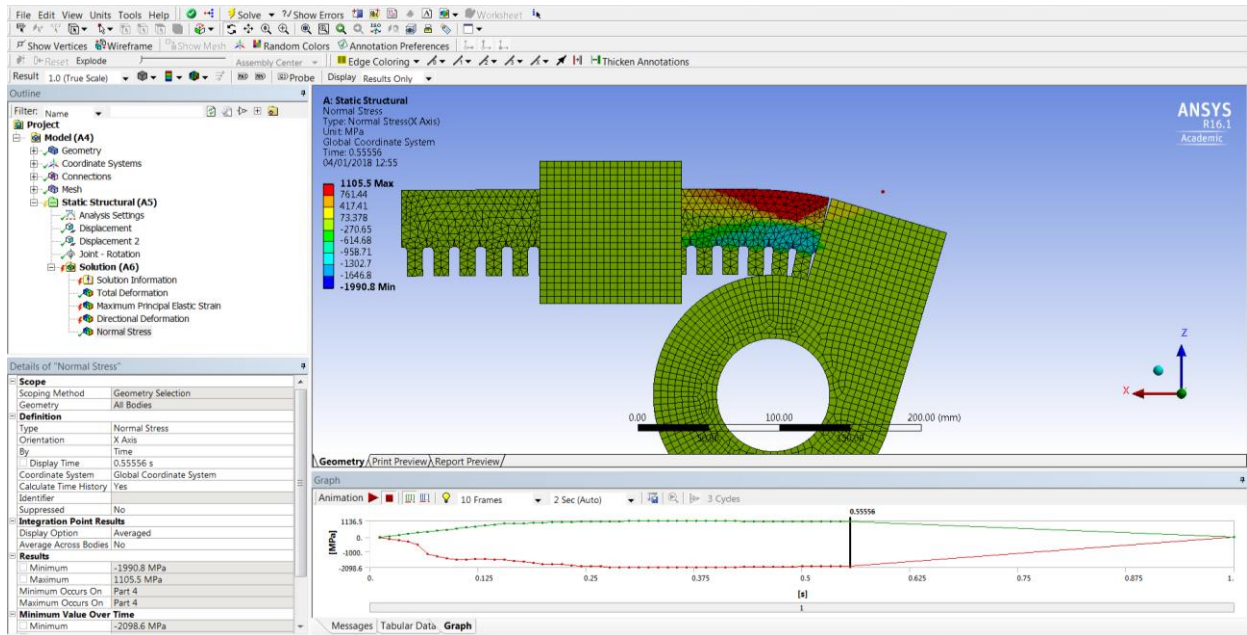


Figure 139 40mm back iron, 60.5mm total width

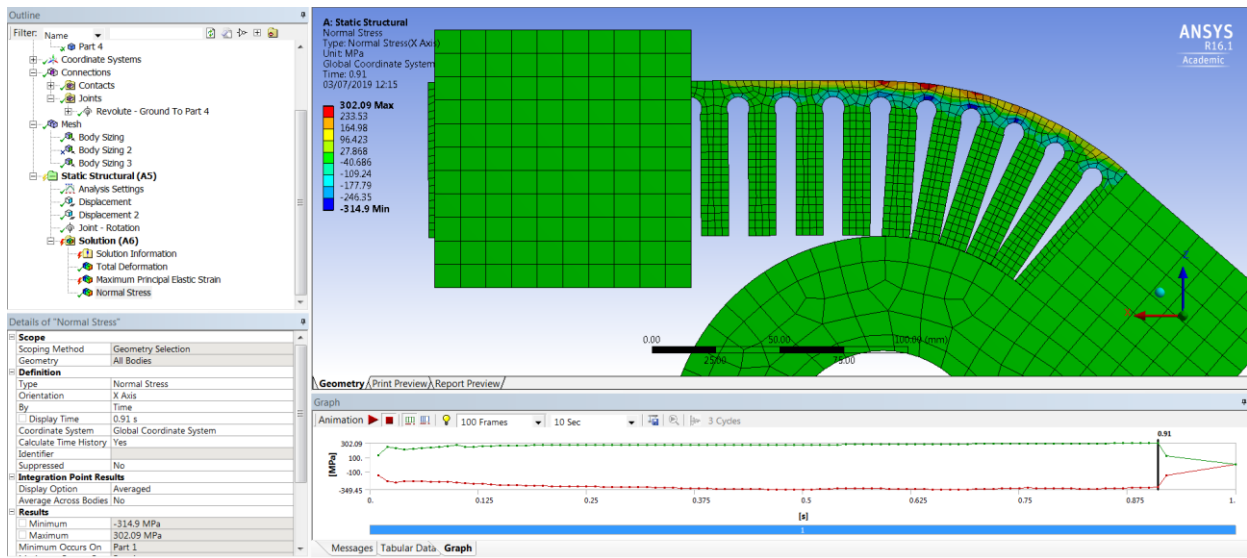


Figure 140 New design A - 10mm back iron, 60.5mm total width

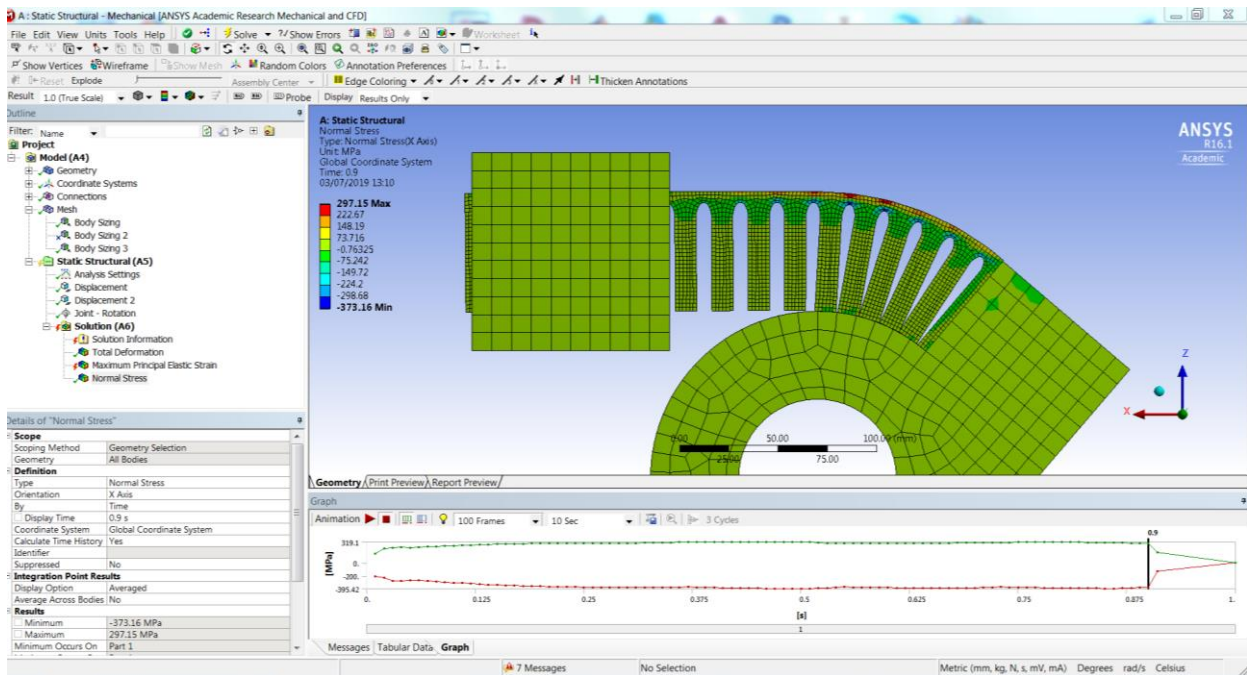


Figure 141 New design B - 10mm back iron, 60.5mm total width

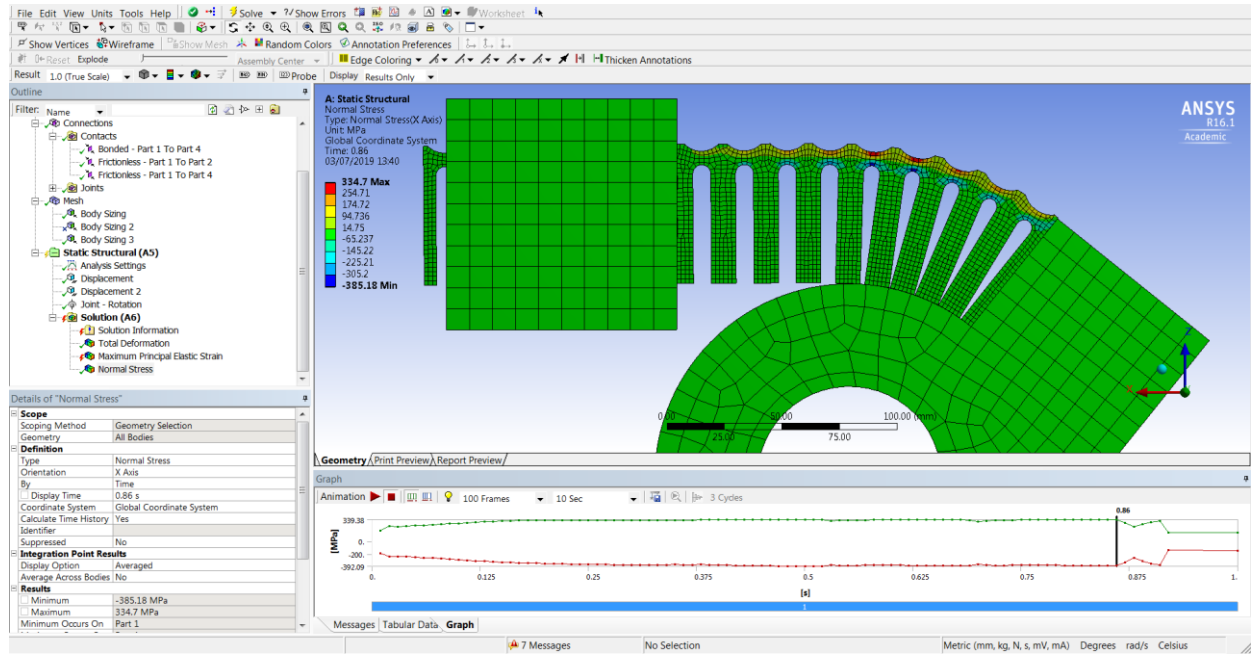


Figure 142 New design C - 10mm back iron, 60.5mm total width



11.3 Appendix C

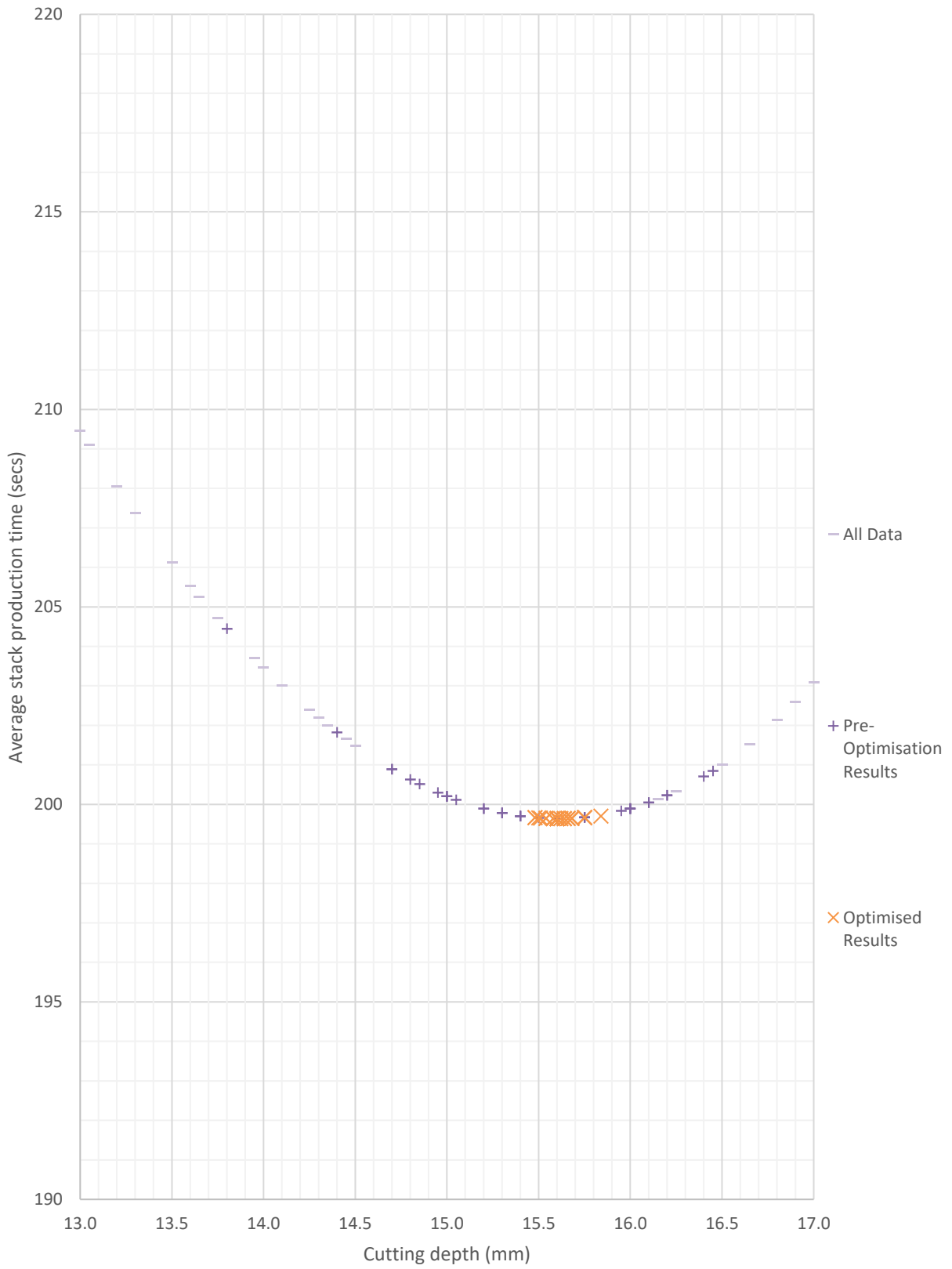


Figure 143 Optimised data set for production times

11.4 Appendix D

Laser Cutting Thickness & Speed Chart											
		500W	1000W	1500	2000W	3000W	4000W	6000W	8000W	10000W	12000W
	Thick	speed m/min	speed m/min	speed m/min	speed m/min	speed m/min	speed m/min	speed m/min	speed m/min	speed m/min	speed m/min
CS (Q235A)	1	7.0-9.0	8.0-10	15-26	24-30	30-40	33-42	35-42	35-42	35-42	35-42
	2	3.0-4.5	4.0-6.5	4.5-7.0	4.7-6.0	4.8-7.5	5.2-8.0	6.0-8.0	6.2-10	7.0-12	10-13
	3	1.8-3.0	2.4-3.0	2.6-4.0	3.0-4.8	3.3-5.0	3.5-5.5	3.8-6.5	4.0-7.0	4.2-7.5	4.5-8.0
	4	1.3-1.5	2.0-2.4	2.5-3.0	2.8-3.5	3.0-4.2	3.1-4.8	3.5-5.0	3.5-5.5	3.5-5.5	3.5-5.5
	5	0.9-1.1	1.5-2.0	2.0-2.5	2.2-3.0	2.6-3.5	2.7-3.6	3.3-4.2	3.3-4.5	3.3-4.5	3.3-4.8
	6	0.6-0.9	1.4-1.6	1.6-2.2	1.8-2.6	2.3-3.2	2.5-3.4	2.8-4.0	3.0-4.2	3.0-4.2	3.0-4.2
	8		0.8-1.2	1.0-1.4	1.2-1.8	1.8-2.6	2.0-3.0	2.2-3.2	2.5-3.5	2.5-3.5	2.5-3.5
	10		0.6-1.0	0.8-1.1	1.1-1.3	1.2-2.0	1.5-2.0	1.8-2.5	2.2-2.7	2.2-2.7	2.2-2.7
	12		0.5-0.8	0.7-1.0	0.9-1.2	1.0-1.6	1.2-1.8	1.2-2.0	1.2-2.1	1.2-2.1	1.2-2.1
	14			0.5-0.7	0.7-0.8	0.9-1.4	0.9-1.2	1.5-1.8	1.7-1.9	1.7-1.9	1.7-1.9
	16				0.6-0.7	0.7-1.0	0.8-1.0	0.8-1.5	0.9-1.7	0.9-1.7	0.9-1.7
	18				0.4-0.6	0.6-0.8	0.65-0.9	0.65-0.9	0.65-0.9	0.65-0.9	0.65-0.9
	20					0.5-0.8	0.6-0.9	0.6-0.9	0.6-0.9	0.6-0.9	0.6-0.9
	22					0.4-0.6	0.5-0.8	0.5-0.8	0.5-0.8	0.5-0.8	0.5-0.8
25						0.3-0.5	0.3-0.5	0.3-0.7	0.3-0.7	0.3-0.7	
SS (201)	1	8.0-13	18-25	20-27	24-30	30-35	32-40	45-55	50-66	60-75	70-85
	2	2.4-5.0	7.0-12	8.0-13	9.0-14	13-21	16-28	20-35	30-42	40-55	50-66
	3	0.6-0.8	1.8-2.5	3.0-5.0	4.0-6.5	6.0-10	7.0-15	15-24	20-30	27-38	33-45
	4		1.2-1.3	1.5-2.4	3.0-4.5	4.0-6.0	5.0-8.0	10-16	14-21	18-25	22-32
	5		0.6-0.7	0.7-1.3	1.8-2.5	3.0-5.0	4.0-5.5	8.0-12	12-17	15-22	18-25
	6			0.7-1.0	1.2-2.0	2.0-4.0	2.5-4.5	6.0-9.0	8.0-14.0	12-15	15-21
	8				0.7-1.0	1.5-2.0	1.6-3.0	4.0-5.0	6.0-8.0	8.0-12.0	10-16
	10					0.6-0.8	0.8-1.2	1.8-2.5	3.0-5.0	6.0-8.0	8.0-12
	12					0.4-0.6	0.5-0.8	1.2-1.8	1.8-3.0	3.0-5.0	6.0-8.0
	14						0.4-0.6	0.6-0.8	1.2-1.8	1.8-3.0	3.0-5.0
	20							0.4-0.6	0.6-0.7	1.2-1.8	1.8-3.0
	25								0.5-0.6	0.6-0.7	1.2-1.8
	30								0.4-0.5	0.5-0.6	0.6-0.7
	40									0.4-0.5	0.5-0.6
Alu	1	4.0-5.5	6.0-10	10-20	15-25	25-38	35-40	45-55	50-65	60-75	70-85
	2	0.7-1.5	2.8-3.6	5.0-7.0	7-10	10-18	13-25	20-30	25-38	33-45	38-50
	3		0.7-1.5	2.0-4.0	4.0-6.0	6.5-8.0	7.0-13	13-18	20-30	25-35	30-40
	4			1.0-1.5	2.0-3.0	3.5-5.0	4.0-5.5	10-12	13-18	21-30	25-38
	5			0.7-1.0	1.2-1.8	2.5-3.5	3.0-4.5	5.0-8.0	9.0-12	13-20	15-25
	6				0.7-1.0	1.5-2.5	2.0-3.5	4.0-6.0	4.5-8.0	9.0-12	13-18
	8				0.6-0.8	0.7-1.0	0.9-1.6	2.0-3.0	4.0-6.0	4.5-8.0	9.0-12
	10					0.4-0.7	0.6-1.5	1.0-2.0	2.2-3.0	4.0-6.0	4.5-8.0
	12					0.3-0.45	0.4-0.6	0.8-1.4	1.5-2.0	2.2-3.0	4.0-6.0
	16						0.3-0.4	0.6-0.8	1.0-1.6	1.5-2.0	2.2-3.0
	20							0.5-0.7	0.7-1.0	1.0-1.6	1.5-2.0
	25								0.5-0.7	0.7-1.0	1.0-1.6
	35									0.5-0.7	0.7-1.0

Table 35 Alternative laser cutting machine speeds (MachineMFG, 2019)

## 11.5 Appendix E

**Table 1: Parameters for laser cutting of mild steels with laser cutting oxygen including pressure and volume requirements**

Material thickness mm (in)	Laser power W	Nozzle standoff mm (in)	Nozzle diameter mm (in)	Oxygen pressure bar (psi)	Gas volume m <sup>3</sup> /h (scf/h)	Cutting speed m/min (in/m)
0.5 (.02)	500	0.3-0.6 (.01-.02)	0.6-0.8 (.03-.04)	3.5-6.0 (50-90)	2.0 (70)	15.0 (600)
1.0 (.04)	800	0.3-0.6 (.01-.02)	0.6-0.8 (.03-.04)	3.5-6.0 (50-75)	1.8 (64)	11.0 (440)
2.0 (.08)	1,000	0.3-0.8 (.01-.03)	0.6-1.2 (.03-.05)	2.5-4.0 (35-60)	3.0 (105)	7.0 (280)
4.0 (.16)	1,000	0.3-0.8 (.01-.03)	0.6-1.2 (.03-.05)	2.0-4.0 (30-60)	2.7 (95)	4.0 (160)
6.0 (1/4)	1,000	0.5-1.0 (.02-.04)	1.0-1.5 (.04-.06)	1.5-3.0 (20-45)	3.2 (115)	2.5 (100)
8.0 (.32)	1,500	0.5-1.0 (.02-.04)	1.2-1.5 (.05-.06)	1.5-2.5 (20-35)	3.0 (105)	2.0 (80)
12.0 (1/2)	1,500	0.5-1.0 (.02-.04)	1.2-1.5 (.05-.06)	1.0-2.0 (15-30)	2.4 (85)	1.0 (40)
18.0 (3/4)	2,000	0.5-1.0 (.02-.04)	1.2-1.5 (.05-.06)	0.5-1.0 (7-15)	1.4 (50)	0.5 (20)
25.0 (1.0)	4,000	0.5-1.0 (.02-.04)	1.5-2.0 (.06-.08)	0.5-0.7 (7-10)	1.3 (46)	0.5 (20)
25.0 (1.0)	6,000	0.5-1.0 (.02-.04)	2.0-2.3 (0.08-0.09)	0.5-0.7 (7-10)	1.5 (52)	0.9 (36)

*Table 36 Indicative laser setting parameters for mild steel settings (BOC, 2021)***Table 4: Parameters for laser cutting of aluminium alloy AlMg3, the table refers to dross-free cuts, cutting gas: laser cutting nitrogen**

Material thickness mm (in)	Laser power W	Nozzle standoff mm (in)	Nozzle diameter mm (in)	Nitrogen pressure bar (psi)	Gas volume m <sup>3</sup> /h (scf/h)	Cutting speed m/min (in/m)
1.0 (.04)	1,800	0.3-0.6 (.01-.02)	1.2-1.5 (.05-.060)	12.0 (180)	11.0 (390)	8.2 (320)
2.0 (.08)	1,800	0.3-0.6 (.01-.02)	1.2-1.5 (.05-.060)	14.0 (210)	15.0 (530)	3.6 (140)
3.0 (.12)	3,000	0.3-0.8 (.01-.03)	1.2-1.5 (.05-.060)	14.0 (210)	15.0 (530)	2.5 (100)
4.0 (.16)	3,000	0.3-0.8 (.01-.03)	1.8-2.2 (.07-.085)	14.0 (210)	35.0 (1,240)	1.8 (70)
6.0 (1/4)	4,000	0.5-1.0 (.02-.04)	2.0-2.4 (.08-.090)	16.0 (240)	40.0 (1,410)	1.8 (70)
8.0 (3/8)	4,000	0.5-1.0 (.02-.04)	2.0-2.5 (.08-.100)	16.0 (240)	45.0 (1,590)	0.8 (30)
12 (1/2)	5,000	0.5-1.0 (.02-.04)	2.0-2.5 (.08-.100)	18 (260)	53 (1880)	0.5 (19)
15 (3/8)	6,000	0.5-1.0 (.02-.04)	2.0-2.5 (.08-.100)	16 (230)	47 (1670)	0.4 (16)

See page 19(\*)

*Table 37 Indicative laser setting parameters for aluminium settings (BOC, 2021)***Copper alloys**

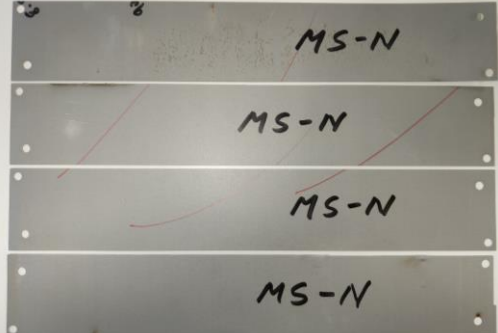
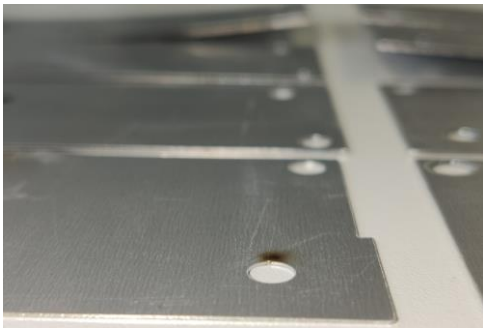
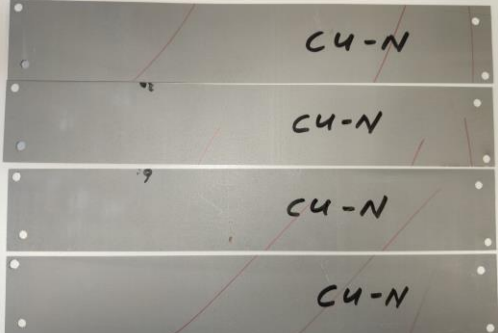
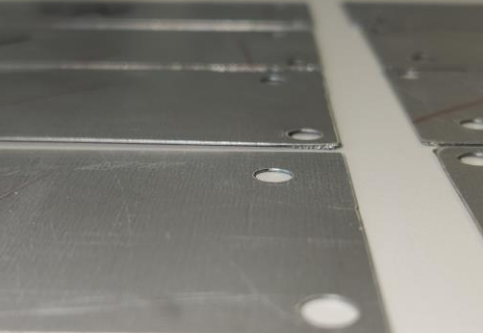
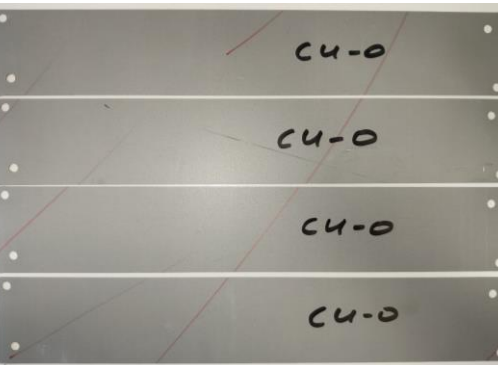

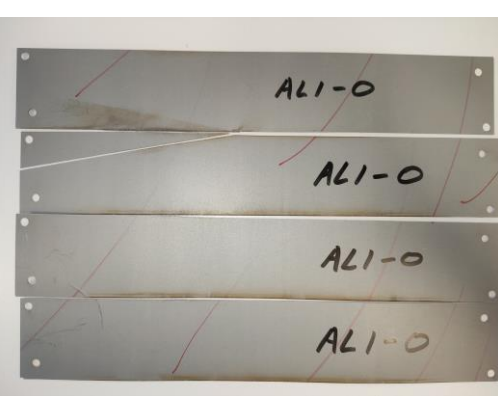
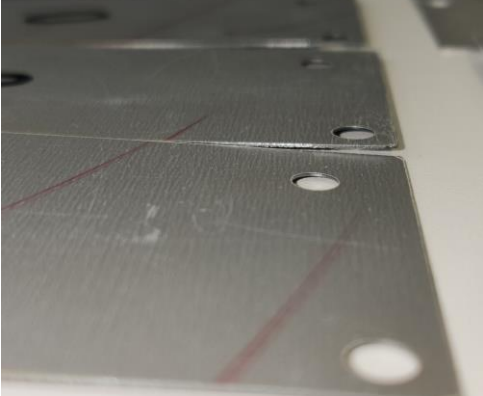
The high reflectivity and thermal conductivity of copper make cutting of this material quite a challenge. Precautions must be taken to avoid re-reflections of the laser beam and subsequent damage to the resonator.

Brass is one of the important copper alloys (copper-zinc alloy), and has lower reflectivity and thermal conductivity than copper. It is therefore easier to cut with CO<sub>2</sub> lasers. Very high laser power and a short focal length of the lens – about 63mm (2.5 in) are beneficial.

Oxygen-cutting is preferable when cutting brass and other copper alloys with CO<sub>2</sub> lasers. Oxygen is better suited as a cutting gas, as the oxide layer at the cut front improves absorption of the laser beam. Both low oxygen pressures of up to 6 bar (85 psi) and high oxygen pressures of up to 20 bar (300 psi) are used. When cutting brass at high oxygen pressures of up to 20bar (300psi), proper ventilation of the working area must be provided to avoid dangerous enrichment of the atmosphere with oxygen. The maximum sheet thickness that can be cut is 4-5mm (0.16-0.20 in). Sometimes, high-pressure nitrogen is also used to cut copper alloys.

*Figure 144 Indicative laser setting parameters for copper settings (BOC, 2021)*

11.6 Appendix F

 <p>MS-N MS-N MS-N MS-N</p>		<p>GOOD</p>
 <p>CU-N CU-N CU-N CU-N</p>		<p>POOR</p>
 <p>CU-O CU-O CU-O CU-O</p>		<p>POOR</p>
 <p>ALI-O ALI-O ALI-O ALI-O</p>		<p>POOR</p>

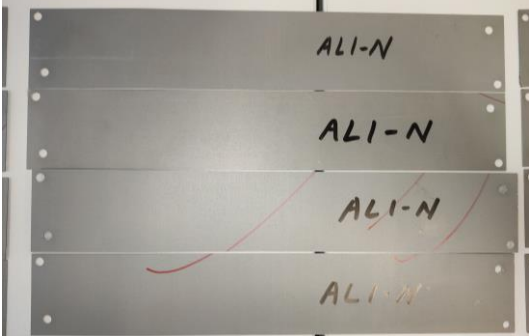
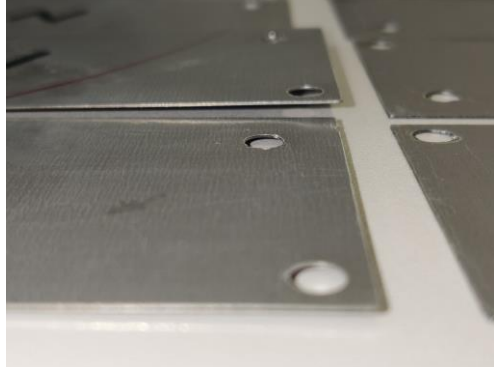

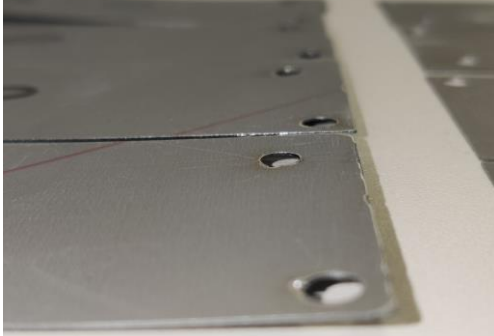
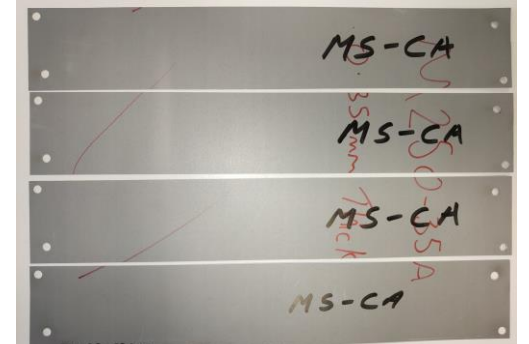

		<p>GOOD</p>
		<p>POOR</p>
		<p>GOOD</p>

Table 38 Single laminate trial cuts



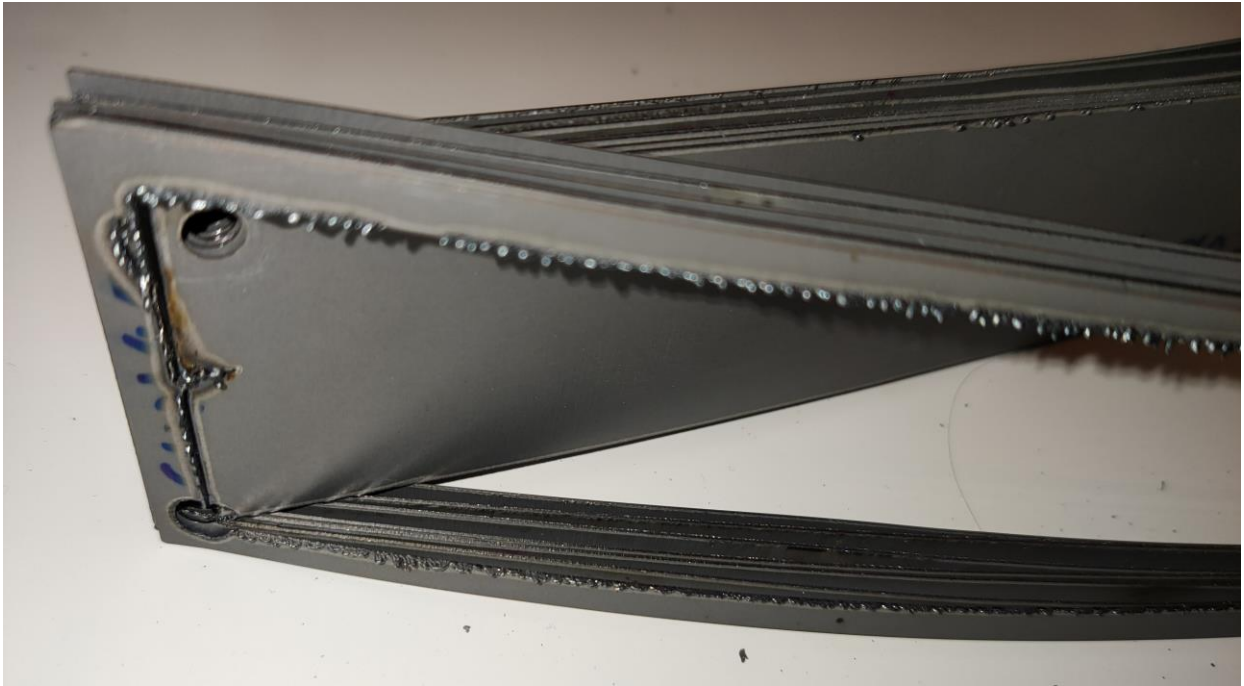
Figure 145 STACK 2



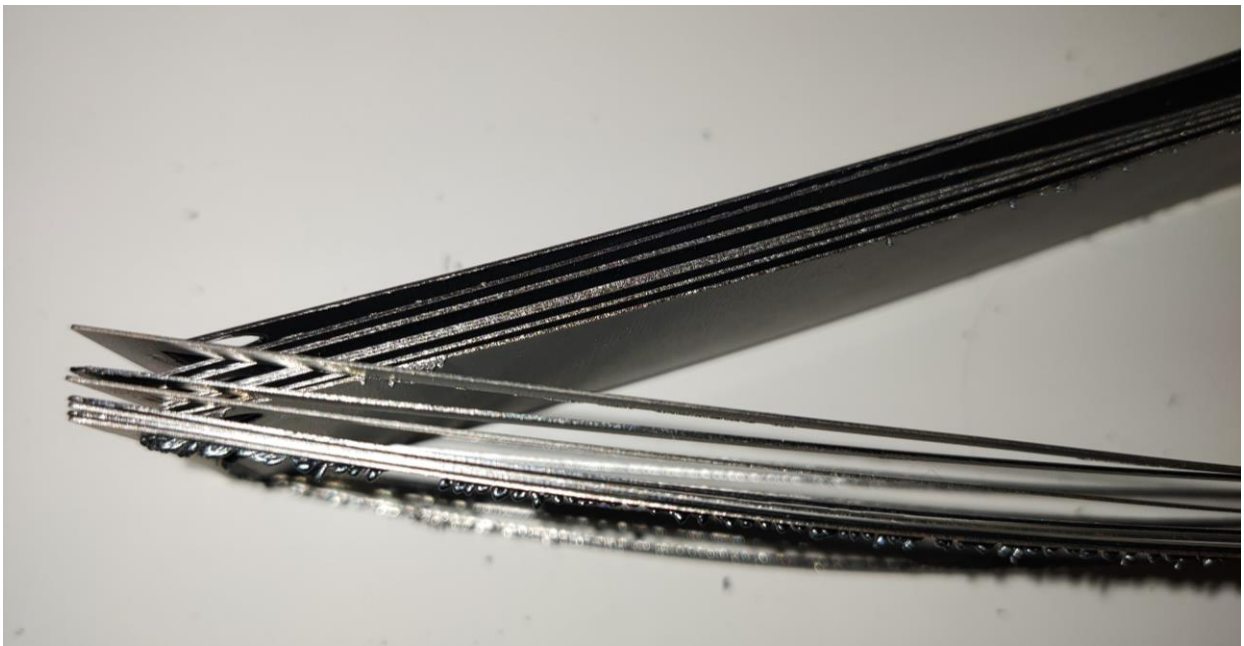
Figure 146 STACK 2



Figure 147 STACK 4



*Figure 148 STACK 3*



*Figure 149 STACK 3*

11.7 Appendix G

	< overall opinion (x/5)	identifier	Review of cut				notes
			Rating	Colour	Edges / Burrs	Seperation	
			/5	/5	/5	/5	
<b>ALI N - STACK 1</b>	2.86	<b>1</b>	5.00	5	5	5	
		<b>2</b>	4.33	4	4	5	black marking on back face
		<b>3</b>	3.67	3	3	5	
		<b>4</b>	2.67	2	3	3	
		<b>5</b>	1.67	2	2	1	
		<b>6</b>	1.33	2	1	1	
		<b>7</b>	1.33	2	1	1	

Table 39 Polystromata cutting trial results for Aluminium + Nitrogen laser cutting settings



	< overall opinion (x/5)	identifier	Review of cut				notes
			Rating	Colour	Edges / Burrs	Seperation	
			/5	/5	/5	/5	
<b>MS N - STACK 2</b>	2.43	<b>1</b>	4.00	5	4	3	
		<b>2</b>	3.00	3	4	2	
		<b>3</b>	2.33	2	4	1	
		<b>4</b>	2.67	3	4	1	
		<b>5</b>	1.67	1	3	1	
		<b>6</b>	1.67	2	2	1	
		<b>7</b>	1.67	2	2	1	

Table 40 Polystromata cutting trial results for Mild steel + Nitrogen laser cutting settings

	< overall opinion (x/5)	identifier	Review of cut				notes
			Rating	Colour	Edges / Burrs	Seperation	
			/5	/5	/5	/5	
<b>Cu N - STACK 3</b>	3.71	<b>1</b>	5.00	5	5	5	
		<b>2</b>	4.33	4	4	5	
		<b>3</b>	4.33	4	4	5	
		<b>4</b>	4.00	4	3	5	
		<b>5</b>	3.67	4	3	4	slightly stuck to layer 6. very little force to separate
		<b>6</b>	2.67	4	2	2	joined to 5& 7
		<b>7</b>	2.00	2	1	3	very stuck to layer 6

Table 41 Polystromata cutting trial results for copper + nitrogen laser cutting settings

	< overall opinion (x/5)	identifier	Review of cut				notes
			Rating	Colour	Edges / Burrs	Seperation	
			/5	/5	/5	/5	
<b>MS CA - STACK 4</b>	2.24	<b>1</b>	3.67	4	4	3	stuck to 2
		<b>2</b>	3.33	3	4	3	stuck to 1
		<b>3</b>	2.67	3	3	2	stuck to 4
		<b>4</b>	1.67	2	2	1	
		<b>5</b>	1.67	2	2	1	
		<b>6</b>	1.33	2	1	1	
		<b>7</b>	1.33	2	1	1	

Table 42 Polystromata cutting trial results for Mild Steel + Compressed Air laser cutting settings

11.8 Appendix H

Production rates				Costs							
			Stamp	Laser			Stamp	Laser			
hours	Time to produce quantity	$t_u$	3099	164146	Energy costs	$C_E$	£3,934	£369,328			
secs	av. laminate production rate	$t_{lam}$	0.39	20.68	Machine & Machining	$C_{ao}$	£11,289,266	£1,200,000			
secs	av. stack production rate	$t_{stack}$	112	5909	Maintenance	$C_{am}$	£286,000	£5,714,286			
£	Overhead costs	$C_O$	£ 619,860	£131,316,446	Consumables & other	$C_c$		£2,249,299			
								Total costs (Machining)	$C_{\Sigma o}$	£11,579,200	£9,532,912
								Total costs (inc raw Mats)	$C_{\Sigma s}$	£17,076,686	£145,726,984
								Av. Stack Cost	$C_{\bar{x}}$	£170.77	£1,457.27
								Energy costs			
£/hr	Overhead rate	$C_t$	£ 200.00	£ 200.00	£ / kWh	RATE	$C_{ew}$	£ 0.25	£ 0.25		
	Operation per minute	$\alpha_o$	300	2.73	£ / kJ	RATE	$C_{ej}$	£ 0.000069	£ 0.000069		
	laminates cut per operation	$\beta$	1	1.00							
%	FORCE FACTOR OF SAFETY	F	2		kJ	Inner circumference	$E_{ic}$	0.053			
kN	INNER CIRCUMFERENCE	$P_{ic}$	152.53		kJ	Outer circumference	$E_{oc}$	0.091			
kN	OUTER CIRCUMFERENCE	$P_{oc}$	261.10		kJ	slots	$E_{slots}$	0.072			
kN	SLOTS	$P_{slots}$	205.63		kJ	Die position return	$E_m$	1.766			
kN	TOTAL FORCE / STROKE	$P_{\Sigma}$	619.26		kg	Die Mass	$E_{DM}$	200			
mins	Maintenance time	$t_m$	240		m	Die Travel	$L_{DT}$	0.3			
mins	die change over	$t_D$	480		kW	Laser power rating	$E_L$		3		
m/sec	laser cutting speed	$U_c$		0.099	kW	Laser Power usage	$E_p$		9		
	laminates cut (best case)	$n_{LC}$		1	Machining & other costs						
m	actual cutting stack depth	$L_L$		0.00035	Die cost	$C_D$	£240,197				
mins	change over time	$t_L$		1.000	HRC	Tool Hardness	H	62			
mins	total operations required	$n_O$		28571429		Number of strokes until tool failure	$n_u$	617672			
mins	Laser maintenance	$t_j$		120		Tools required to produce stacks	$n_D$	47			
								Cost of performing maintenance	$C_m$	£1,000	
								Number of strokes until tool maintenance	$n_s$	100000	
								Number of tool maintenance occurrences	$n_m$	286.00	
								Number of machines purchased	$n_L$	4	
								Laser cutter	$C_L$	£300,000	
								/operator	Gas	$C_G$	£0.05
								/100 hours:	other consumables	$C_{co}$	£500
									Maintenance costs	$C_j$	£2,000
								operations:	Operations until maintenance	$n_j$	10000

Table 43 Results based on monostroma cutting operations (single sheet cut per operation)

11.9 Appendix I

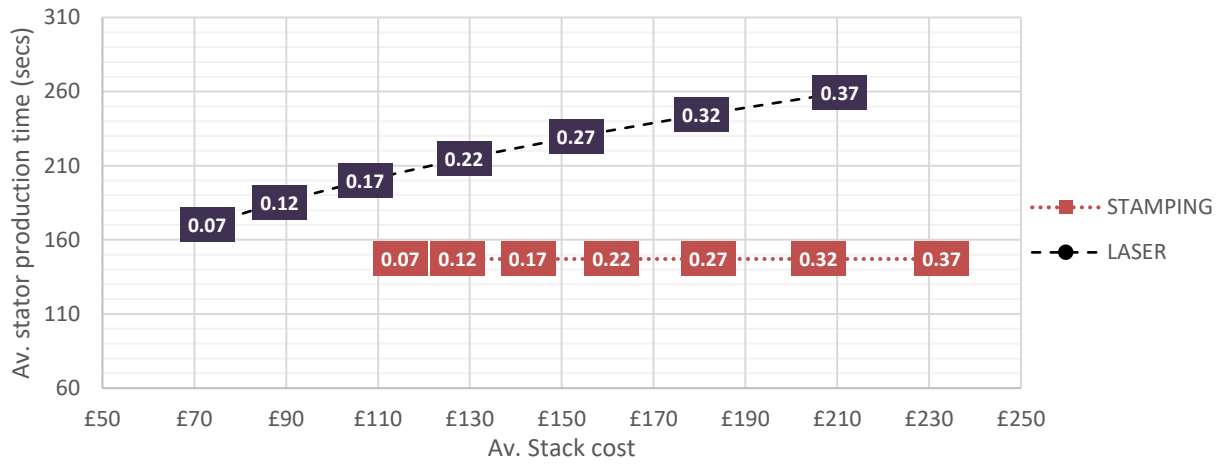


Figure 150 0.25 mm

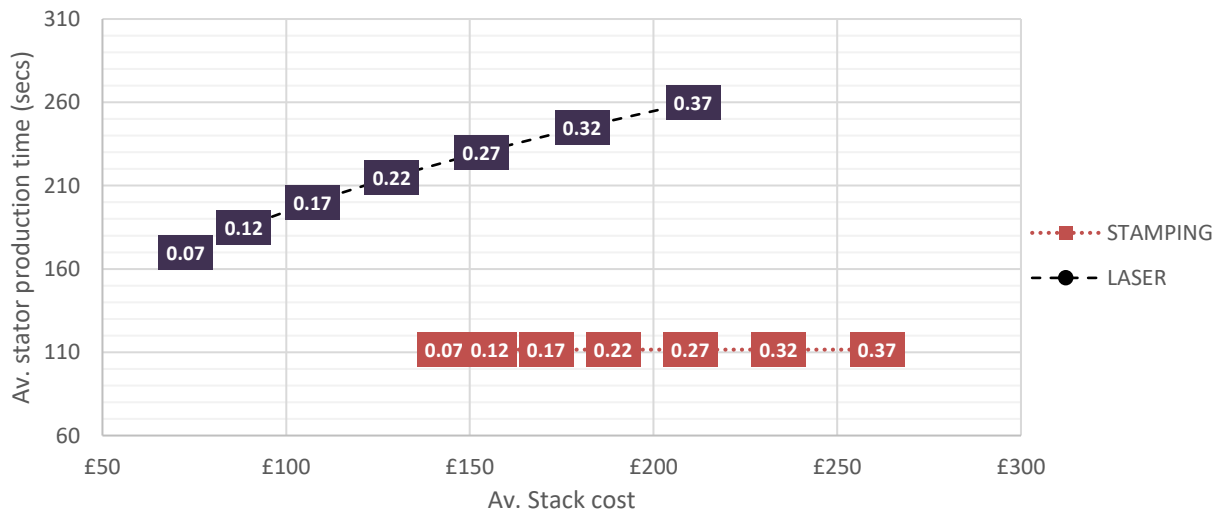


Figure 151 0.35mm

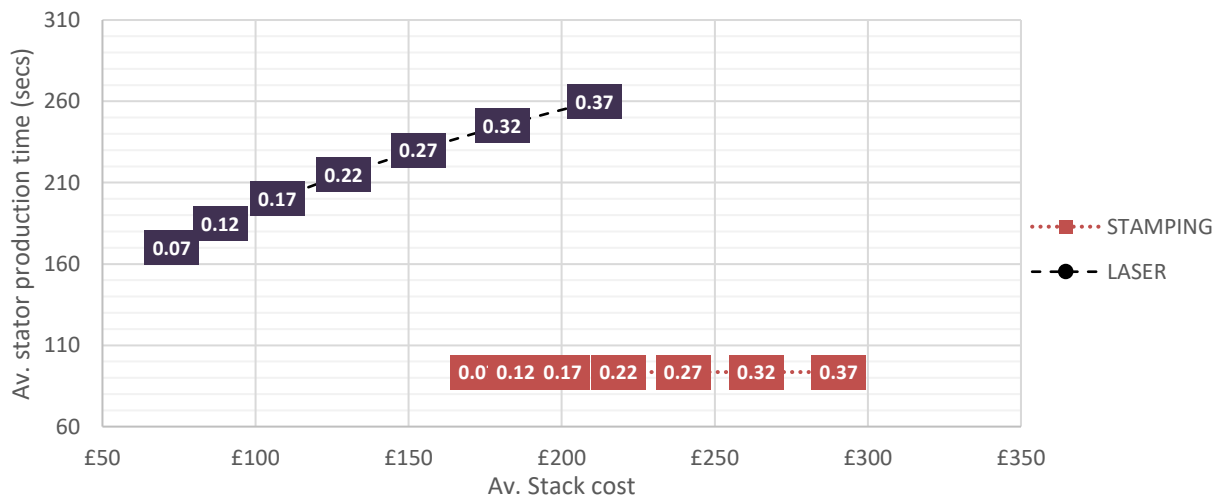


Figure 152 0.45mm

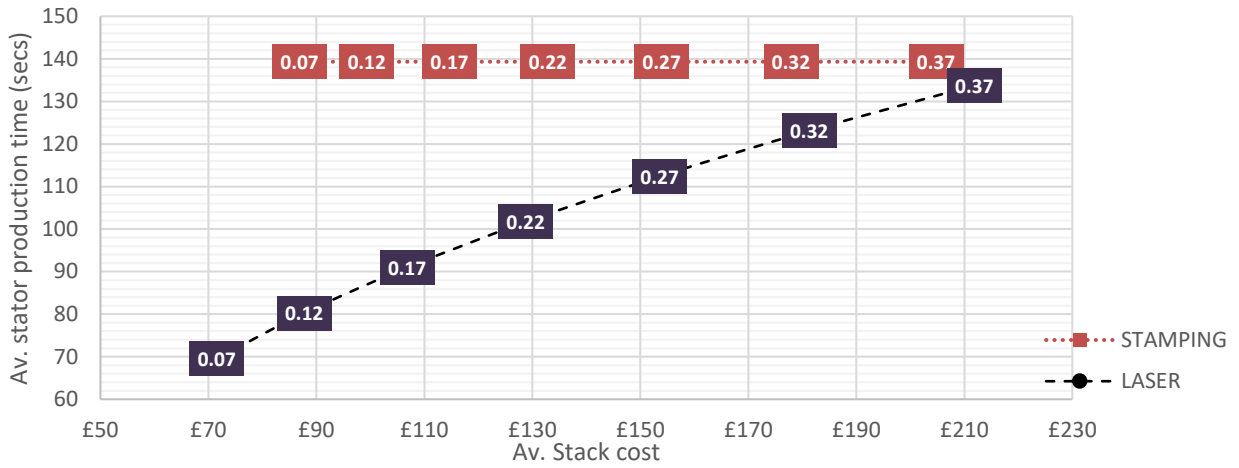


Figure 153 0.25mm thick

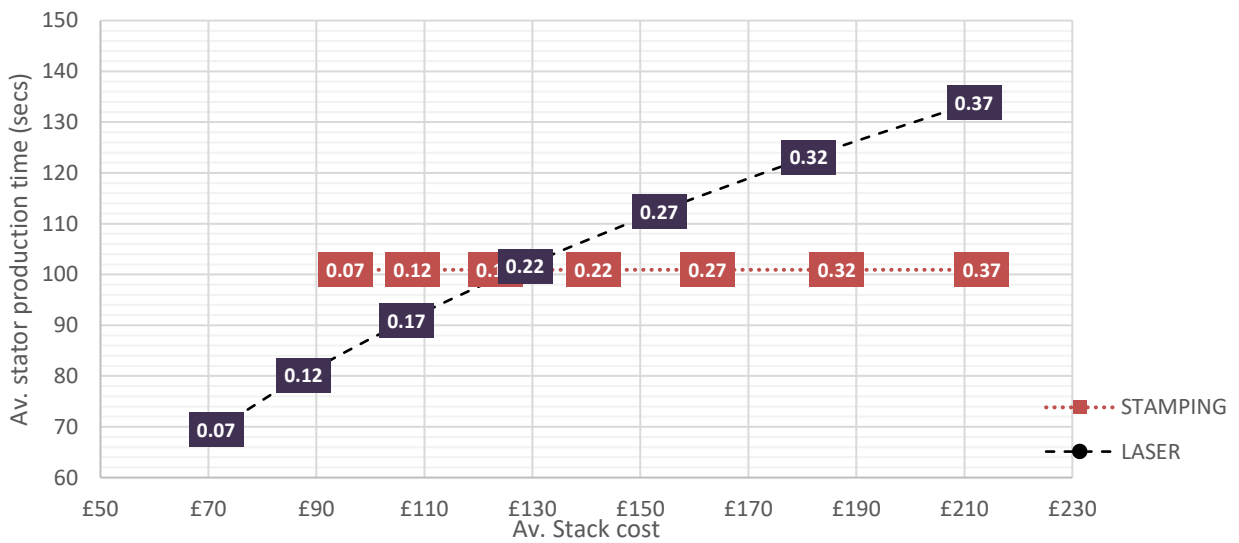


Figure 154 0.35mm thick

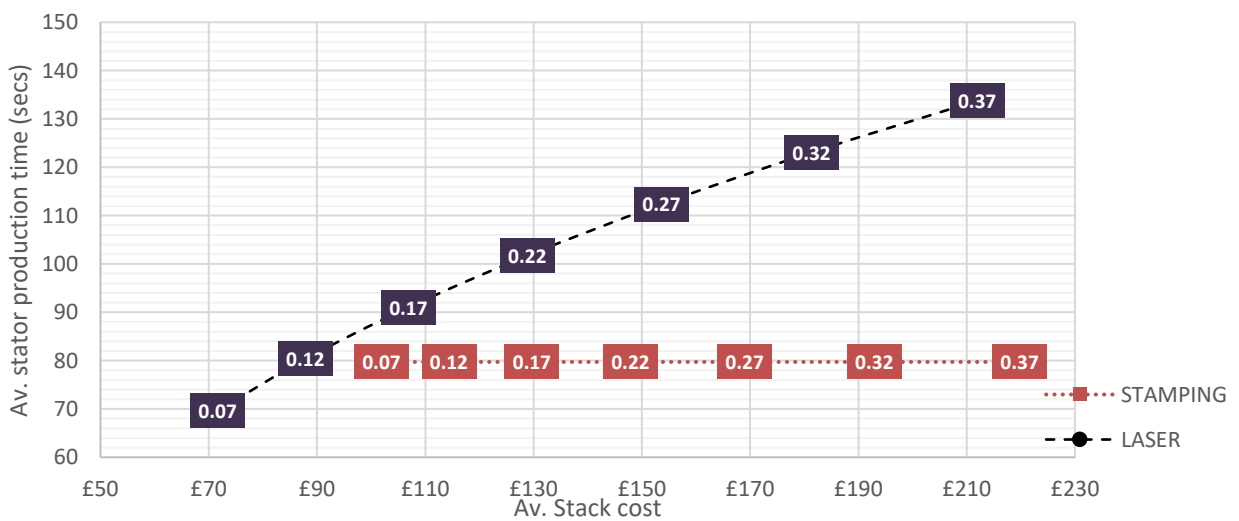


Figure 155 0.45 thick